ASPECTS OF VISUAL PROCESSING IN RELATION TO SEARCH PERFORMANCE

by

Patrick Matthew Forsyth

Thesis submitted for the degree of
Doctor of Philosophy

to

THE CITY UNIVERSITY

Department of Optometry and Visual Science

May 1987

CONTENTS

LIST OF TABLES

LIST OF FIGURES

ACKNOWLEDGEMENTS

I would like to thank my supervisors, Professor R.W.G.Hunt and Dr J.L.Barbur, for their encouragement, help and patience throughout the project. Thanks are also due to Dr J.L.Barbur for the use of his optical apparatus, interfaces and computer, the versatility of which enabled the results reported in chapters 3 and 4, encompassing four different experimental procedures, to be produced without the construction of new equipment, in a relatively short time.

I acknowledge with thanks the financial support of RSRE.

I would like to thank the following, and acknowledge their help:

- Dr [redacted] of RSRE for his continuous interest in the project, and his help in obtaining the equipment needed for it,
- Miss J.Wilson for the use of her version of Dr G.Burton's program for probit analysis,
- Dr J.M.Findlay for his stimulation and help in working out the programme of experimentation on the eye movements of the hemianopic subject,
- [redacted] for constructing the modified version of his eye tracker,
- Dr W.D.Thomson for preparing the computer programs used in the saccadic contrast threshold comparison (chapter 9), and helping to run this experiment.

I have had the help of several fellow students and members of my family who have acted as subjects and I am grateful to them all for their patience and cooperation, but I must thank particularly [redacted] and [redacted] the extent of whose help will be apparent in the frequent occurrence of their initials in the figures and tables.

I am very grateful to both the sponsors of the project and The City University for giving me the enjoyable opportunity to acquire practical experience of electronic circuit building and computer programming, and partially to make

DECLARATION

I grant powers of discretion to the University Librarian to allow this thesis to be copied in whole or in part without further reference to the author. This permission covers only single copies for study purposes, subject to normal conditions of acknowledgement.

ABSTRACT

This investigation has aimed to provide data required for a model of visual search performance, and to test models of visual processing.

Psychophysical thresholds have been measured over a range of visual field angles for luminance and colour contrast, motion displacement and speed discrimination, for small, uniform, briefly presented stimuli on a large uniform background. These are reported as threshold functions and as visual lobes, and show how these functions vary with target diameter, visual field position, target velocity and background luminance. Eye movements and pupil responses to similar stimuli were also examined, and threshold levels of stimulation, amplitudes and latencies of response were measured.

In this study foreknowledge of target position made little difference to detection performance, but the use of a suddenly appearing and disappearing stimulus gave very different thresholds to one that appeared gradually. For stimuli close to threshold, luminance contrast correlated well with visual lobe area, whereas chromatic contrast did not. The contrast required for saccadic response was similar to that for a threshold level of detection.

Speed discrimination thresholds were lowest for target velocities near 3^{o}/sec, changing little with increasing eccentricity. Displacement thresholds for detecting motion were proportional to target speed, for speeds from 5^{o}/sec to 50^{o}/sec, and were almost constant for speeds from 2^{o}/sec to 5^{o}/sec, suggesting a model using a single time delay at high speeds, and a range of time delays at lower speeds.

A hemianope showed a normal pupil light reflex, but little response in his blind hemifield to a counterphase grating of the same mean luminance as the surround. These findings suggest that response to such a stimulus requires a direct projection to the striate cortex.

The same subject responded to flashed stimuli in his blind hemifield with saccades of normal latency and accurate mean amplitude, but with greater variability than to stimuli in his normal hemifield. His contrast threshold for saccades in his blind hemifield was higher than normal, but stray light has been virtually ruled out as an explanation of these results.

GLOSSARY:

BRODMAN AREA 8.....(includes) Frontal Eye Fields
BRODMAN AREA 17.....Striate cortex v1
BRODMAN AREA 18.....Parastriate cortex V2, V3 and V4
BRODMAN AREA 19.....Peristriate cortex v5 (motion)
CORPUS CALLOSUM.....Commissure connecting left and right lobes of the cerebrum
CIE.....Commission Internationale d'Eclairage
CRANIAL NERVE II....Optic nerve
CRANIAL NERVE III...Oculomotor nerve
CRANIAL NERVE IV....Trochlear nerve (>sup oblique muscle)
CRANIAL NERVE VI....Abducens nerve (>lat rectus muscle)
CT.....Computerised Tomography
D.....Dioptre
LED.....Light emitting diode
LS.....Lateral Sulcus
MESENCEPHALON.....midbrain
MLF.....Medial Longitudinal Fasciculus
OLIVARY NUCLEUS.....(part of) pretectal nucleus
PLEXIFORM LAYER.....network of nerve cells (in the retina)
PPRF.....Paramedial Pontine Reticular Formation
STS.....Superior Temporal Sulcus
TROXLER FADING.....Local adaptation of the peripheral retina during voluntary fixation.
VEP.....Visually Evoked Potential
W-CELLS.....Ganglion cells with large receptive fields - slow conducting axons (pupil constrictor pathway)
X-CELLS.....Tonic ganglion cells - sustained response - small receptive field - slow conducting axons - colour
Y-CELLS.....Phasic ganglion cells - burst response - fast conducting axons -movement.

INTRODUCTION

1.1 GENERAL INTRODUCTION

The factors affecting human visual search performance are of interest not only in those tasks which rely on visual search (such as in aviation, motoring, radiology, monitoring Visual Display Units, military operations and product inspection), but also to those who have to design the equipment used in them, and more fundamentally for the light they throw on the neural organisation of the human visual system.
Contributions to the field have been made by scientists of many disciplines, using a great variety of experimental paradigms.

Visual search is a complex function which involves several stages of visual processing. In order to understand and model visual search performance, sufficient experimental data are required on each process which contributes to the detection, recognition and identification of a given target in a complex visual scene. Information of interest when considering a generalised model of search performance includes:

a) Absolute detection thresholds as a function of target eccentricity. When the task is to find stationary objects saccadic eye movements are not likely to be triggered by the stimulus, and therefore the subject must consciously scan the visual field either in a random way or by following a predetermined strategy. Within each fixation period (i.e., a glimpse) the target may be at any given eccentricity with respect to the fixation point. A model of search performance will need a prediction of the probability of detecting the target for particular conditions of the visual presentation. Besides target eccentricity these include target size, target motion, luminance and chromatic contrast, average retinal illuminance, background structure and also target structure.

b) Eye movement control in response to moving or briefly presented targets. Search conditions which involve the detection of either moving or briefly presented targets (i.e., targets which appear suddenly in the visual field) differ from those for stationary targets in that the onset of the peripheral stimulus or the transient component associated with target movement can trigger off specific saccades so as to bring the peripheral target under foveal examination as required for a recognition task. The search procedure can, therefore, be quite different to that utilised for stationary targets.

c) Once a target image has been detected and brought under foveal examination, other visual processes take over which result in target recognition. This stage may involve analysis of the spatial covariance of the principal elements in the target structure, the results of which can be used to place the target in a given category. A complete model of visual search would, therefore also include a final stage on pattern recognition.

This particular study attempts to use restricted and simplified visual stimuli to examine the effect of a number of these factors, and to report them in a form suitable for incorporation in a model of human search performance, as part of a larger project in which other factors have been studied by other workers.

For this purpose, threshold data were gathered for a number of possible variables, over as wide a visual field subtense as possible. These are presented as plots of threshold or of probability of detection versus visual field angle. The latter are known as Visual Lobes. In the course of gathering these data the opportunity was taken to examine eye movement and pupil response to similar stimuli, and to look at the effect of attention on the performance of these tasks.

Since it was possible to study the performance of an observer with a lesion of the right optic tract on some of these tasks, the results were used to draw some conclusions on the role of projections to the striate cortex and to the mid-brain in these activities.

The threshold data on motion detection and velocity discrimination suggest some conclusions on the validity of a model of human motion detection.

Chapters 3 to 9 recount the various experiments performed, and chapter 10 summarises the conclusions. This chapter will review the general background to the topics investigated, and chapter 2 discusses the experimental equipment and methods used in each experiment. In both chapters 1 and 2 the sections are in general numbered to correspond with the chapter number of the relevant experiments. Tabulated experimental results can be found in Appendix 1, and the circuit diagrams of special purpose interfaces are in appendix 2.

The initial part of the work (covered in chapter 3) was done on a maxwellian view optical bench instrument which was already available in the department. This could provide a very wide range of luminance and contrast, but was limited in field size to 46^{o}, and was not capable of producing equiluminous colour stimuli. Because of these limitations the later work was mostly largely done on projection screen arrangements, which had a more limited luminance range, but greater field angle, and a more natural binocular mode of viewing. The stimulus sizes and luminances used in the two parts of the study overlapped, and the results are compared in chapters 5 and 8.

1.2 A BRIEF REVIEW OF THE HUMAN VISUAL SYSTEM.

OPTICAL ARRANGEMENT

The optical arrangement of the human eye is shown in Figure 1.1, together with typical values of the principal dimensions for a normal eye. The imaging performance is far from perfect, being affected particularly by chromatic aberration and by veiling glare from scattered light.

DIRECTIONAL CONTROL.

The direction of gaze is controlled by a set of muscles which normally act to move both eyes together. These are shown in figure 1.2. It can be seen that there is some small degree of torsional control, but most of the motion is in the form of rotation about a point about 13mm behind the front surface of the cornea, whereas the optical nodal point is about 7mm behind the cornea. The entrance pupil is about 3mm behind the front surface of the cornea, so that as the eye rotates, the entrance pupil moves.

PUPIL CONTROL.

The aperture of the optical system is controlled by the pupillomotor muscles, the circumferential sphincter controlling contraction, (miosis) and the radial muscle controlling dilation, (mydriasis). Since the front surface of the cornea provides most of the refractive power of the eye, the diameter of the entrance pupil is larger than the real pupil by a factor of about 1.12.

PHYSIOLOGY OF THE RETINA.

The imaging light passes through the network of blood vessels supplying the retina, and through the layers of neural cells which process signals from the sensory cells (the rods and cones), and carry them away from the retina.

The rod system is effective primarily at low levels of illumination, below about $10cd/m^2$. Its spectral sensitivity is shown in figure 1.3 A. This has been derived from the absorption spectrum of rhodopsin, the rod light-

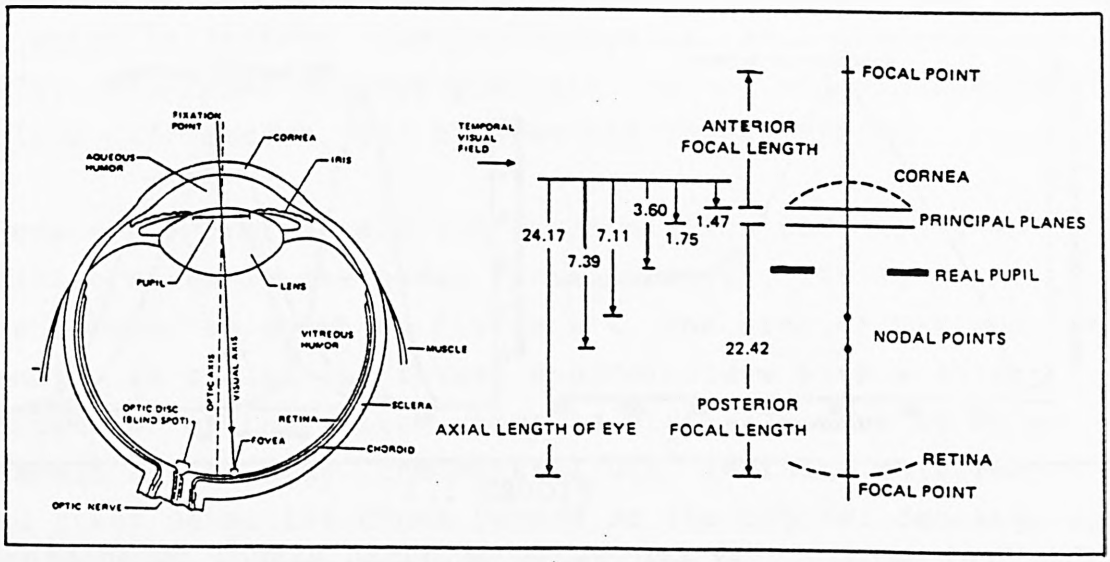

FIGURE 1.1

Cross-section of a typical human eye (a), and its main optical parameters (b). (From Farrell and Booth, (1984))

FIGURE 1.2

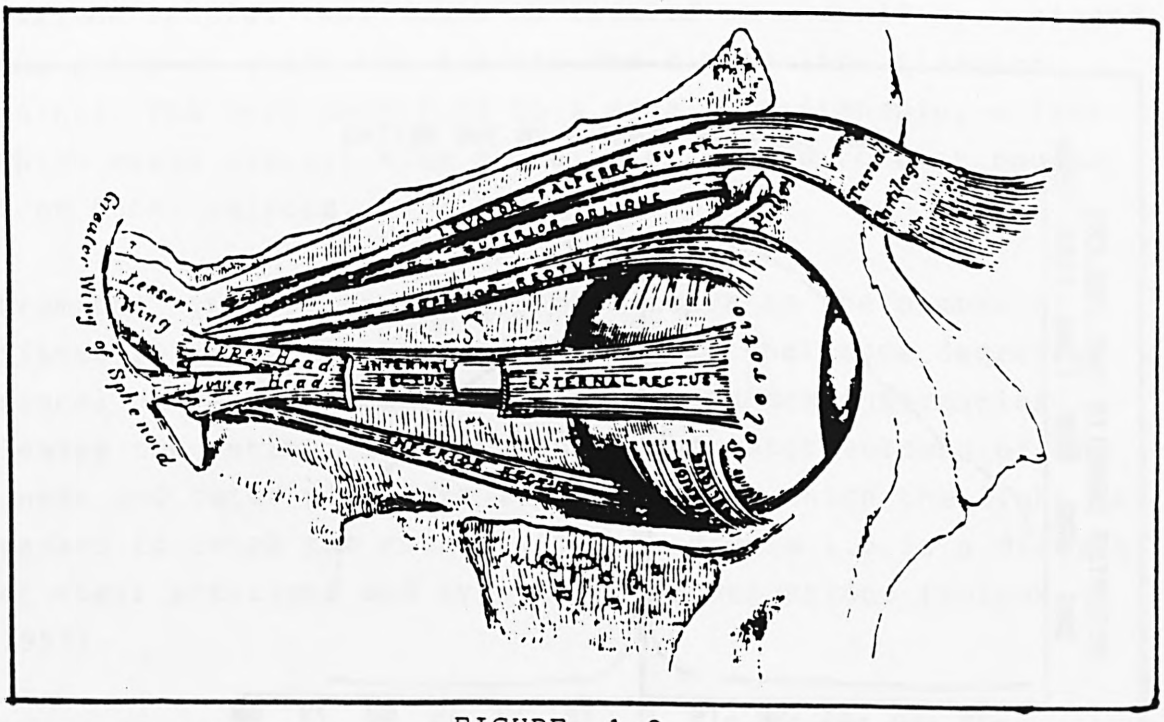

FIGURE 1.2

Diagram of the oculomotor muscles of the right human eye. (From Gray's Anatomy, 1854.)

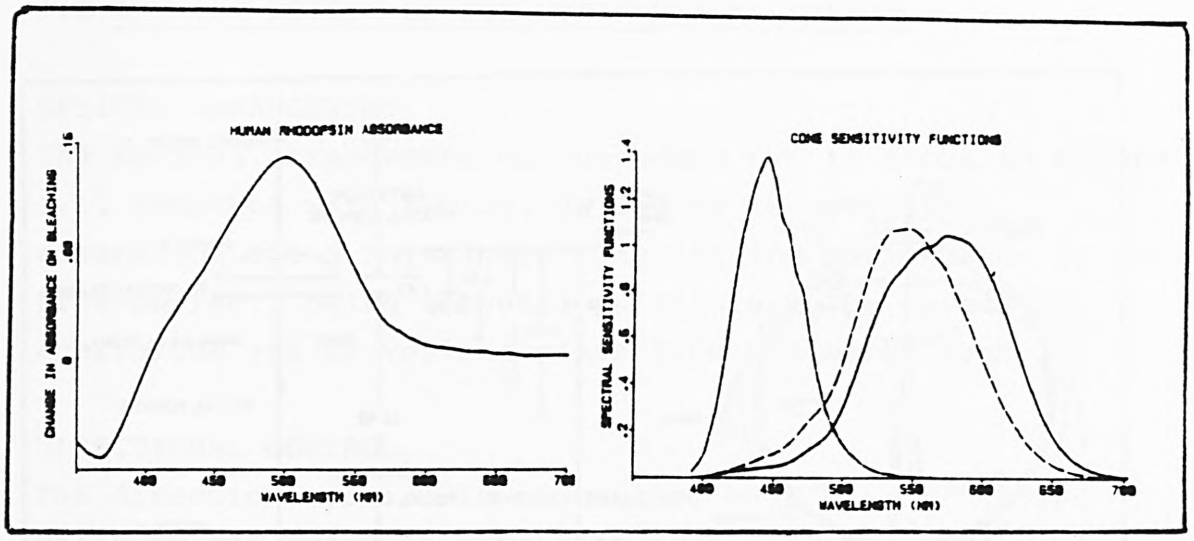

FIGURE 1.3

Spectral sensitivity functions of human visual receptors: (a) Rods (replotted from Brown and Wald (1963)). This shows the difference in absorbtion which occurs on bleaching the rod pigment in the presence of hydroxylamine. (b) Red, Green and Blue cones (replotted from Estevez (1979)). This shows the sensitivities of the three cone types, derived from colour matching data and corrected for an equal quantum spectrum.

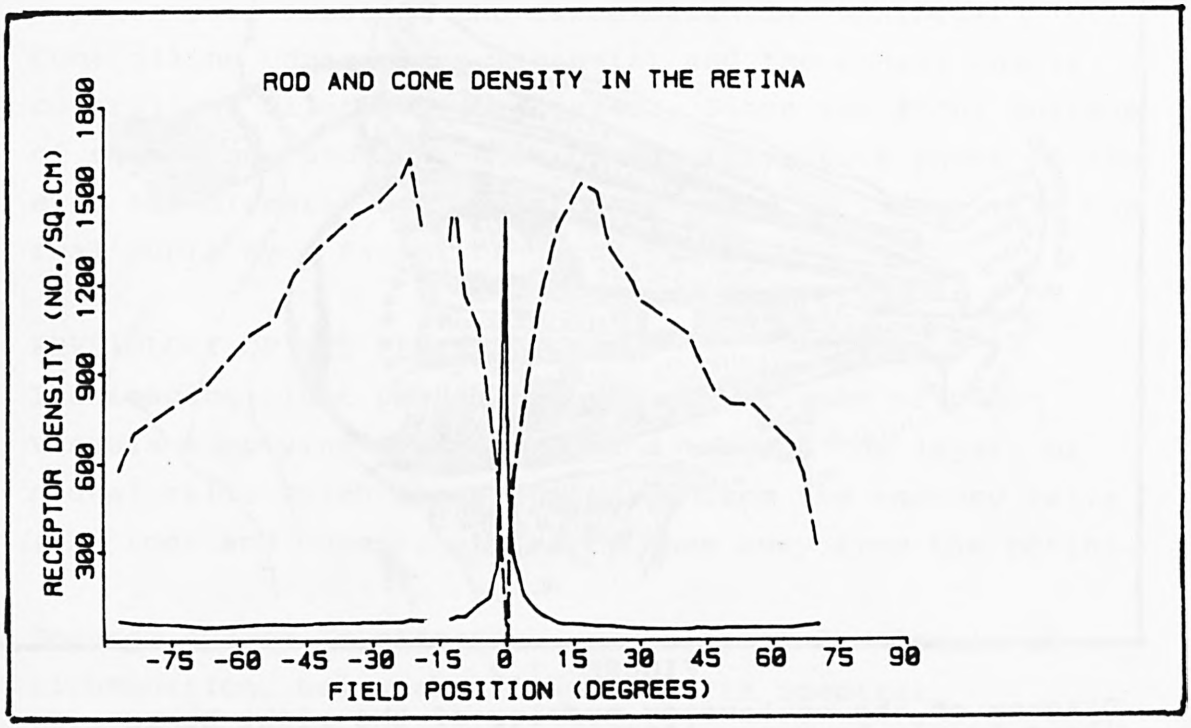

FIGURE 1.4

Distribution of rods and cones in the human retina. (replotted from Oesterberg (1935)).

sensitive pigment (Brown and Wald, 1963). Corresponding data for the three classes of cones are shown in figure 1.3 B, which is derived from psychophysical data (Estevez, 1979). The cones mediate photopic vision, and provide both colour information, and high acuity foveal vision.

There are approximately 110 - 125 million rods and 4 - 7 million cones in the human retina (Polyak, 1957), distributed as shown in figure 1.4. The area of maximum cone density is called the fovea, and coincides with a slight depression on the retina which is virtually free of blood vessels and of rods. The central 0.5^{o} contains only red and green sensitive cones packed at the highest density, and the central 2^{o} contains 90% of all the cones in the retina. The nerve fibres (approximately 1 million (Polyak 1957)) converge on one area of the retina - the blind spot - which is about 16^{o} to the nasal side of the fovea, and leave the eye as the optic nerve.

From the above, it follows that the eye has no colour vision and only poor visual acuity at low light levels, and that maximum spatial resolution is limited to a small area around the point at which one directs one´s gaze (the fixation point). The very centre of this area is tritanopic, a fact which makes distant blue signal lights hard to distinguish from other colours.

From the ratio of the number of sensors to the number of fibres in the optic nerve, it is clear that some degree of signal processing occurs before the sensory information leaves the retina. This occurs in the interneurones of the inner and outer plexiform layers through which the light has passed to reach the rods and cones. Figure 1.5 is a diagram of their positions and type of interconnections (Polyak, 1957).

The following summary of the functions of the interneurones is drawn mainly from reviews by Zrenner (1983) and Masland (1986) of electrophysiological studies and photomicrography

and autoradiography of selectively labelled cells. One class of bipolar cells transmits the output of individual rods or cones, another type transmits centre/surround signals to the ganglion cell layer (see figure 1.6), the collection and interaction of signals from several cones being performed by the horizontal cells which lie in the outer plexiform layer, close to the bipolar cells. Bipolar cells have been identified which receive input exclusively from rods and others which only receive blue sensitive cone input, others which respond positively to a red centre and negatively to a green surround, others to a green centre and a red surround, and yet others which respond negatively to red centres and positively to green surrounds, and vice versa.

Between the bipolar cells and the ganglion cells lie the amacrine cells, different types of which are now known to perform a variety of signal processing functions; some provide transient signals at the onset or offset of rod stimulation, others provide directionally sensitive signals (Barlow and Levick, 1965; Vaney, 1985), others transmit rod output to the ganglion cells, so that the same ganglion cell can function in photopic or scotopic conditions.

Phasic ganglion cells (Y - type cells) respond to light stimulation of their receptive fields with a burst of spikes, or a cessation of spikes. They have a centre/surround opponent field, but are not sensitive to colour, their spectral response being similar to the photopic luminous efficiency curve. Their axons conduct impulses faster than the tonic ganglion cells. The tonic ganglion cells (X - type cells) respond to stimulation with a sustained train of impulses, or the cessation of a train, and mostly provide the variety of colour opponent responses already described for the bipolar cells. They have smaller receptive fields than the phasic cells. The proportions of the different types of ganglion cell vary with retinal eccentricity, the phasic cells becoming relatively more numerous outside the macular area.

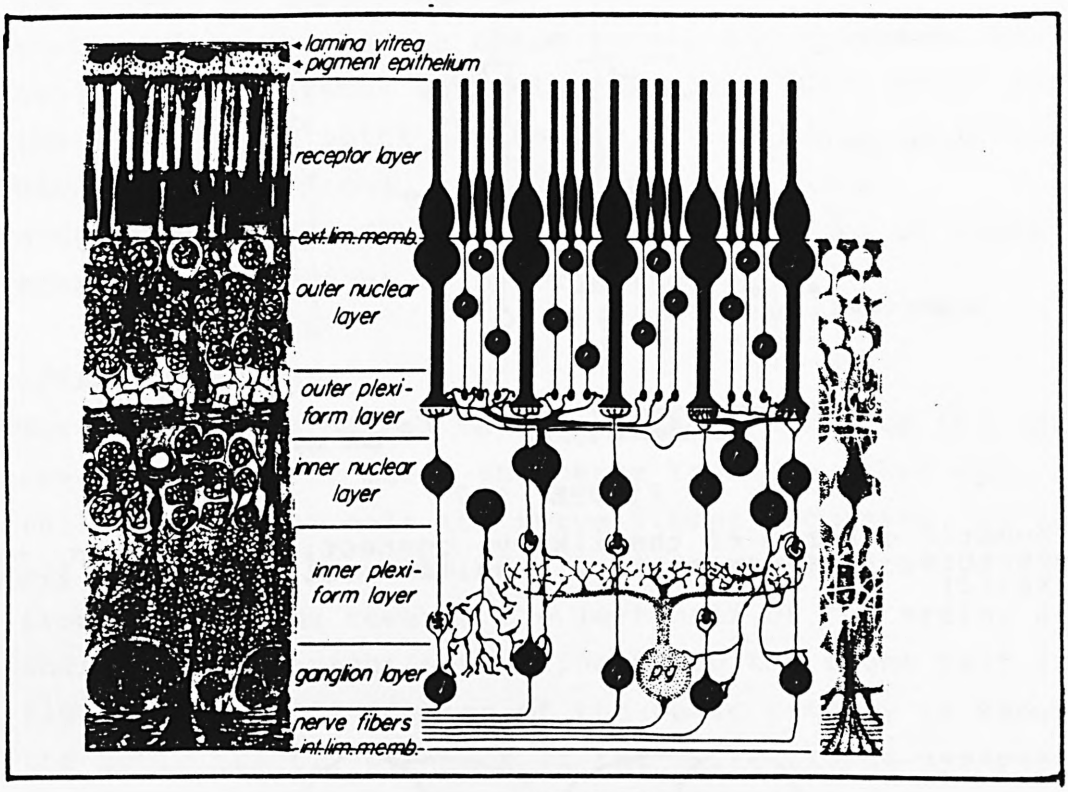

FIGURE 1.5

Diagram of the receptors and neurons in the retina. (from Polyak (1957)).

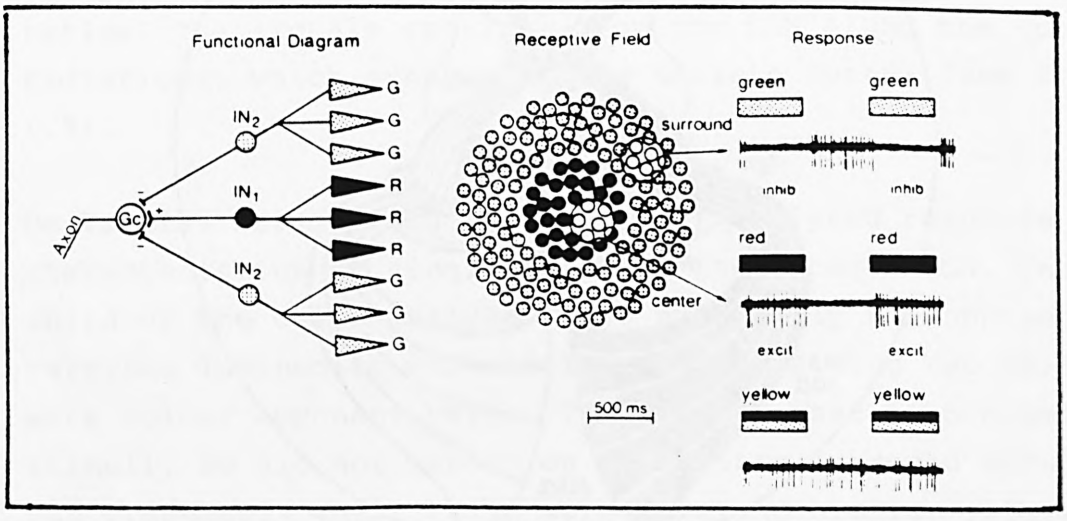

FIGURE 1.6

Organisation of centre-surround detectors (from Gouras and Zrenner, 1982)

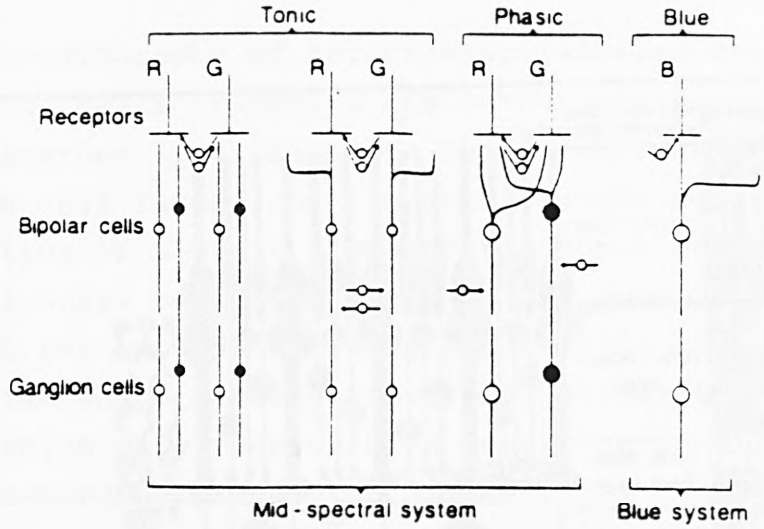

FIGURE 1.7

Schematic diagram of the likely connections between the receptors, interneurons and ganglion cells. (from Zrenner (1983).)

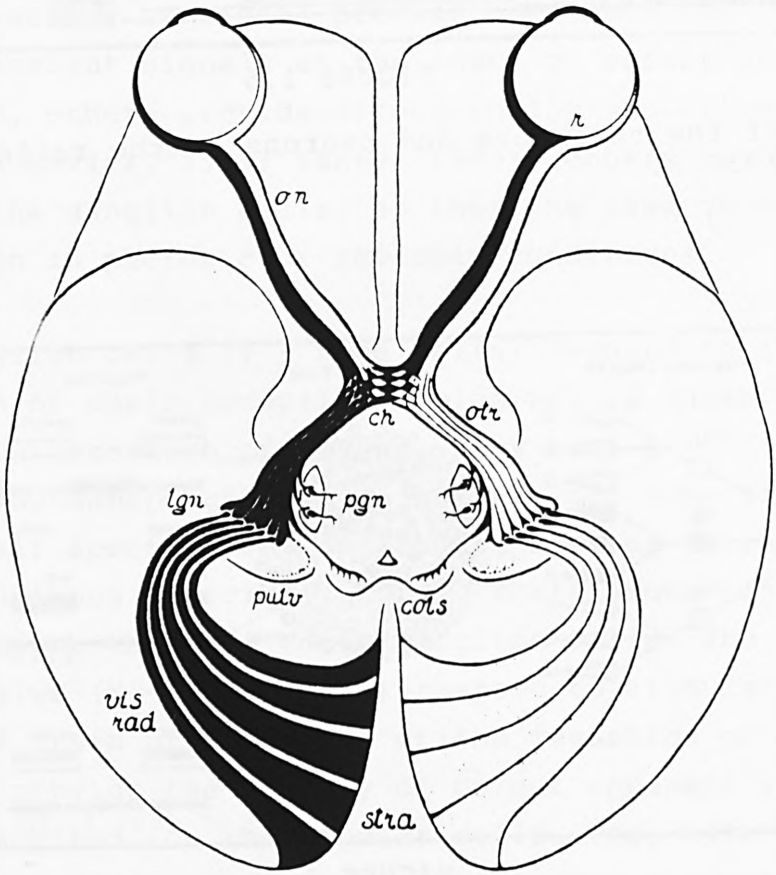

FIGURE 1.8

Neural pathways from the retina to the striate cortex (from Polyak (1957). r: retina, on: optic nerve, ch: chiasma, o tr: optic tracts, lgn: lateral geniculate nucleus, pgn: pregeniculate nucleus, col s: superior colliculus, pulv: pulvinar, vis rad: optic radiation, str a: striate cortex.

The number of ganglion cells is probabably similar to the number of fibres in the optic nerve, and to the number of cells in the Lateral Geniculate Nucleus (LGN) which forms the first relay point on the way to the brain (Williams and Warwick, 1980; Stone, 1983). Figure 1.7 shows diagrammatically (Zrenner, 1983) the way some of these elements are thought to be organised.

AFFERENT PATHWAYS

The optic nerve passes back from the eyeball to the optic chiasma, where it meets the nerve from the other eye. At this point about half the nerve fibres decussate, so that all the fibres from the left hemiretina of each eye continue from the chiasma towards the left half of the brain, and those from the right hemiretina go to the right half (see figure 1.8). This section of the optic pathway is known as the optic tract. 70% - 80% of the nerve fibres synapse at the Lateral Geniculate Nucleus, in 6 well organised layers which map different areas of the retinal field. Most of the remaining 20% or so of fibres project to the superior colliculus, where they contribute to eye movement control. Some fibres also project to midbrain areas and particularly the pretectal nuclei, and contribute to the pupil light reflex. The signals continue from the LGN along the optic radiations, which synapse at the striate cortex (see figure 1.9).

De Valois, Abramov and Jacobs (1966) analysed response characteristics of single cells in the macaque LGN. One third of the cells analysed were spectrally non-opponent, carrying luminosity information, the remaining two thirds were colour opponent cells. The authors used monochromatic stimuli, so did not report on any centre/surround structure, but presumably their cells were carrying similar information to the retinal ganglion cells later analysed by Gouras and Zrenner (1982).

VISUAL CORTEX

The organisation of the visual cortex has been reviewed by Hubel and Wiesel (1979) and by Zeki (1978 and 1985). Within the striate cortex adjacent striae map corresponding parts of the visual field from each eye. The cells in any one vertical column descending from the surface of the cortex are all sensitive to edges of the same orientation within the visual field, adjacent columns having peak sensitivity to slightly different orientations.

A group of columns within a millimetre or two includes a full range of orientations corresponding to one area of the retina, the macular area of the retina occupying a large proportion of the visual cortex, so that the area of cortex per retinal ganglion cell receptive field is approximately constant (Drasdo, 1977). Since receptive fields increase in area towards the periphery, a scaling factor can be derived, relating visual angle to, for instance, visual acuity, receptive field density or cortical area. This cortical magnification factor can be used to scale peripheral stimuli to provide equal thresholds for many visual properties throughout the visual field.

The striate cortex is organised as 6 layers roughly parallel to its surface, with distinct functions and patterns of connection to the rest of the visual areas. One layer of cells has concentric centre/surround fields, like the retinal ganglion cells. In the same layer (IV) above these, are simple cells which respond to a short bar of fixed orientation. In the other layers the cells respond best to moving bars, or to bars of indeterminate length. Layer V cells project to the superior colliculus, and layer VI cells project back to the LGN (Stone, 1983).

The prestriate cortex has been shown, in monkeys at least, to be divided into at least six functional areas (Zeki, 1978, Hubel & Wiesel,1979), receiving their initial input from the striate cortex (V1). Area V4, for instance is specialised in colour detection (Zeki, 1985) and area V5 in

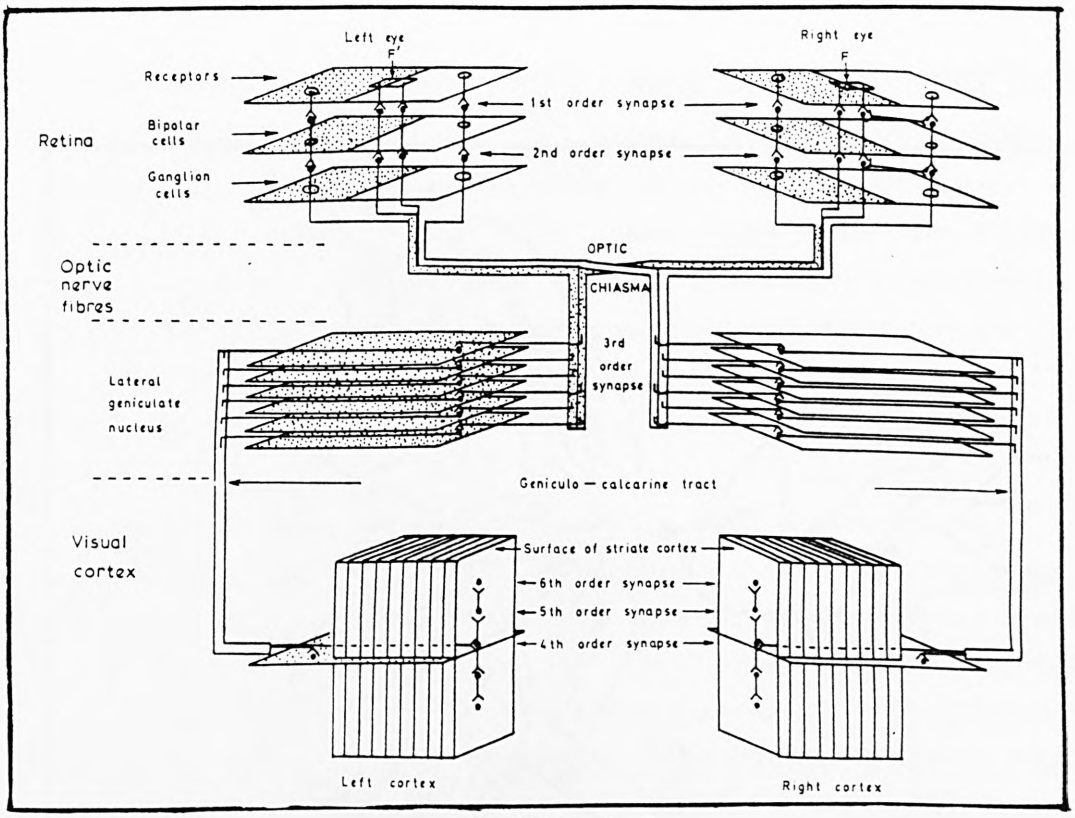

FIGURE 1.9

Neural pathways from the receptors to the cortex. (from Ruddock (1975).)

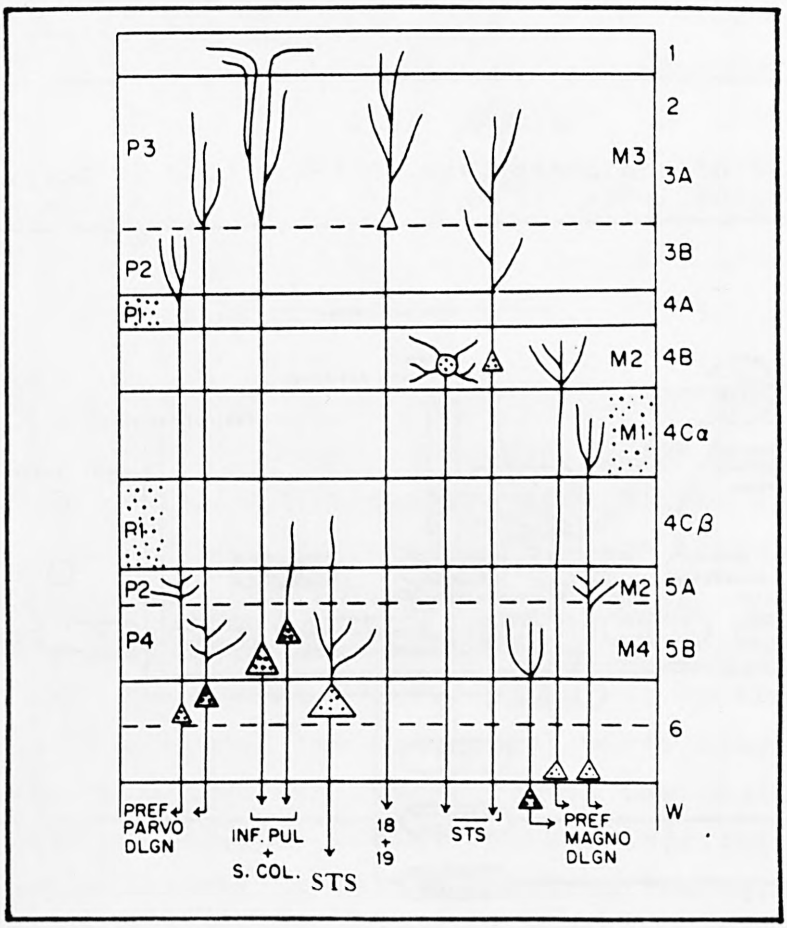

FIGURE 1.10

Functions of layers of the striate cortex. From Lund et al.,(1975)

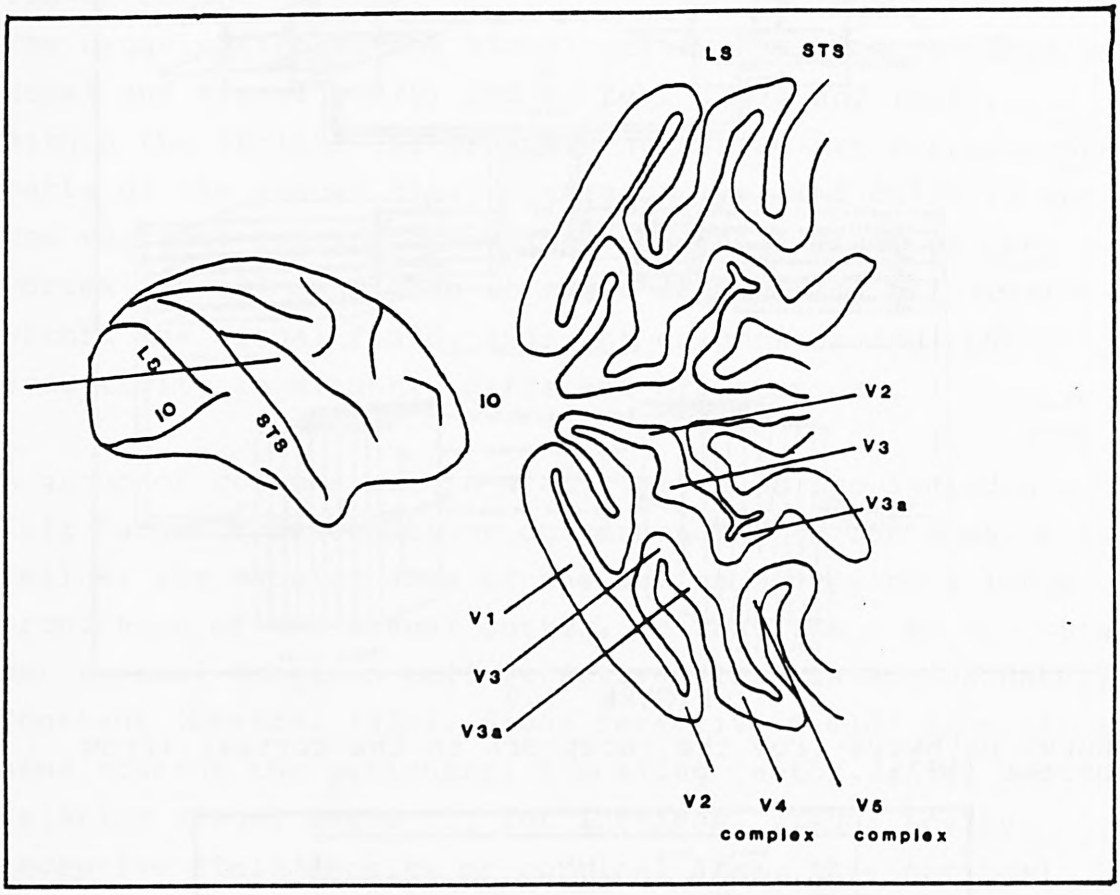

FIGURE 1.11

Visual Areas of the prestriate cortex of the Monkey, and their functions (Zeki (1985))

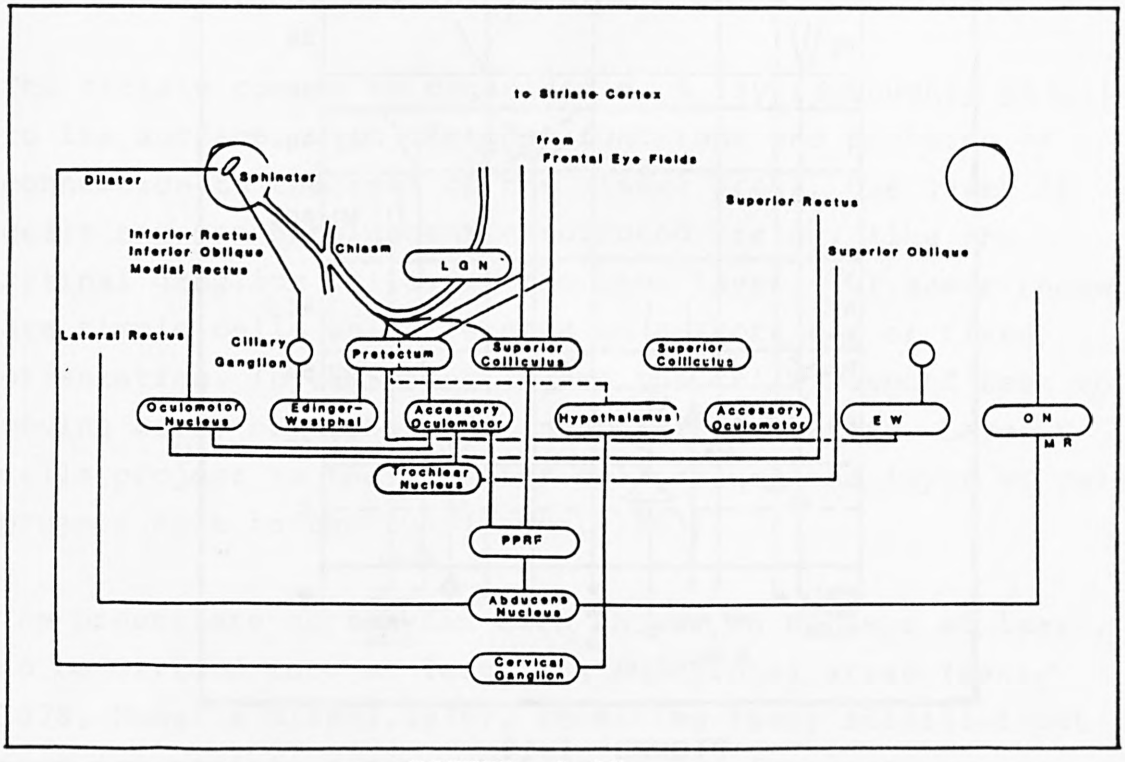

FIGURE 1.12

Schematic diagram of part of the oculomotor control system

motion detection (Zeki, 1974). Many of these areas have interconnections across the corpus callosum with the corresponding area in the other half of the brain (Zeki,1985), see figure 1.11. Each area maps the visual field in a way appropriate to its function, the areas functioning in parallel, and passing information on in turn to the other areas.

EFFERENT PATHWAYS

The nervous pathways which cause contraction of the pupillomotor muscles are indicated in figure 1.12. Pupil constriction is controlled via the parasympathetic nervous system. Some retinal ganglion cell axons bypass the LGN and synapse at the olivary nuclei of the pretectum (Pierson and Carpenter,1974). The pretectum also receives input via various routes from the visual cortex and frontal eye fields. Interneurons connect the pretectal nuclei to both the ipsilateral and contralateral Edinger-Westphal nuclei (Zinn, 1972), thus providing a pathway for both the direct and consensual light reflex. The Edinger-Westphal nuclei in turn send axons to the ciliary ganglion, and thence to the constrictor muscle of the iris. The pupil dilator muscle is controlled by the sympathetic nervous system, the signal emerging from the the brainstem and reaching the muscle via cranial nerve V (Williams and Warwick (1980)).

Efferent signals from the frontal eye fields and the striate cortex go via the superior colliculus to the nuclei of the motor nerves of the ocular muscles (see figure 1.12). Parts of the visual cortex also connect, via the accessory oculomotor nuclei, with the oculomotor nuclei and trochlear nuclei. These are paired structures, one on each side of the midline. They are connected (Keller, 1980) to the ipsilateral muscles of the eye except where otherwise noted. The oculomotor nuclei are connected via the oculomotor nerve to the inferior oblique, medial rectus, inferior rectus and (contralateral) superior rectus muscles. The lateral rectus is controlled via cranial nerve VI from the abducens nuclei. The (contralateral) superior oblique muscle is controlled

via the accessory oculomotor nuclei, the trochlear nucleus, and the trochlear nerve (cranial nerve VI).

The control of visual saccades has been investigated by Fuchs, Kaneko and Scudder (1985). The neural command to produce a step rotation of the eyes is generated in the pontine and mesencephalic regions of the brain. A neural 'Pulse generator' operates there which is activated by inhibition of "PAUSE" neurons. These neurons appear to operate nonselectively for all saccades, and appear to be concerned only with the initiation and timing of saccades ('WHEN' system). The burst neurons in the pulse generator discharge selectively depending on the direction and amplitude of the saccade. They thus receive a second input from the visual system coding the saccade spatial characteristics (the 'WHERE' system).

As can be seen above, pathways exist for information from the retina to reach the oculomotor centres by at least three possible routes, namely:

a) retina > superior colliculus > oculomotor centres,
b) retina > LGN > visual cortex > superior colliculus > oculomotor centres
c) retina > LGN > visual cortex > Frontal eye fields > oculomotor centres.

Lesion studies in monkeys have demonstrated that saccades can be mediated through at least these three pathways. Schiller, True and Conway (1979) showed that lesioning both superior colliculus and frontal eye fields left rhesus monkeys unable to respond with saccades to visual stimuli; however lesioning either centre alone did not eliminate this ability. Likewise Mohler and Wurtz (1977) had shown that combined visual cortex and superior colliculus lesions eliminated visual saccades, following visual stimulation of the affected area of the visual field, but less severe deficits occurred with lesions in each individual centre. Ablation of the superior colliculus of the monkey led to

saccades with longer latency, and more intense stimuli were needed to elicit them, whereas the effect of visual cortex lesions appeared to be a reduction in the accuracy of the movement, without altering the mean latency.

1.3 EFFECT OF STIMULUS SIZE, VELOCITY AND BACKGROUND LUMINANCE ON CONTRAST THRESHOLDS.

"Contrast" in this study will be taken as:

$$\frac{\text{(luminance of target) - (luminance of adapting field)}}{\text{(luminance of adapting field)}}$$

In many cases it is more conveniently reported in terms of $\log_{10}$(contrast). Since the targets used are all small compared with the background, and (except in chapter 7) consist of uniform discs differing in colour or luminance from the background, rather than gratings, the luminance of adapting field is taken to be that of the background.

The classical work in this field is Blackwell's (1946) "Tiffany" experiments, in which two million threshold observations were made with a large number of observers and a range of contrasts (positive and negative), stimulus areas and exposure times. The large numbers involved point to one of the classic problems: the inherent variability of psychophysical threshold data. The use of negative contrasts (i.e. stimuli darker than the background) produced similar thresholds to positive contrasts, except for large stimuli with low background luminances, where negative contrast thresholds were 20% lower than positive contrasts.

The interpretation of such data was studied by Swets, Tanner and Birdsall (1961) on the basis of signal detection theory. They postulated an ideal observer, whose stimuli are subject to noise, and whose Receiver Operating Characteristic relates his criterion of detection to his contrast threshold. They found that a real observer can detect a

stimulus which is one standard deviation above noise.

Exposure time - beyond a minimum of about .3 sec, is not an important factor. For shorter times, Bloch's law applies (i.e. threshold is inversely proportional to flash duration) (Overington, 1976).

For very small stimulus diameters, less than 10 minutes of arc, Ricco's law applies, i.e. threshold contrast is inversely proportional to stimulus area (Ronchi and Novakova 1971). For diameters greater than 100 minutes of arc, changes in stimulus size - in the centre of the visual field and under photopic conditions - have little effect on threshold. The intermediate range is covered by Blackwell (1946), see Figure 1.13 (replotted from Blackwell's data).

All of the work reviewed above has referred to foveal or parafoveal observation. The fall-off of visual sensitivity in the periphery is shown by normal perimetric field testing as in figure 1.14. These plots are for one eye at a time. Wolf and Gardiner (1963) report that there is an area of lower threshold in the nasal hemiretina corresponding to the blind spot in the other eye, however these observations were made with a fully dark-adapted eye, and pertain to rod vision only.

In 1977 Rovamo, Virsu and Nasanen (1978) measured contrast thresholds for stationary peripheral gratings and Koenderink et al (1978) measured contrast thresholds for moving sine wave patterns for variations of spatial frequency, velocity and target size. Both groups found that if the size of the targets is scaled by the inverse of the cortical magnification factor, or by the visual acuity at that eccentricity, contrast thresholds do not change with eccentricity. Koenderink et al (1978) found that there was a unique combination of spatial frequency and velocity at any eccentricity for the lowest contrast threshold.

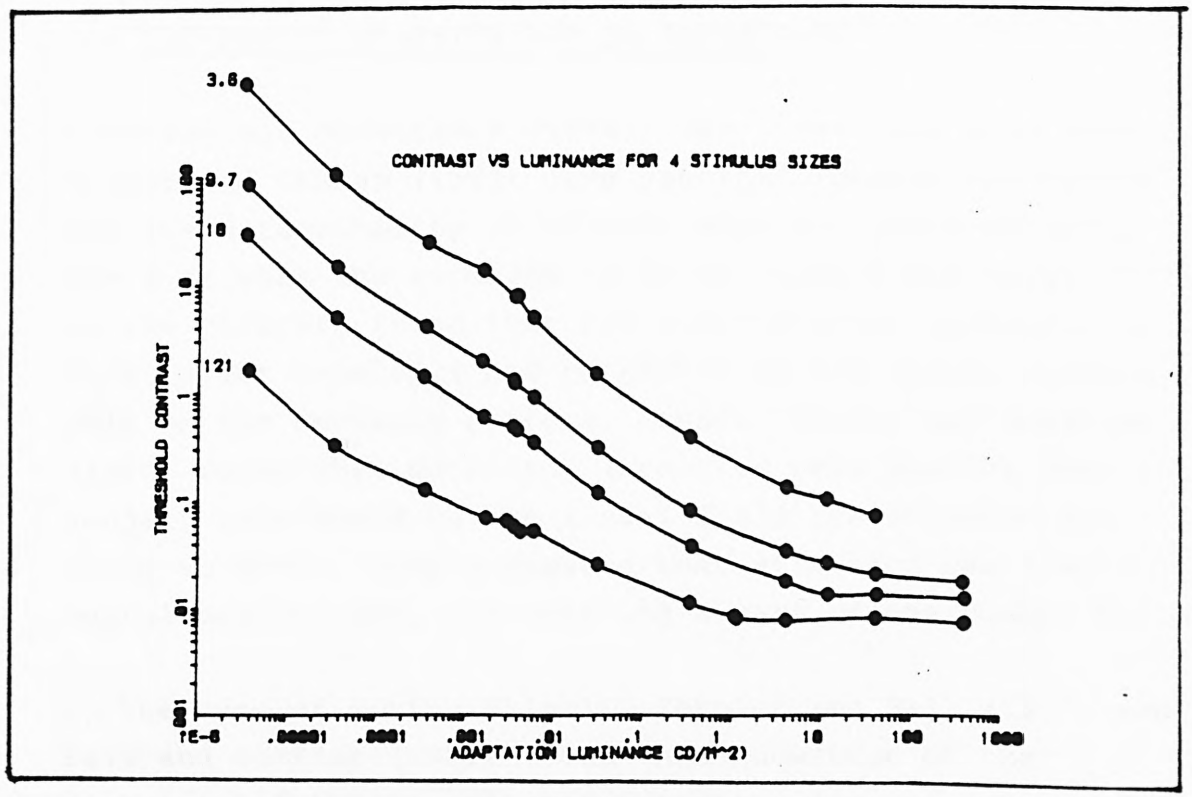

FIGURE 1.13

Threshold contrast as a function of size and luminance. Each line represents a different diameter target, labelled with its diameter in minutes of arc. (Replotted from Blackwell (1946)).

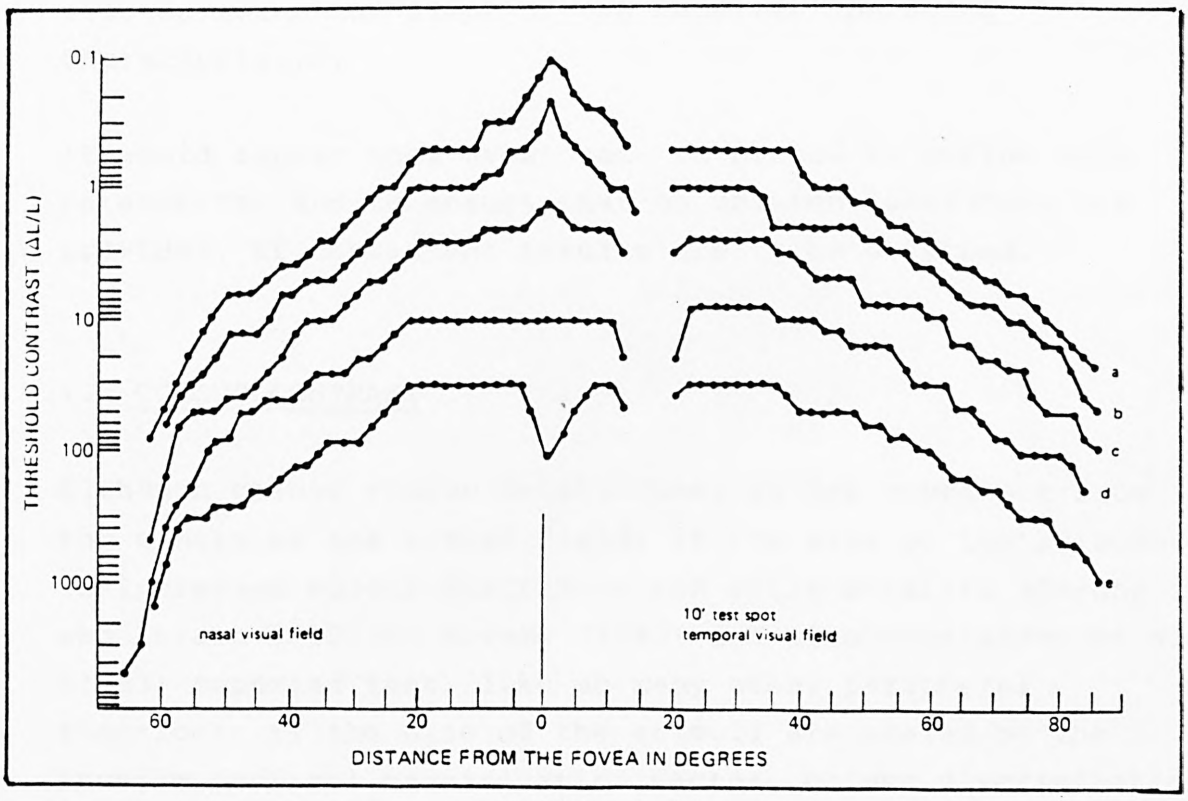

FIGURE 1.14

Perimetry for a range of background levels of luminance. a:0.85 ml, b:0.085 ml, c:0.0085 ml, d:0.00085 ml, e:0.000085 ml. (From Harvey and Poppel, (1972).)

1.4 THE EFFECT OF ATTENTION ON THRESHOLD.

Cohn and his co-workers (1974, 1981, 1984) and also Davis, Kramer and Graham (1983) have reported lowered thresholds for the detectability of stimuli when the observer knows where or what the stimulus is to be. Lappin and Uttal (1976) on the contrary found that for their stimuli (patterns of dots) prior knowledge had no effect on the visual process, only on the decision process. Posner, Snyder and Davidson (1980) found that detection latencies were shorter when the subject knew where in the visual field the stimulus was going to occur. They suggested that attention was like a mental searchlight, illuminating a part of the visual field.

In the case of moving stimuli, Sekuler and Ball (1977) and Ball and Sekuler (1981) found that knowledge of the direction of motion enhanced detectability and increased speed of reaction. Cohn and Lasley (1974) predict from Signal Detection Theory that uncertainty of any orthogonal parameter describing one of a set of equally likely non-overlapping stimuli will decrease its detectability, and also decrease the slope of the Receiver Operating Characteristic.

It would appear that great care is needed to define such parameters, and to ensure that no unintentional cues are provided, if consistent results are to be obtained.

1.5 COLOUR CONTRAST

Although colour vision deteriorates as one moves out from the centre of the visual field, if the size of the stimulus is increased colour discrimination still persists (Gordon and Abramov, 1977). Rovamo (1983) and also Noorlander et al (1983) reported that, like so many other peripheral functions, if the size of the stimuli are scaled by the inverse cortical magnification factor, colour discrimination becomes comparable throughout the visual field.

One consequence of the cone spectral sensitivity functions shown in figure 1.3 is that the eye is more sensitive to differences in spectral stimuli at wavelengths near 500 nm and 570 nm, where the relative sensitivities of two sets of cones are changing rapidly (see figure 1.15).

Colour differences may be represented using the CIE 1931 standard observer data. This is based on work by Guild and by Wright, who measured the response of a number of observers to red, green and blue primaries. They used different primaries, and the CIE system used linear transformations of these sets into a further set, which comply with the requirements that the standard observer functions should have no negative sensitivities, and also that the green spectral sensitivity function should match the (previously determined) CIE photopic luminous efficiency function. The resulting set of spectral sensitivity functions, although derived for small area colour matching, and incorporating a slightly non-typical luminous efficiency function, are very widely used in specifying colour tolerances, colour standards and gamuts of available colours (Wright, 1986; Hunt, 1986 and Robertson, 1986).

If the expression

(spectral radiance)x(CIE colour matching function)

is integrated over the visible spectrum, responses of the standard observer to the light source can be calculated. These are generally represented as X,Y and Z, and are known as CIE tristimulus values. Y is proportional to the luminance. If X, Y and Z are then normalised by dividing by (X+Y+Z) the normalised values of X and Y (usually written x and y) can be used to specify the chromaticity. A colour can then be represented graphically by plotting these chromaticity coordinates on a chromaticity diagram. It has to be born in mind however that the CIE primaries used were never intended to match the sensitivities of the human cone receptors, and even if they did, the resulting chromaticity representation would not represent equal differences in

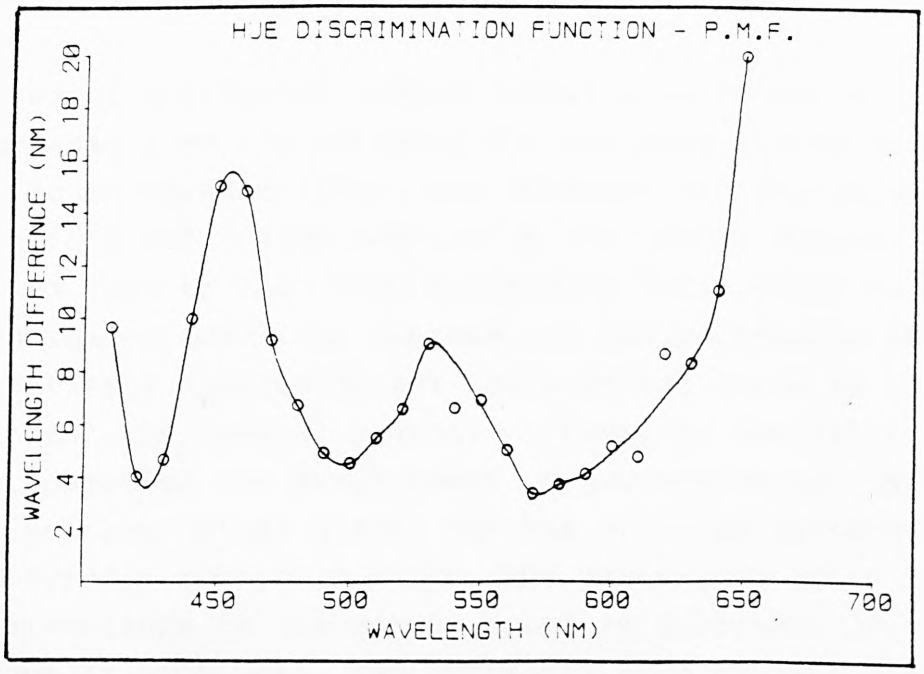

FIGURE 1.15

Example of a spectral hue discrimination function (Subject: PMF at age 23)

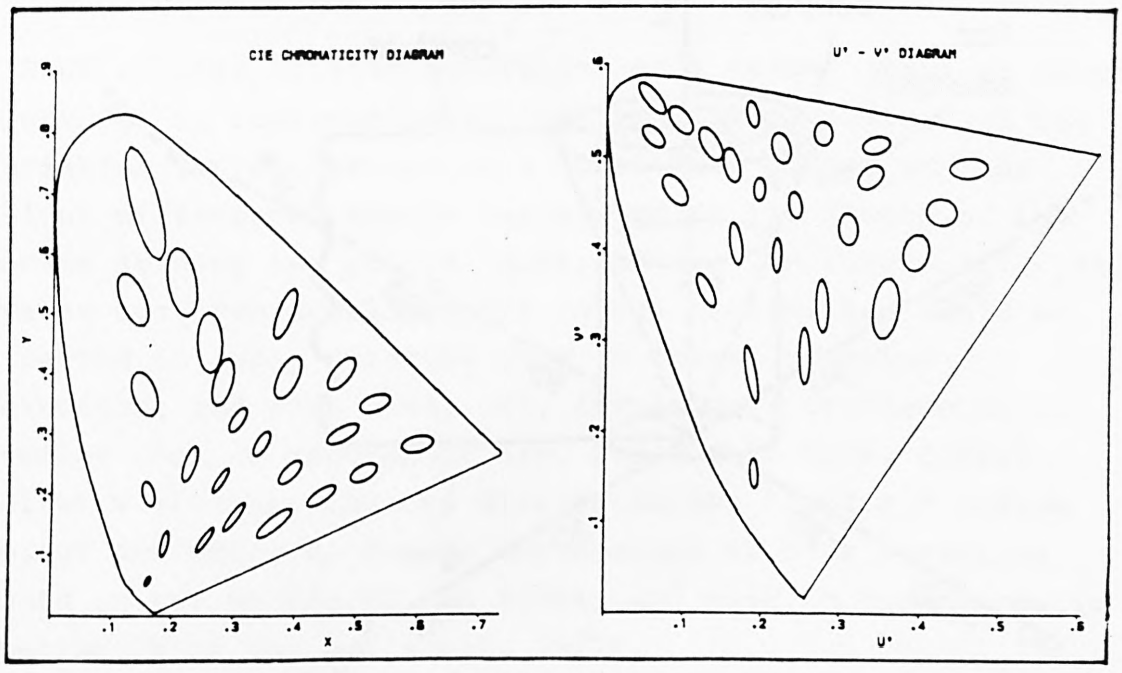

FIGURE 1.16

Original Macadam ellipses plotted on a CIE x-y diagram, and on a u' - v' diagram.

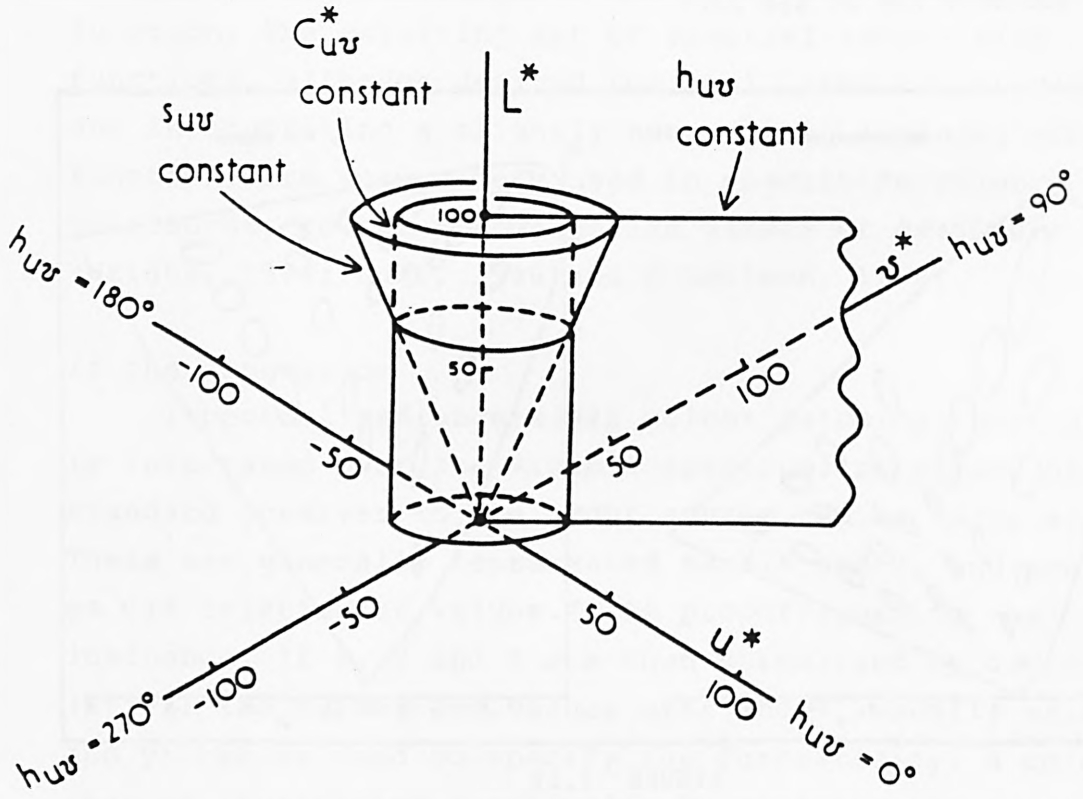

FIGURE 1.17

The CIELUV colour solid. L* is the correlate of the concept of lightness, S_{uv} is the correlate of the concept of saturation, C* is the correlate of the concept of chroma, and h_{uv} is the correlate of the concept of hue. (From Hunt (1977).)

colour by equal distances.

The colour difference needed foveally to render a stimulus detectable from its surroundings has been extensively studied by MacAdam (1942) who measured the standard deviations for colour matches of 105 sample colours, and related them to the 'Just Noticeable Difference' in colour or luminance (JND). He represented the variations on the CIE chromaticity diagram by what have become known as MacAdam ellipses. The Optical Society of America, and later the CIE have sponsored the development of successive approximations to a Uniform Colour Space. The aim of these systems has been to provide a metric in which JNDs measure the same length in all directions in the colour space in question, including changes in lightness. Two currently used systems are CIELUV and CIELAB. The latter system is intended for surface colours only, whereas the present study is concerned with stimuli which may be lighter than the adapting field.

CIELUV relates tristimulus values to a colour space in which lightness is represented as the vertical ordinate, and hue variation is represented on a horizontal plane, so that colour differences should correspond to the length of the vector joining two points (Hunt, 1977), see figure 1.17. The system has been developed for foveal vision, and would be expected to apply directly only to foveal stimulus detection, and even then, only for stimuli of diameter greater than 30 minutes of arc. Below this size, foveal colour vision has reduced discrimination to blue - yellow colour differences, due to the absence of blue sensitive cones in the centre of the fovea, and also to the chromatic aberration of the eye (Hunt, 1977).

Figure 1.16 shows Macadam's original ellipses plotted on the CIE 1931 chromaticity diagram, and also on the u' - v' diagram, which is effectively a projection of CIELUV space onto a plane of constant lightness. The ellipses shown are plotted so that each semi-axis represents ten JND's. The approximation to uniformity is clearly poor in the Blue

corner (and could be improved by the use of nonlinear transformations) but is good near the neutral point, and the system has the overwhelming advantage that its use is internationally agreed. The colours used in the current study are all within .02 units on this diagram of the neutral point.

The best way to predict colour appearance when the eye is adapted to light different from the reference white for which the colour space has been constructed has been the subject of much recent work. The simplest approach is the von Kries transformation, in which the tristimulus values of a colour are linearly transformed by matrix multiplication, the coefficients being calculated to transform the adapting field tristimulus values to those of the reference white.

This is only approximately adequate even for conditons of high illumination (Hunt, 1982). Nayatani, Takahama and Sobagaki (1986) propose a von Kries transformation modified by the inclusion of noise components, followed by a nonlinear (power law) transformation, a ratio stage to derive opponent signals, and further logarithmic transformation to derive the various colour percepts. This is a developement of a model by Hunt (1982) where the successive signal processing stages of the visual system are similarly modelled. He suggests that the power law (square root in his case) transformation occurs at the horizontal cells and that the bipolar cells perform a subtraction to provide opponent signals. The later interpretative stages are presumably cortical. Nayatani et al place the von Kries adaptation transformation at the earliest stage of signal processing, implying the taking of a ratio between the global level of sensitivity of the relevant class of cones and the activity of a particular cone.

Ramachandran and Gregory (1978) reported that the perception of motion ceases at isoluminance, as does stereopsis (Lu and Fender, 1972). However, Mullen and Baker (1985) came to the opposite conclusion. The Ramachandran and Gregory stimuli

were in fact alternating between two positions, and were in apparent motion, whereas Mullen and Baker used very high refresh rates and their stimuli were more akin to real, continuous motion. Cavanagh, Boeglin and Favreau (1985) found, with Ramachandran and Gregory, that segregation of a central square in an equiluminous random dot kinetogram was lost, but state that the perception of motion remained, although much weaker than when luminance contrast was present. Troscianko and Gregory (1985) studied the effect of various isoluminous stimuli on the peripheral retina. They classify visual mechanisms into short-range ones, which require exact position information and are disabled at isoluminance, and long-range mechanisms, which still function at isoluminance. Stimuli which appear and disappear remain detectable at isoluminance, and are an example of the latter class.

1.6 SACCADIC EYE MOVEMENTS

In order to investigate detection thresholds in the periphery of the visual field it is necessary to suppress the normal eye movements intended to place the image of the stimulus on the fovea. However, a normal search activity would include a saccade towards a stimulus, followed by a conscious classification of the resulting foveal image. The relevance to search of visual thresholds for the detection of peripheral stimuli depends on the assumption that the same pathways are involved, or at least that the pathways have the same latency and threshold.

Fischer and Boch (1983) found that in monkeys, there are saccades with two different ranges of latencies, and consider that the "express saccades" take place via the superior colliculus, without the signals being processed by the visual cortex. Mohler and Wurtz (1977) showed that, in the absence of the superior colliculus, saccades had longer latency and higher threshold, whereas, in the absence of the visual cortex, saccades were less accurate. The system

involving the superior colliculus is phylogenetically more primitive, and might be expected to be less important in the higher vertebrates. Fischer and Ramsperger (1984) have extended these findings to human subjects.

Studies of subjects who have suffered lesions to the optic tract and therefore cannot process visual signals in the striate cortex show that they are sometimes able to make appropriate saccades to targets within the blind part of their visual field, (e.g. Poppel, Held and Frost, 1973, Barbur, Ruddock and Waterfield, 1980). Such saccades are usually less accurate than those to a stimulus in an unimpaired part of the visual field.

The investigations of neural pathways reviewed in section 1.2 have indicated separate 'where' and 'when' pathways controlling saccades. Behavioural studies have converged on a similar model (Becker and Jurgens, 1979; Findlay, 1983). These studies postulate two parallel processes, each receiving visual input during the preparation of a saccade. The 'when' system determines the instant at which a saccade will begin and triggers whenever activated above a critical threshold level. Triggering may occur without direct visual input (voluntary saccades) or as a result of visual stimulation by the appearance or movement of a target.

Triggering of the 'when' threshold does not determine the spatial characteristics of the saccade. These must be provided by the 'where' system. For saccades triggered by a peripheral visual target, the 'where' system can be considered as a map of target locations which can be updated by new visual information. The latency of a visually generated saccade is usually quoted as about 200 ms for human beings, and the fact that the spatial characteristics of the saccade can be modified as little as 80 ms before the start of the movement provides further support for the two channel model.

The effect of this modification is frequently to produce a saccade directed to an intermediate location between two successive positions of the target. This implies some degree of temporal and/or spatial integration in the 'where' system. Another result of behavioural experiments also suggests spatial integration in the processing of visual location for saccades. Findlay (1982) calls this the 'centre of gravity' or 'global' effect. When a subject makes a saccade to a target consisting of two elements at neighbouring positions in the visual periphery, the saccade tends to land at an intermediate position rather than on either element even if the subject's conscious intention is to scan the elements sequentially (Findlay, 1982; 1983). When the relative visual properties of the target, such as its size or intensity, are varied, the saccade size varies in a systematic way (Findlay, 1982; Deubel, Wolf and Hauske, 1984). Although the subject can modify this behaviour by conscious attention (Findlay, 1985), the 'default' option normally causes saccades to land on the centre of gravity of the visual stimulus (Ottes, van Gisbergen and Eggermont, 1985).

1.7 PUPIL RESPONSE TO VISUAL STIMULATION

Whereas some saccades are under conscious control, the pupil response to a stimulus is not, and therefore provides a useful indication of how another type of threshold varies with visual field position, without involving a decision criterion of the subject.

A normal pupil undergoes continuous and irregular fluctuations in diameter, as well as systematic changes in response to sudden changes of retinal illuminance, large accommodation changes and certain psychosensory stimuli (Lowenstein and Lowenfeld, 1969). Kahneman (1973) reports that the pupil dilates during periods of thought; this would defocus the foveal image and perhaps enhance the sensitivity of the periphery. If this is the case it is an argument for

avoiding maxwellian viewing for search performance experiments, since this would defeat such an enhancement.

The latency of the pupil light reflex is 180 to 200ms, with a maximum response after about 940ms (Zinn, 1972), and its threshold may be close to the absolute visual threshold for a particularly sensitive observer (Alpern, Ohba and Birndorf, 1974). The magnitude of these responses, the behaviour of the pupil during dark adaptation, its effect on grating acuity as well as the function of pupil response in general have been thoroughly investigated in numerous studies (Crawford, 1936, Alpern and Campbell, 1962, Barlow, 1972, Woodhouse, 1975, Woodhouse and Campbell, 1975).

Harms (1956) examined the use of pupillometry as a method of investigating visual field defects. He concluded that all functional disorders of the visual field produce impaired pupil response, irrespective of the site of the lesion.

More recent investigations have shown that certain stimulus parameters can produce systematic changes of pupil size. For example, temporal modulation of a uniform stimulus field at a constant mean luminance level produces a small constriction of the pupil which depends both on the frequency and the modulation depth of the stimulus (Varju, 1964, Troelstra, 1968). Contrast reversal of a checkerboard pattern or alternation between a uniform field and a checkerboard pattern of equal mean luminance were found to cause similar pupillary responses (Ukai, 1985, Slooter and van Norren, 1980). Such observations have either been associated with non-linear processes prior to the pretectal region (Troelstra, 1968), or have been taken to represent a light reflex driven by local luminance changes (Ukai, 1985, Slooter and van Norren, 1980).

1.8 MOTION PERCEPTION IN THE VISUAL FIELD

The perception of motion appears to be a fundamental function of the visual system, present in all seeing species. Nakayama (1985) suggests that image motion processing might contribute to depth perception, time to collision, assessment of the boundaries of objects, in assessing one's own position and velocity, in driving pursuit eye movements, the detection of low spatial frequency stimuli as well as the perception of moving objects.

Lee (1980) and Lishman (1981) point out how much information can be extracted by a mathematical analysis of the optic flow field, in particular time to contact can be predicted from it, without any assumptions of scale or magnification, and this would be a valuable and basic use of the visual system.

Legge and Campbell (1981) conclude that the threshold for detecting an instantaneous displacement is dependent on the motion sense (rather than the position sense) and is of the order of 1.5 minutes of arc. In the presence of a structured visual field this falls to .3 minutes of arc.

Finlay (1982) in a concise review article, finds that, contrary to popular impression, the fovea is more specialised for motion detection than the periphery, although moving objects have a lower peripheral contrast threshold than stationary ones.

Motion of an image across the retina of course stimulates different receptors and ganglion cells as it traverses them, but the processing of visual signals into a sensation of motion is likely to be a cortical function, which may take place in visual area MT or V5, (Zeki 1974, Albright et al, 1984, Allman et.Al.,1985). In the cat Duysens, Orban and Cremieux (1984) found cells in the striate cortex which respond best to low velocities, whereas such cells were not

found earlier in the visual pathway, in the LGN.

Allman, Miezin and McGuinness (1985) found very large surround fields in the MT area of the cortex which are optimally stimulated by backgrounds moving in the opposite direction to the central receptive field, and suggest they may be involved in figure-ground discrimination and depth perception. Efferent nerve fibres from MT extend to the mid-brain, and probably contribute to the control of eye movements. There are also connections to other motion processing areas in the cortex. (Nakayama, 1985).

1.9 CONCLUSION

In this chapter the background to the various topics studied has been reviewed. Some more specifically relevant prior work is discussed in the appropriate chapters, together with some aspects of the experimental method.

EQUIPMENT AND METHODS

2.1 PSYCHOPHYSICAL METHODS.

For those experiments where probability of visual detection lobes were required, there was no alternative to presenting the required stimulus a large number of times and recording the proportion of times that it was detected. The stimuli were interleaved with those at different eccentricities to avoid adaptation or Troxler fading. Stimuli often had to be carefully selected in order that probabilities over a reasonable range of visual angles should be neither 0 nor 1.

For threshold determinations, there are three types of psychophysical method available:

the method of adjustment, in which the subject adjusts the stimulus until he judges it to be at threshold;

the method of constant stimuli, in which a series of stimuli at several fixed levels are presented, and the subject has to respond with a yes or a no to the question 'did you see this presentation?';

The two alternative forced choice method, in which the subject has to say in which of two periods of time the presentation occurred.

In the case of other psychophysical experiments there are other methods which may be appropriate, such as subthreshold summation, binocular matching, masking with a known level of noise, or the production of a visual after effect, but for this investigation, the primary requirement was to generate probability of detection curves, so a threshold method based on the method of constant stimuli was considered to be the most closely comparable to the lobe type of presentation. For this purpose three variants of staircase procedures were used.

One variant utilised a series of stimuli which differed from the preceding stimulus by a decreasing amount, the direction of change depending on the preceding response, so that at any stage it was possible to correct an erroneous response within two further steps. The steps continued to decrease until the step size was within the acceptable error. This generally required 12 to 16 steps, and allowed the determination of a set of thresholds at 6 different eccentricities within an acceptable time limit, usually about 20 minutes. In some experiments the step sizes were chosen empirically, but later an exponential function was used.

A second variant was based on the principles of Adaptive Probit Estimation, as described by Watt and Andrews (1981). This method uses a constant step size, and aims to present as many stimuli as possible on the straight line portion of the psychometric curve, but not at the 50% probability level, since this would be trying for the observer. In order to do this, a preliminary estimate of the threshold and standard deviation is necessary. The method has the added advantage that, for a relatively small amount of observers effort, an estimation could be made of standard deviation as well as of the 50% probability level. This in turn allowed the reconstruction of complete psychometric curves, from which probability of detection lobes for a variety of stimuli could be predicted. The equations used to estimate the 50% probability level and standard deviation were those of Dixon and Mood (1948). Although Finney (1964) has since urged caution in the use of this method rather than probit analysis, it is so fast that the doubtful reliability of the measure of standard deviation seems acceptable in these cases where standard deviation is not the primary parameter sought, and in any case can be estimated by other means, since each experiment was replicated a number of times.

The third variant used a constant small step size, and the 50% threshold was calculated as the average of the last 6 reversals. It was used for some motion discrimination

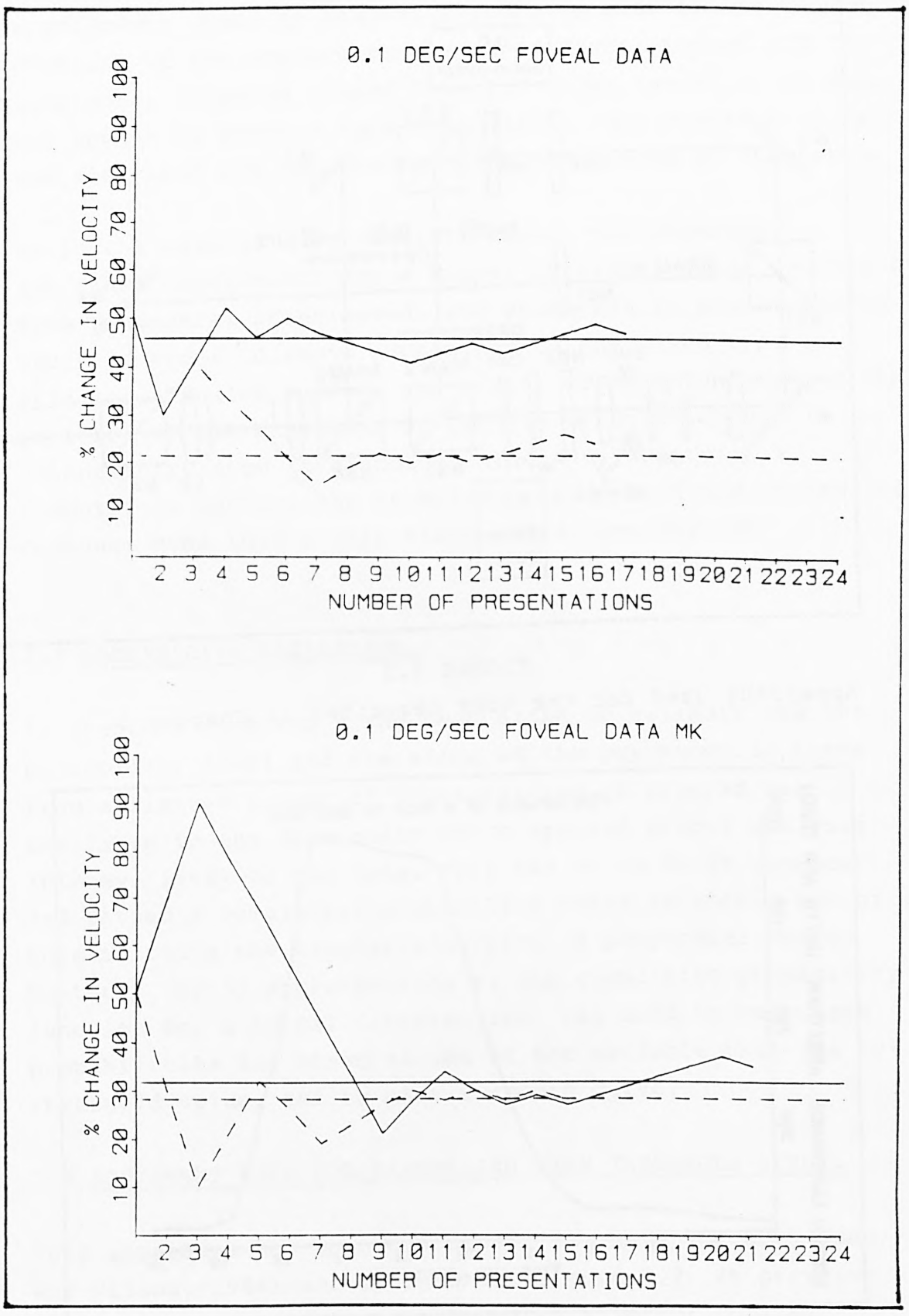

FIGURE 2.1

Examples of staircases used to determine a velocity discrimination threshold. Solid line: stimulus moving from Right to left, broken line: stimulus moving from left to right. Observer: MK. Initial velocity: 0.1°/sec. The horizontal lines represent the mean of the last 6 reversals, and are taken as the 50% threshold.

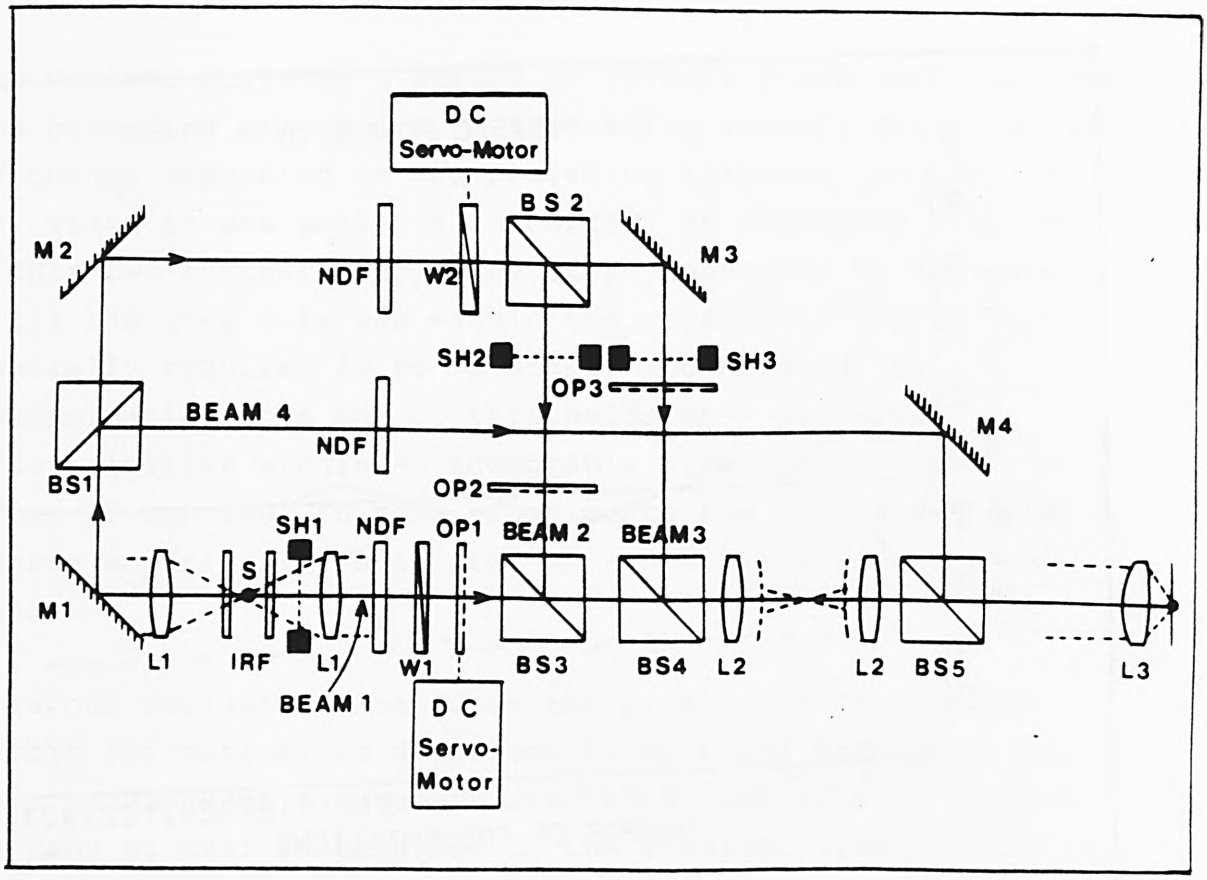

FIGURE 2.2

Apparatus used for the work described in Chapter 3.

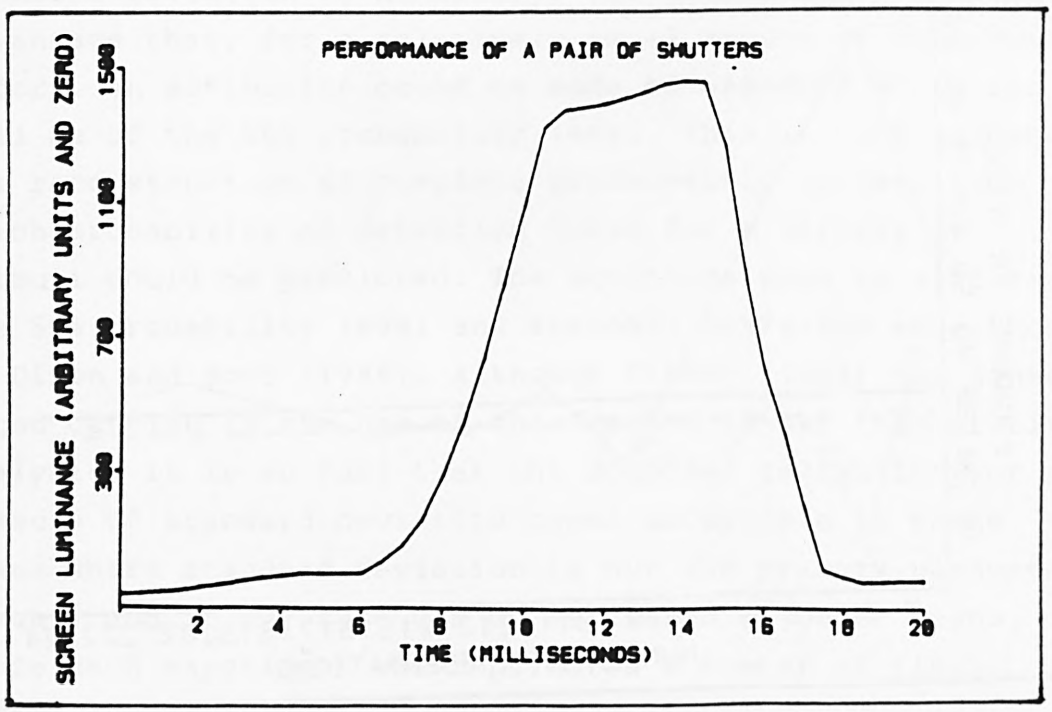

FIGURE 2.3

Plot of time versus photocurrent (obtained from the Nicolet storage oscilloscope) to examine the performance of the pair of Forth Instruments shutters installed in the Carousel projectors used in Chapter 5. The base line represents the screen luminance when one projector was in operation.

experiments when the variability of the results had caused distrust of the equipment, the experimental method and the observers. Although slower than the other variants, it did not appear to produce less variability (see figure 2.1). It was also used for the eye movement thresholds of chapter 9.

As in the case of lobe determinations, the separate staircase experiments for a number of visual field positions were in general interleaved, and presented in pseudo-random order in order to avoid adaptation to any given type of stimulus, Troxler fading, the effect of foreknowledge of the position of the stimulus, or fatigue affecting one eccentricity more than another. The availablity of a computer to control the stimulus presentation and record the response made this a very minor added complication.

2.2 PROBABILITY ESTIMATION.

In chapters 3, 6 and 9 the need arose to estimate the 50% probability level and the slope of the psychometric curve from a limited number of probabilities. A program was available in the department which applied probit analysis (Finney, 1964) to the data. This ran on an HP 85 computer and fitted a cumulative probability curve to such a set of points, using the simplex algorithm. A polynomial due to Hastings (1955) approximating to the cumulative probability function for a normal distribution, was used to calculate probabilities for other values of the variable than the 50% threshold value, and to plot a smooth curve.

2.3 EQUIPMENT USED FOR MAXWELLIAN VIEW THRESHOLD STUDY.

This apparatus has been described elsewhere (Barbur, Dunn, and Wilson, 1986) and is shown in figure 2.2. It provides a monocular, maxwellian view, based on a set of optical benches, with retinal illuminance level, target position, target velocity and stimulus duration in any of four beams all under the control of a Macsym 2 computer. In order to

immobilise his head, the subject bites on a dental impression which is fixed relative to the optical bench. The responses of the subject to a stimulus presentation are made by pressing one of two buttons, the computer storing the responses in an array appropriate to that particular stimulus.

Programs were written to measure contrast thresholds for a selected set of visual field positions at a preset target velocity, target diameter and retinal illuminance, and to measure visual lobes for the same variables. Variants of these programs were used in which the target increased in luminance from below threshold up to the required value, over a fraction of a second, so as to avoid the temporal stimulus of the sudden appearance of the target.

Calibration procedures for the maxwellian view system.

1) Visual field position and target size. First the object planes were adjusted so that the images were at the resting focus of the subject's eye for each of the three optical paths used. Next the target servo-system was adjusted so as to bring its position potentiometer to the middle of its range. The position of the target aperture was then manually adjusted so that its projected image coincided with a permanent mark on the centreline of the optical system.

   A graticule was placed at the object plane, and its projected image on a wall was measured. 10 cm at the object is represented by 203 mm on the wall. The distance from wall to artificial pupil is 1038 mm. Hence 1 mm in the object plane represents a visual field angle of 1.12^{o}.

   The apertures in a series of metal plates were measured with a travelling microscope, and their angular subtenses calculated (see table 2.1).

Plate	Aperture diameter	Angular subtense
A	.38 mm	0.5 ^{o}
B	1.04 mm	1.4 ^{o}
C	1.96 mm	2.6 ^{o}
D	3.00 mm	4.0 ^{o}
E	4.09 mm	5.5 ^{o}

TABLE 2.1
Calibration of target sizes

2) Target position potentiometer calibration. The target servomotor was driven manually to position the image of the target over each mark on the projected graticule scale, and the potentiometer reading was noted. A least squares straight line was fitted to these points, from which it was calculated that:

Potentiometer voltage = -0.0531x(Field eccentricity) + 1.67

3) Retinal illuminance calibration.
An Oriel photometer head was placed 390 mm from the pupil plane, its calibration equation being:

$$\text{Luminous intensity} = \frac{P \times 475 \times 390^2}{1.629 \times 10^{-5} \times 1000^2} \text{ candelas}$$

So the retinal illuminance is $P \times 4.435 \times 10^6$ trolands (see Westheimer, 1966). Hence the illuminance contributions of the three beams were:

	photometer units	retinal illuminance (trolands)
Target beam	0.112×10^{-6}	4.967×10^5
Background beam	0.830×10^{-7}	3.681×10^5
Fixation beam	0.308×10^{-7}	1.357×10^5

In this particular maxwellian view system the image of the light source at the pupil is smaller than the observer's pupil, so it is not necessary to measure the subject's pupil size.

4) Calibration of the neutral density wedge used to control the illuminance of the target beam.

The photometer was set up as in the previous paragraph, and the stepper motor advanced 10 steps at a time. From the tabulated readings the mean density change per step was calculated to be 0.0104.

2.4 TELESPECTRORADIOMETRY

The method employed to generate a colour stimulus made it difficult to adjust the colour of the stimulus relative to its background, so that an accurate means of measuring the colours and luminances of the projected images was required. A telespectroradiometer was assembled, based on a similar device in use elsewhere in the department, and interchangeable with it. It consists of an Applied Photo-Physics grating monochromator, combined with a high efficiency photometric telescope (model 2020-31) which has a range of acceptance angles from 3^{o} to 4 minutes of arc, and a digital radiometer (Model DR-2), both supplied by Gamma Scientific. The radiometer includes a photomultiplier and amplifier, and a shutter which automatically protects the photomultiplier when not in use. An interface was built to link this to a computer, providing an instrument amplifier for the analogue output of the radiometer, and a stepper motor drive for the grating (see appendix 2). Electrical noise due to the stepper motor drive was avoided by delaying the measurement of the radiometer output until after the stepper motor had stopped. Programs were written to take radiometric readings at 2nm intervals throughout the visible spectrum, and to multiply these by the CIE colour matching functions to provide CIE chromaticities and

luminances. The radiometer output was calibrated by reference to a standard lamp for which NPL spectral radiances were available.

2.5 APPARATUS FOR COLOUR VISUAL LOBES.

The requirement for this experiment was to present brief colour stimuli against a large uniform background, without providing a cue as to the position at which the stimulus will appear within the visual field. The stimuli in any one experimental run must appear in an unpredictable order, and the subject has to record whether or not the stimulus was detected. Each stimulus must appear enough times to build up a reliable probability of detection. It was decided to use a projection system, so that a transparency which included a coloured target could be projected in place of one which only included the background.

The basic equipment for this work consisted of a pair of matched projectors fitted with completely silent, relatively fast tachistoscope shutters. These were controlled by a drive circuit which opened one shutter and closed the other simultaneously, on receipt of a single digital signal (see appendix 2) The opening and closing time of the shutters was measured with a Pin photodiode and Nicolet storage oscilloscope, with the result shown in figure 2.3. The response time for closure of either shutter is slightly longer than the time for opening, so that there is an increase in screen luminance for about 8 milliseconds. Although the subject was aware that something had changed, this increase in field luminance was not perceptible.

PREPARATION OF TARGET SLIDES.

The slides were prepared as photographic transparencies, using a grey background (approximately Munsell value 5) on which were placed discs of coloured paper which had been selected from a pilot trial to produce transparencies in which the projected luminance of the stimulus spot approximately matched that of the background.

A method exists to provide a uniformity of illumination of a screen better than 0.1% (Marriage, 1955) using two lamps placed 1.05x(screen width) apart, and 1.18x(screen width) away from the screen. Since both the projector lens and the camera lens produce some unavoidable vignetting, it was necessary to illuminate the grey photographic background non-uniformly in order to yield an approximately uniform field on projection. To do this, the background was lit with two fluorescent colour matching lamps, placed as shown in figure 2.4. The lamps were placed 1.44x(screen width) apart, and 0.77x(screen width) away from the screen. The luminance and colour temperature achieved (in conjunction with the third projector fitted with a Cinemoid 41 blue filter) with the 36mm projection lens used to provide the illuminated field subtending 100^{o} to the observer were:

	Centre	Edge
Luminance (cd/m^2)	15.4	13.0
Colour Temperature (^{o}K)	5250	5520

It is highly desirable to use a colour temperature higher than that of a tungsten lamp since colour discrimination is better in conditions approaching daylight.

The colour patches used for preparing the slides were chosen from the Pantone series of samples, and die-cut to the smallest diameter that could adequately be reproduced on the screen, without problems of definition, flare or graininess. The film used was Kodachrome 25, which is reputed to have the highest resolution of any available colour film. Nevertheless, the reproduced stimulus subtended about 24 minutes of arc at the observer's eye, when using a 36mm projection lens. Since some data were required with a smaller stimulus, some lobes were also measured using a 55mm projection lens, which produced a smaller target size, but also a smaller field of view.

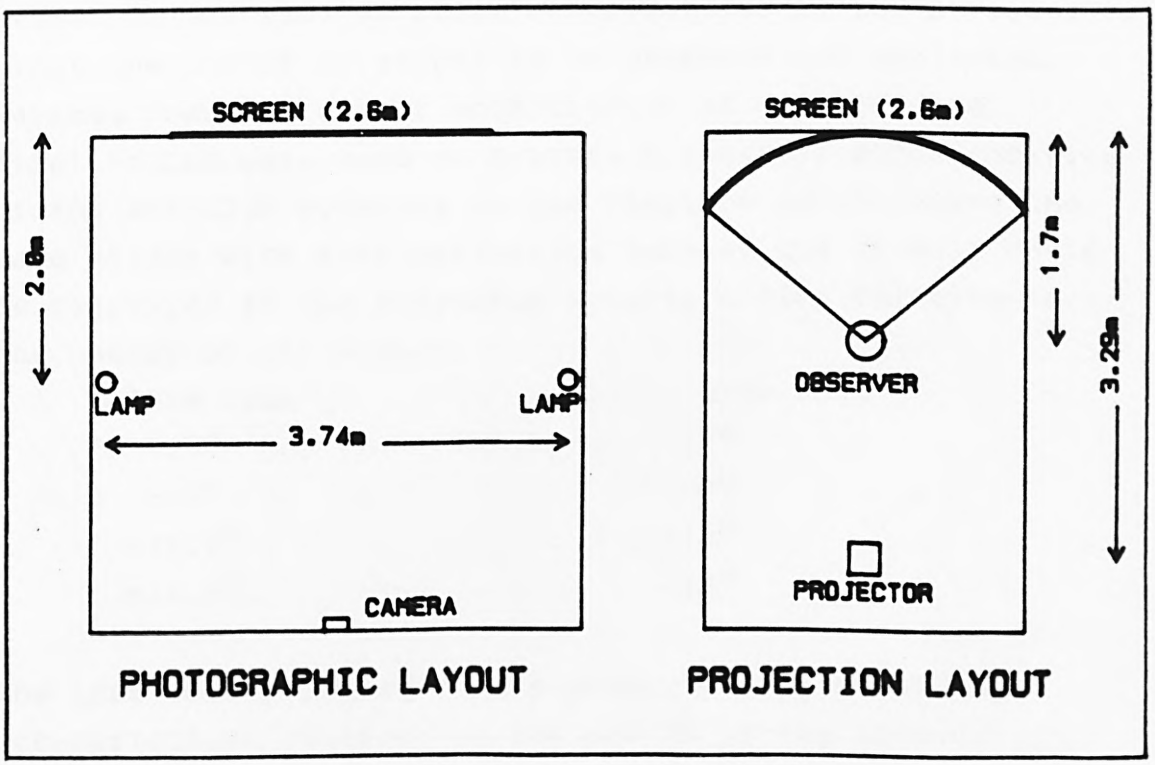

FIGURE 2.4

Diagram of the arrangement used to photograph the original art work used to produce transparencies for colour lobes.

PROJECTION CONDITIONS.

The subject was seated in a fixed seat about 1.7 m from a cylindrical screen, presenting a uniform visual field 100° wide and 40° high, as shown in figure 2.4. The observing conditions for both stimulus sizes are tabulated below.

	36mm lens	55mm lens
Screen luminance (cd/m^2)	15	40
Adapting field colour temperature (°K)	5200	4700
Field size (width x height in degrees)	100x40	56x40
Stimulus diameter (minutes of arc)	24	16
Duration of display of stimulus (seconds)	0.3	0.3

The screen luminance is that due to two projectors; one producing the background or target-and-background field, and the other providing uniform blue illumination through a Strand Electric Cinemoid No. 41 filter.

In view of the results obtained from the previous study on attention and mode of stimulus presentation, and in order to limit the number of slides to be prepared and projected, various combinations of eccentricity of stimulus and fixation LED were used to provide a range of eccentricities of the stimulus relative to the fixation point. Using the same slides with both projection lenses, the stimuli could be displayed at the following eccentricities relative to the centre of the screen:

36mm lens	55mm lens
+.5°	+2°
-.5°	-2°
+21.5°	+17°
-21.5°	-17°

The LEDs were embedded in the screen at the following eccentricities relative to the centre of the screen:

-19.5° -12.5° -2° -0.5° +0.5° +2° +12.5° +19.5°

The eccentricity for a given presentation was selected pseudo-randomly by the computer from a limited subset of the possible combinations, chosen to provide a series of visual field positions which were more closely spaced near the fovea than towards the periphery. The appropriate LED and slide were displayed using specially built interfaces described in appendix 2, and a Kodak Random Access Carousel projector, model S-RA 2000. Because of the wide range of positions in which the fixation light could appear, all intermediate LEDs were arranged to flash on briefly in turn, so that the fixation light appeared to travel across the screen, and was therefore easy to follow.

The projectors were supplied from a constant voltage transformer to avoid problems of light fluctuation due to voltage variation.

Various common slide projection problems were encountered:

Fading of the transparencies.
Since the stimuli were only projected briefly, and the shutter protected the slide from the radiation of the projector lamp most of the time, this was only a problem for the slides used for the adapting field. In order to overcome this difficulty a large number of duplicates were exposed for this purpose, and the slides changed each day. The blue Cinemoid filter was also subject to fading, and was changed every two or three days. Telespectroradiometer readings of the projected stimuli made before and after the main set of observations showed no consistent change.

Drift of focus.
The phenomenon of popping did not occur during the short time the stimuli were illuminated, but it made it difficult to set up the focus accurately, so the transparencies were mounted between glass. This introduced Newtons rings (interference fringes), which were avoided by using etched "Anti-Newton ring" glass. This in turn led to a visible etch pattern on the screen, which was not

obtrusive at the designed viewing distance, and provided a satisfactory solution to the problem.

Dust.
On trials made without glass slide mounts, this proved an insuperable problem, as any dark spots on the screen could be mistaken for the intended stimulus, or at least distract the observer when the stimulus was displayed. When the transparencies were mounted between glass, any dust settling on the outside of the mount was well out of focus, but extreme care was needed in mounting the slides. A jig was used to locate the stimulus spot correctly in the mount, silk gloves and a cotton hat were worn, an anti-static "ion gun", camel hair brush , an aerosol pack of clean air and much patience were needed to obtain clean slides. In the case of the projectors providing the adapting field and the added blue illumination, the slides and filters were kept out of focus to avoid the dust problem.

Accuracy of location of the stimulus spot on the screen.
The combination of the errors of location of the stimulus spot in the slide mount, and of the slide in the projector produced random errors of up to 0.5^{o}. Before each run each stimulus was projected at least twice, and the projector alignment adjusted. At the same time the display was examined for freedom from dust, and the adapting field was matched to the stimulus field, by visual comparison of the two alternating fields.

The projector providing the background field was supplied from a phase controlled power regulator, which allowed the lamp output to be adjusted over a sufficient range to match the background slide to the background of the stimulus slide.

2.6 EQUIPMENT AND METHODS FOR EYE MOVEMENT STUDY.

The subject was seated as described in the previous section, viewing the same screen, with the same projection equipment. His head was restrained by a padded frame and strap, and he wore a spectacle frame carrying infra-red eye movement sensors (Haines Optoelectronic Developments, Model 53). This instrument uses light emitting diodes and sensors peaking at 830 nm to detect and compare light scattered from the left and right sides of each limbus, and is tolerant of stray light. With careful adjustment it can be used to record over a range of $\pm$ 20^{o} with a resolution of 20 minutes of arc over the central 5^{o}.

Any one of 6 patterns of stimuli were projected onto the screen by the random access projector equipped with a 93mm focal length lens. This was placed 3 m from the screen, and for this experiment the matched projector was turned off, so that operation of the shutters simply presented the stimulus pattern on the screen. The series of light emitting diodes embedded in the screen were used for fixation and for calibrating the eye tracker.

The fixation LEDs, shutter and stimulus selection were again controlled by the Macsym 150 Measurement and Control System, which also stored the eye movement signals for a period of 600 ms following the appearance of the stimulus, so that eye movements during that period could be instantly displayed, and subsequently plotted and analysed. The analogue signal from the eye tracker was sampled once every millisecond, the mean of each group of 5 samples was then converted into a visual angle, and displayed and stored for later analysis.

A second projector equipped with a 36mm lens provided constant uniform background illumination of the screen. The background luminance (except where otherwise noted) was 9.5 cd/m^{2} and the stimulus luminance was a maximum of 139 cd/m^{2}. The LED subtended about two minutes of arc and had a luminance of 23 cd/m^{2}. The luminances of the test

stimuli, the background field and the fixation light were measured with a LMT Model 1000 luminance meter.

One experimental run, lasting about 20 minutes, would generally include 10 presentations of each of the stimulus patterns, in random order.

The eye movement monitor was recalibrated after about every 20 presentations. The calibration procedure required the subject to look at a series of fixation points on the screen and to indicate when steady fixation had been achieved by pressing a response button. For each fixation point the analogue signal from the eye tracker was smoothed by averaging 50 samples. A look-up table was then generated by fitting a least squares straight line to the four points within 4^{o} of fixation and straight line interpolation used to fit a line through the 6 outer points to extend the calibration curve to 21^{o} either side of the fixation point. In some of the later experiments 15 calibration points were used, and straight line interpolation used to fit a line through all of them. The raw calibration points and the interpolated curve were then displayed and examined by the experimenter before proceeding with further measurements. If the calibration curve was asymmetrical, covered an insufficient range, or was not monotonic the sensor frame would be adjusted, and the calibration procedure repeated. A more efficient method of adjustment is to use an infra-red closed circuit television system to view the beams of radiation striking the limbus, but this was not available at the time.

Each presentation was preceded by an initial test of the eye tracker signal so as to ensure appropriate steady fixation, and to check that head movement had not rendered a recalibration necessary. If a fixation error was detected this was indicated by an intermittent tone, and flashing of the fixation light.

EXPERIMENTAL ACCURACY.

The selection of time delays was under computer control with a resolution of .0165 seconds which was adequate for the purpose. The timing of the eye movement record depended on the time to actuate the shutter. Separate trials using the recording oscilloscope showed that this was repeatable to within 1 ms, at 4 ms from fully closed to fully open (see figure 2.8). It also depended on the time for the computer to acquire each analogue signal, which was 1.6 $\pm$0.1 ms, and was dependent on the clock rate of the computer.

The measurement of eye position was also influenced by changes in head position since the last calibration, and by inaccuracies in the interpolated calibration curve. The straight line interpolation was not always accurate, especially when the required curve was a pronounced sigmoid. The shape of the curve depended on the precise position of the sensors relative to the limbus (see figure 2.5). In some cases it was almost a straight line out to 20^{o}. and in others it was close to a sinusoid with maximum and minimum at about $\pm 25^{o}$. However, once the sensors had been adjusted to the face of the subject, the shape of the curve varied little from run to run. Fortunately, in most cases absolute knowledge of eye position was not so important as saccade latency and amplitude. Where absolute knowledge of eye position was required, the accuracy of calibration could usually be checked by examining the trace in question to see where the saccade eventually landed. For later runs this was systematised, and the subject was asked to press a response button when he had actually acquired the target, and the eye position at that time was used to recalculate the saccade amplitude.

The results for the author appear to show a consistent calibration error on the left (negative) side. This was because such runs were made without a separate experimenter to adjust the eye tracker, or check the calibration. The runs were done mainly in the course of developing the system, and should not be taken into account for saccade

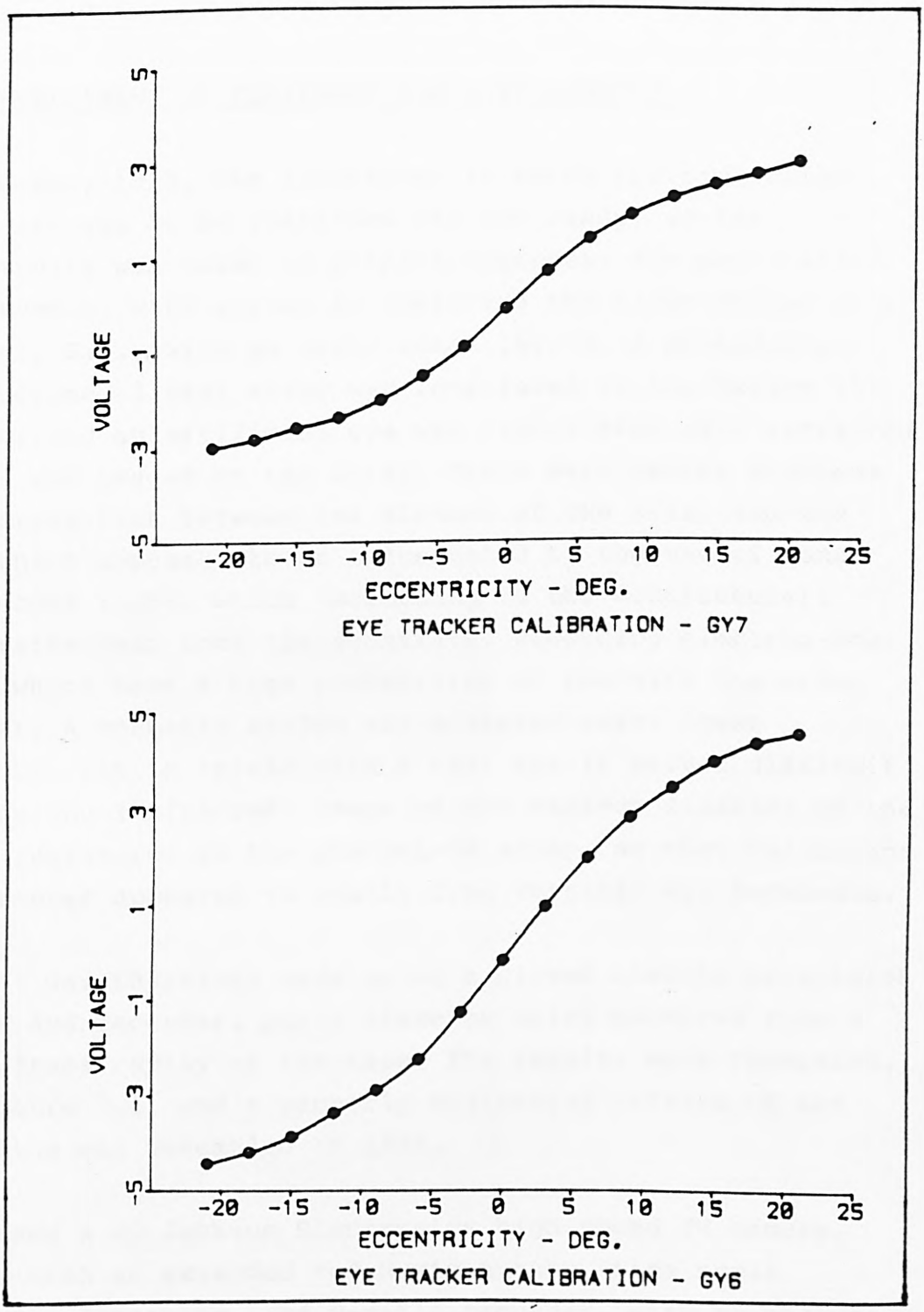

FIGURE 2.5

Examples of calibration curves obtained with the Haines eye tracker.
(The points represent analogue voltages for different fixation positions.)

amplitude distribution considerations.

2.7 DEVELOPMENT OF EQUIPMENT FOR PUPILLOMETRY.

During May, 1984, the laboratory in which the projection equipment was to be installed was not ready, so the opportunity was taken to prepare equipment for pupil size measurement, with a view to measuring the light reflex of a subject, G.Y., with an optic tract lesion. A photodiode self-scanned linear array was interfaced to the Macsym 150 system, and an artificial eye was illuminated with infra red light, and imaged on the array. There were severe problems with cross-talk between one element of the array and the next which appeared to be exacerbated by the use of long wavelength light, which (according to the manufacturer) penetrates deep into the substrate, producing electron-hole pairs which have a high probability of reaching the wrong element. A workable system was achieved using fewer elements, but in trials with a real eye it proved difficult to keep the (infra-red) image of the maximum diameter of the pupil registered on the photodiode array, so that variations in diameter appeared to result from vertical eye movements.

A trial was therefore made using a closed circuit television camera and recorder, pupil diameter being measured from a still frame replay of the tape. The results were promising, see figure 7.1, and a properly engineered version of the apparatus was assembled in 1985.

This used a JD Jackson Electronics high speed TV camera, fitted with an extended red Nuvicon tube, time scale character generator, and U-matic recorder, with an optical bench arrangement providing three stimulus fields. Measurements and stimulation could be carried out in the same eye. A Picasso pattern generator and high resolution CRT display provided the sinusoidal grating stimulus, and a specially designed eyepiece illuminated the iris/pupil boundary using infra-red emitting diodes, with peak emission

at 830 nm. These matched the sensitivity of the Nuvicon well, and required very low current to achieve a good camera signal. The tapes carrying the record of pupil response to stimuli included a frame by frame identification of time since the start of each presentation, and were analysed manually, with the aid of a pair of calipers, the arms of which were connected by a potentiometer, so that an analogue signal representing pupil diameter could be stored for each frame. The calipers were calibrated against the image of a graticule which was placed at the pupil plane before each experiment. The pupil boundary was easy to recognise by eye, but was not uniform enough for machine recognition, and further development of the illumination system was necessary to permit this (see Barbur, Thomson and Forsyth, 1987).

2.8 APPARATUS FOR MOTION THRESHOLDS.

For this work a large binocular field was required, with the ability to place a moving stimulus at any point on it. A projection system was chosen, in which two Carousel S-AV 1050 projectors illuminated a flat screen from an off-axis position, and the subject was seated on the axis of the screen, as shown in figure 2.7. The subject's chair, (and chin rest frame when used) could be moved to positions from 1 m to 3 m from the screen. The projectors and associated equipment were mounted on a movable tower which was generally placed 3 m from the screen, although it could be moved up to 2 m from the screen in order to allow higher visual field velocities. The screen illumination was not completely uniform (see table 2.2) but this was compensated for by maintaining target contrast at a fixed ratio above the contrast threshold for the speed range, displacement and visual field position at which it was presented.

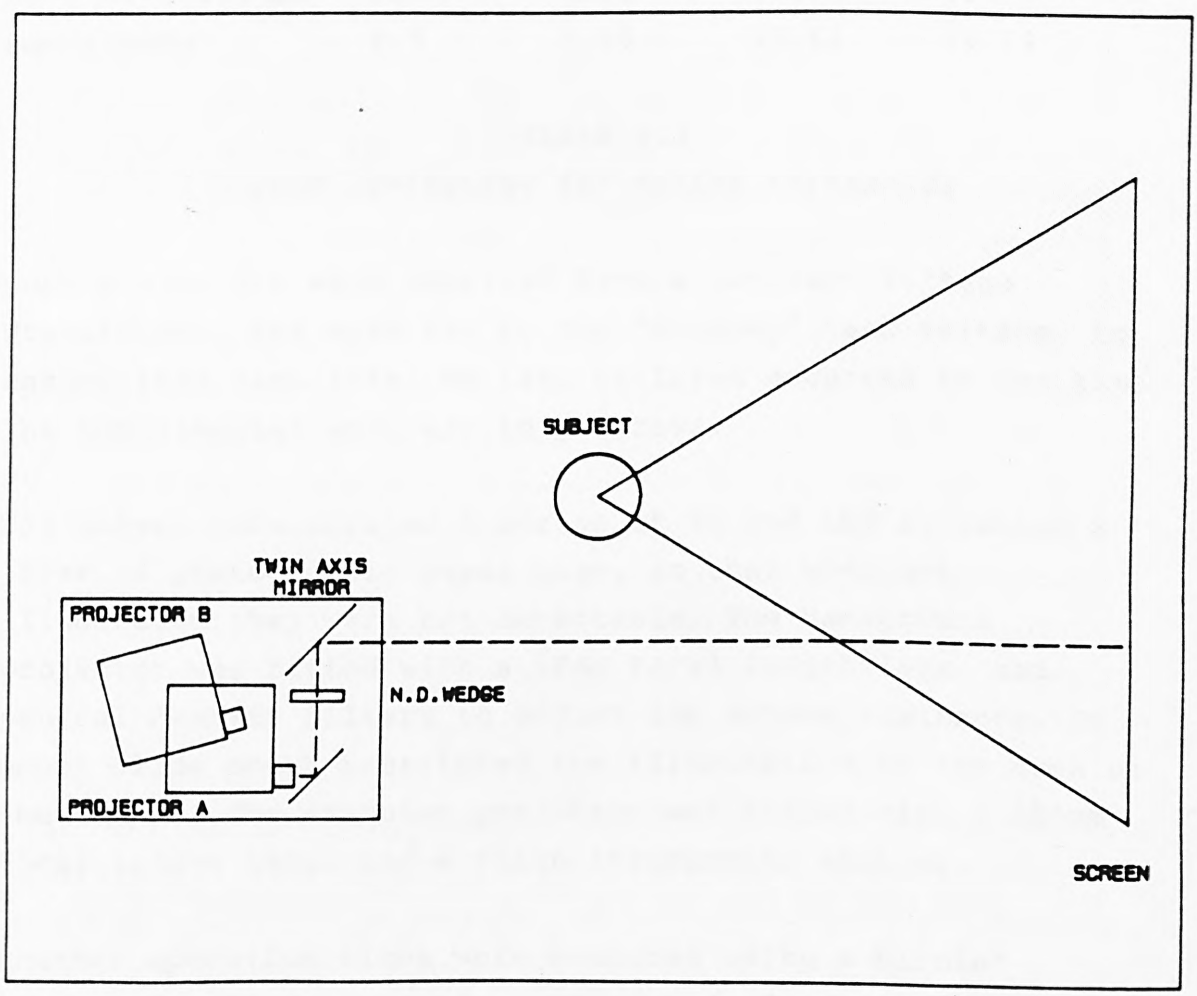

FIGURE 2.7

Layout of projectors and optical components for motion thresholds.
(Projector A provided the target image, which was steered by the twin axis mirror. Projector B provided the background illumination.)

Low spd geometry.	Screen-mirror=1.8 m.		Observer-screen=3.25m		
Eccentricity	-15	-10	0	5	10
Target+0.8 Density	2.1	3.6	9.1	12.5	14.1
background	9.9	15.1	21.3	23.6	28.8

	Screen-mirror=1.8 m.		Observer-screen=2 m	
Eccentricity	-30	-25	-10	0
Spot diameter	15mm	14mm	12mm	12mm
Spot with 0.8 ND	.8	1.9	10.7	6.1
Background	8.4	11.8	19.8	23.4

High spd geometry.	Screen-mirror=3 m.		Observer-screen=1 m	
Eccentricity	-20.7	-10.7	9.3	19.3
Spot diameter	9mm	8mm	8mm	8mm
Spot with 0.8 ND	3.8	4.35	5.2	5.7
Background	9.5	9.88	10.61	11.09

TABLE 2.2
Screen luminances for motion thresholds

Both projectors were supplied from a constant Voltage Transformer, and were set to the "Economy" lamp voltage, to ensure long lamp life. No lamp failures occurred in the time the experimental work was in progress.

The screen incorporated a series of 96 red LED's, behind a layer of photographic paper base, so that when not illuminated they were not detectable. The background projector was fitted with a 36mm focal length lens, and neutral density filters to adjust the screen luminance. An empty slide mount restricted the illumination to the area of the screen. The stimulus projector was fitted with a 180mm focal length lens, and a Forth Instruments shutter.

Shutter operation times were measured using a Nicolet Storage oscilloscope, and a pin photodiode, the output of which was amplified by a battery driven operational amplifier. For some experiments the 7ms minimum exposure time that this shutter provided was too long, and an

additional shutter (made from a small loudspeaker) was fitted in the object plane. This had a small but just adequate amplitude, and a minimum exposure time of 2ms. Figure 2.8 illustrates the time course of stimulus luminance with each shutter at its minimum exposure time. The effective time for the Forth Instruments shutter to open was less than for an identical shutter described in section 2.5, since in the present case only the central portion of the projector field was used. The fast shutter was not silent, but for this particular purpose this was immaterial. The shutter blade was cemented to the loudspeaker cone and had a travel of about 1mm. It was necessary to control this with a pulsed power supply to avoid bounce.

A linear neutral density wedge driven by a stepper motor was placed close to the projection lens, with a similar wedge arranged with the gradient at 180^{o} to ensure uniform illumination across the field. For these particular experiments this was probably unecessary, but was retained to ensure the equipment was of general value for later work.

A Twin Axis Mirror drive, supplied by McLennan Servo Supplies, was placed immediately after the wedge. The mirror was driven by two servomotors, and its position sensed by two potentiometers. A tachogenerator was coupled to each motor, and the motors were driven by McLennan PM121-T servo-amplifiers acting in a velocity control mode. An interface to the computer was provided (see appendix 2) to ensure that the mirror could never be forced against its limit positions.

A Macsym 150 Measurement and Control Computer was connected to the position potentiometers, servo drives, stepper drive, shutter drives and LED drive unit, providing control of the stimulus position, velocity, luminance, duration and of the fixation point position.

A library of subroutines was written to control stimulus speed and position in terms of the subject's visual field

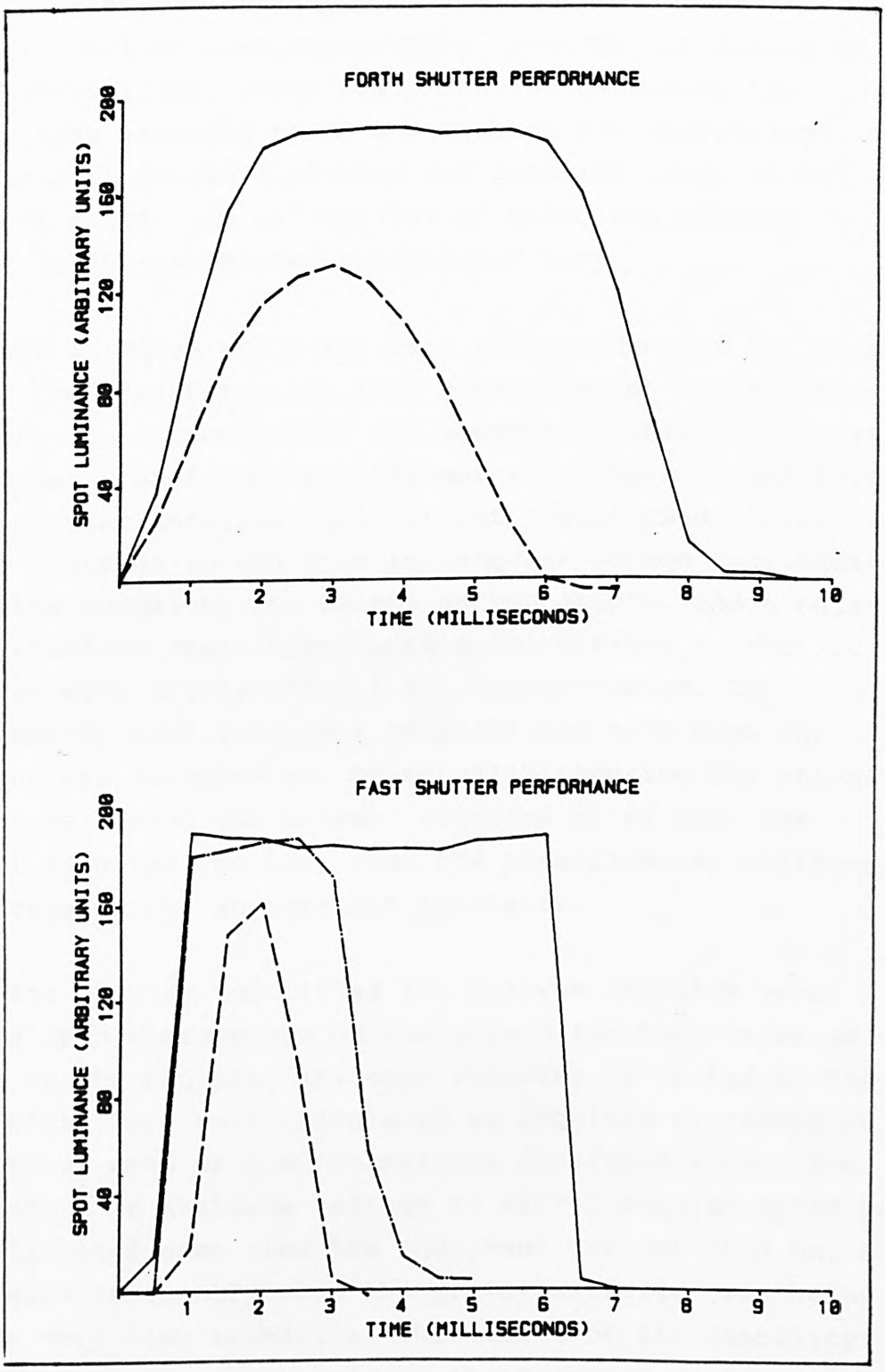

FIGURE 2.8

Plots of the time versus photocurrent trace obtained from the Nicolet storage oscilloscope to examine the performance of the Forth Instruments shutters installed in the Carousel projectors used in Chapters,6 and 8, and the fast-acting shutter used in Chapter 8. Key to nominal shutter open times: Forth shutter; 7ms (solid line), 6ms (broken line). Fast shutter; 6ms (solid line), 2ms (chain dot line), 1.5ms (broken line).

coordinates, to provide calibration routines for wedge position vs screen luminance, stimulus position and velocity, shutter opening duration, and various checks of these calibrations. (Routines and drive circuitry had already been provided by Dr W.D.Thomson for controlling the LED display.) Screen luminance was measured using an LMT luminance meter, the calibration of which was checked against an NPL-calibrated substandard lamp.

Since the stimulus projector beam was incident on the mirror at 45^{o}, the transformation from potentiometer voltage to observers field coordinates was somewhat involved; one set of routines transformed potentiometer voltages to and from mirror angular position, another set transformed mirror angular position to and from rectangular screen coordinates, taking the normal to the mirror as the origin, and a third set of routines transformed screen coordinates to and from the observer's angular visual field coordinates. The potentiometer equations were recalibrated each time the equipment was switched on, by manually steering the stimulus to three points on the screen indicated by an LED. The computer selected the LED, read the potentiometer voltages, and calculated the appropriate constants.

The mirror angular velocities for a given stimulus speed depended upon whereabouts on the screen the spot happened to be, and so the required analogue voltages to be fed to the servo-controllers were calculated as required by reference to the three sets of transformations described above. The relationship of analogue voltage to mirror angular speed was also calibrated each time the equipment was switched on, and indeed more frequently when the drive controller was being used for very slow speeds, at the limits of its stability. This was carried out entirely by the computer, a least squares straight line being fitted to 20 points relating analogue voltage to mirror speed. Figure 2.6 shows examples.

EXPERIMENTAL ACCURACY

In order to investigate the speed stability, tests were

made, using the subroutines employed for the experiments, in which the spot was swept across the entire width of the screen. The speeds were stable and accurate even when some oscillation of the servo system was occurring. This test was used to adjust the servo feedback for the slowest speed range.

The Macsym timer function depends on mains frequency, and was not sufficiently reliable or precise for some of the short times required, so an empty loop routine was provided for times shorter than 3 seconds. This was also used for shutter control, and was calibrated using the Nicolet Storage Oscilloscope.

The Macsym programming language is a compiled Basic, so these multiple transformations did not unduly delay the progress of the experiment.

Some imprecision was however introduced by noise in the potentiometer system, which required some averaging to be carried out in order to get a stable signal. By the time sufficient samples had been collected the mirror had moved significantly, and could have passed the required position. Required and actual position were monitored, and were generally within 30 minutes of arc.

A further source of imprecision at higher speeds was due to the time required to accelerate the mirror to full speed, but this was compensated by adding an empirical constant to the equation predicting stimulus position at the time the shutter was to open.

Most of the transformations and calibrations are straightforward, but the transformation from mirror angular position to screen rectangular coordinates requires a little explanation.

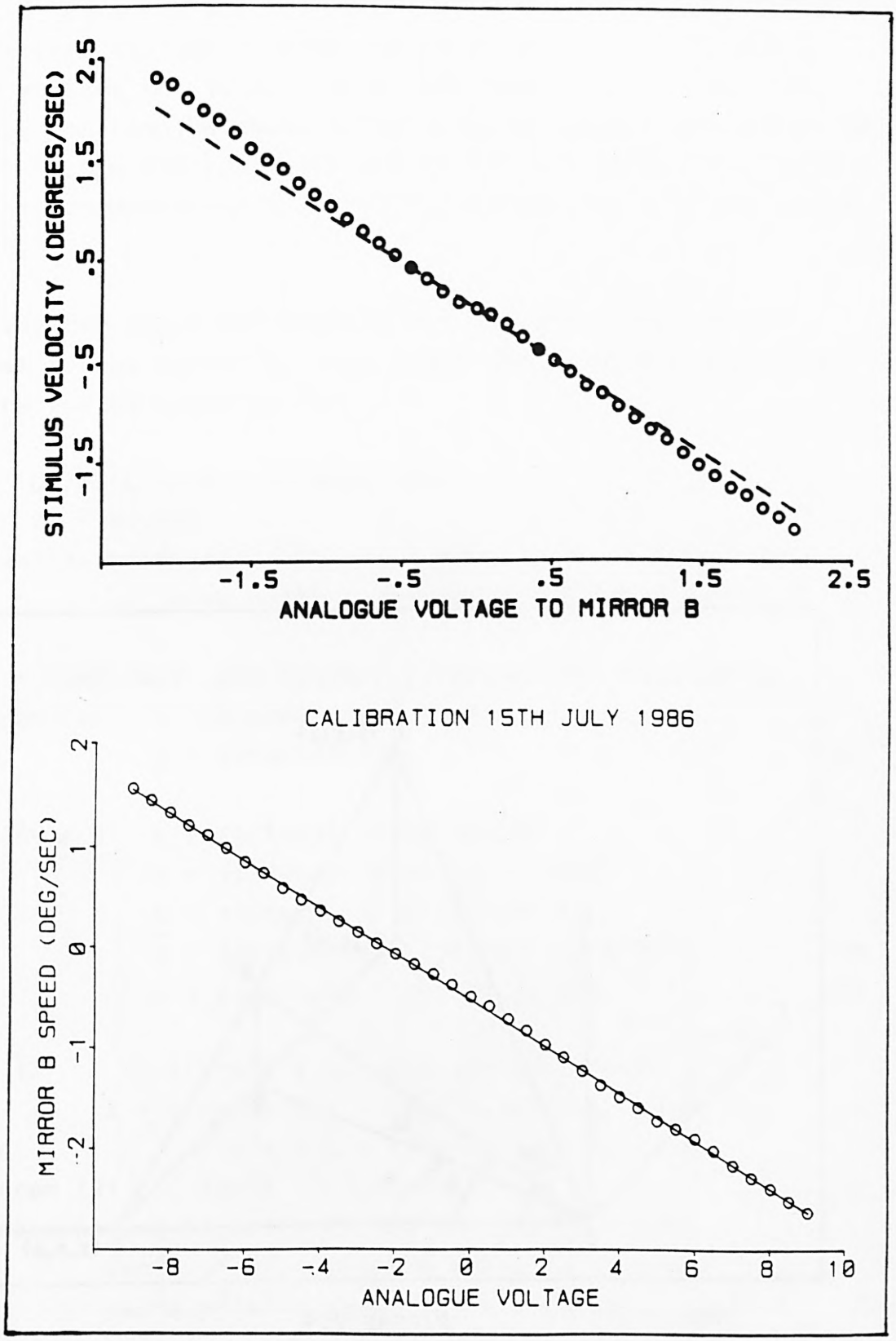

FIGURE 2.6

Examples of voltage vs angular velocity calibration curves (for the Two-axis mirror drive used in Chapter 8. The first one was unsatisfactory, and required some adjustment of the servo-controller.)

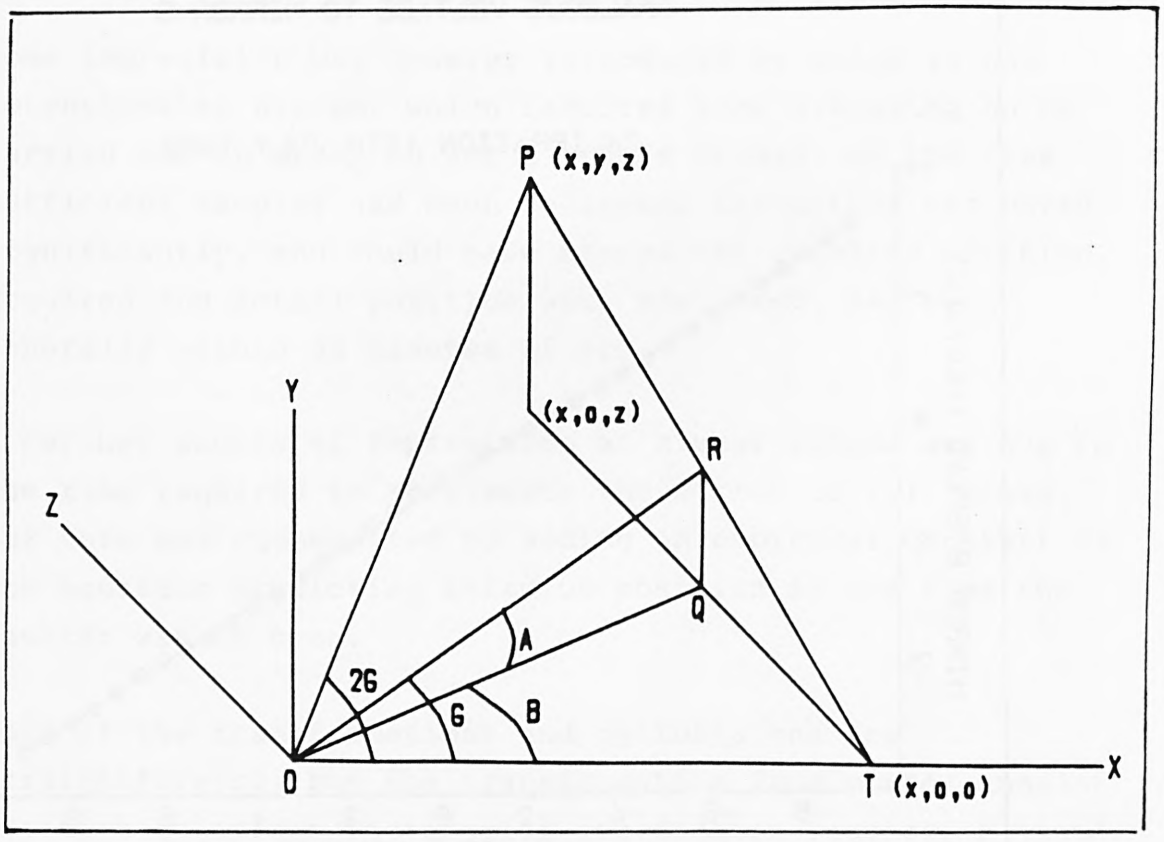

FIGURE 2.9

Diagram to develop the geometrical transformation to convert from mirror angular position to position of the stimulus on the screen.
(The projector beam is incident along XO, the mirror is at O with normal along OR, and the reflected beam is OP. A and B represent the position of the mirror about its two axes of rotation.)

In figure 2.9 OXYZ is a system of rectangular coordinates with O being the point on the mirror where the stimulus beam XO strikes it, and P being the point where the reflected beam strikes the screen, with coordinates x,y,z. Let the mirror position be characterised by the angles its normal OR makes to the Y=0 plane (A) and to the Z=0 plane (B). Point Q is the projection of R on the Y=0 plane, and T is the point x,0,0.

Calling the angle XOR between the incident beam and the normal to the mirror G, then angle XOP between the incident and reflected beams is 2G.

Then $QR = OQ.\tan A = x.\tan A/\cos B$

and $TQ = x.\tan B$

by similar triangles $z/TQ = y/QR = \tan 2G/\tan G$

so $z/(x.\tan B) = y/(x.\tan A/\cos B) = \tan 2G/\tan G$ (1)

$\cos G = \cos A.\cos B$ and $\tan 2G = 2.\cos G.\sin G/(\cos^2 G-\sin^2 G)$

so from (1) $y = z.\tan A/(\tan B.\cos B)$

or $y = z.\tan A/\sin B$ (2)

Also from (1) $x = (z/\tan B).(\tan G/\tan 2G)$

or $x = (z/\tan B).(2\cos^2 G-1)/2\cos^2 G$

or $x = (z/\tan B).(1-1/(2.\cos^2 G))$

so $x = (z/\tan B).(1-1/(2.\cos^2 A.\cos^2 B))$ (3)

or $x = z.(1/\tan B-1/(\cos^2 B.\sin 2B)$ (4)

From (3) $1/\cos^2 A = 2.\cos^2 B.(1-(x/z).\tan B)$

so $1 + 1/\cos^2 A = 1 + 2\cos^2 B.(1-(x/y).\tan B)$

hence $\tan^2 A = 1 + 2\cos^2 B.(1-(x/y).\tan B)$

but from (2) $\tan^2 A = y^2.\sin^2 B/z^2$

so, eliminating A, and dividing through by $\cos^2 B$

$\tan^2 B.y^2/z^2 = 1/\cos^2 B + 2(1-(x/y).\tan B)$

or $\tan^2 B.y^2/z^2 = \tan^2 B - 1 + 2(1-(x/y).\tan B)$

or $(y^2+z^2).\tan^2 B + 2xz.\tan B - z^2 = 0$

hence $\tan B = (z/(z^2 + y^2).\{ +/- /(x^2+y^2+z^2)- x\}$ (5)

and from (5) and (2) $\tan A = y.\sin B/z$ (6)

Equations (2),(4),(5) and (6) form the basis of the transformation of coordinates routines, except that x and y above take the normal from the screen to the mirror as the origin, rather than the centre of the screen, and B is zero when the mirror is normal to the incident beam, rather than at 45° to it. The only inverse trigonometric function available on the Macsym is arctan.

2.9 EQUIPMENT USED FOR COMPARING PSYCHOPHYSICAL AND SACCADIC CONTRAST THRESHOLDS.

In order to make a valid comparison of two types of contrast threshold, that for a psychophysical staircase method with the threshold at which accurate saccades could be made, use was made of the automatic pupillometry equipment, the development of which followed from the work described in chapter 7. This is fully described in Barbur, Thomson and Forsyth (1987).

2.10 DETAILS OF OBSERVER'S VISION.

All observers had healthy eyes and visual acuity (corrected) of 6/6 or better. For maxwellian view experiments the optical system was adjusted to each observer, and for viewing projection presentations the observers wore their normal correction, except that as noted PMF wore +1D to adjust his resting accommodation to view the projection screen. The observers used in colour observations had normal colour vision as tested by the 100 hue test.

Name	age	sex	Name	age	sex	right eye	left eye
emmetropes			presbyopes			(correction required)	
JLB	33	m	PAF	51	f	add +2.00DS	add +2.00DS
PSB	18	m	PMF	56	m	add +2.00DS	add +2.00DS
PCD	27	m	myopes				
RMF	22	m	HDP	24	m	-4.50/-0.75x180	-2.75/-1.25x180
			WDT	27	m	-1.25/-0.75x170	-1.25/-0.75x170
			hyperope				
			GY	32	m	+1.25DS	plano

THE EFFECT OF TARGET CONTRAST, SIZE AND VELOCITY ON PROBABILITY OF DETECTION AT VARIOUS ECCENTRICITIES.

Summary.

Contrast thresholds and visual lobes were measured for a range of conditions. These included target diameters from .033° to 5.5°, glimpse durations from 0.1secs to 1 second, background retinal illuminances of 4.17 and 2.57 log trolands, and target positions from -20° to +20°.

Contrast threshold curves appear to belong to a family - varying in a consistent way with stimulus size and velocity.

Apart from divergencies of lobe shape which may be artefacts, the lobes measured also look as if they belong to a common family, getting broader as contrast target velocity or diameter increases.

Visual lobes could be predicted from the corresponding threshold plots, using a generalised frequency of seeing curve.

3.1 INTRODUCTION.

To investigate all the variables mentioned in section 1.1 over a sufficient range of field size required the construction of a purpose-built set-up. Whilst this was being designed and constructed, time was made available on an existing experimental equipment for visual studies, described briefly in section 2.3. It was scheduled for use for this study for a period of about 5 weeks, (later extended to two months), and because of the time restriction the variables studied have been restricted to those shown below. It is the results with this equipment which form the subject of this chapter.

Summaries of the observational results are tabulated in Appendix 1, and are shown graphically in figures 3.7 to 3.26, at the end of the chapter.

3.2 VARIABLES STUDIED.

a) Target sizes of $.033^{o}$, $.133^{o}$, $.5^{o}$ and 1.4^{o}; larger target diameters were examined in a pilot experiment (see figures 3.7 and 3.8), but these gave misleading results. If the target covers an angle which is large compared to the size of the illuminated background, or if it is close to the boundary of the illuminated background field, the effective contrast cannot be calculated as:

$$\frac{\text{(Luminance target - luminance of background)}}{\text{Luminance of background}}$$

since the adapting field is some combination of the dark field surrounding the 46^{o} background field, the background field, and the target itself, the exact value depending on the eccentricity of the target. Furthermore in the case of moving targets, presentations where the edge of the target crosses the fixation point are more easily seen than those where the target envelopes the fixation point throughout the glimpse. The plots in figure 3.8 showing thresholds for the two largest moving targets subtending 4^{o} and 5.5^{o}, show a distinct double hump resulting from a higher threshold when the target is at the fixation point. The two smallest target sizes were introduced after the preliminary findings had been reviewed, and were the subject of more limited tests.

b) A glimpse length of .33 seconds; this is a commonly used glimpse length, since it corresponds to about the normal interval between saccades (e.g. Megaw and Bellamy, (1979)), and avoids inconsistencies in fixation behaviour during stimulus presentation. A range of glimpse lengths from 0.1 second to 1 second were briefly examined during preliminary tests (see figure 3.9), and showed little variation in thresholds.

c) The adapting field was a uniform circular background of 48^{o} total subtense, with target presentations limited to $\pm 20^{o}$ from the fixation point, along the horizontal meridian. On the temporal side of the field the blind spot affected presentations of moving targets between about 14^{o} and 19^{o}, and no stimuli were presented in this region.

d) Two levels of background illuminance; these fell broadly in the photopic region at 14800 trolands and 370 trolands.

e) Three velocities of target movement, 0^{o}/sec, 1^{o}/sec and 3^{o}/sec; some trials were made at 2^{o}/sec (see figure 3.10) but these were not significantly different from those at 1^{o}/sec. Since at 3^{o}/sec a 1.4^{o} disc spans an angle of 2.4^{o} in the .33sec glimpse time, higher speeds would be difficult to relate to a specific position on the visual field.

f) The stimuli consisted of uniformly illuminated circular targets.

g) No variations of chromaticity were introduced into this first experiment. Partly this was due to the time limitation, and partly because the optical arrangement made it impossible to introduce chromaticity changes without at the same time introducing luminance changes relative to the background, since the target and background beams are superimposed additively, through a beamsplitter cube.

h) 3 observers have been used; the author (PMF) was the primary subject, with the other observers repeating some of the essential visual lobes.

Thus the main study concerns two target sizes, 3 velocities, two background luminances, and at least 11 positions in the

visual field. For each of these 132 sets of conditions a minimum of 20 presentations was needed to establish a stable figure for a probability of detection, and 8 to 16 for a contrast threshold.

3.3 EXPERIMENTAL PROCEDURE.

After some trial runs, the procedure adopted was as follows: The target size and background illuminance would be selected and a run made with stationary presentations of the target in order to produce a table of thresholds (i.e. levels of target illuminance which, when superimposed on the background illuminance, produced a 50% probability of detection). A series of lobe determinations was next made with a range of contrast levels, and a contrast selected (still with the target stationary) such that the target was always detected when presented at the fixation point, but not always detected when presented 1.5^{o} away from the fixation point on either side. This contrast was maintained for further lobe determinations to be made at target velocities of 1^{o}/sec and 3^{o}/sec. The contrasts selected are shown in table 3.1.

Since the equipment and some of the observers were only available for a limited time, threshold determinations were made for the moving targets as well, since the thresholds carried more information than the lobes, and the data obtained might be useful later in the project.

Each run, whether it was to determine a visual lobe or a threshold plot, consisted essentially of a separate series of stimulus presentations for each eccentricity, the presentations of differing eccentricity being interleaved in random order so that the observer could not predict where the next stimulus would appear. For some early trials he was also unaware of exactly when the stimulus would appear (within the interval between 1 and 4 seconds after a warning sound), but this temporal variation was abandoned as it led to unreliable results due to unavoidable blinks and saccades.

After each stimulus presentation, the observer was required to indicate whether he had detected it by pressing a "yes" or a "no" response button. The option of being unsure was not permitted.

In the case of a lobe determination each stimulus was of the same contrast, selected as described above, and presented 10 times in each run. Such a run was always made at least twice, often on different days.

In the case of a threshold determination a staircase method was used, of the first type described in section 2.1. At the final step a "Yes" response would cause a decrease in target illuminance of about .03 log trolands, and a "No" response would cause an increase of the same amount.

After 10 or so runs in one day, the author's consistency and repeatability declined, and he became prone to false positive responses. (Volunteer observers usually found it difficult to continue with these observations.) Because of this and computer availability, a day's observations were usually confined to mornings only, and to not more than about 1200 responses. The repeatability is illustrated in figure 3.1. The repeatability of the lobes from a single run is not as good as that of the thresholds since a probability of 0.1 is the result of just one positive response. Probabilities of 0 or 1 appear with no error bar since these represent conditions where the stimulus was never seen or always seen, but do not indicate a high degree of precision since any sufficiently small or large stimulus would give these results.

3.4 THRESHOLD RESULTS.

The results are summarised graphically in figures 3.7 to 3.14 at the end of the chapter, and are tabulated in appendix 1. The thresholds were measured using the method described above at the same conditions as those used for

visual lobe determination. Comparisons were made using a series of target sizes up to 5.5° subtense, also using a grating target with a periodicity of 5 cycles/degree, and using a series of glimpse lengths from .1 to 1 second. The larger target sizes showed less variation with eccentricity, since the targets spanned two or more nominal sampling positions, and the smallest targets show a very large increase in threshold contrast in the periphery. Glimpse length, in the range studied, makes little difference to the position or shape of the threshold curve.

Figure 3.1 indicates the variability of both the threshold and the visual lobe data. The error bars represent the standard deviation of the measurements, not the standard error.

Target diam. degrees	Background retinal illum. log trolands	Added retinal illum at target log trolands	contrast %	Foveal thresh'd contrast
1.4	4.17	2.97	6.3	3.4
1.4	2.57	1.37	6.3	5.7
0.5	4.17	3.15	9.5	7.2
0.5	2.57	1.57	10.0	6.8
0.133	4.17	{	}	6.5
0.133	2.57	{ lobes not	}	12.3
0.033	4.17	{ measured	}	56.4
0.033	2.57	{	}	105.2

TABLE 3.1

Conditions used for the main series of experiments. (For each condition, 11 eccentricities and 3 speeds were presented)

Full psychometric curves were then measured for a few conditions, by presenting the target 20 or so times at one eccentricity, and 10 different contrast levels (See figure 3.2). These support the claim made by Blackwell (1946) that

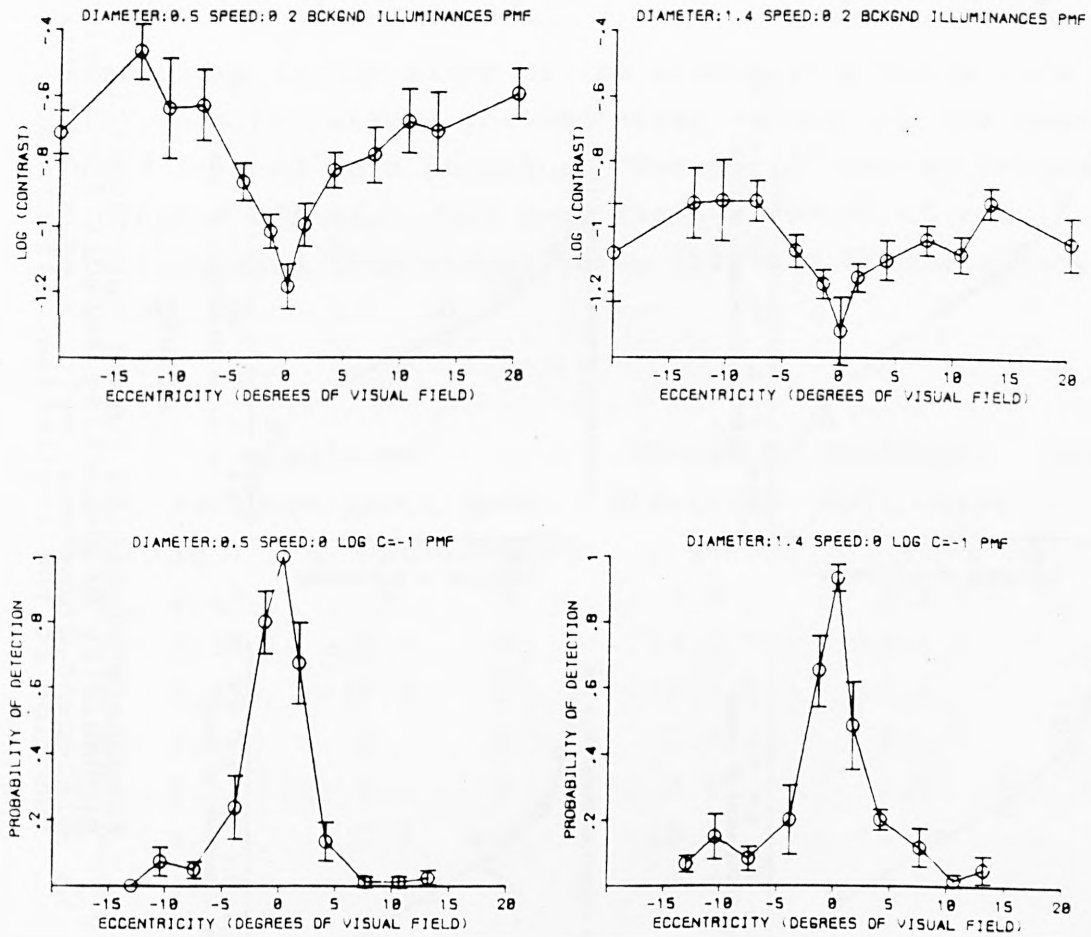

FIGURE 3.1

An indication of the repeatability of individual measurements for stationary targets of diameters 0.5^{o} (left) and 1.4^{o} (right). Top row: contrast thresholds, lower row: visual lobes. The error bars indicate the standard deviation of 6 to 9 experimental runs.

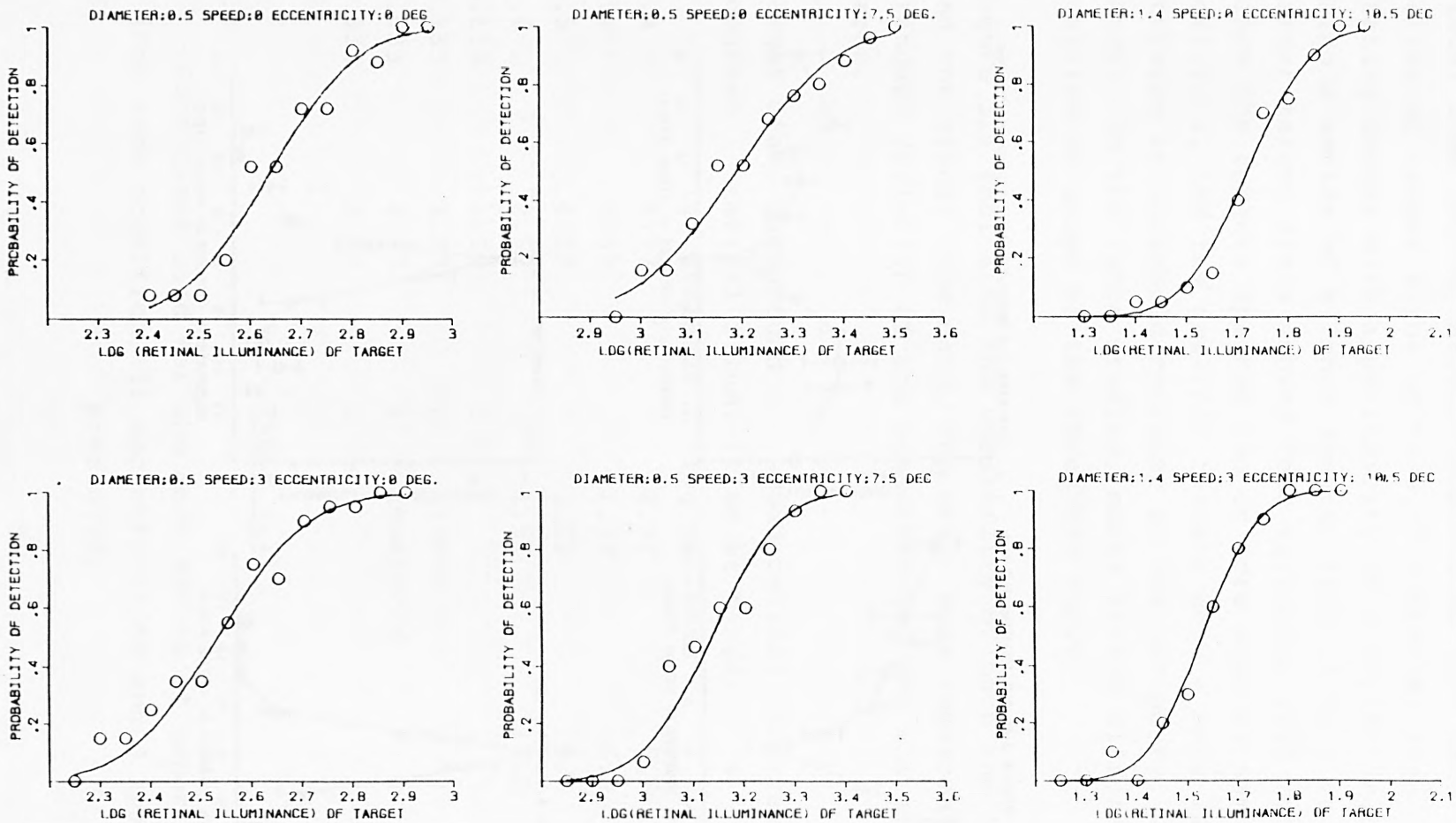

FIGURE 3.2

Frequency-of-seeing curves (psychometric curves). For the probability of detecting stimuli for a selection of different diameters, velocities and eccentricities, as a function of the log(retinal illuminance) of the target.

the shape of the curve varies little with the conditions, over the range examined. A complete set of such curves, together with the appropriate threshold curve, could be used to predict visual lobes for a range of contrasts. Making the assumption that the psychometric curve has a constant slope, corresponding to a standard deviation of 0.14, visual lobes were calculated from some of the threshold curves measured, and compared with those obtained directly (See figures 3.15 and 3.16). In practice, variations in standard deviation over the range encountered made little difference to the shape of the predicted lobes. See for example figure 3.17.

Variations in the slope of the probability curve (see Table 3.2) seem to reflect the certainty with which the observer could respond to a stimulus. Thus a 1.4° moving target, presented off axis, was more easily identified and distinguished from visual noise than a 0.5° stationary target.

conditions				Threshold contrasts		Std. Dev
Diam.	Backgrnd	Ecc.	Speed	Staircase	full curve	
deg.	lg T	deg.	deg/sec	%	%	
1.4	4.17	0	0	3.7	2.1	.18
1.4	2.57	-10.5	0	14.3	14.1	.10
1.4	2.57	-10.5	3	10.7	11.4	.09
0.5	4.17	0	0	7.0	2.9	.14
0.5	4.17	0	3	3.8	2.3	.14
0.5	4.17	7.5	0	12.6	10.3	.16
0.5	4.17	7.5	3	9.4	9.1	.11

TABLE 3.2

Comparison of threshold contrasts found from the frequency of seeing curve for a target of known eccentricity, with those from the exponential staircase method for a randomly positioned target.

It is interesting to compare these results with those of other investigations. The contrast threshold for the detection of a foveal 0.5^{o} target under the conditions of this experiment was 2.9%. This is intermediate between that reported by Harvey and Poppel (1972) who used a $.17^{o}$ stimulus diameter and whose curves show an optimum contrast of 10%, and of Watson, Barlow and Robson (1983), who used a patch of sinusoidal grating of $.43^{o}$ diameter, drifting at about $.6^{o}$/sec., and whose lowest contrast threshold was 1.44%. Blackwell (1946) reported 3.3% threshold contrast for a target diameter of 0.3^{o}. In chapter 5 some slightly lower contrast thresholds are reported. In a preliminary experiment a patch of high contrast grating subtending 2^{o} was substituted for the uniform disc stimulus, and for this target the threshold contrast dropped to 2.4%.

Blackwell (1946) presents an average probability curve for a large number of contrast threshold measurements which corresponds to a standard deviation of 0.48. He fitted his curve on a linear scale of contrast, whereas the curves of figure 3.2 plot log (contrast) against probability. Since very few points are available at low probabilities the difference is not important. Figure 3.3 shows Blackwells curve and a set of points representing a log (contrast) curve of standard deviation 0. 17. This is within the range values shown in table 3.2.

Inspection of figures 3.7 to 3.14 suggests that there is no consistent difference between corresponding contrast thresholds in the two hemifields or, with the exception of targets of diameter 0.133^{o} or smaller, at the two levels of background retinal illuminance used in this experiment. The results can therefore be summarised by taking the mean of all measurements made at a given eccentricity, target size and velocity, regardless of hemifield or retinal illuminance level (see table 3.3 and figures 3.4 and 3.5). These figures demonstrate the change in threshold function with changes in velocity and target size. The lower threshold indicated in this figure for extreme

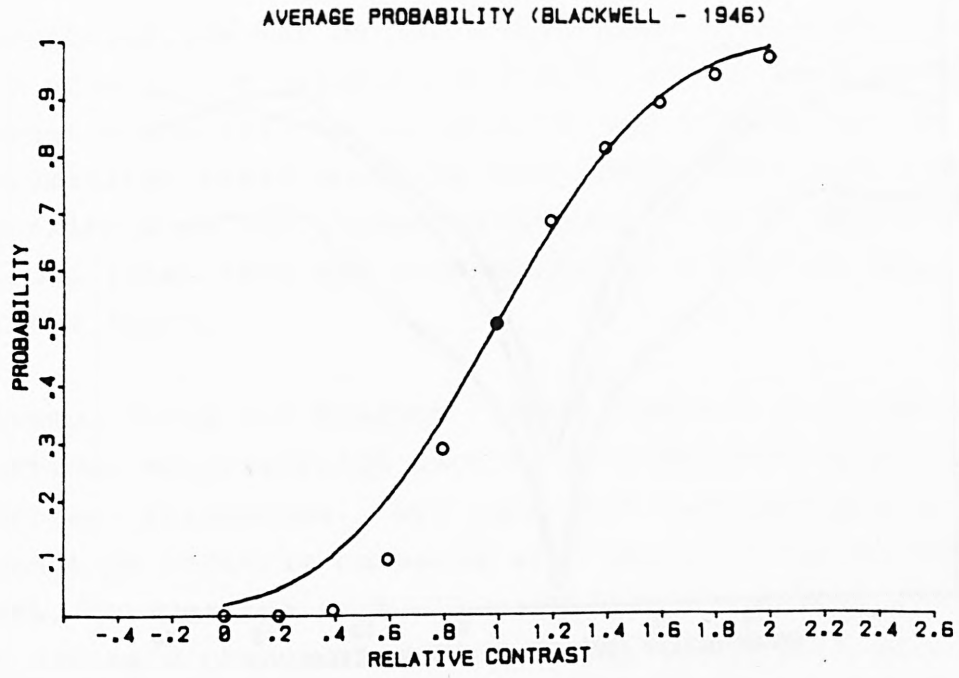

FIGURE 3.3

Average probability curve (Blackwell, 1946) sigma=0.46. The points represent a curve of the type shown in figure 3.2, sigma=0.17.

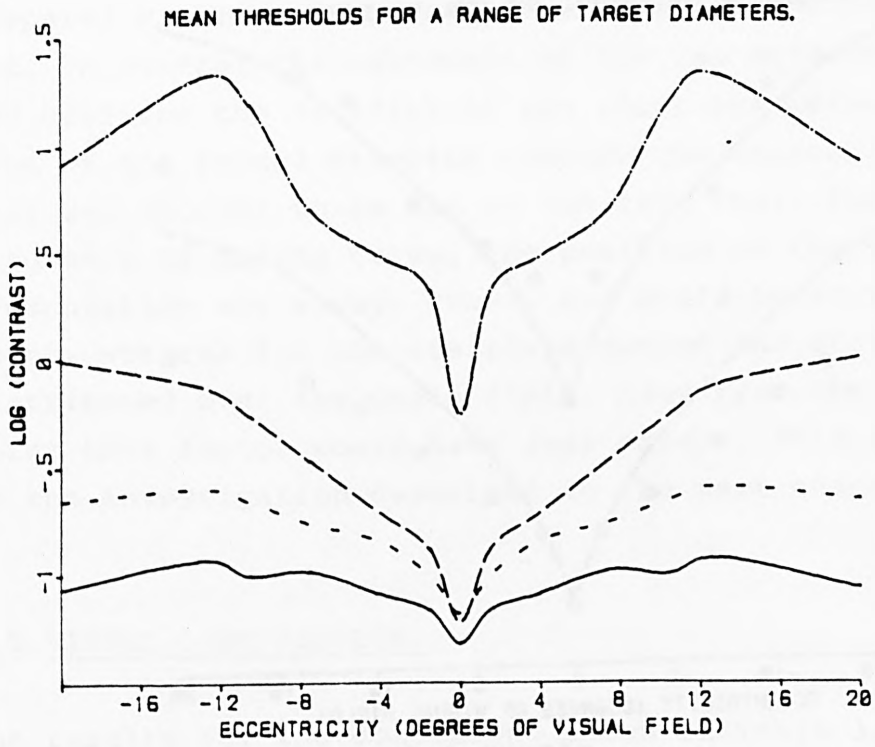

FIGURE 3.4

Mean contrast thresholds, derived from raw data by averaging left and right hemifields and both background illuminance levels. Stationary targets. Broken and dotted line: diameter 0.033°. Broken line: diameter 0.133°. Dashed line: diameter 0.5°. Solid line: diameter 1. 4°.

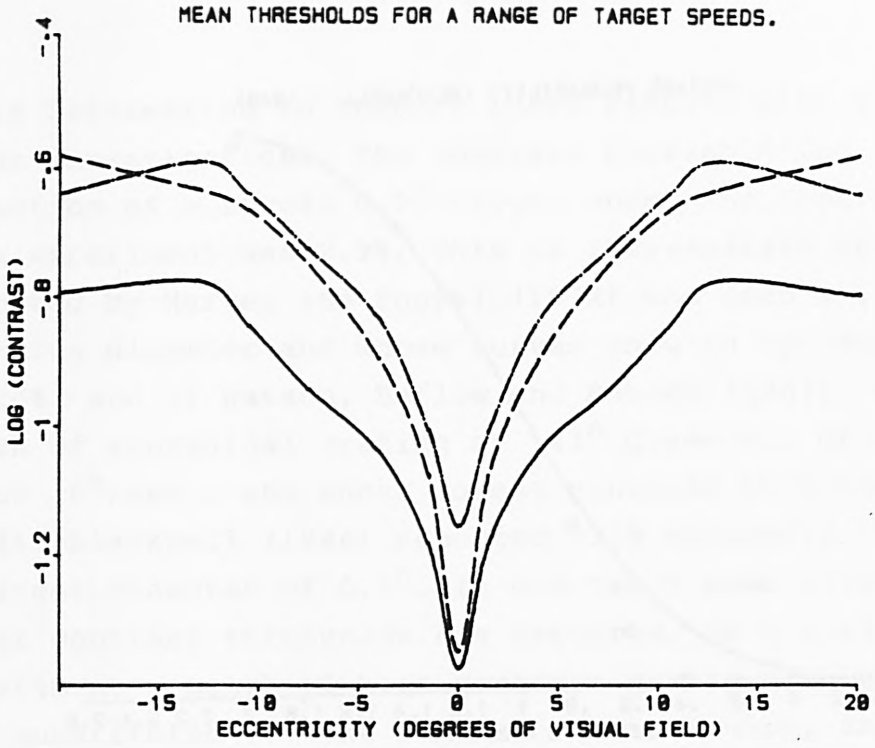

FIGURE 3.5

Mean contrast thresholds, derived from raw data by averaging left and right hemifields and both background illuminance levels. Target diameter: 0.5^{o}. Broken and dotted line: stationary target. Dashed line: speed=1^{o}/sec. Solid line: speed=3^{o}/sec.

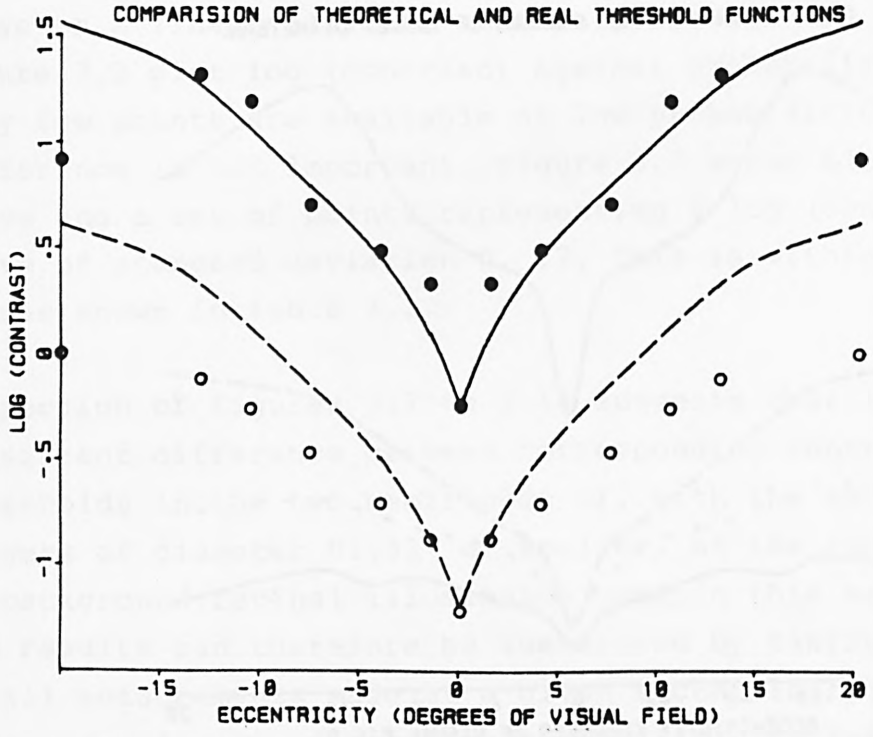

FIGURE 3.6

A comparison of mean experimental threshold data, as in figure 3.5, with threshold functions derived from the cortical magnification factor, M (Rovamo, 1978). The predicted threshold curve has been based on the measured foveal contrast threshold, and scaled by a factor M^{2} at each eccentricity. Stationary targets. Filled circles: diameter 0.033^{o}. Open circles: diameter 0.133^{o}.

eccentricities may be due to the nearness of the stimulus to the edge of the illuminated field. Any stray light from the target which fell on the part of the retina outside the illuminated field would be more easily detected, and contribute to the threshold detection performance. The visual lobes have not been measured in regions near the edge of the field.

Rovamo, Virsu and Nasanen (1978) reported that the inverse cortical magnification factor could be used to predict contrast thresholds. They used high contrast gratings which cannot be directly compared with the circular targets used here, however the cortical magnification factor can be used to estimate changes in contrast threshold with eccentricity, and this is done in figure 3.6. As might be expected, the prediction is best for stimulus sizes which are small compared to the fovea.

The thresholds found from the frequency of seeing curves are compared with those found by the staircase method in Table 3.2. In general the agreement of the two methods is good, and confirms the validity of the staircase method. In the case of one foveal stimulus however the agreement is poor. This was thought to be due to the fact that, for the frequency of seeing curve, the position of the next presentation was always known, and would be at the fixation point, whereas for the staircase method the attention was distributed over the whole field. Away from the fixation point this factor would have less effect. This problem led to the investigation described in the next chapter.

3.5 VISUAL LOBE RESULTS.

The results for the conditions shown in Table 3.1 are plotted in figures 3.18 to 3.20. Figure 3.18 shows the effect on lobe shape of increasing speed. If this is compared with the upper part of figure 3.15 (a series of lobes produced by increasing the target contrast), It can be

seen that the broadening of the lobe due to increases in velocity is similar to that due to increases in contrast.

A technique was developed in the work to be described in chapter 5, where lobe area is correlated with a parameter such as contrast. Applying this procedure to the visual lobe series' of table 3.5:

Stationary target, diameter=0.5°;
Lobe area = (percent contrast) x 1.46 -10.19 corr. coeff.=1.0

Speed=3°/sec, diameter=0.5°;
Lobe area = (percent contrast) x 1.97 - 9.62 corr. coeff.=1.0

Log(contrast)=-1.2, target diameter=1.4°;
Lobe area = (speed,°/sec) x 1.36 + 6.16 corr. coeff.=0.84

log(contrast)=-1.01, target diameter=0.5°;
Lobe area = (speed,°/sec) x 2.09 + 5.10 corr. coeff.=0.93

Thus for a 0.5° target, the effect of changing from a stationary target to one moving at 3°/sec looks similar to the effect of increasing contrast by about 4%.

These lobes, sampled at 11 points on the horizontal meridian of the visual field, show a number of dips and peaks, which could be due to false positive responses, or insufficient observations. A few further lobes were therefore measured, sampled at 27 different eccentricities between -18° and +18° (see figure 3.21) These do not eliminate the peaks and dips, rather the reverse. They indicate the position of the blind spot, between 14° and 17° on the temporal side. A dip in sensitivity at +7.5° seems common even with plots which are an aggregate of 28 target presentations at each of the 25 eccentricities examined.

Results of lobes obtained with a second subject confirm the general threshold level and lobe sizes, and also a degree of spikiness.

3.6) EFFECT OF SUDDEN APPEARANCE AND DISAPPEARANCE OF THE TARGET.

In the course of making the observations it was often felt that it was the temporal stimulus as the target appeared or disappeared that made detection possible. In this respect the manner of the experimental presentation differed from the real life situations it was hoped to relate it to. (It also differed in that the subject was instructed to fixate on one spot, a point which is discussed further in chapter 9, and in the simplified nature of the visual field presented.)

To see if this was invalidating the results, some trials were made in which the target increased in luminance over 0.74sec, and the fall in luminance was masked by obscuring the entire field at the end of the glimpse for 0.5sec. Thresholds were measured in this condition with both 1.4^{o} and 0.133^{o} targets.

The results determined with the 1.4^{o} target (figure 3.24) show little difference between the contrast thresholds for the gradual and the sudden appearance; the gradually appearing target is slightly more difficult to detect when both are stationary, and slightly easier to detect when both are moving. In the case of the 0.133^{o} target however, the gradually appearing stationary target is more difficult to detect than the suddenly appearing one, particularly at the fovea, whereas when both are moving at 3^{o}/sec the rate of appearance makes no difference (see figure 3.23). It does therefore appear that the sudden appearance and disappearance of the target masks the effect of movement on detectability. Both movement and sudden appearance produce temporal change at the receptors: both these changes produce lower thresholds. Figures 3.25 and 3.26 show the results of some brief visual lobe experiments with the same stimuli.

3.7 CONCLUSIONS.

Apart from divergencies of lobe shape which may be artefacts, the lobes measured look as if they belong to a common family, getting broader as contrast, target velocity or diameter increases. The subsidiary peaks found on many lobes are discussed further in section 5.5.

The foveal values of contrast thresholds measured in this study are similar to those found for comparable stimuli by previous workers, in particular the value found for a 0.5^{o} diameter stimulus of 2.9% compares well with the value of 3.3% reported by Blackwell (1946) for a 0.3^{o} stimulus.

The desirability was felt of monitoring eye movements. Saccades were often made involuntarily to the place where the stimulus was thought to have been. If these had been analysed they could have indicated the existence of false positive responses. However, such equipment was not available for use with the maxwellian view optical system.

When the sudden appearance and disappearance of the target was avoided, the effect of movement was more pronounced than in the main series of tests. In other words, the conditions of the main series of experiments may minimise the effect of target movement in increasing the probability of detection. It would appear that small stationary stimuli in a visual display are more easily detectable if changes in the display are made in sudden steps, rather than gradually.

Visual lobes can be predicted from the corresponding threshold plots, by using a generalised frequency of seeing curve. This would provide more reliable data for stimuli where the probability of detection is low, for the same expenditure of observer's time.

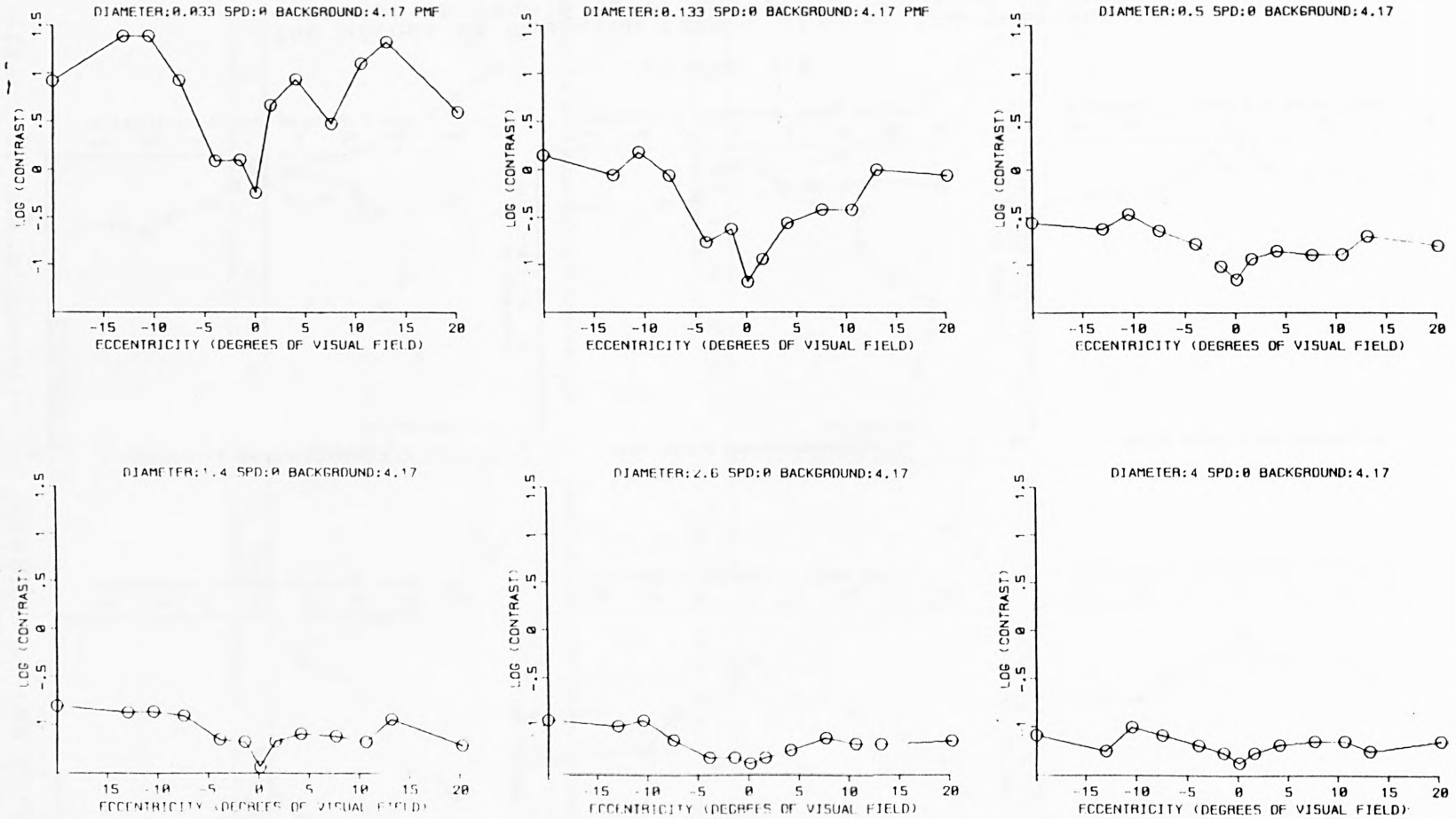

FIGURE 3.7

The effect of changing target size on the relation of contrast threshold to visual field position. Target diameters from 0.033^{0} to 4^{0} are shown, for a stationary target against a background of log(retinal illuminance) of 4.17 log trolands.

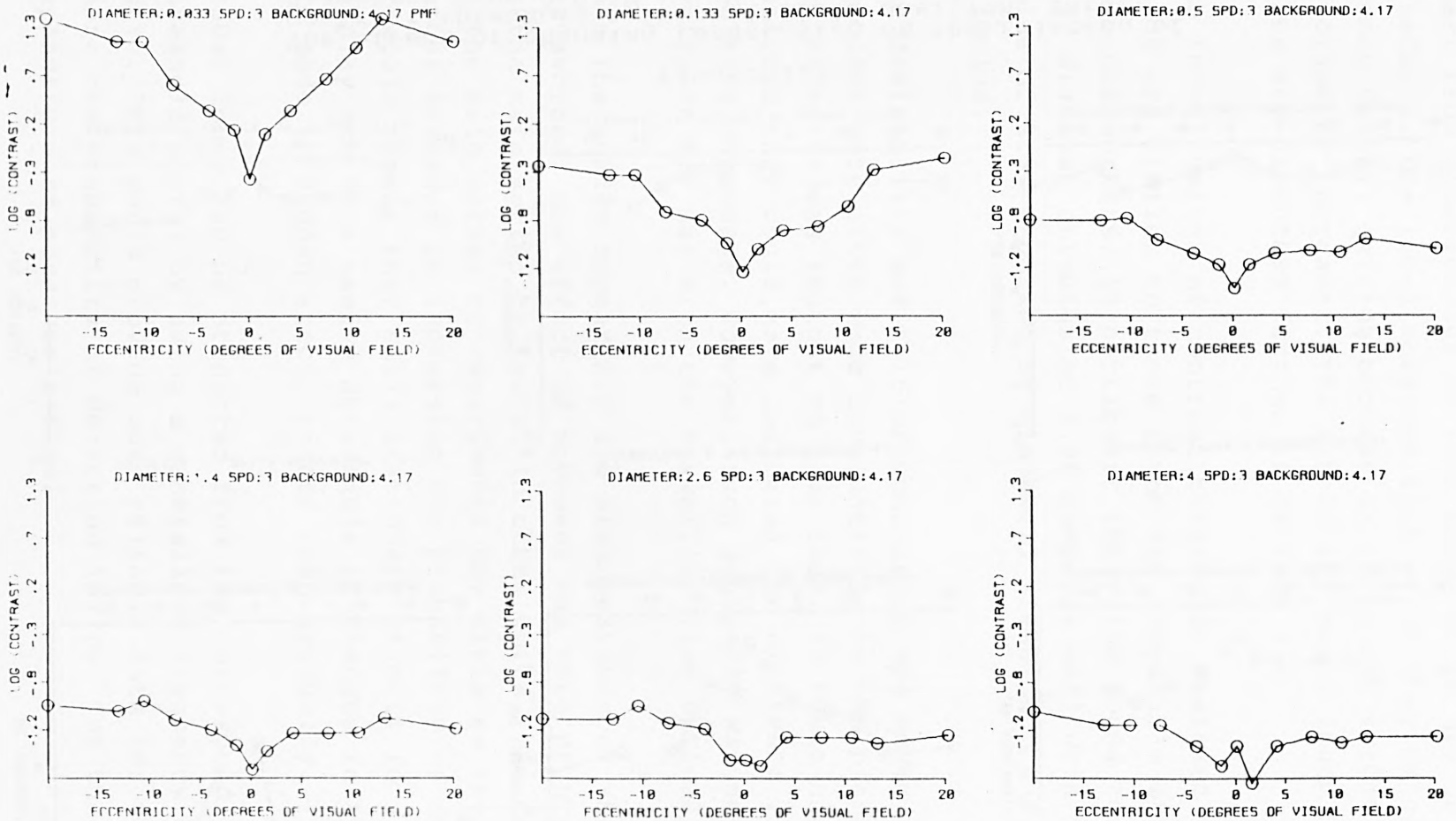

FIGURE 3.8

The effect of changing target size on the relation of contrast threshold to visual field position. Target diameters from 0.033^{o} to 4^{o} are shown, for a target speed of 3^{o}/sec., against a background of log(retinal illuminance) of 4.17 log trolands.

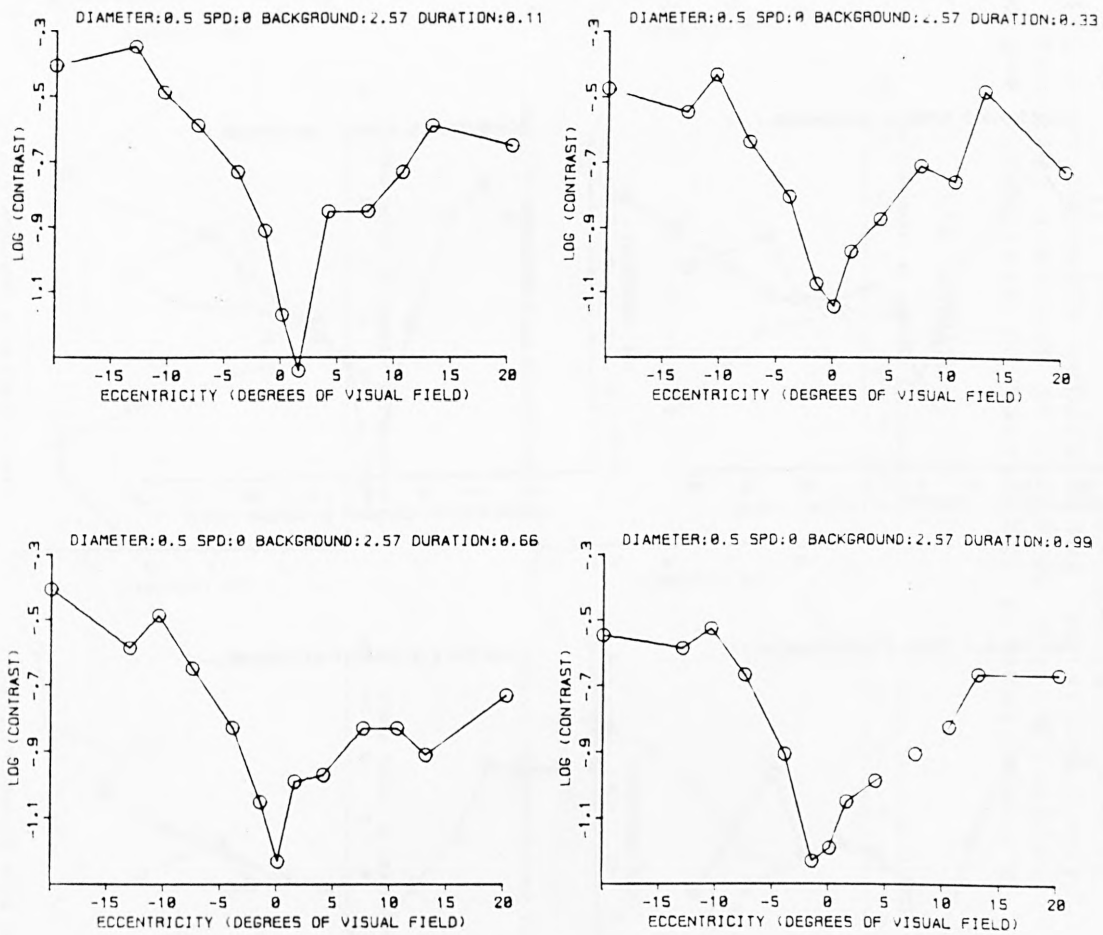

FIGURE 3.9

The effect of changing stimulus duration on the relation of contrast threshold to visual field position. The target appeared for from .11 sec. to .99 sec. The target diameter was 0.5°, and was stationary. The background was of log(retinal illuminance) 2.57 log trolands.

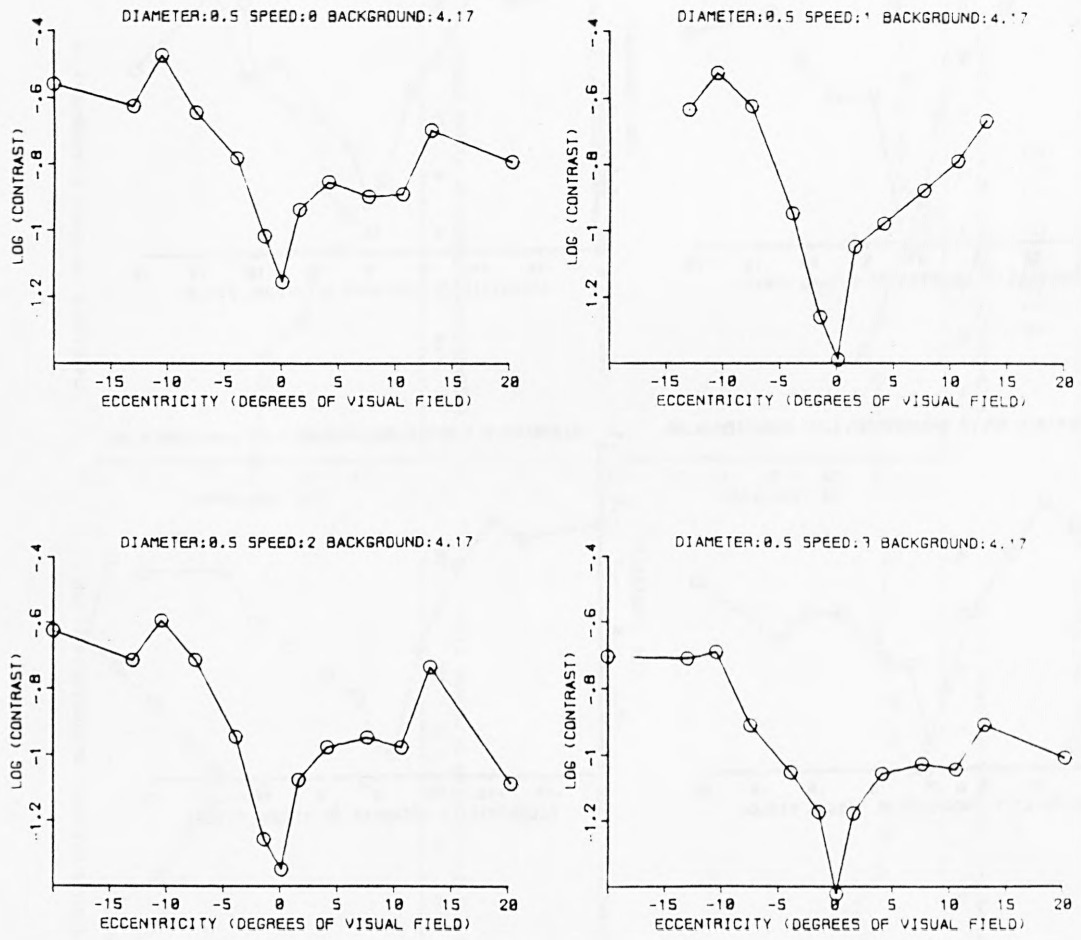

FIGURE 3.10

The effect of target speed on the relation of contrast threshold to visual field position. Target speeds of from 0°/sec. to 3°/sec. are shown, for a target diameter of 0.5°, against a background of log(retinal illuminance) of 4.17 log trolands.

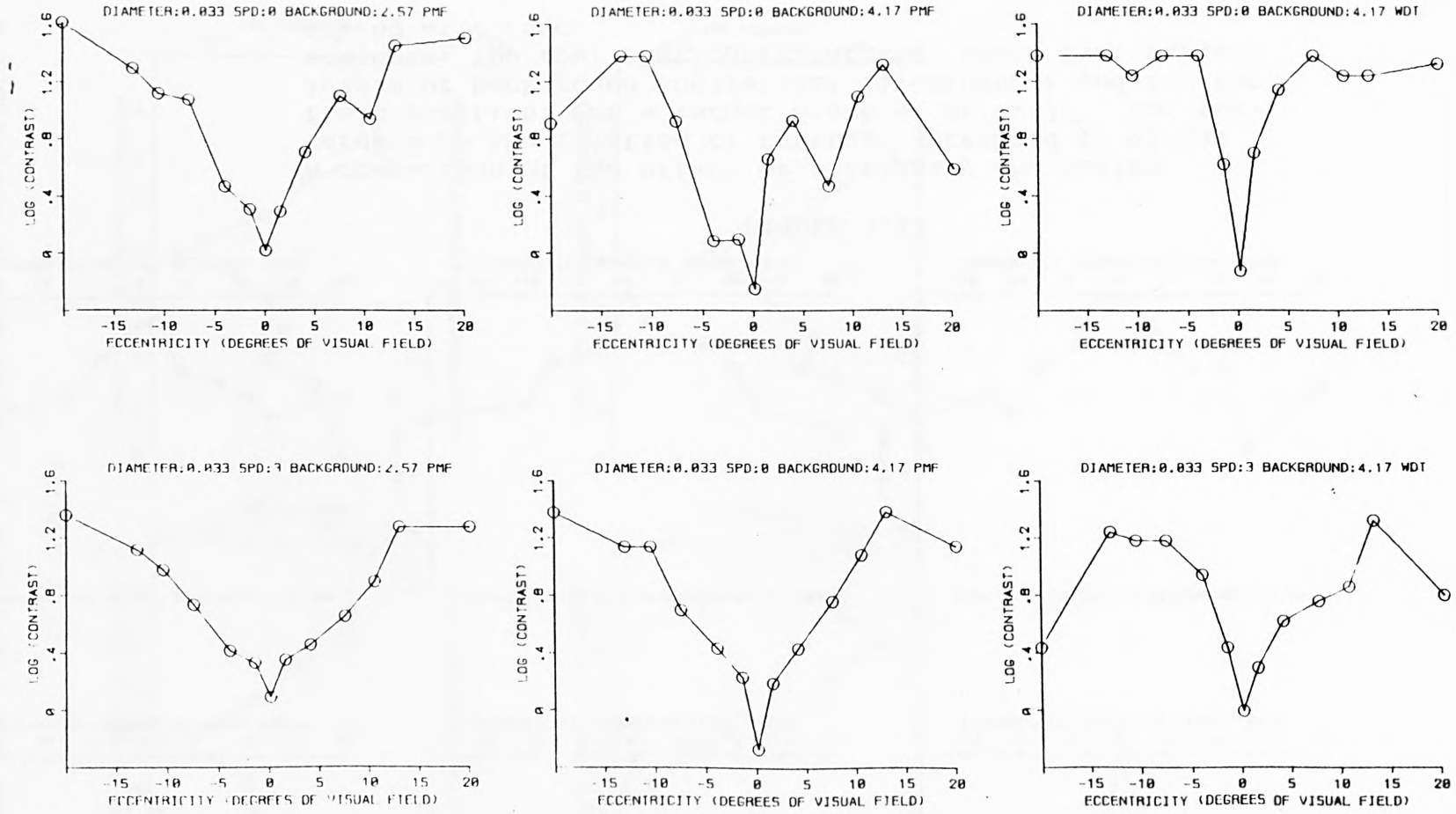

FIGURE 3.11

A comparison of the effect of stationary and moving targets on the relation of contrast threshold to visual field position. For a target diameter of 0.033^{o}, for two levels of background log(retinal illuminance) and for two subjects. Top row: stationary targets. Lower row: targets moving at 3^{o}/sec.

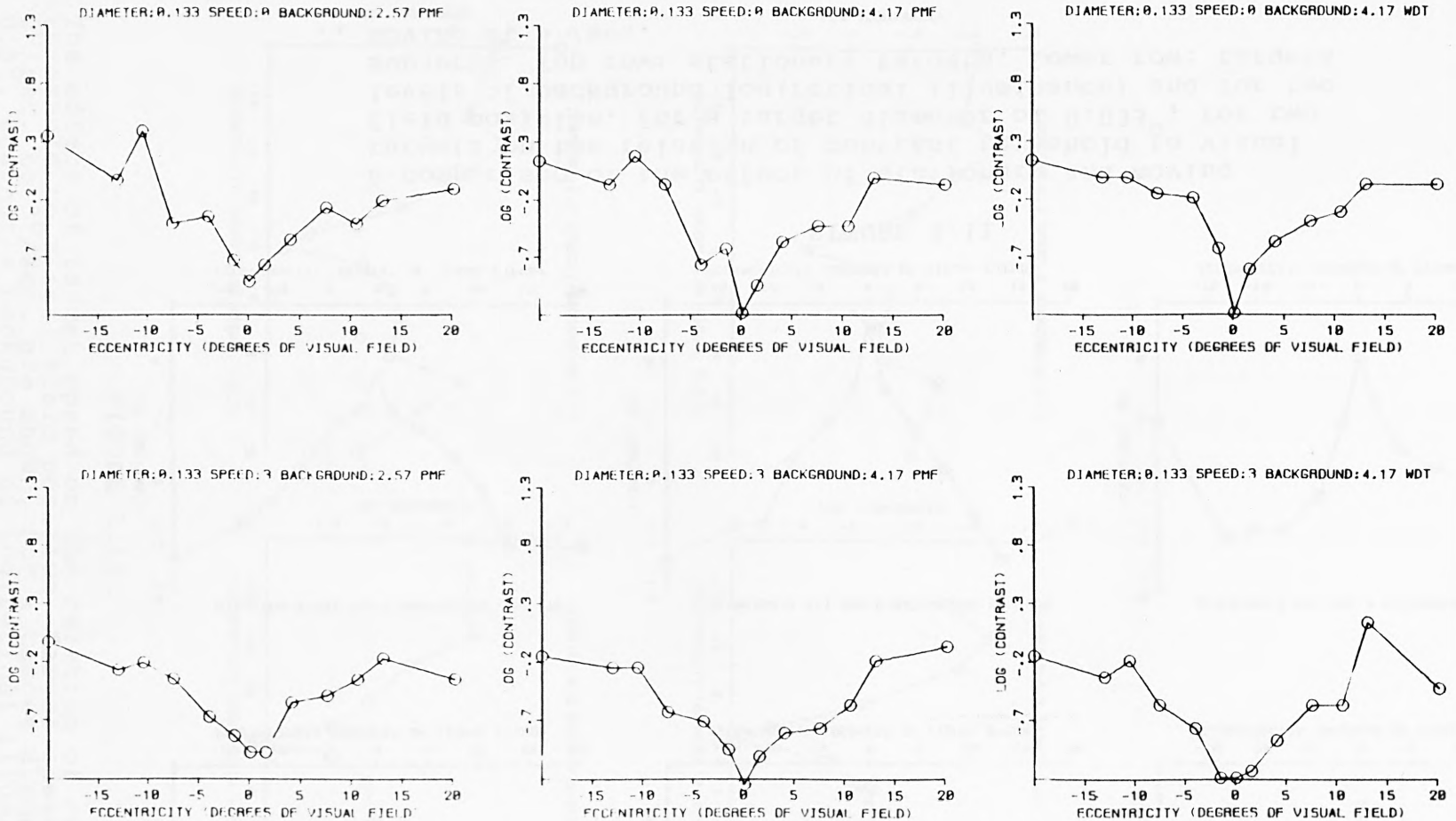

FIGURE 3.12

A comparison of the effect of stationary and moving targets on the relation of contrast threshold to visual field position. For a target diameter of 0.133^{o}, for two levels of background log(retinal illuminance) and for two subjects. Top row: stationary targets. Lower row: targets moving at 3^{o}/sec.

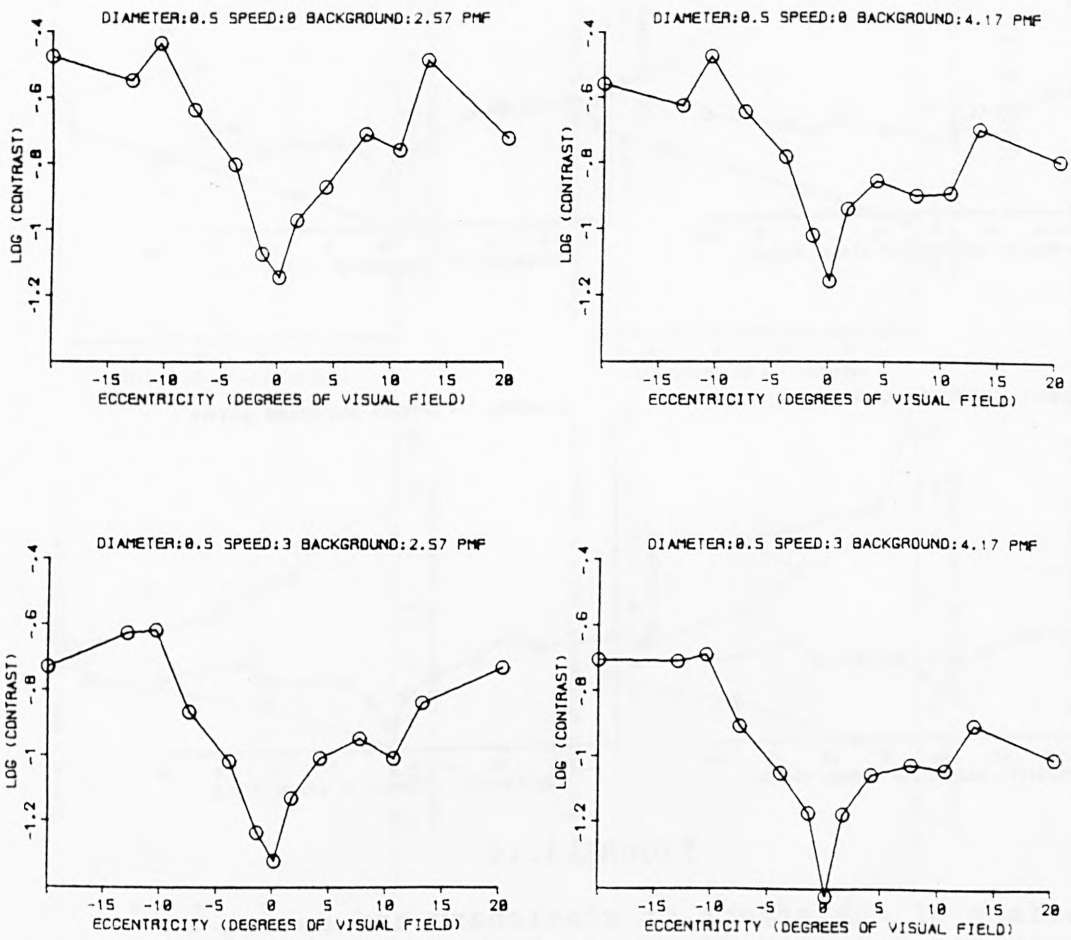

FIGURE 3.13

A comparison of the effect of stationary and moving targets on the relation of contrast threshold to visual field position. For a target diameter of 0.5^{o}, for two levels of background log(retinal illuminance). Top row: stationary targets. Lower row: targets moving at 3^{o}/sec.

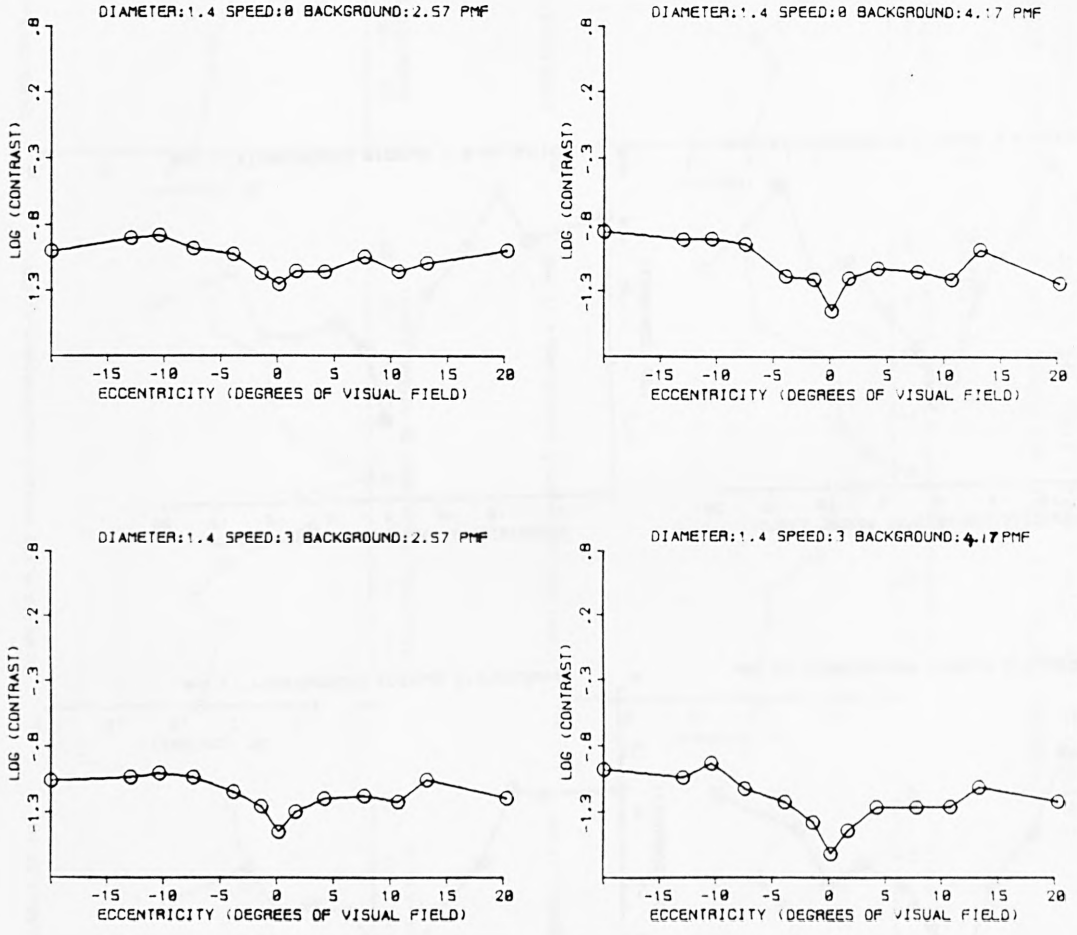

FIGURE 3.14

A comparison of the effect of stationary and moving targets on the relation of contrast threshold to visual field position. for a target diameter of 1.4°, for two levels of background log(retinal illuminance). Top row: stationary targets. Lower row: targets moving at 3°/sec.

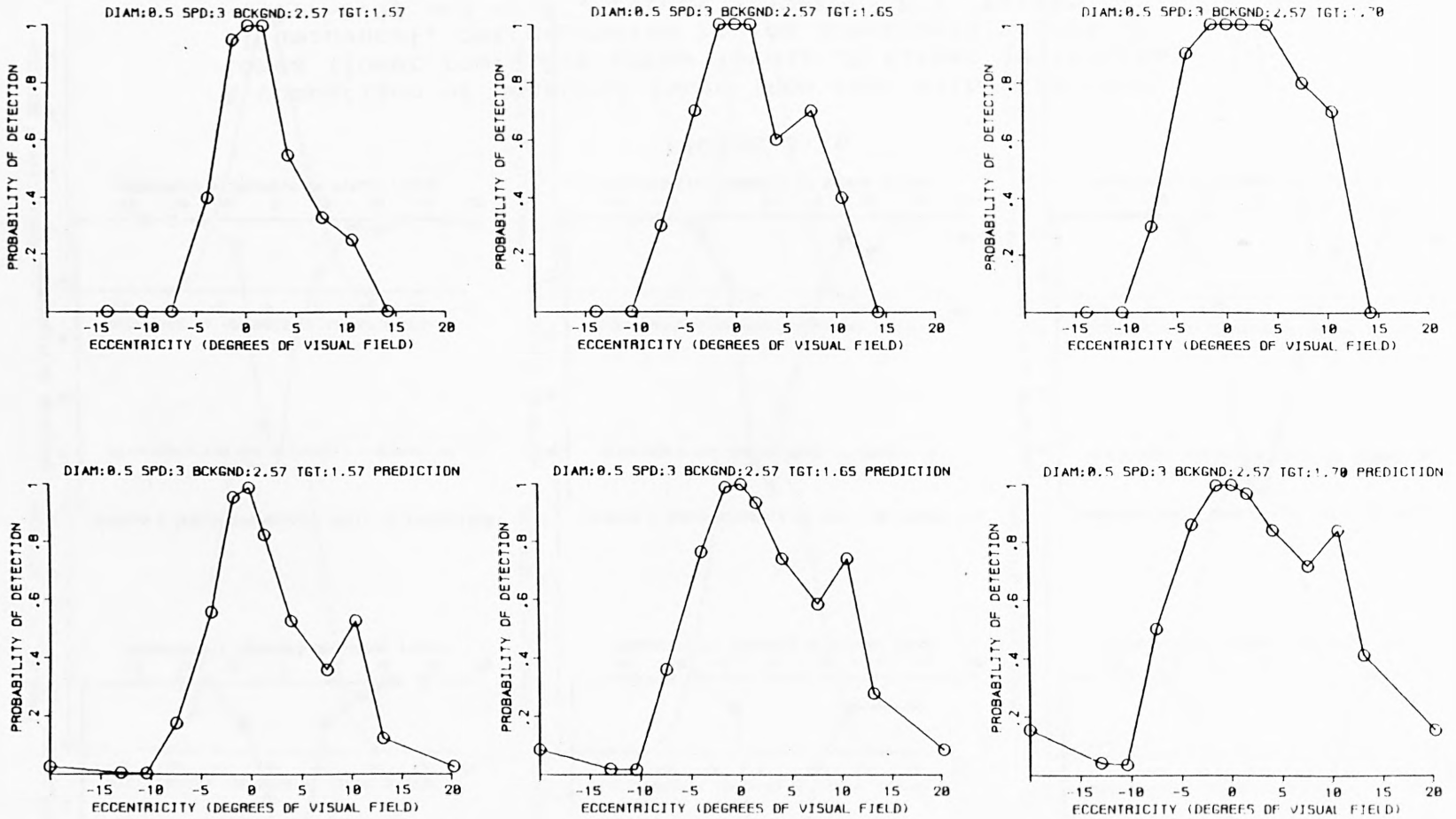

FIGURE 3.15

A comparison of measured lobes (top row) with predicted lobes (lower row). For three levels of target log(retinal illuminance), corresponding to log (contrast) values of -1.0, -0.92 and -0.87. Target diameter: 0.5. Stationary target. Background log(retinal illuminance): 2.57.

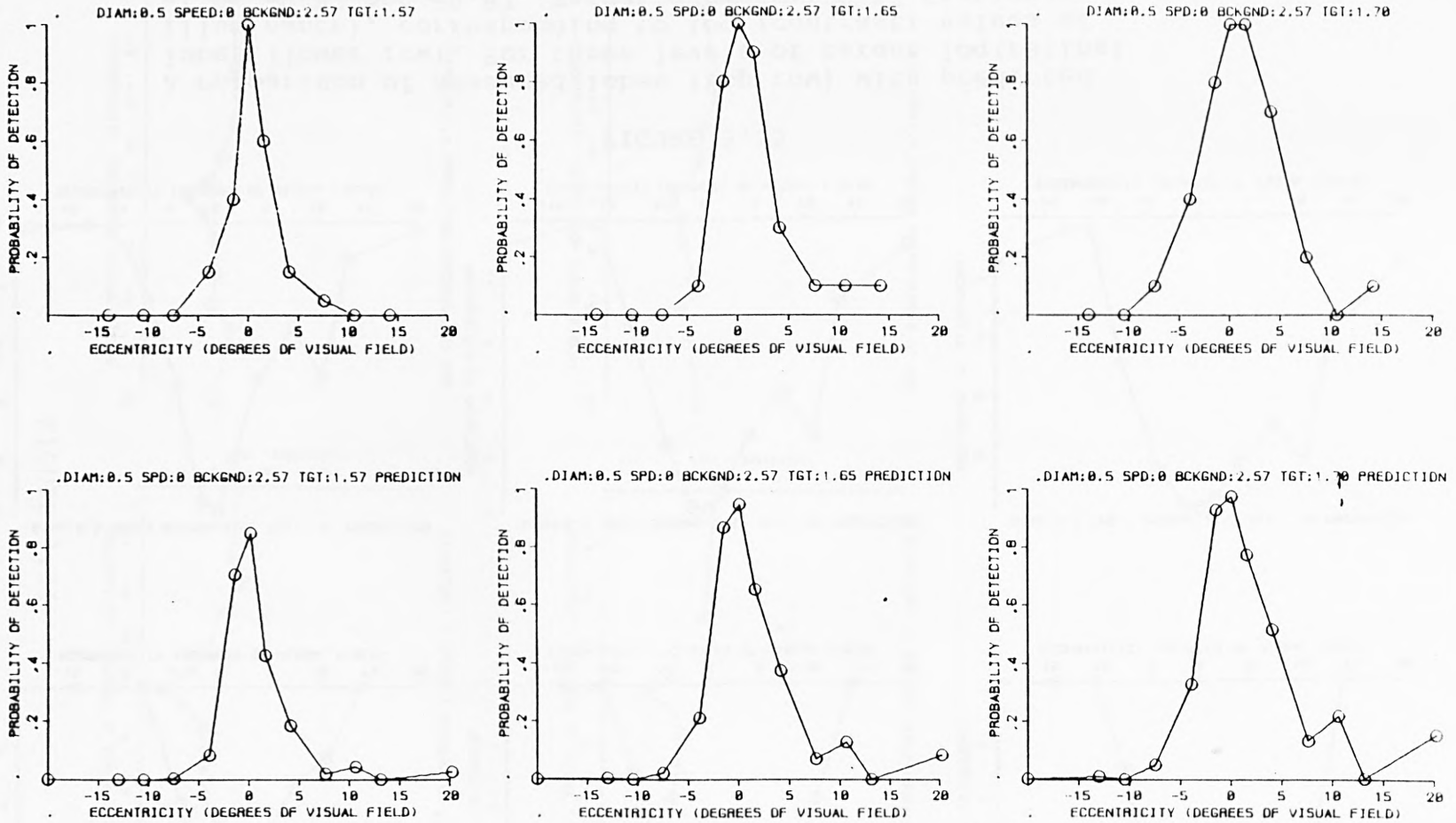

FIGURE 3.16

A comparison of measured lobes (top row) with predicted lobes (lower row). For three levels of target log(retinal illuminance), corresponding to log (contrast) values of -.10, -0.92 and -0.87. Target diameter: 0.5. Target velocity: 3^{o}/sec. Background log(retinal illuminance): 2.57.

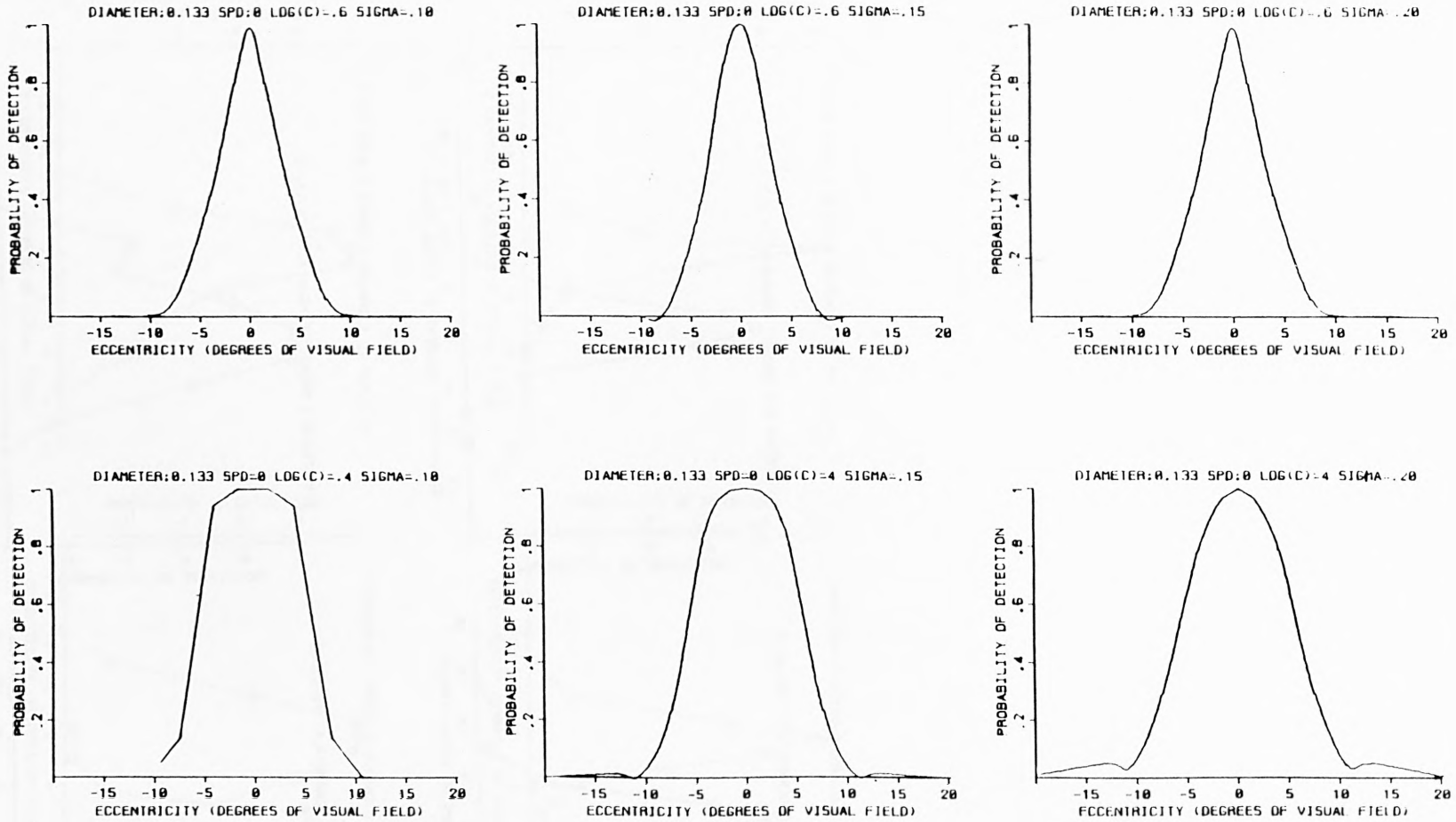

FIGURE 3.17

A series of predicted lobes for a range of values of standard deviation. Target diameter: 0.133^{o}. Stationary target. Top row: 0.4 log(contrast). Lower row: 0.6 log(contrast). The threshold data used for this prediction is a mean of the left and right hemifield data for background log (retinal illuminance) levels of 2.57 lt and 4.17 lt.

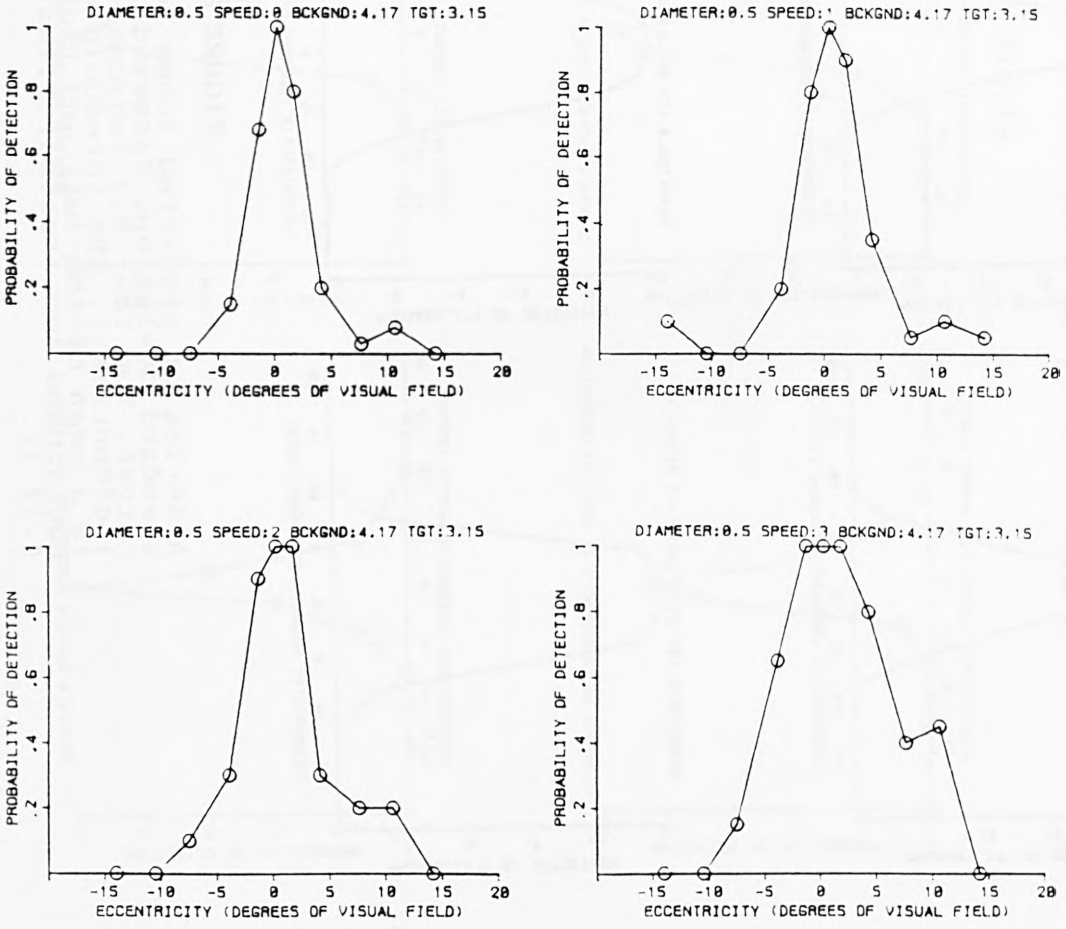

FIGURE 3.18

A comparison of the effect on visual lobes of a range of target velocities. From 0^{o}/sec. to 3^{o}/sec. for a target diameter of 0.5^{o}. Background log(retinal illuminance): 4.17 lt. Log (contrast): -1.02.

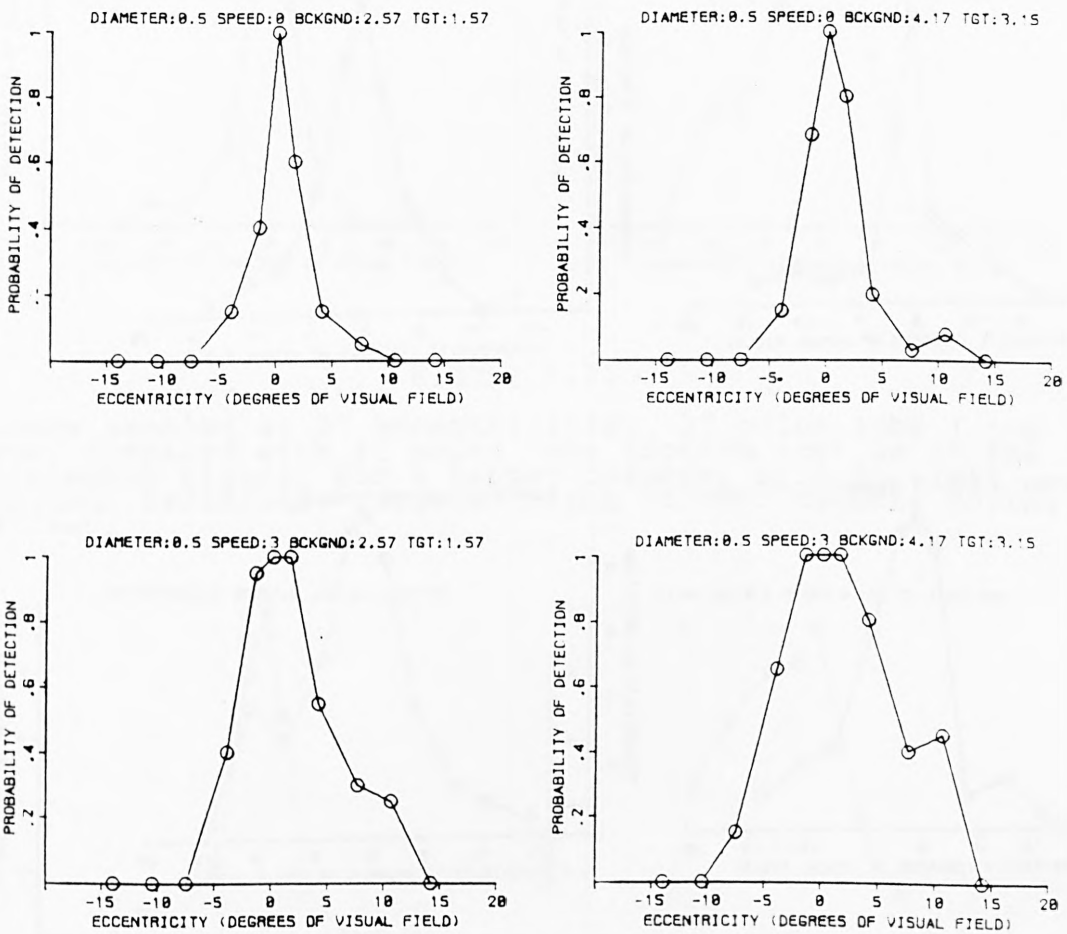

FIGURE 3.19

A comparison of the effect on visual lobes of stationary and moving targets. For a target diameter of 0.5°, and log (contrast) of about -1, for two levels of background retinal illuminance. Top row: stationary targets. Lower row: targets moving at 3°/sec.

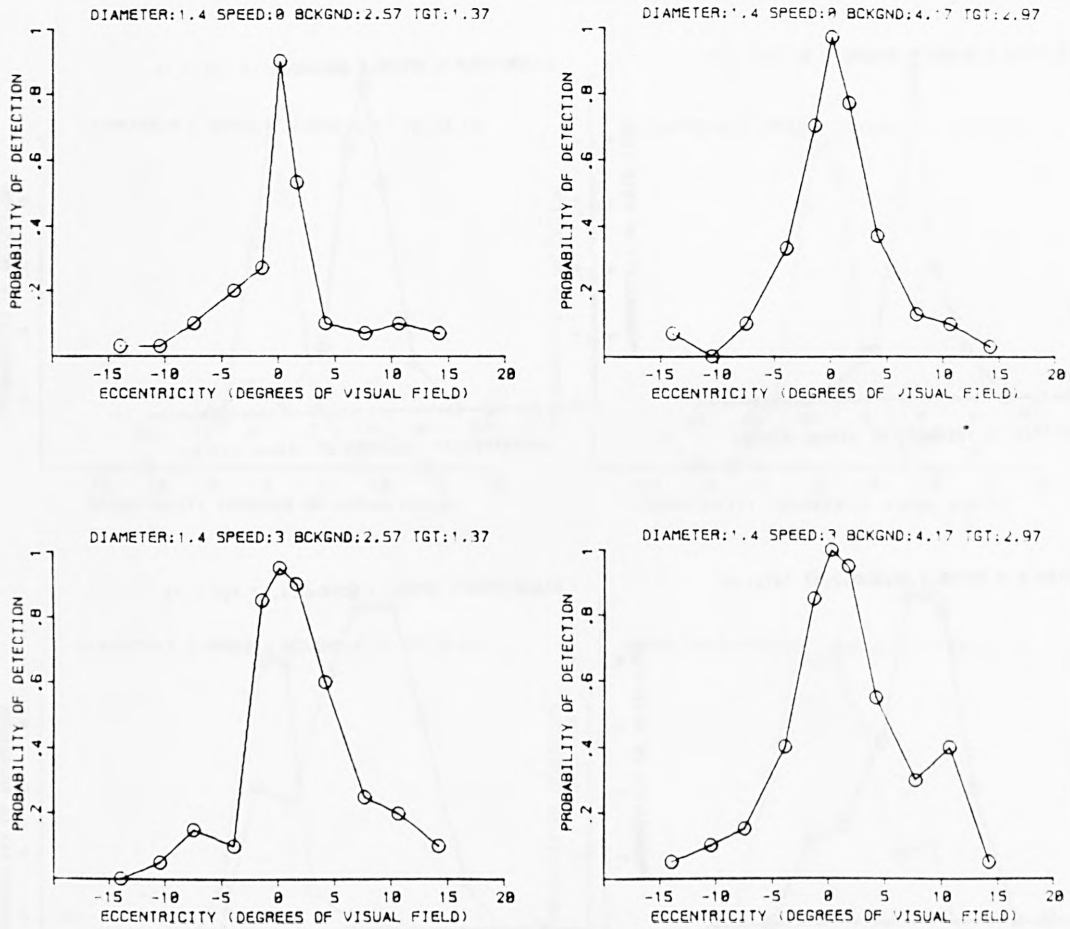

FIGURE 3.20

A comparison of the effect on visual lobes of stationary and moving targets. For a target diameter of 1.4°, and log (contrast) of 1.2, for two levels of background retinal illuminance. Top row: stationary targets. Lower row: targets moving at 3°/sec.

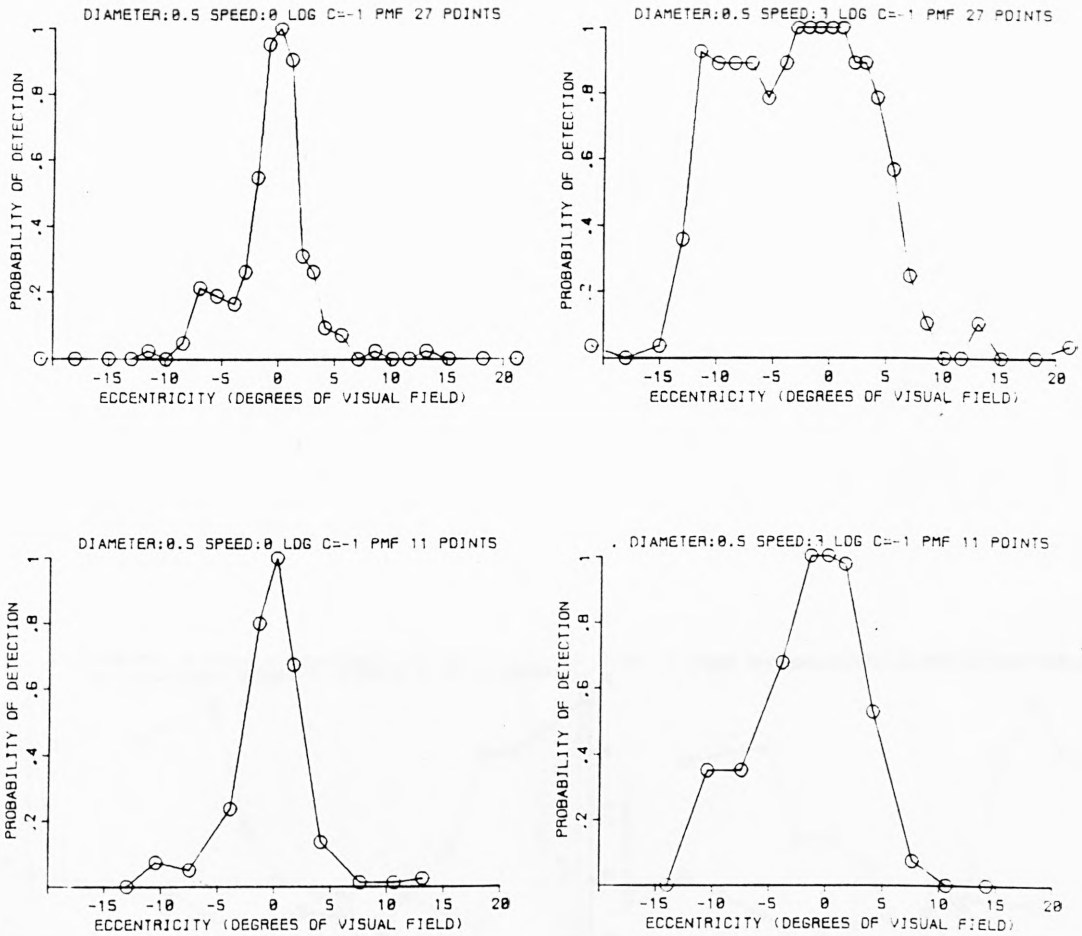

FIGURE 3.21

Lobes sampled at 27 eccentricities. 27 point lobe (top row) compared with 11 point lobe (bottom row) as in the preceding figure, for a target diameter of 0.5^{o}. left column: stationary targets. Right column: targets moving at 3^{o}/sec.

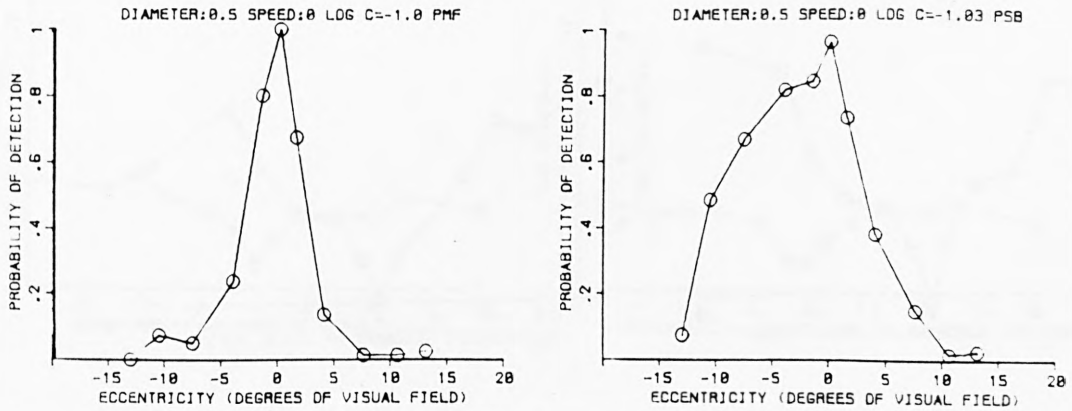

FIGURE 3.22

A lobe measured by an inexperienced observer (PSB). Compared with that measured by the author, for a stationary target, of diameter 0.5^{o}, log (contrast) about -1.0

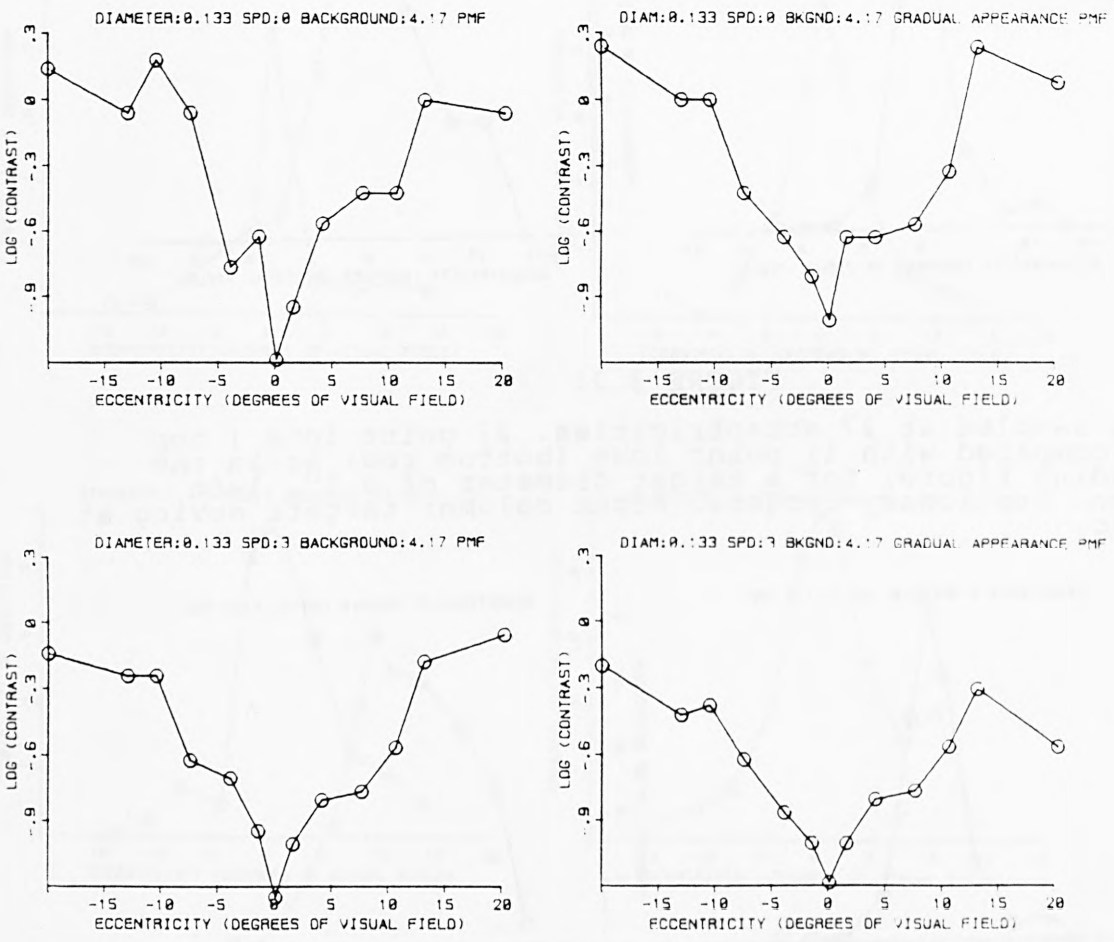

FIGURE 3.23

The effect on contrast thresholds of gradual appearance of the target. Gradual appearance (right column) compared with the instantaneous appearance and disappearance used in the preceding figures (left column). Top row: stationary targets. Lower row: targets moving at 3°/sec. Target diameter: 0.133°. Background log(retinal illuminance): 4.17 log trolands.

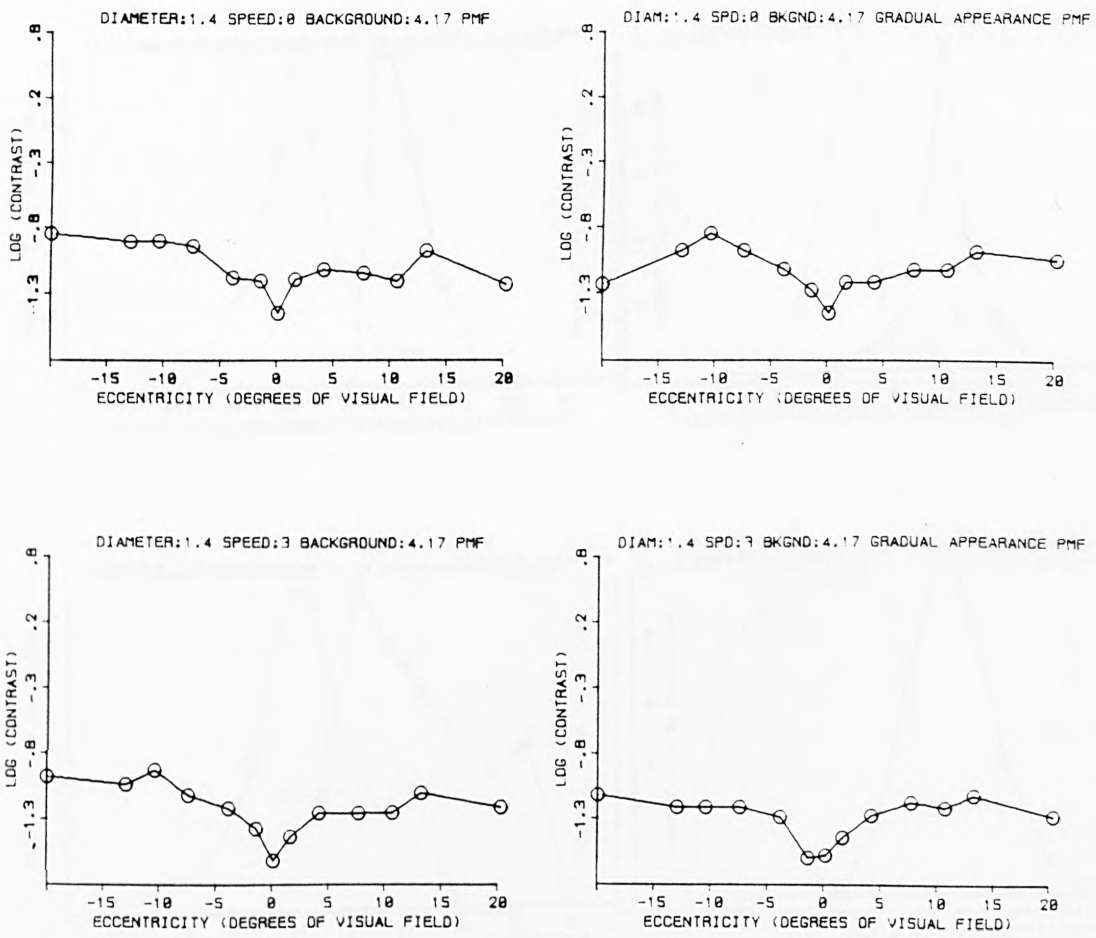

FIGURE 3.24

The effect on contrast thresholds of gradual appearance of the target. Gradual appearance (right column) compared with the instantaneous appearance and disappearance used in the preceding figures (left column). Top row: stationary targets. Lower row: targets moving at 3°/sec. Target diameter: 1.4°. Background log(retinal illuminance): 4.17 log trolands.

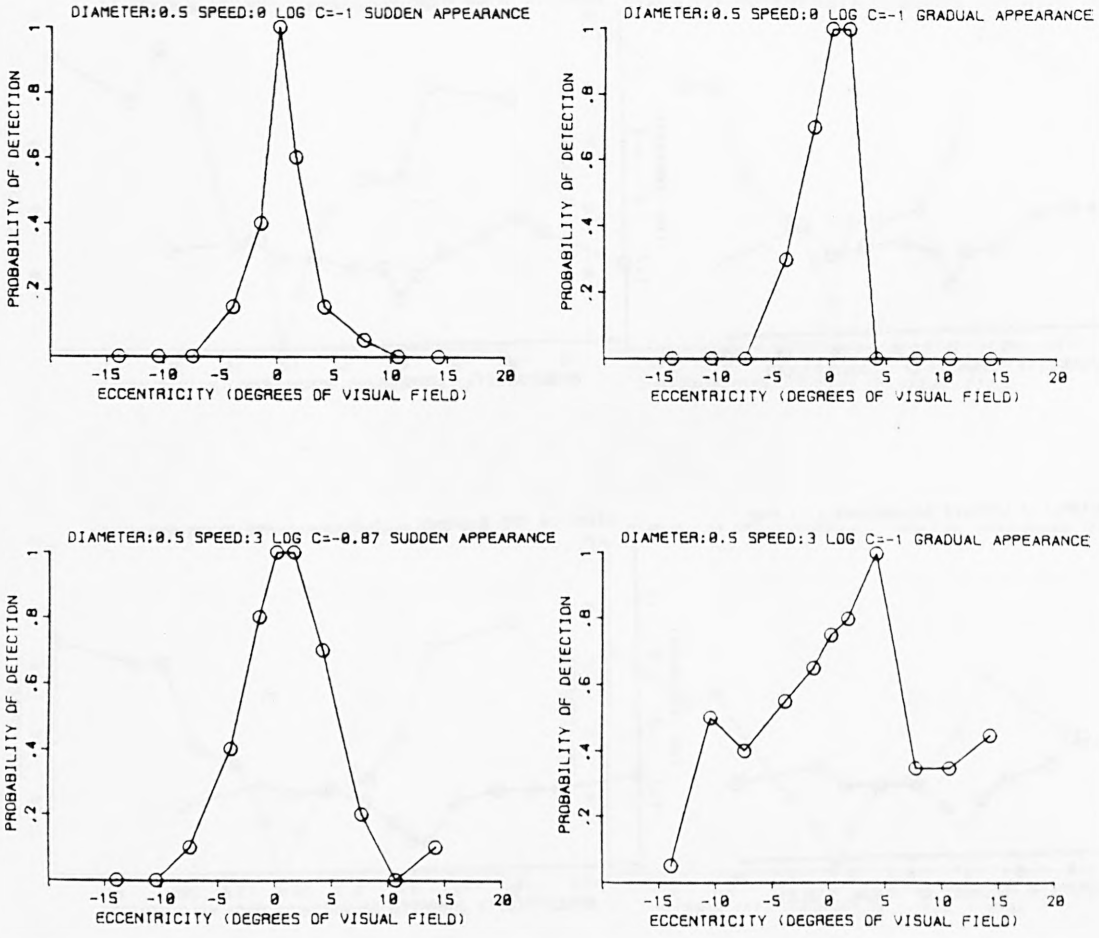

FIGURE 3.25

The effect on visual lobes of gradual appearance of the target. Gradual appearance (right column) compared with the instantaneous appearance and disappearance used in the preceding figures (left column). Top row: stationary targets. Lower row: targets moving at 3°/sec. Target diameter: 0.5°. Log contrast:-1.

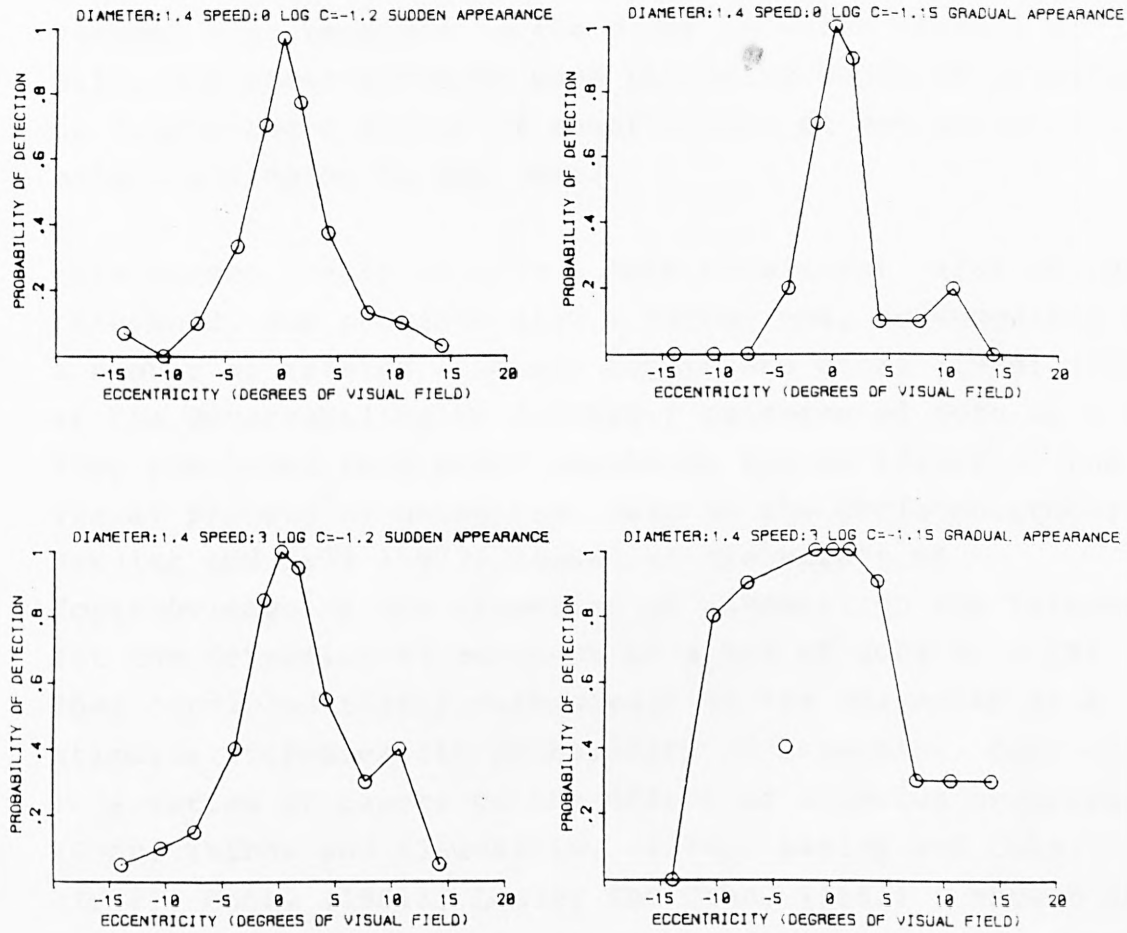

FIGURE 3.26

The effect on visual lobes of gradual appearance of the target. Gradual appearance (right column) compared with the instantaneous appearance and disappearance used in the preceding figures (left column). Top row: stationary targets. Lower row: targets moving at 3^{o}/sec. Target diameter: 1.4^{o}. Log contrast:-1.15 to 1.2.

THE EFFECT OF ATTENTION ON DETECTION THRESHOLDS.

Summary.
The order in which stimuli were presented was examined to see if randomising the sequence in which stimuli at different eccentricities were presented affected the probability of detection. Whereas fatigue affected the results very rapidly, a randomised sequence produced results not significantly different from presenting all of the stimuli at one position in the visual field in a series, or with foreknowledge of the approximate field position.

4.1 INTRODUCTION.

In the course of the work described in chapter 3 it had been assumed that randomising the order in which stimuli of different eccentricities were presented would be preferable to completing a series of observations at one eccentricity, before moving on to the next.

This seemed likely to give a more consistent value of each threshold, and probably also a higher one, as suggested by a number of related studies. Lappin and Uttal (1976) looked at the detectability of different patterns of dots on a CRT. They concluded that prior knowledge had no effect on the visual process of detection, only on the decision process. Sekuler and Ball (1977) looked at the effect of foreknowledge of the direction of movement on the threshold for the detection of movement of a set of dots on a CRT. They concluded that foreknowledge of the character of a stimulus increases its probability of detection. Cohn et al, in a series of papers on the effect of stimulus uncertainty (Cohn, Thibos and Kleinstein, (1974), Lasley and Cohn, (1976), Cohn, (1981), Lasley and Cohn, (1981)) showed that uncertainty about signal parameters depresses sensitivity to those visual signals, in line with the Swets, Tanner theory of signal detectability (Swets, Tanner and Birdsall, (1961)). Posner, Snyder and Davidson (1980) in a study of reaction times to the presence of supra-threshold peripheral

and central stimuli, suggest that attention operates like a spotlight, but is not related to the distance from the fixation point. They conclude that knowledge of where a stimulus is to occur aids detection, but knowledge of its form does not help. Davis, Kramer and Graham (1983) studied the effect of variations of contrast, spatial frequency, position and cueing on the detectability of gratings presented on a CRT. This was a pattern detection study, but it also showed a significant effect of position clues in detecting the position of the stimuli.

4.2 EXPERIMENTAL PROCEDURE.

Preliminary trials suggested that fatigue was an important factor, so each run was restricted to about 20 minutes. In order to establish the probability of detection curve for each stimulus within that time an adaptive staircase procedure was used, based on the Adaptive Probit Estimation of psychometric functions described by Watt and Andrews, (1981). The apparatus used was the same as in the previous chapter.

Three modes of presentation were programmed. In one the stimuli were interleaved and presented in random order with a sound cue that did not indicate visual field position. In another, the threshold was established for each stimulus in turn, that stimulus being presented repeatedly until sufficient data had been accumulated. There was some concern that this mode of presentation could give rise to some adaptation to the repeated stimulus, so in the third mode, alternate left and right hemifield stimuli were presented at each eccentricity, each presentation being preceded by a sound cue which indicated on which side the stimulus was about to appear.

In each run five visual field positions were explored: -10^{o}, -4^{o}, 0^{o}, 4^{o}, 10^{o}. Altogether two stimulus velocities (0^{o}/sec and 3^{o}/sec), two stimulus diameters (0.133^{o} and 0.5^{o}) and three observers were used. Since

the restriction of runs to 20 minutes each meant that each stimulus (in each of two or three modes) could only be presented 8 times, each run was performed 8 times.

4.3 RESULTS.

A first attempt to investigate this problem used one observer, and the first and second mode described above. Table 4.1 shows the thresholds and standard deviations, estimated by the method of Dixon and Mood (Finney,1964), for a range of experimental conditions. These standard deviations show the variability within a run. The last row for each condition shows the standard deviation estimated from the measured results of all eight runs, and shows the variability from run to run. In most cases it is close to the within-run variability. There is no obvious difference in thresholds or in variability between the two modes of presentation (the difference is significant ($p>0.05$) in 5 cases out 40, of which only one showed a higher threshold for the random order of presentation). This could have been due to the effect of foreknowledge of stimulus position being countered by some form of adaptation to the repeated stimulus.

A second investigation was therefore made, using three observers, and comparing the first mode of presentation (random order) with the third one described above, in which the position of the stimulus is cued, and alternated between left and right hemifields. The order in which the two modes were presented within any one 20 minute run was alternated from run to run. The individual results are summarised in appendix 2, tables 4.3 to 4.6. Table 4.2 summarises the mean contrast thresholds and contrast differences for "random" vs "cued" presentation, and an analysis of the same data for the effect of fatigue, as the difference in threshold between the second experiment in the run and the first, regardless of whether the trial was cued or random.

	-10 deg	-4 deg	0 deg	+4 deg	+10 deg
Diam/speed					
0.133°, 0°/sec					
random threshold	3.836	3.584	3.132	3.599	4.215
within run s.d.	0.135	0.159	0.177	0.150	0.173
between runs s.d.	0.175	0.081	0.148	0.108	0.194
0.133°, 0°/sec					
repetition threshold	3.826	3.585	3.060	3.606	4.274
within run s.d.	0.116	0.115	0.145	0.139	0.144
between runs s.d.	0.196	0.176	0.194	0.143	0.238
0.133°, 3°/sec					
random threshold	3.600	3.408	2.987	3.500	3.966
within run s.d.	0.067	0.079	0.161	0.075	0.117
between runs s.d.	0.047	0.036	0.053	0.034	0.039
0.133°, 3°/sec					
repetition threshold	3.665	3.424	3.011	3.520	3.911
within run s.d.	0.096	0.073	0.090	0.078	0.136
between runs s.d.	0.031	0.048	0.063	0.038	0.027
0.5°, 0°/sec					
random threshold	3.354	3.241	2.910	3.337	3.645
within run s.d.	0.146	0.079	0.086	0.168	0.162
between runs s.d.	0.072	0.075	0.014	0.047	0.067
0.5°, 0°/sec					
repetition threshold	3.401	3.340	2.919	3.426	3.679
within run s.d.	0.125	0.069	0.117	0.190	0.080
between runs s.d.	0.051	0.058	0.029	0.038	0.029
0.5°, 3°/sec					
random threshold	3.131	3.071	2.774	3.197	3.364
within run s.d.	0.149	0.105	0.119	0.079	0.080
between runs s.d.	0.016	0.036	0.030	0.026	0.046
0.5°, 3°/sec					
repetition threshold	3.205	3.102	2.790	3.234	3.418
within run s.d.	0.067	0.037	0.136	0.090	0.071
between runs s.d.	0.014	0.030	0.027	0.050	0.045

TABLE 4.1

The effect of randomising the order of presentation on contrast thresholds. Units: log trolands of target retinal illuminance increment. Background luminance 4.17 lt. Subject: PMF

	-10 deg	-4 deg	+4 deg	+10 deg
RMF0 rnd	3.859	3.706	3.530	3.592
RMF0 CUED	3.856	3.659	3.451	3.515
RMF0 1ST	3.790	3.656	3.475	3.510
RMF0 2ND	3.925	3.710	3.506	3.597
RND-CUED	0.003	0.047	0.079	0.077
2ND-1ST	0.135	0.054	0.031	0.087
std dev	0.120	0.065	0.069	0.075
RMF3 RND	3.625	3.503	3.353	3.351
RMF3 CUED	3.638	3.523	3.429	3.353
RMF3 1ST	3.580	3.480	3.354	3.312
RMF3 2ND	3.683	3.546	3.428	3.393
RND-CUED	-.013	-.020	-.076	-0.002
2ND-1ST	0.103	0.066	0.074	0.081
std dev	0.063	0.089	0.071	0.078
PMF0 RND	3.756	3.513	3.420	3.494
PMF0 CUED	3.883	3.482	3.365	3.425
PMF0 1ST	3.687	3.443	3.310	3.379
PMF0 2ND	3.952	3.521	3.417	3.484
RND-CUED	-.127	0.031	0.055	0.069
2ND-1ST	0.265	0.078	0.107	0.105
std dev	0.181	0.087	0.090	0.083
JLB0 RND	3.596	3.198	3.036	3.079
JLB0 CUED	3.723	3.134	2.985	3.062
JLB0 1ST	3.546	3.130	3.000	3.050
JLB0 2ND	3.773	3.203	3.021	3.091
RND-CUED	-.127	0.064	0.051	0.017
2ND-1ST	0.227	0.073	0.021	0.041
std dev	0.209	0.086	0.058	0.053

TABLE 4.2

The effect of foreknowledge and fatigue on contrast threshold. The units are log trolands of the target retinal illuminance increment. Background luminance 4.17 lt.

Each threshold is the mean of 8 measurements, so the standard error of the difference of the means is 0.5 x (standard deviation) and the 5% significance level is approximately 0.82 x (standard deviation) Out of 16 measurements of the differences (4 visual field positions for 3 subjects, one of whom made observations of a moving as well as a still target) only 4 reached the 5% significance level. In the case of the analysis for the effect of fatigue all but 4 results reached the 5% significance level.

4.4 CONCLUSIONS.

An analysis of these results suggests that fatigue, is a significant source of threshold elevation even in an experimental session as short as 20 minutes, whereas uncertainty of the position at which the stimulus is going to appear is not significant.

These results do not appear to support the widely reported conclusion that thresholds decrease when more independent ("orthogonal") characteristics of the stimulus are known in advance of the stimulus appearance. This difference may be due to the rather limited number of different positions at which the stimulus could appear in this experiment, or to the different nature of the threshold being studied. However, the initial assumption that the order of presentation should be random is probably justified as a method of minimising variations due to fatigue and to Troxler fading, and because it is closer to the real life search procedure this study is concerned with.

It had been noted during the experiments of chapter 3 that there were two different ways in which one could fixate, but the selection was not always under conscious control: in one way one would stare at the fixation point, as if expecting to see the stimulus foveally, in the other one would direct one's gaze at the fixation point, but maintain one's

attention more widely spread. Perhaps the effect of fatigue was that the observer tended to revert to the former mode. However Mertens (1956) found that there was a slightly greater probability of detection for peripheral flashes if the observer had general attention for the whole field, rather than special attention for the peripheral direction in which the flash was in fact going to occur. Mertens suggested that this may be the result of the extra fatigue involved in maintaining special attention for one particular extra-foveal area, without actually looking at it.

THE EFFECT OF COLOUR ON SEARCH PERFORMANCE.

Summary

The probability of detection of a small circular target across the central 60^{o} of the visual field has been measured for a range of target colours. The targets used in this investigation subtended a visual angle of either 16 or 24 minutes of arc. The experimental data show no obvious relationship between probability of detection and chroma. Luminance contrast (positive or negative) was overwhelmingly the dominant factor affecting detectability. Subsidiary lobes either side of the main one were often found. An experiment using selective chromatic adaptation suggests that these may be due to rod activity.

5.1 INTRODUCTION

The primary aim of this investigation was to obtain experimental data under specified conditions of illumination which could then be used to model the effect of target colour and movement on search performance in human vision.

This chapter is concerned largely with the effect of target colour and chromatic adaptation produced by the background on the probability of target detection as a function of target eccentricity in the visual field. The data which are required for modelling are represented as "visual lobes" for specified spectral distributions of the background and test target, from which are calculated the tristimulus values for both, as well as the difference in chromaticity coordinates and luminance.

The effect of chromatic adaptation, and hence the relative sensitivity of different receptor types, may be important since previous results (some of which are reviewed in chapters 6 and 7), suggest that threshold detection data reflect early stages of visual processing. Hence the relative distribution of rod and cone receptors as a function of eccentricity, and their level of adaptation, may

have a large effect on the shapes and sizes of the visual lobes. In line with this argument, chapter 4 showed that, under the conditions of this experiment, knowledge of target location does not affect the probability of target detection. On the other hand, the state of the eye's light adaptation, which affects the relative contribution of different cone types and of rod receptors to the detection of the target, would be expected to cause significant changes to the shape of the visual lobe.

5.2 METHOD.

In order to distinguish between the effects of colour and of luminance contrast, it was necessary to display the stimuli in a way which permitted them to have the same luminance as the surround, as well as higher or lower, and also allowed them to differ in colour. Thus it was not possible to use methods of display which added the stimulus to the background illumination, since this always results in an increase in luminance. Furthermore the conditions of interest required a field of view of 100^{o}. These conditions could not be met using a Maxwellian view optical system.

It was therefore decided to use a pair of projectors fitted with fast acting shutters to display first a uniform adapting field, and then to switch instantly to a matched field which also included the test target. One problem with such a system is the comparatively low light level, another is the low colour temperature of the projection lamps, which is below the optimum for colour discrimination. Both these difficulties were overcome by using a third matched projector, fitted with a blue filter. This raised the colour temperature to within the range of daylight ($5250^{o}K$) and the adapting field luminance to a level of practical interest ($14cd/m^2$ to $40cd/m^2$ or about 2 to 2.6 log trolands). This level is broadly in the photopic region and is similar to that used by, for instance, Goillau (1983) in his study of the effect of display subtense on eye movement

search. It has been suggested (Farrell and Booth (1984)), that rods begin to play a part in vision for scene luminances below 10cd/m^2, or a retinal illuminance of about 2 log trolands. The lower background level used in the work reported in the first chapter was 2.57 log trolands.

When the subject was confronted with a uniformly illuminated screen subtending 100^o by 40^o, with a small LED to fixate on, it was difficult to maintain the fixation light in focus, as there was insufficient stimulus for the accommodation reflex. Spectacles were therefore obtained to bring the resting focus to the screen distance of 1.7 m when needed.

Trials were made to check the effect of imperfect setting of the projectors on the probability of target detection. The slide was first defocussed by 0.2 D (by adjusting the best focus to a point 1.25m in front of the screen, when the target appeared considerably more blurred than was likely to occur due to errors of adjustment) and an additional lobe measured. Next, the projector supplying the adapting field was deliberately mismatched to the projector supplying the stimulus field. The screen luminance of the adapting field was 21 cd/m^2, and that of the stimulus field was set at 14cd/m^2. The screen luminances were also measured when the two projectors had been matched visually, and were closer than 5%. In both cases the lobes were similar to those measured normally (see figure 5.19 at the end of the chapter). The lobe widths at 50% probability of detection were as follows:

Normal measurement	Defocused stimulus	Mismatched luminance
54^o	55^o	50^o

5.3 PHOTOMETRY AND COLORIMETRY OF THE STIMULI.

The target slide and background for each colour were projected with the added blue illumination, as for the observations, and the spectral radiance functions for both target and surround recorded using the telespectroradiometer described in chapter 2. This was done for some slides using the 55mm projection lens, but the granularity of the film and the small size of the spot made these measurements less reliable. All the slides were measured using the 36mm lens, and the photopic luminance, scotopic luminance and CIE tristimulus values calculated. Linear regressions were run for three major colorimetric parameters for the two sizes of target with the following results:

$CONTRAST_{55} = 0.867 * CONTRAST_{36} + 0.686$

correlation coefficient=0.987

$CHROMA_{55} = 0.995 * CHROMA_{36} + 1.051$

correlation coefficient=0.974

$L^*u^*v^*\ vector_{55} = 1.007 * L^*u^*v^*\ vector_{36} + 0.632$

correlation coefficient=0.977

The colorimetric results from the 55mm lens were close to, and correlated well with, those from the 36mm lens, and the regression line was used to predict colorimetric data for the 55mm lens in those cases where it had not been measured.

The tabulated colorimetric data for each target slide are summarised in Table 5.1.

Slide	Area of lobe	L*	u*	v*	Relative chroma	Photopic contrast	Scotopic contrast	L*u*v* vector
Tray 1								
4	24.204	100.540	+17.939	+8.764	19.966	+1.4	+3.6	19.973
5	61.397	105.701	+12.896	+16.268	20.759	+15.5	+2.6	21.528
6	16.604	97.029	-24.763	+3.031	24.947	-7.5	-2.9	25.124
7	52.159	93.567	-26.849	-8.439	28.144	-15.7	-5.1	28.870
8	33.208	94.416	-18.774	-12.797	22.721	-13.8	-3.3	23.397
9	49.506	103.828	+12.520	-0.550	12.532	+10.2	+7.0	13.103
10	60.881	89.430	+16.929	-19.716	25.987	-24.9	-18.7	28.055
11	11.850	98.142	+21.705	-8.869	23.447	-4.7	-5.1	23.521
12	19.125	96.410	+20.666	-13.323	24.588	-9.0	-6.8	24.849
14	16.538	98.680	-21.986	-4.194	22.382	-3.4	+4.1	22.421
15		98.593	-7.305	+5.802	9.329	-3.6		9.434
16	14.688	100.909	-4.320	+11.635	12.411	+2.4	-3.3	12.444
17	15.088	101.903	+12.577	+10.596	16.445	+5.0	-4.0	16.555
18	13.025	100.254	+18.638	+6.354	19.691	+0.7	-7.0	19.693
Tray 2								
1	9.899	101.472	-4.064	+11.100	11.820	+3.9	-1.4	11.911
2	54.868	94.247	-26.669	-13.188	29.752	-14.2	-1.4	30.303
3	57.444	92.593	+17.336	-16.639	24.029	-18.0	-13.1	25.145
4	55.645	92.799	+19.455	-11.044	22.371	-17.5	-15.7	23.501
5	15.785	101.842	+5.207	+8.291	9.791	+4.8	-0.8	9.963
6	7.013	98.510	-9.634	+5.485	11.086	-3.8	-4.3	11.186
7	75.750	106.917	+8.936	+10.092	13.480	+19.0	+10.0	15.151
8	55.377	93.789	-3.704	-5.129	6.327	-15.2	-11.6	8.866

SUMMARY OF LOBES AND COLORIMETRIC DATA. 36mm Lens. Subjects name; PMF

Slide	Area of lobe	L*	u*	v*	Relative chroma	Photopic contrast	L*u*v* vector
Tray 1							
4	18.900	101.299	+18.081	+8.119	19.820	+3.4	19.863
5		105.034	+13.778	+16.210	21.274	+13.6	21.861
6	10.563	96.803	-24.400	+2.968	25.573	-8.0	25.772
7		94.782	-27.118	-8.669	28.470	-12.9	28.944
8	22.175	95.333	-19.629	-12.148	23.084	-11.6	23.551
9	28.988	103.807	+14.706	-0.868	14.732	+10.4	15.236
10		90.210	+19.611	-20.821	28.602	-23.2	30.231
11	10.413	98.590	+26.570	-6.887	27.448	-3.6	27.484
12	10.700	95.983	+20.738	-13.640	24.822	-10.0	25.145
14	10.550	98.950	-22.976	-4.546	23.421	-2.7	23.445
15		98.475	-8.932	+5.854	10.679	-3.9	10.787
16	9.925	101.083	-5.036	+11.956	12.973	+2.8	13.018
17	12.063	101.032	+10.885	+11.110	15.554	+2.7	15.588
18	10.963	99.752	+18.410	+7.515	19.885	-0.6	19.886

SUMMARY OF LOBES AND COLORIMETRIC DATA. 36mm Lens. Subjects name; PMF

TABLE 5.1

Summary of colorimetric data and lobe area for each stimulus

Although the CIE system of colorimetry strictly applies only to foveal colour vision, it was hoped that the size of the lobe for a given target, or its probability of detection in the periphery, would bear some relation to its distance from the background in a uniform colour space. Accordingly the CIELUV colour space, described in section 1.7, was used, and L*,u* and v* were calculated for each target, treating its background as the white point. (Trial calculations treating the background as a grey of fixed L* made little difference to the result, and were also of doubtful validity.) This is equivalent to applying a von Kries transformation to allow for adaptation to the colour of the background.

5.4 PROBABILITY OF DETECTION LOBES.

Each stimulus was presented at each of the selected eccentricities between 20 and 30 times. The probabilities of detection are tabulated in Tables 5.3 to 5.8 in appendix 1. The lobes are presented in sets to facilitate comparison with one another, and the position of the target relative to the background in CIELUV space is plotted for each target. These results are summarised in figures 5.4 to 5.25, which will be found at the end of this chapter.

Since the results suggest that the lobes are symmetrical, the number of presentations at each eccentricity could be doubled by combining the left and right probabilities. This has not been done, in order that the degree of symmetry can be better assessed.

Following examination of the lobes produced, some further lobes were measured for an additional normal subject (see table 5.6 and figures 5.4 to 5.14) and monocularly for the original subject (table 5.7 and figures 5.27 to 5.32).

Some lobes were also produced under conditions selected to maximise the involvement of rod receptors (See table 5.8 and

figure 5.26). The projection conditions for the 'rod vision' lobes were based on those used by Aguilar and Stiles (1954). The background field was illuminated by a filter that cut off wavelengths less than 590nm, at a screen luminance of 6cd/m^2. This was achieved using two projectors fitted with 36mm lenses, each with a Strand Electric Cinemoid filter no. 6. The target was provided by a projector fitted with a 55mm lens, and a narrow band filter transmitting at 537nm. The filter transmission curves are included in figure 5.24 B and 5.24 C. The target slides were opaque, with a 200 micron pinhole arranged to produce an image on the screen at $\pm 5^{o}$ or $\pm 25^{o}$. Because of lens vignetting, different neutral density filters had to be placed over the different pinholes to achieve matched screen luminance at all eccentricities. The luminance of the green stimulus alone was .084cd/m^2. Its diameter on the screen was 25 minutes of arc.

5.5 DISCUSSION.

The shape and size of lobes for the same size and colour of target can be seen to be very similar for the two observers. In general they are symmetrical. The lobes for the two sizes of target for the same colour are also similar, but the lobe for the smaller target is always smaller than that for the larger one. This trend is in line with the data presented in Chapter 3.

The area under each lobe was computed, to provide a simple index of the visibility of each stimulus configuration (see table 5.1). Linear regressions were performed to establish the correlation of this index with various colorimetric parameters. These included the distance between stimulus and background in L* u* v* space (referred to in the appended tables as the L*u*v* vector), the distance on a u* v* plane between stimulus and background (referred to as chroma), as well as scotopic and photopic contrast. Of these only the last showed a clear positive correlation with the area under the lobe (see table 5.2).

Subject	parameter correlated	correlation coefficient
PMF/36mm	Area vs photopic contrast	0.902
	Area vs +ve or -ve contrast	0.930
	Area vs chroma	0.138
	Area vs L*u*v* vector	-0.088
PMF/55mm	Area vs photopic contrast	0.875
	Area vs chroma	-0.175
WDT/55mm	Area vs photopic contrast	0.875

TABLE 5.2

Correlation of lobe area with colorimetric parameters.

Separate regressions were run for targets of both positive contrast (i.e., those lighter than the background) and negative contrast. The regression lines and points for each target are shown in figure 5.3. The equations for the two lines were:

positive contrast;
Lobe area = +3.49x(contrast)+7.27, correlation coeff.= 0.93

negative contrast;
Lobe area = -2.94x(Contrast)+0.54, correlation coeff.= 0.93

Likewise a multiple linear regression relating area with L*, u* and v* indicated a significant correlation only with L*.

Figure 5.1 compares some of the lower contrast monocular lobes with those reported in chapter 3. From this comparison it appears that, under the conditions of this experiment, the detection of low contrast stimuli of similar diameter, duration, visual field position and luminance contrast is easier than under the conditions of chapter 3 (it would be difficult to assess the significance of this difference since none of the lobes were measured under conditions of matched luminance contrast). Although this could be due to the additional chromatic contrast, the differences in viewing conditions, edge definition of the target and luminance measurement techniques makes the similarities more

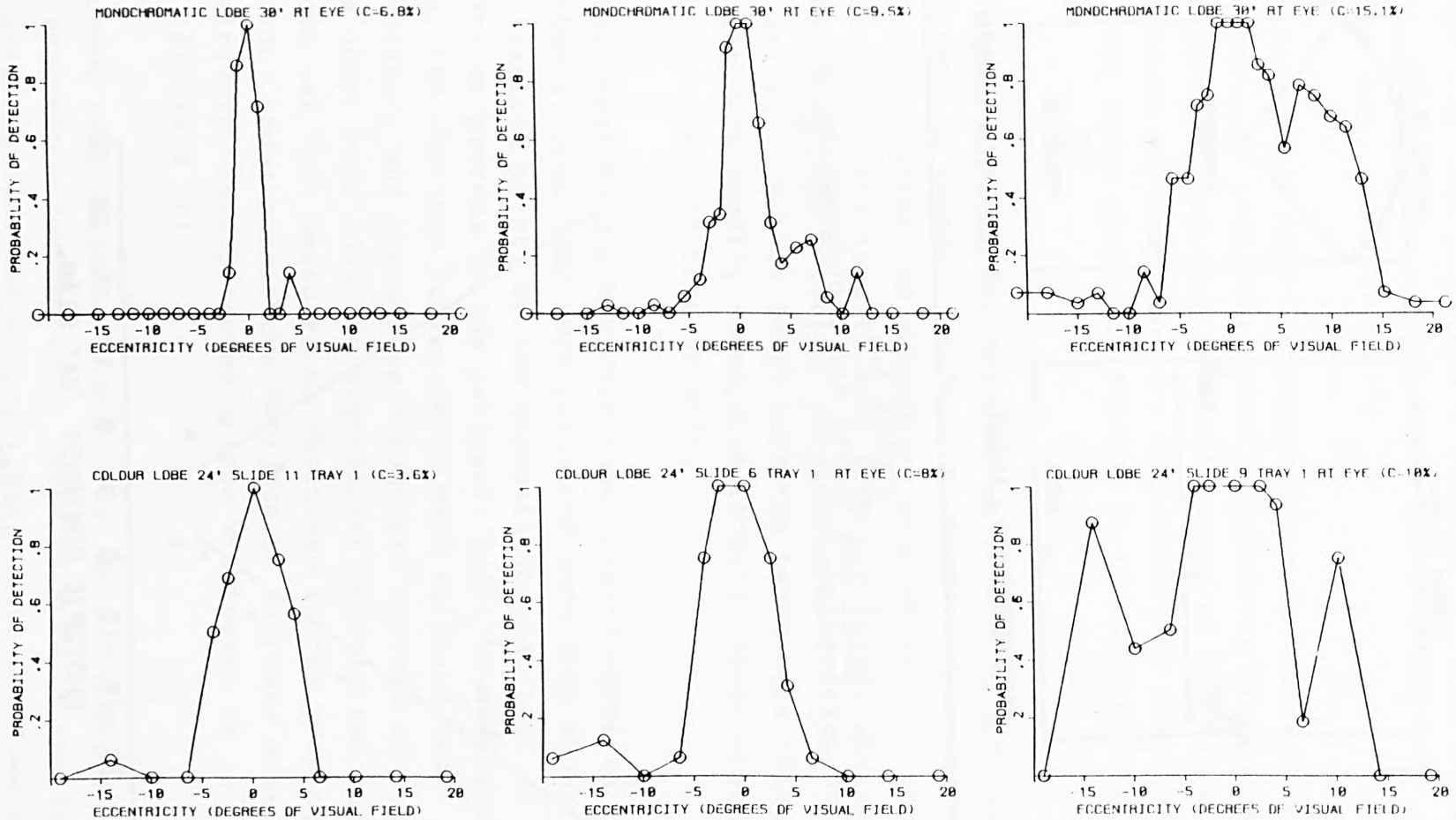

FIGURE 5.1

Visual lobes described in this chapter compared with those of chapter 3. Both are results with the right eye only, those in the upper row are from the 27 point lobes of chapter 3, selected to span the contrast range of those in the lower row.

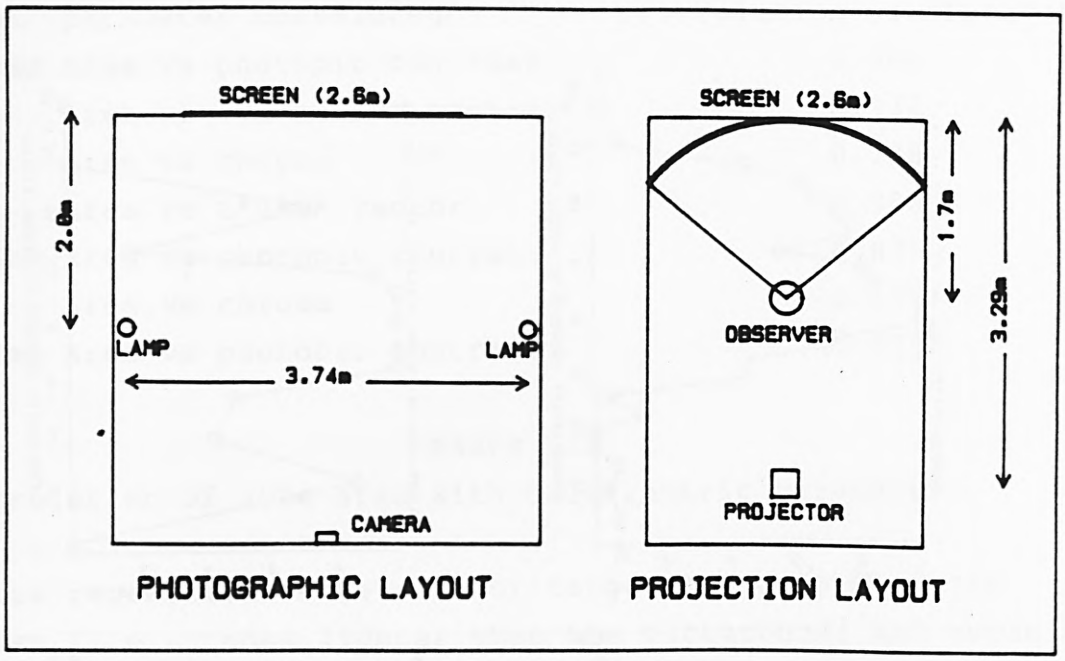

FIGURE 5.2

Layout of camera and lights for photographing the samples, and of observation room.

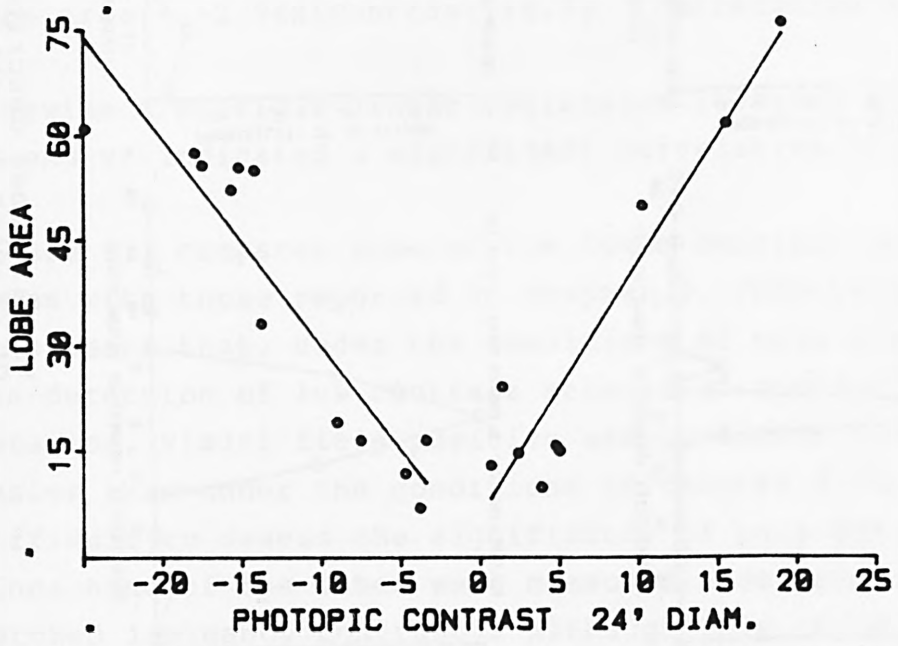

FIGURE 5.3

Correlation of area under each lobe with the luminance contrast of its target. plotted as %). Separate least squares straight lines have been fitted to the positive and negative contrast points.

remarkable than the differences. It will be noted that the rate of change of lobe area with contrast calculated here is higher than that indicated in chapter 3. (2.94 compared with 1.46). However the current lobes are measured with a smaller target size, and binocularly.

Thus it appears that 'Luminance Contrast' is overwhelmingly the dominant colorimetric factor affecting the probability of detection, and over the small range of luminance difference explored, the use of positive or negative contrast makes little difference to the size of the visual lobe.

The shape of the lobes measured in this work and those described in chapter 3 were by no means simple bell shaped curves, but often had subsidiary regions of high probability of detection for targets away from the fovea. The subsidiary peaks, when they occurred, were at eccentricities between 10^{o} and 14^{o}. In this later work the peaks were often at 10^{o} but for very readily detectable targets, peaks appeared at greater eccentricities as well.

It was observed subjectively that targets appeared achromatic when they were presented more than about 10^{o} from the fixation point. On the supposition that part of the detection process in the periphery might be mediated by rods, the scotopic luminance of each surround was calculated, and the scotopic contrast correlated with the area under each lobe. No significant correlation was found. A lobe was then measured as described in the previous section, under conditions designed to suppress cone sensitivity. This produced a lobe with peaks at 10^{o} and at 30^{o} (figure 5.26).

It seems reasonable to suppose that some rod activity might be responsible for the outer peaks of some of the lobes measured. Aguilar and Stiles (1954) quote the zone of maximum rod sensitivity as being 8^{o} to 15^{o}, in good agreement with the zone of the inner lobules found here. The

fact that such lobules were found during the earlier part of the project at retinal illuminances of up to 4 log trolands is more surprising. Oesterberg (1935) measured the maximum number of rods per unit area at about 20^{o} (see figure 1.4). Zrenner(1983) reports an increase in the proportion of phasic to tonic ganglion cells towards the periphery. Rovamo and Raninen (1984) report a maximum value of Critical Flicker Frequency at about 55^{o} eccentricity (for a constant stimulus size and luminance). It is clearly possible that some combination of responses from rods and cones could produce the shape of lobes presented here, or that the variation of temporal response properties across the retina may be a factor, since the targets appeared and disappeared abruptly. Brogan (1987) has also shown lobes with subsidiary peaks in his work on search. In this case they are at 4^{o} to 8^{o} eccentricity.

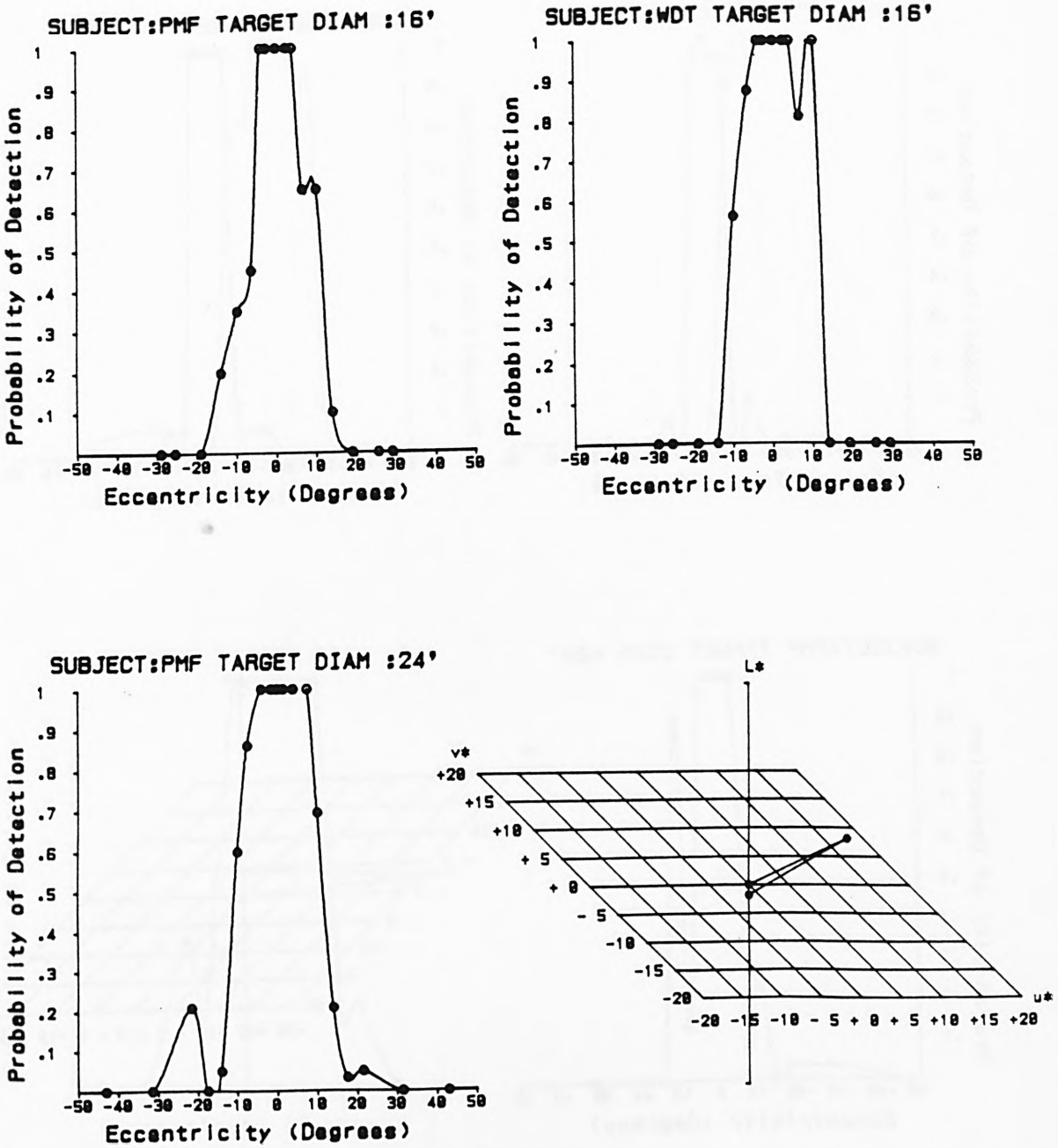

FIGURE 5.4

Visual lobes for 16' diameter stimulus for subject PMF compared with those for a 24' stimulus for PMF and a 16' stimulus for subject WDT. The fourth quadrant shows the relation of the colour of the stimulus to that of its immediate surround, in L* U* V* uniform chromaticity space.

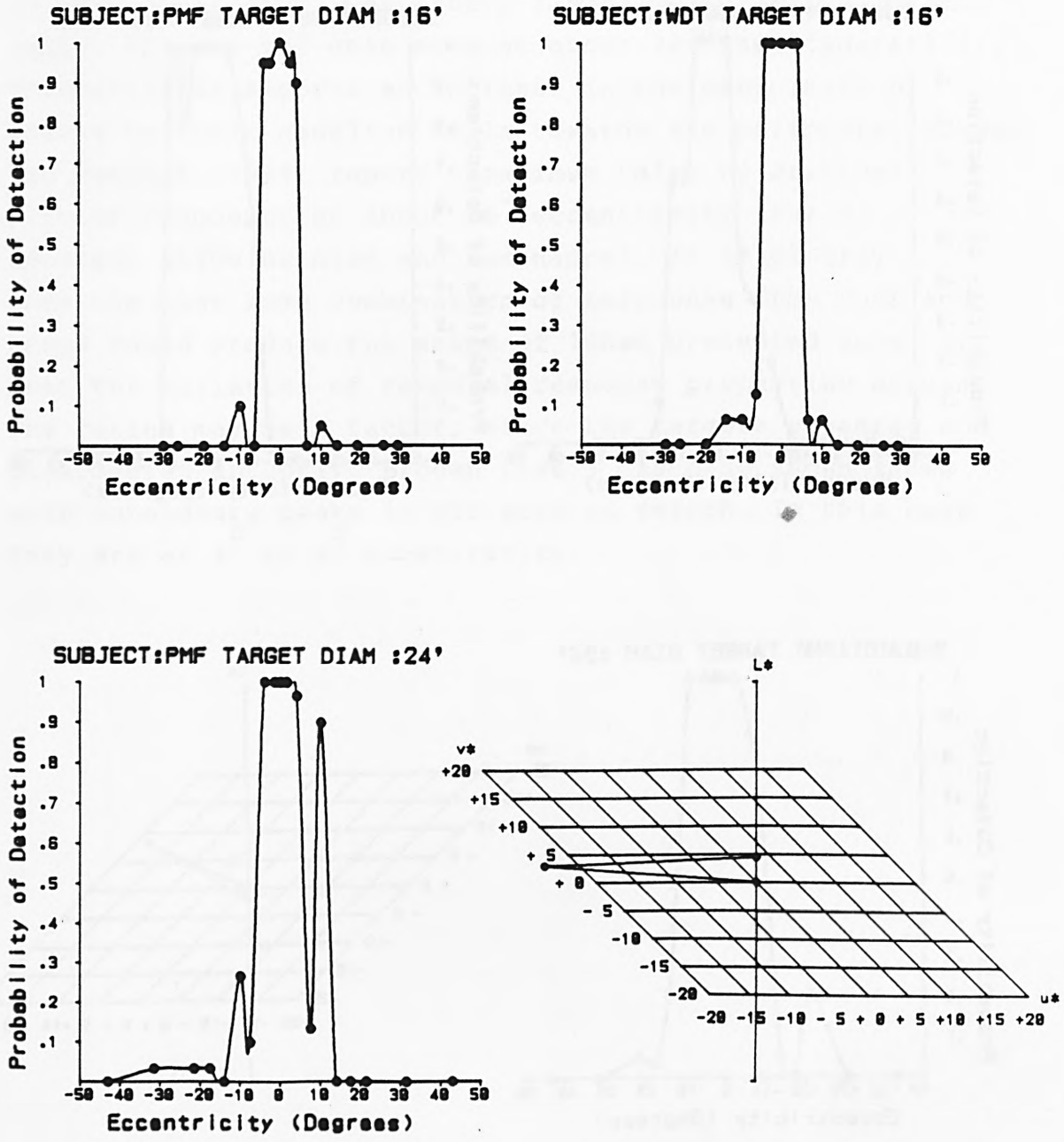

FIGURE 5.5
Visual lobes for 16' diameter stimulus for subject PMF compared with those for a 24' stimulus for PMF and a 16' stimulus for subject WDT. The fourth quadrant shows the relation of the colour of the stimulus to that of its immediate surround, in L* U* V* uniform chromaticity space.

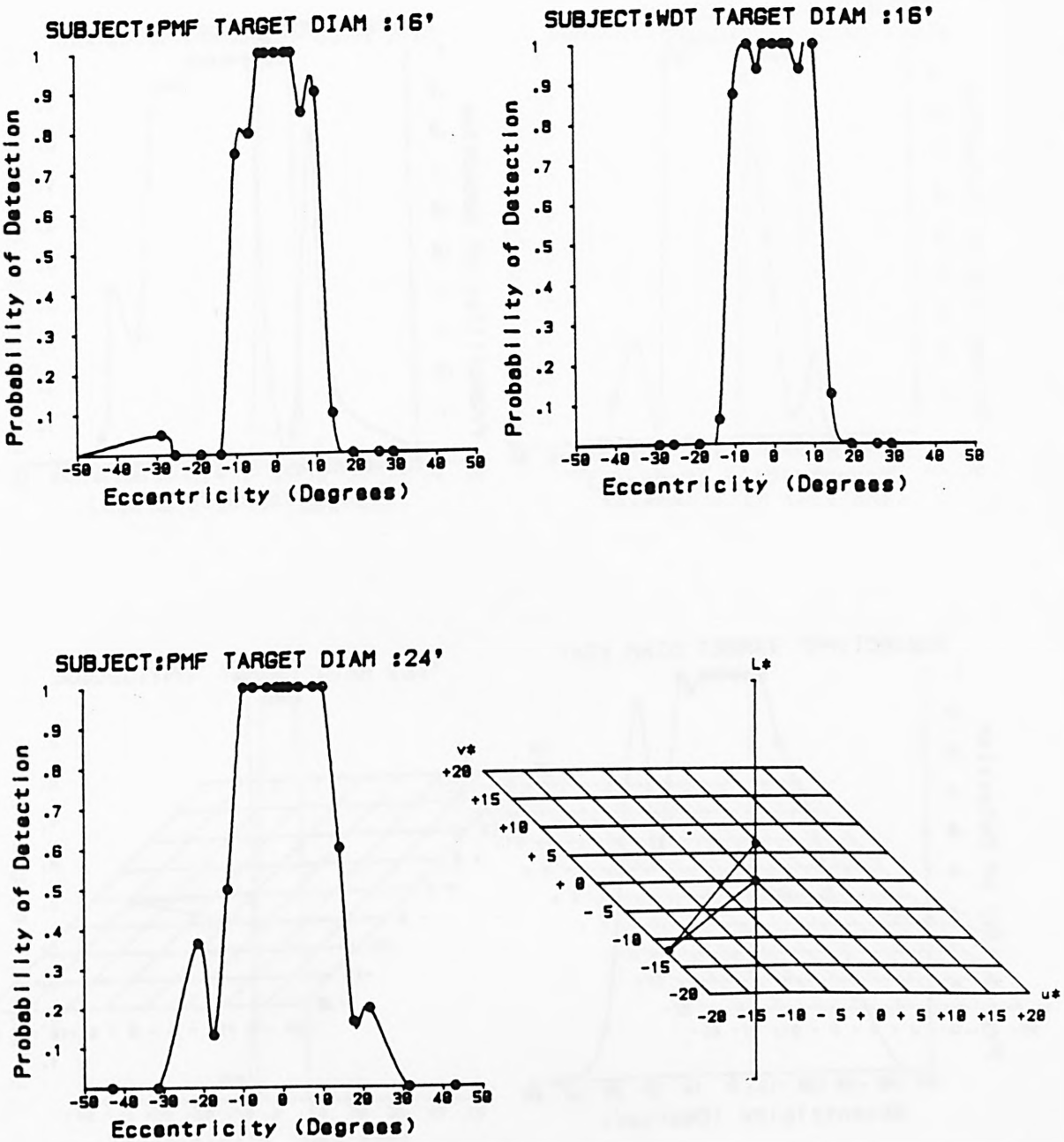

FIGURE 5.6
Visual lobes for 16' diameter stimulus for subject PMF compared with those for a 24' stimulus for PMF and a 16' stimulus for subject WDT. The fourth quadrant shows the relation of the colour of the stimulus to that of its immediate surround, in L* U* V* uniform chromaticity space.

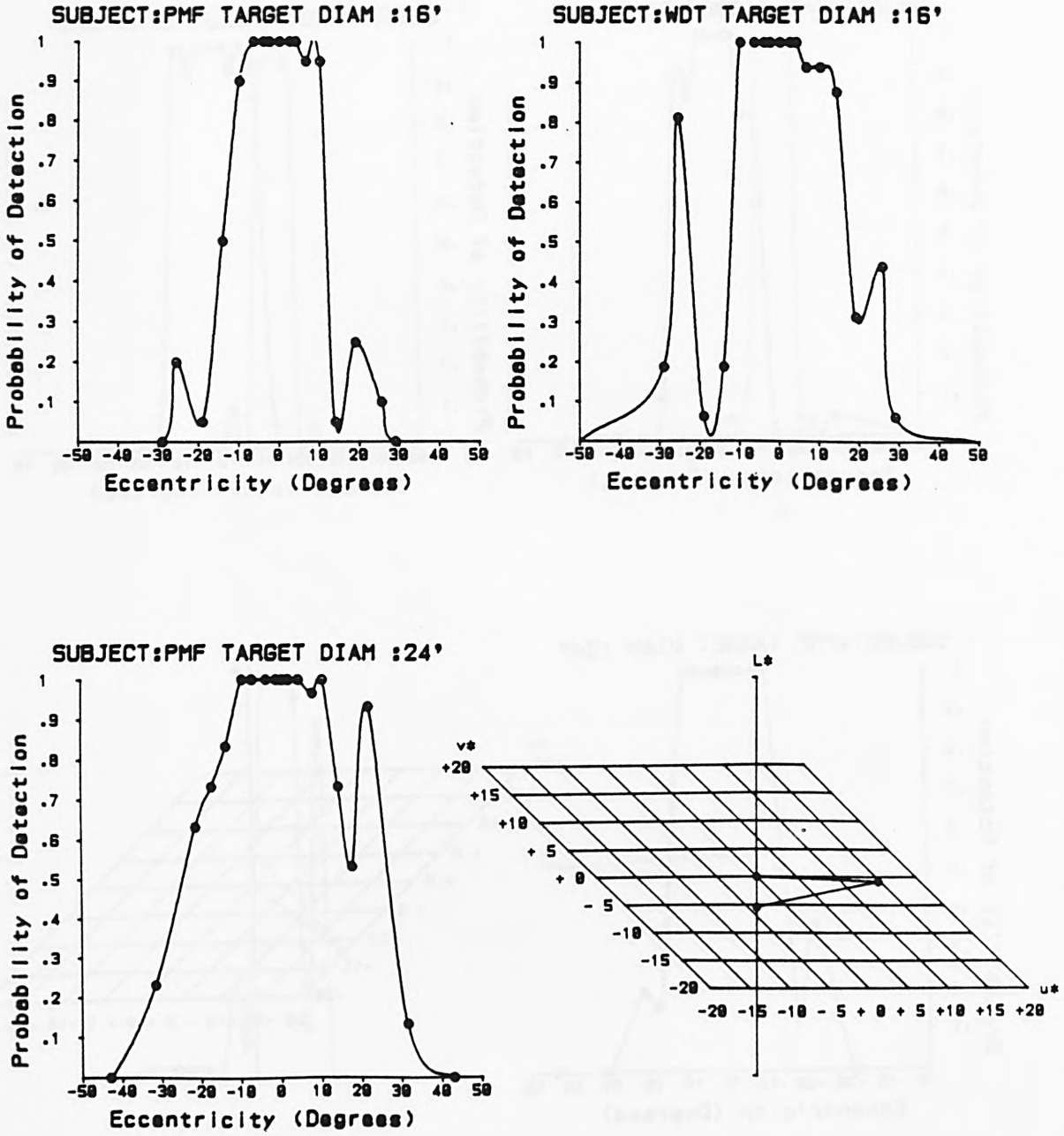

FIGURE 5.7
Visual lobes for 16' diameter stimulus for subject PMF compared with those for a 24' stimulus for PMF and a 16' stimulus for subject WDT. The fourth quadrant shows the relation of the colour of the stimulus to that of its immediate surround, in L* U* V* uniform chromaticity space.

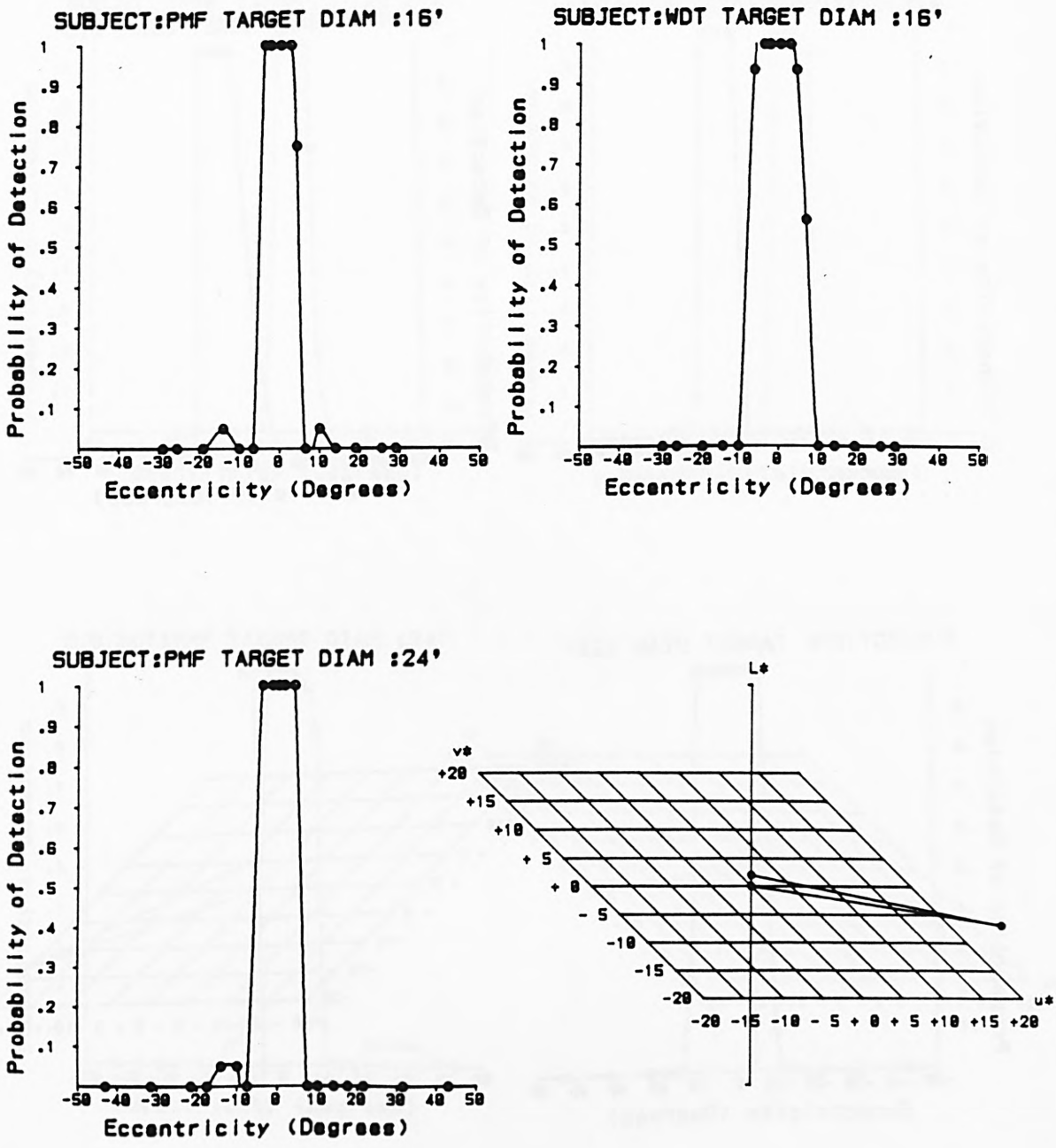

FIGURE 5.8
Visual lobes for 16' diameter stimulus for subject PMF compared with those for a 24' stimulus for PMF and a 16' stimulus for subject WDT. The fourth quadrant shows the relation of the colour of the stimulus to that of its immediate surround, in L* U* V* uniform chromaticity space.

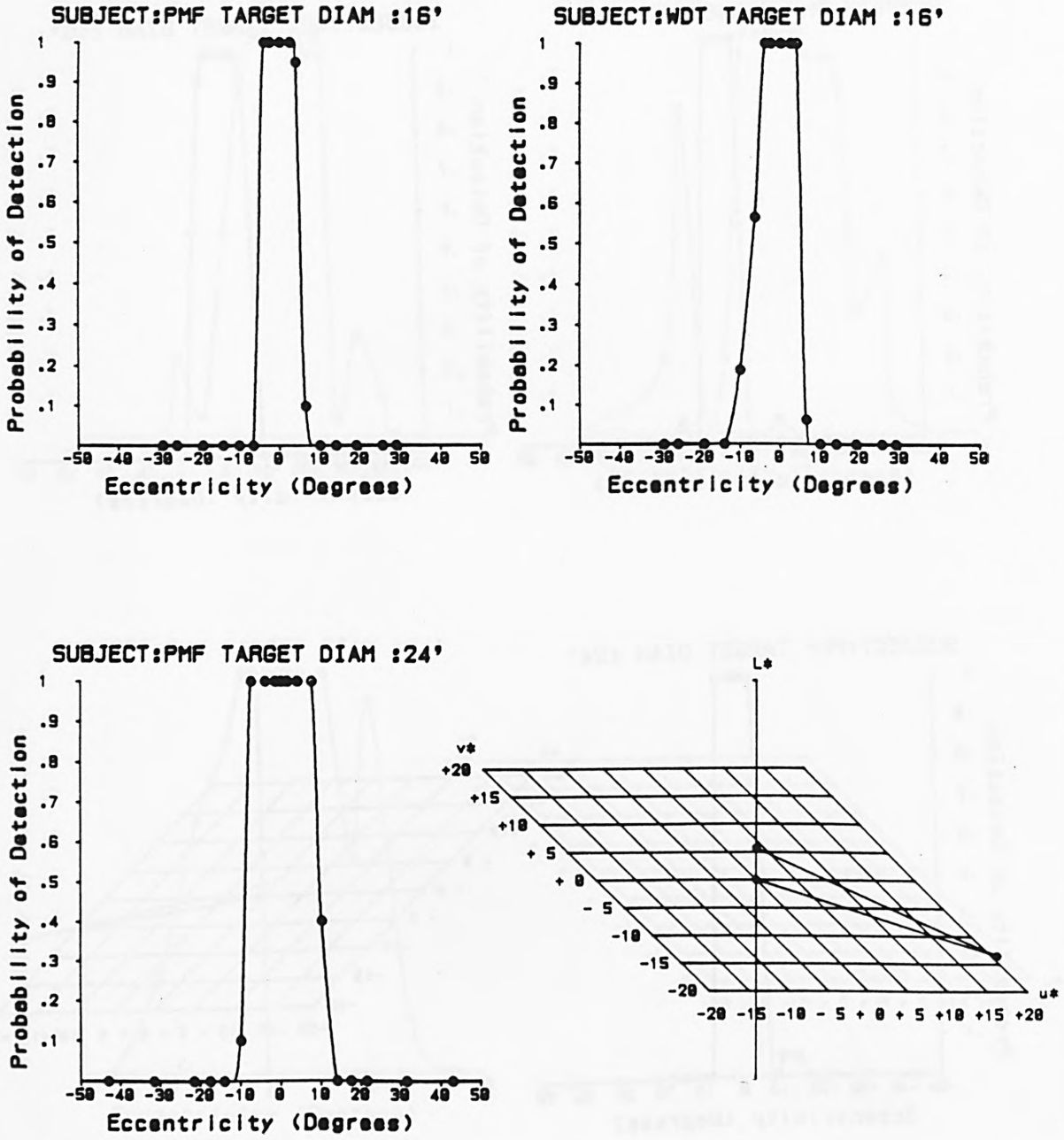

FIGURE 5.9
Visual lobes for 16' diameter stimulus for subject PMF compared with those for a 24' stimulus for PMF and a 16' stimulus for subject WDT. The fourth quadrant shows the relation of the colour of the stimulus to that of its immediate surround, in L* U* V* uniform chromaticity space.

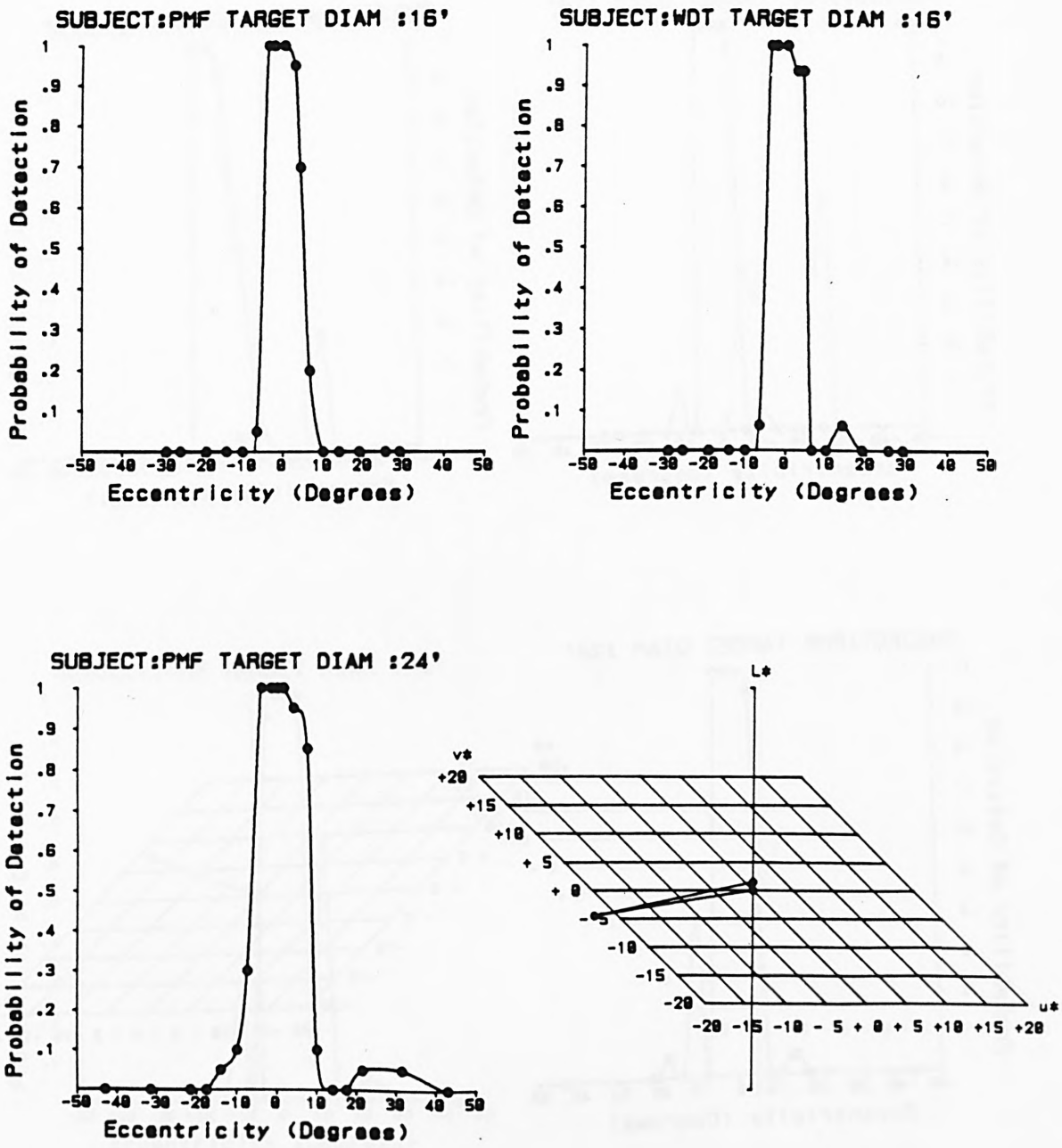

FIGURE 5.10
Visual lobes for 16' diameter stimulus for subject PMF compared with those for a 24' stimulus for PMF and a 16' stimulus for subject WDT. The fourth quadrant shows the relation of the colour of the stimulus to that of its immediate surround, in L* U* V* uniform chromaticity space.

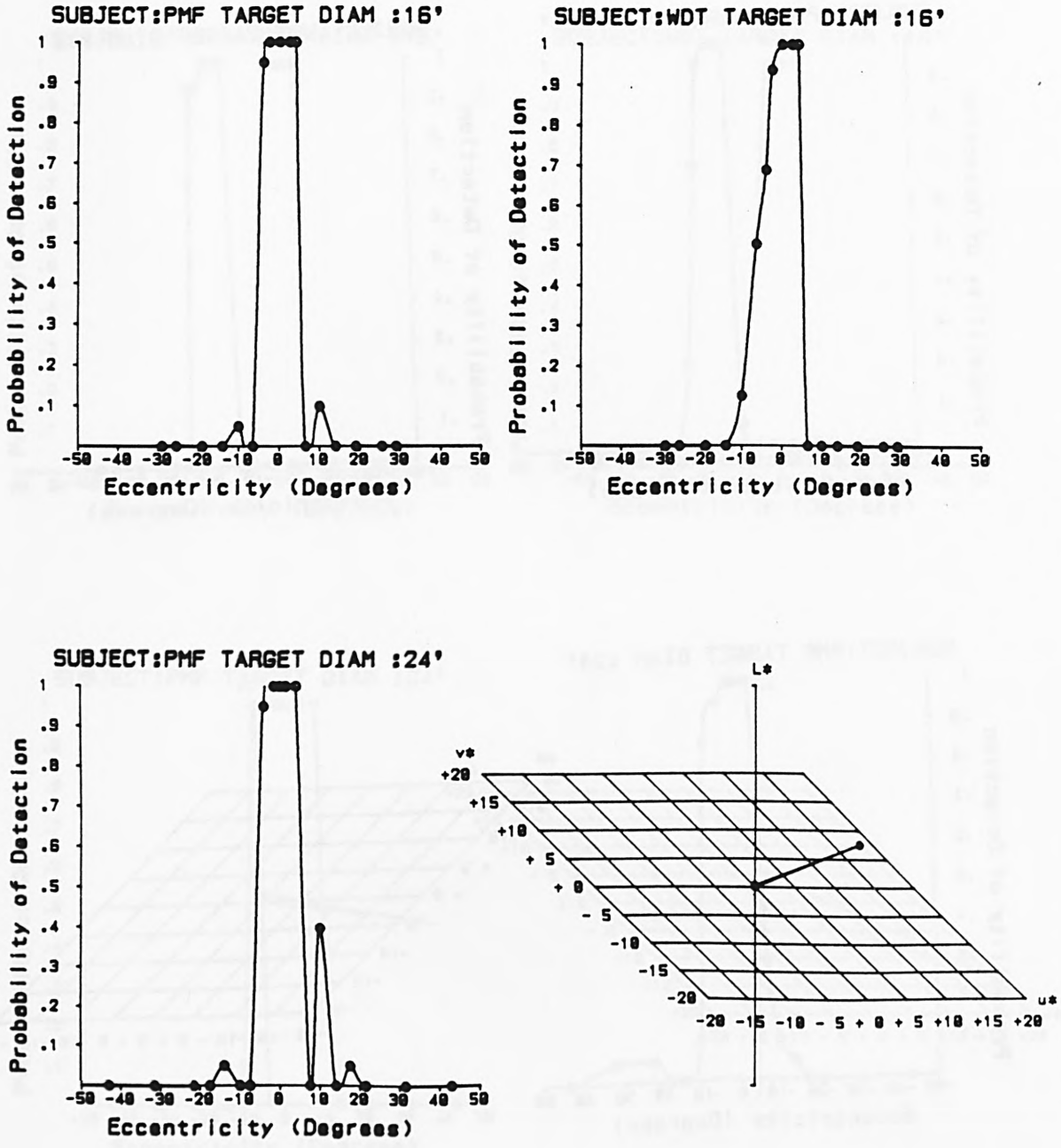

FIGURE 5.11
Visual lobes for 16' diameter stimulus for subject PMF compared with those for a 24' stimulus for PMF and a 16' stimulus for subject WDT. The fourth quadrant shows the relation of the colour of the stimulus to that of its immediate surround, in L* U* V* uniform chromaticity space.

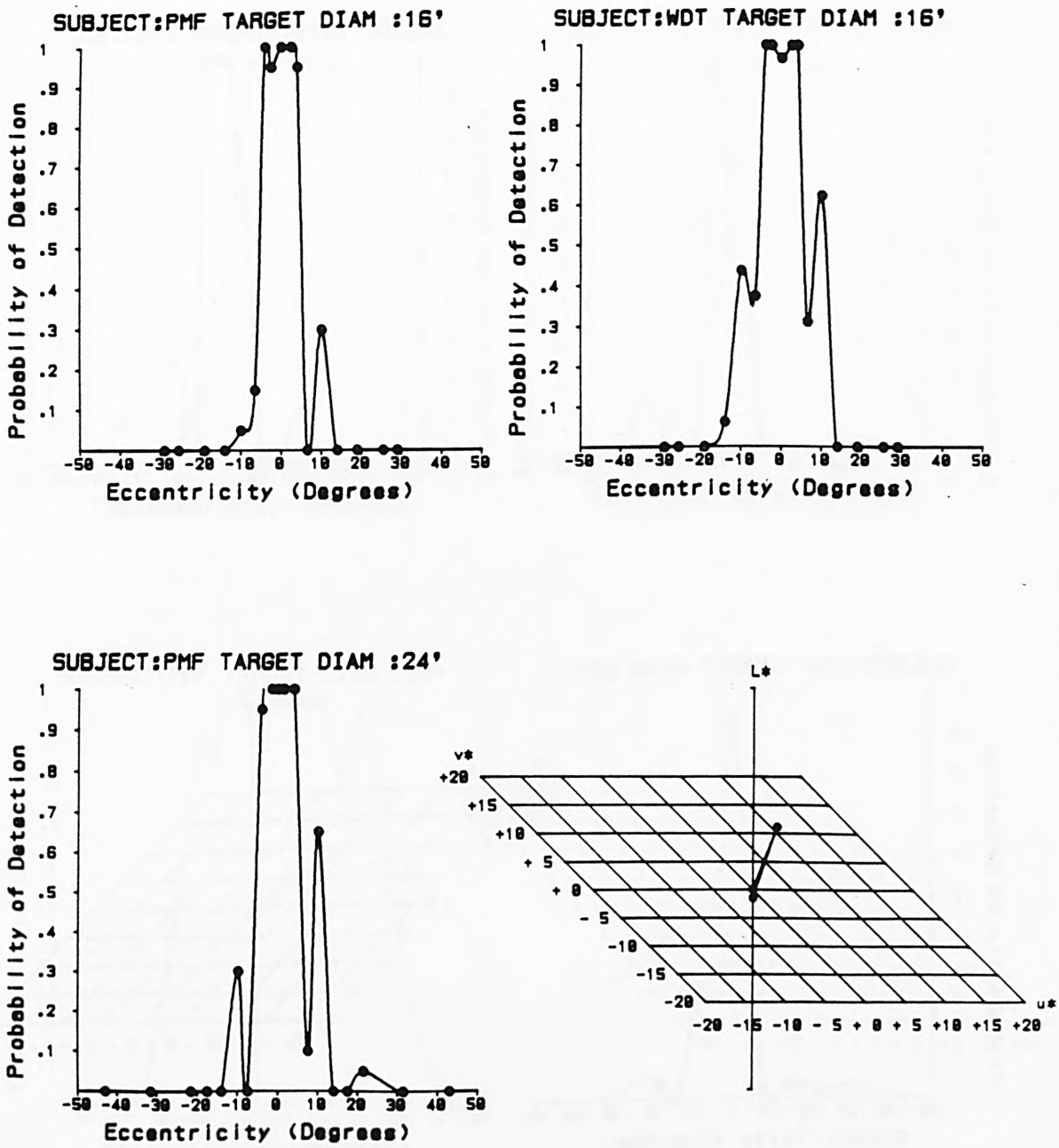

FIGURE 5.12
Visual lobes for 16' diameter stimulus for subject PMF compared with those for a 24' stimulus for PMF and a 16' stimulus for subject WDT. The fourth quadrant shows the relation of the colour of the stimulus to that of its immediate surround, in L* U* V* uniform chromaticity space.

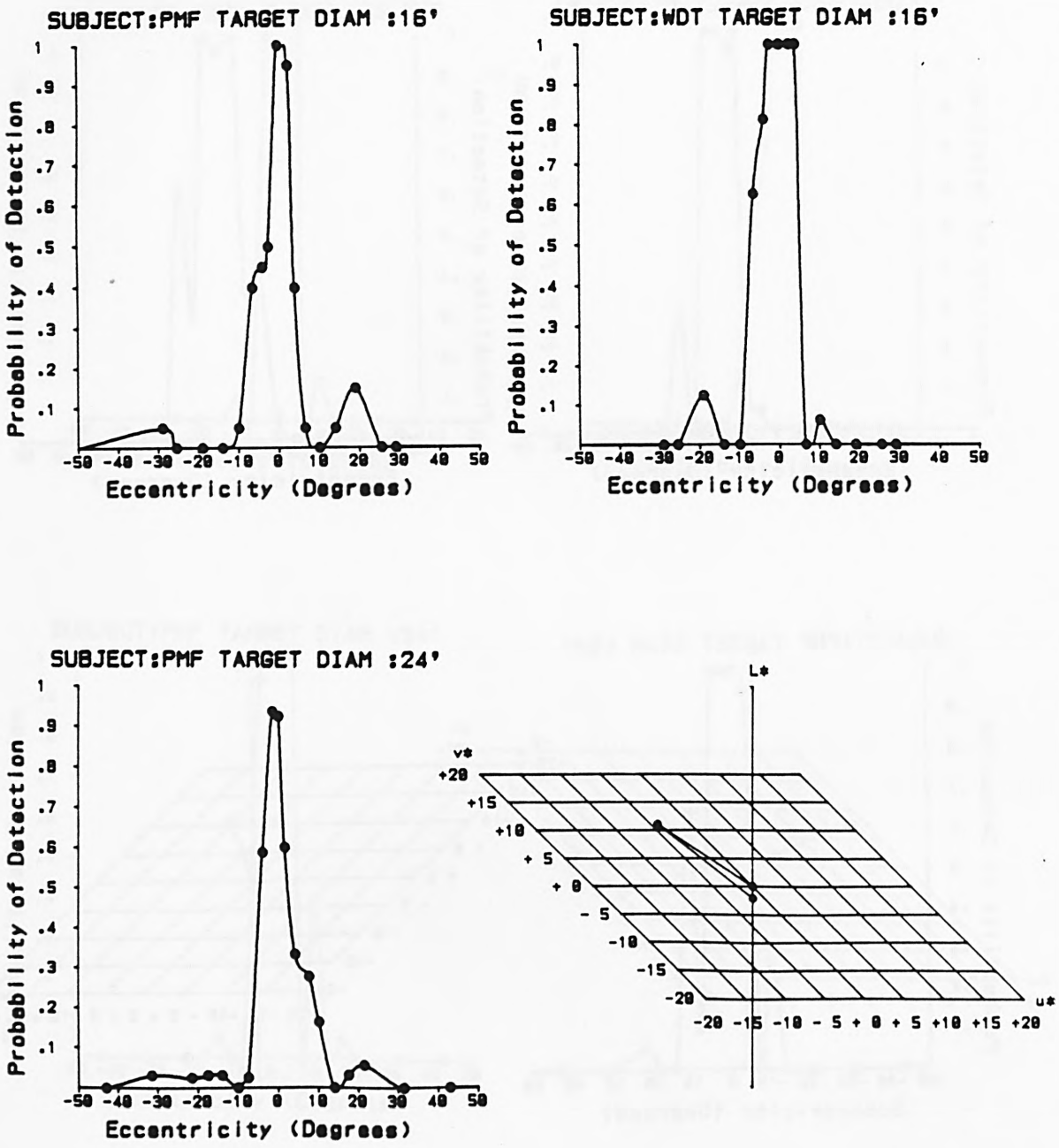

FIGURE 5.13
Visual lobes for 16' diameter stimulus for subject PMF compared with those for a 24' stimulus for PMF and a 16' stimulus for subject WDT. The fourth quadrant shows the relation of the colour of the stimulus to that of its immediate surround, in L* U* V* uniform chromaticity space.

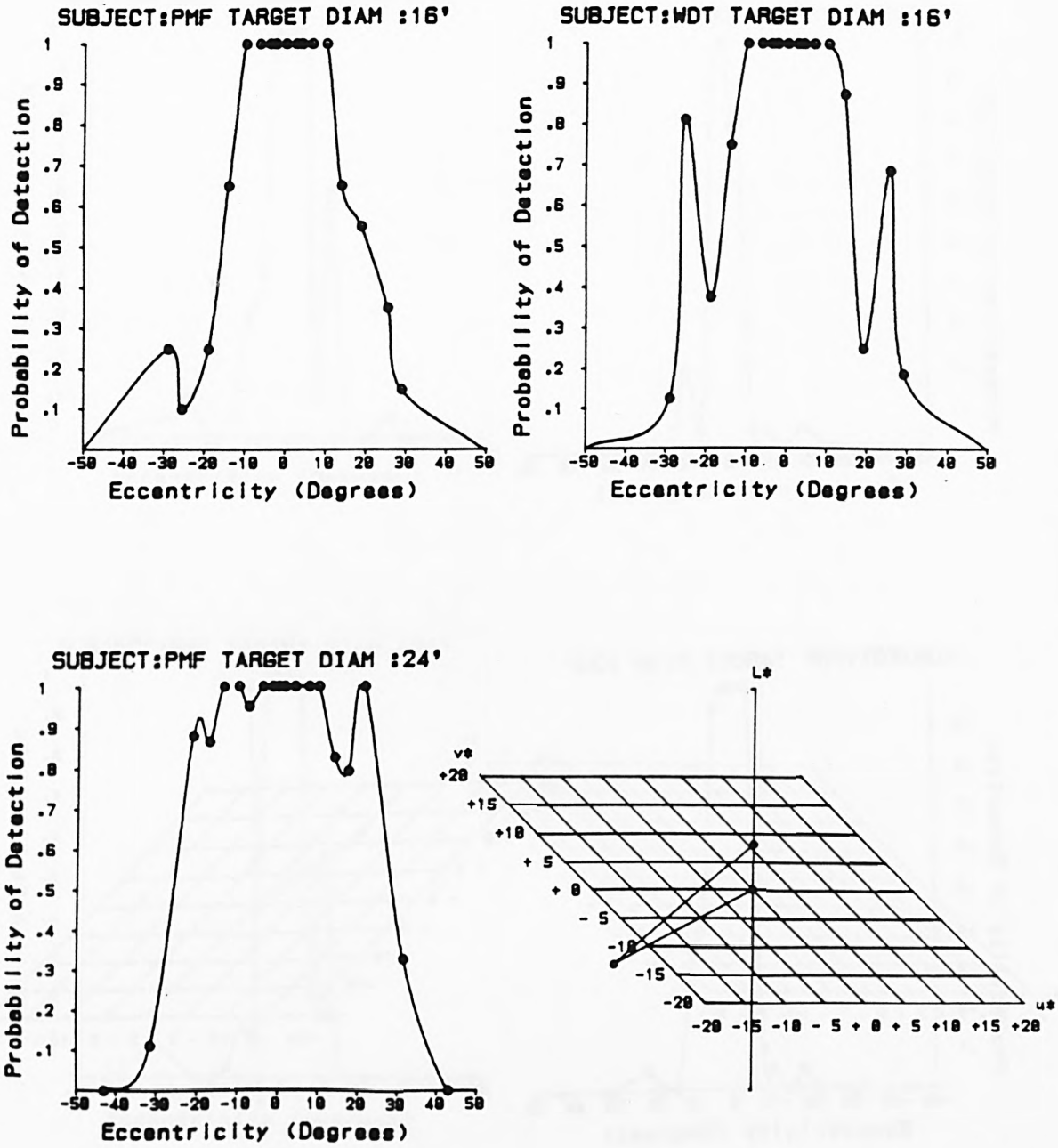

FIGURE 5.14
Visual lobes for 16' diameter stimulus for subject PMF compared with those for a 24' stimulus for PMF and a 16' stimulus for subject WDT. The fourth quadrant shows the relation of the colour of the stimulus to that of its immediate surround, in L* U* V* uniform chromaticity space.

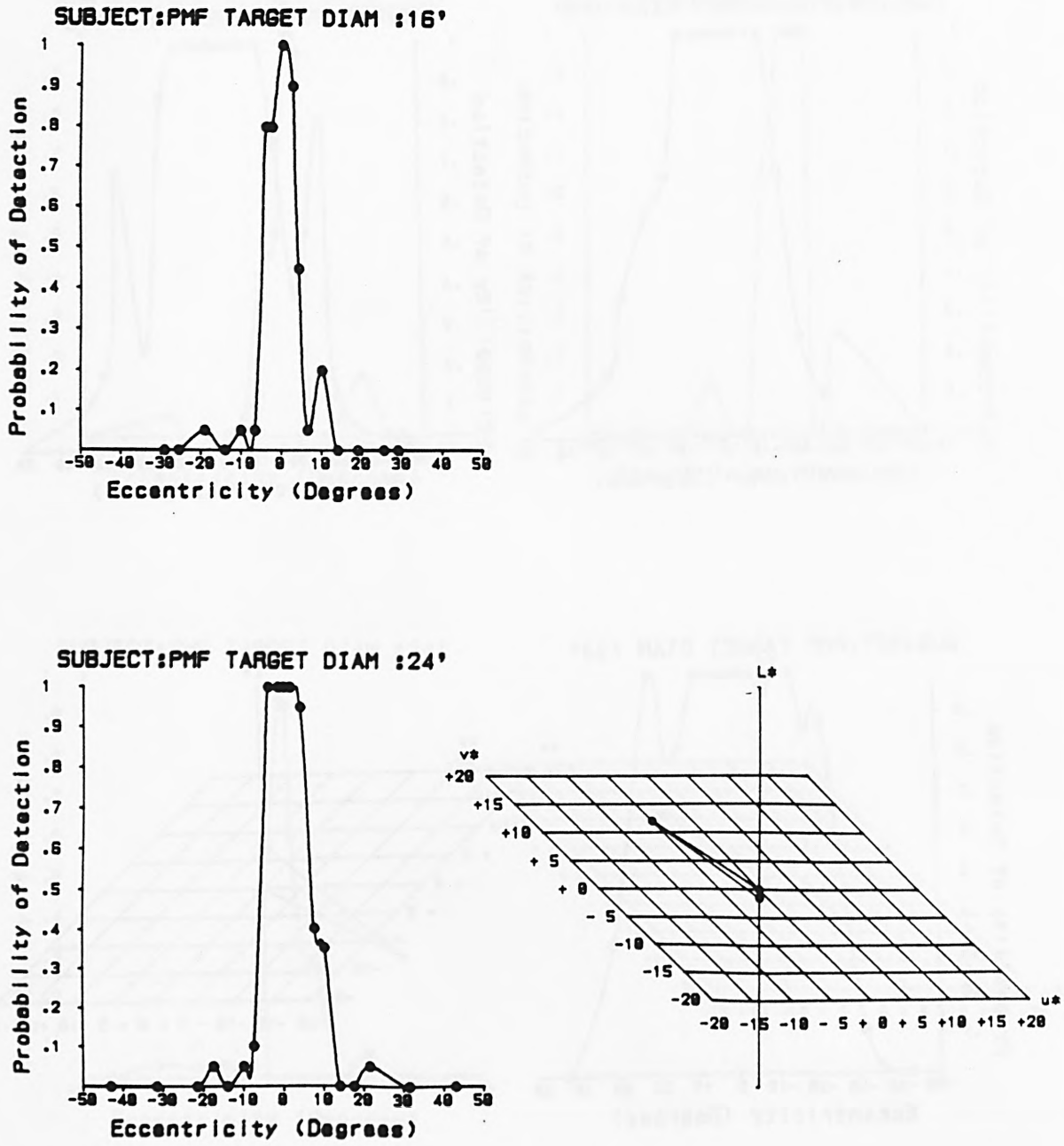

FIGURE 5.15
Visual lobes for 16' diameter stimulus for subject PMF compared with those for a 24' stimulus. The fourth quadrant shows the relation of the colour of the stimulus to that of its immediate surround, in L* U* V* uniform chromaticity space.

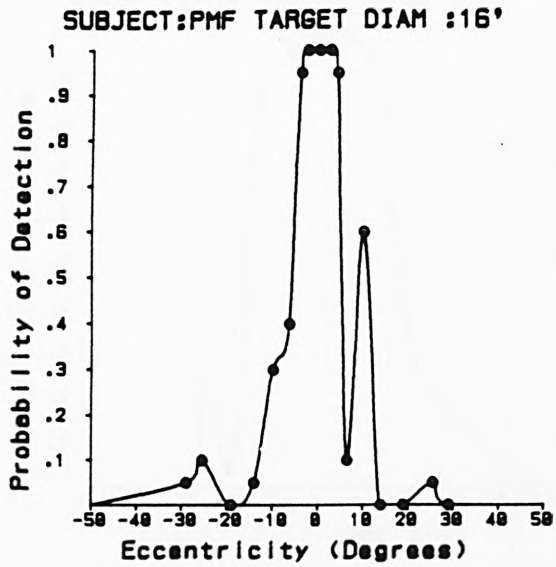

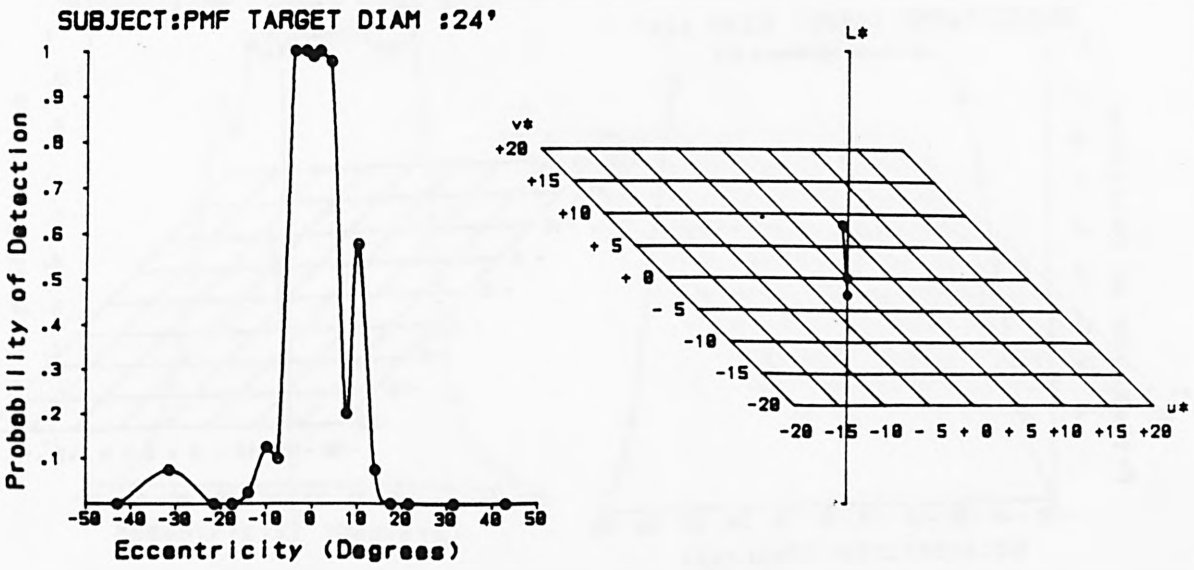

FIGURE 5.16
Visual lobes for 16' diameter stimulus for subject PMF compared with those for a 24' stimulus. The fourth quadrant shows the relation of the colour of the stimulus to that of its immediate surround, in L* U* V* uniform chromaticity space.

SLIDE 7. TRAY 2

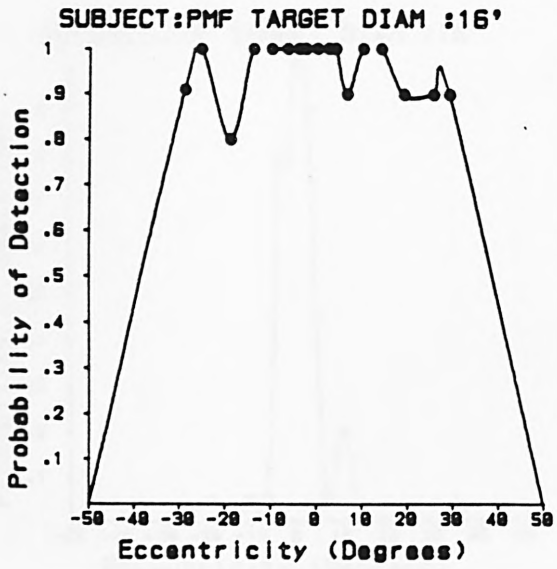

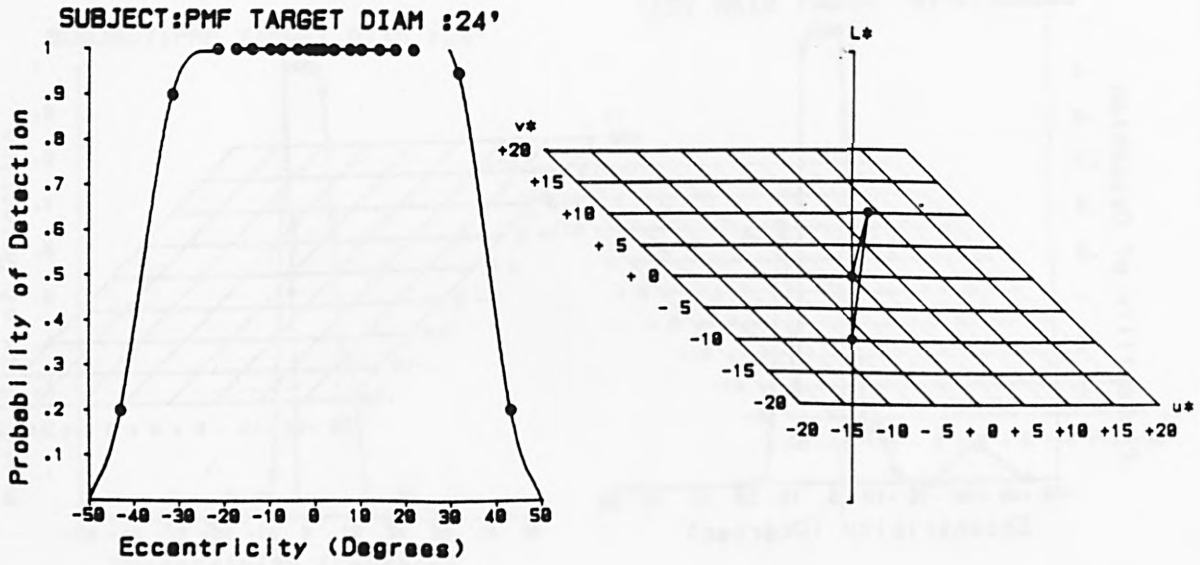

FIGURE 5.17
Visual lobes for 16' diameter stimulus for subject PMF compared with those for a 24' stimulus. The fourth quadrant shows the relation of the colour of the stimulus to that of its immediate surround, in L* U* V* uniform chromaticity space.

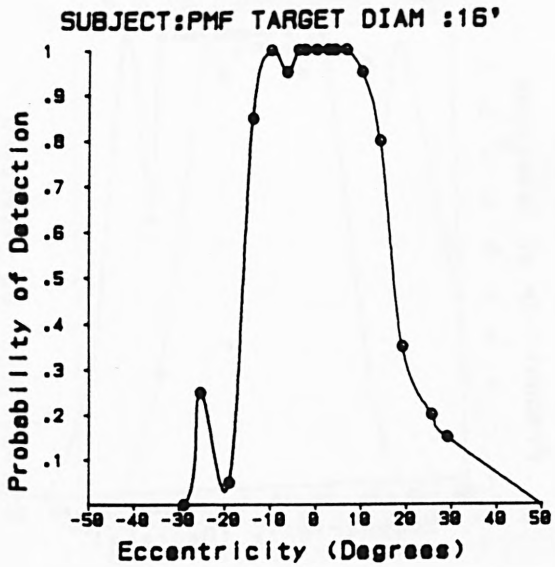

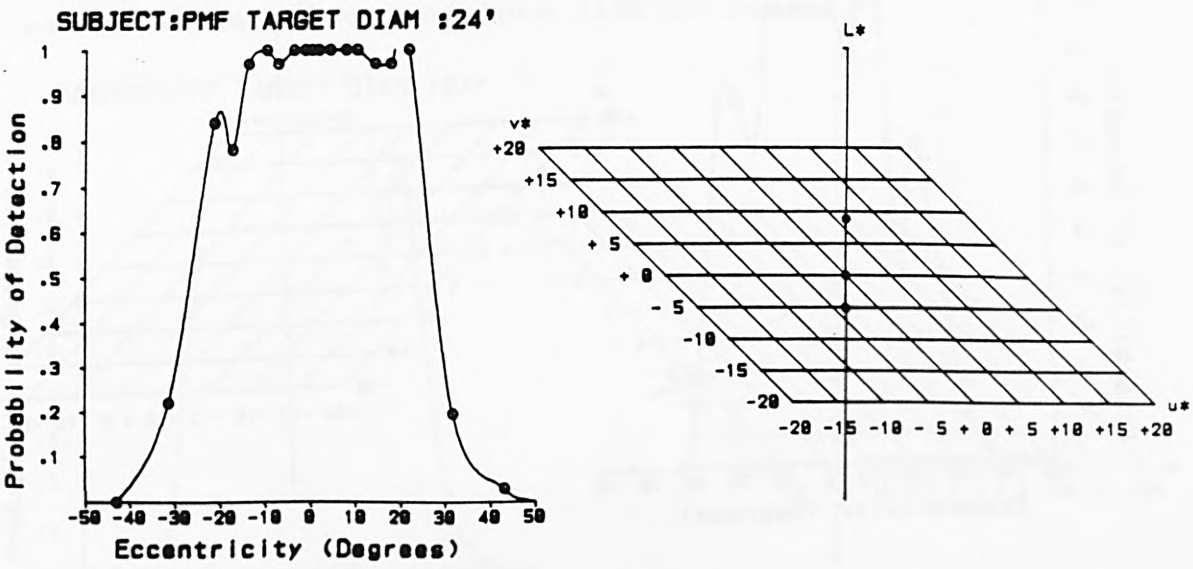

FIGURE 5.18
Visual lobes for 16' diameter stimulus for subject PMF compared with those for a 24' stimulus. The fourth quadrant shows the relation of the colour of the stimulus to that of its immediate surround, in L* U* V* uniform chromaticity space.

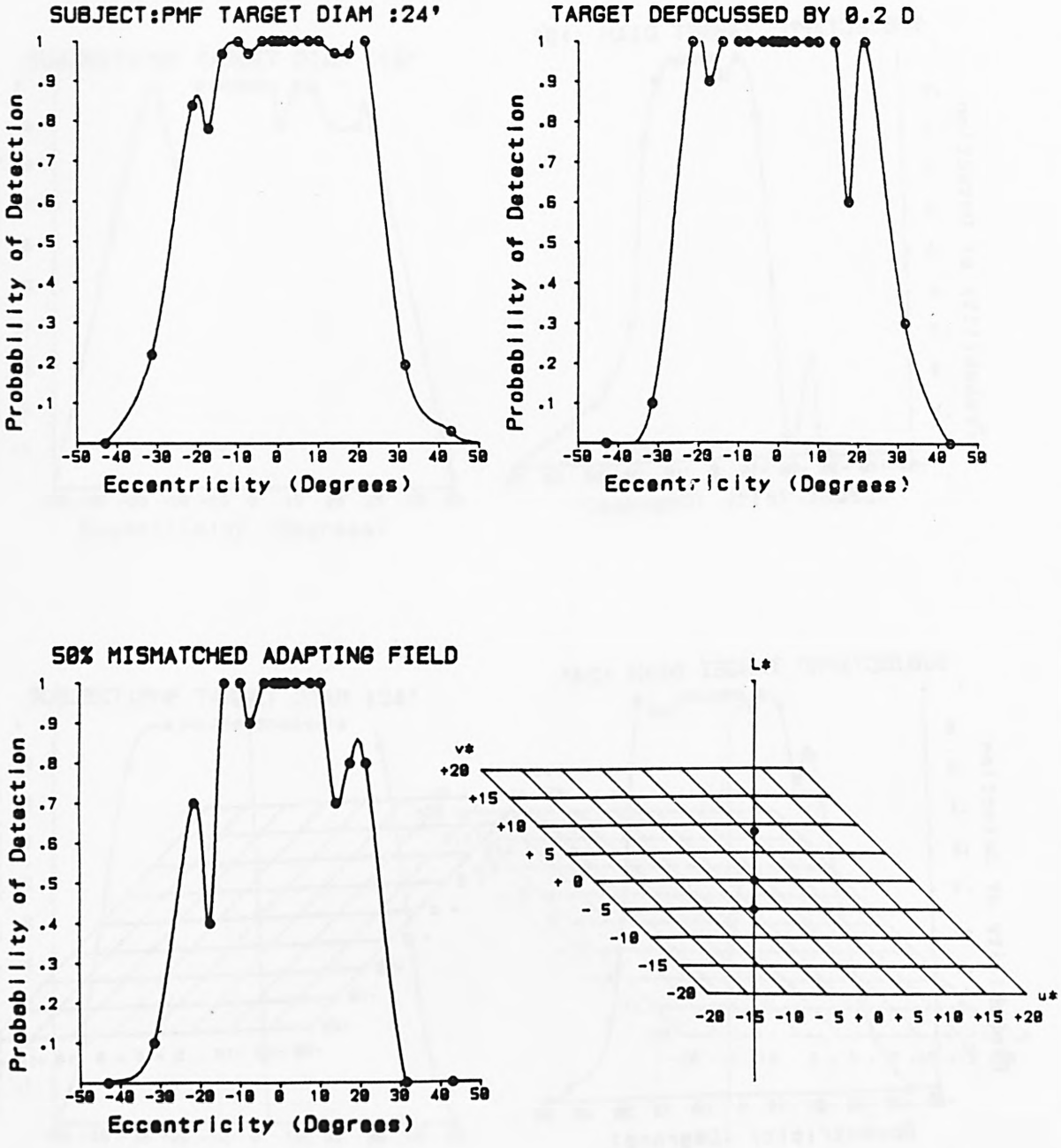

FIGURE 5.19

The effect of errors of focus and of luminance mismatch. Visual lobe for a 24' diameter stimulus for subject PMF compared with that for the same stimulus but deliberately projected defocussed by .2 Dioptres, and for the same stimulus, but with the adapting field slide deliberately projected with a luminance 50% greater than that of the stimulus surround. (This does not affect the spectral distribution of the stimulus or its surround.)

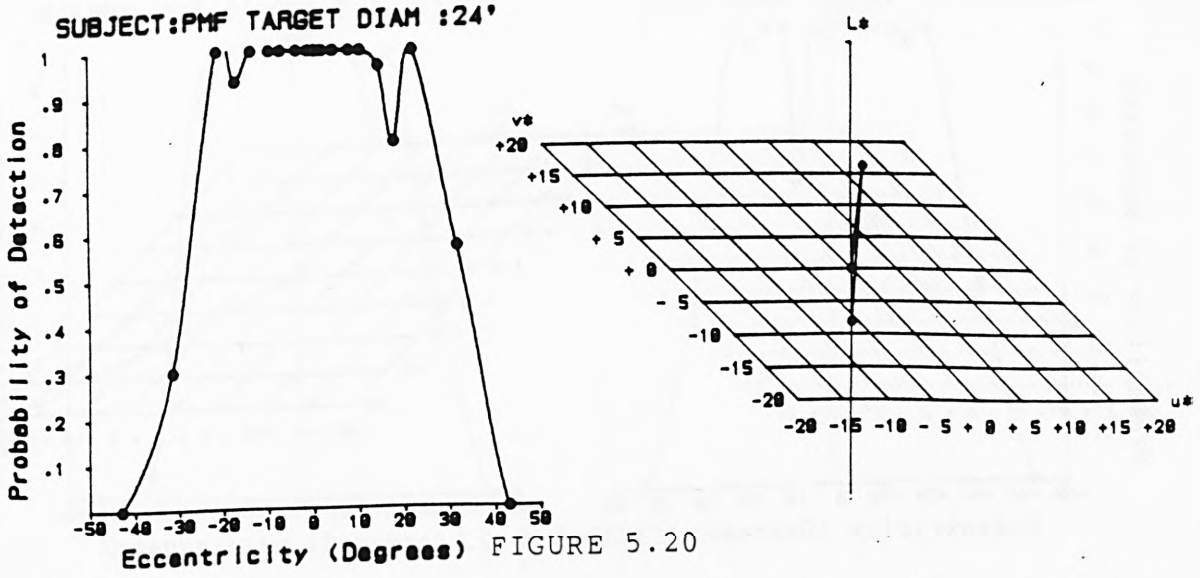

FIGURE 5.20

Visual lobe for a 24´ diameter stimulus for subject PMF and a plot showing the relation of the colour of the stimulus to that of its immediate surround, in L*U*V* uniform chromaticity space. This stimulus was then discarded as it was close in colour and lobe size to others.

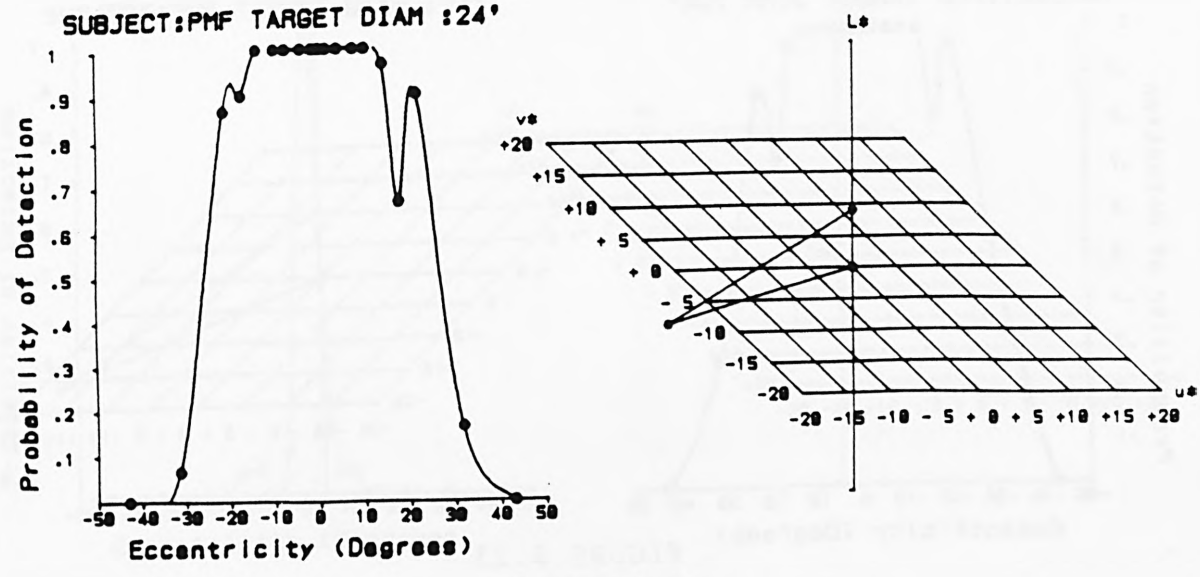

FIGURE 5.21

Visual lobe for a 24´ diameter stimulus for subject PMF and a plot showing the relation of the colour of the stimulus to that of its immediate surround, in L*U*V* uniform chromaticity space. This stimulus was then discarded as it was close in colour and lobe size to others.

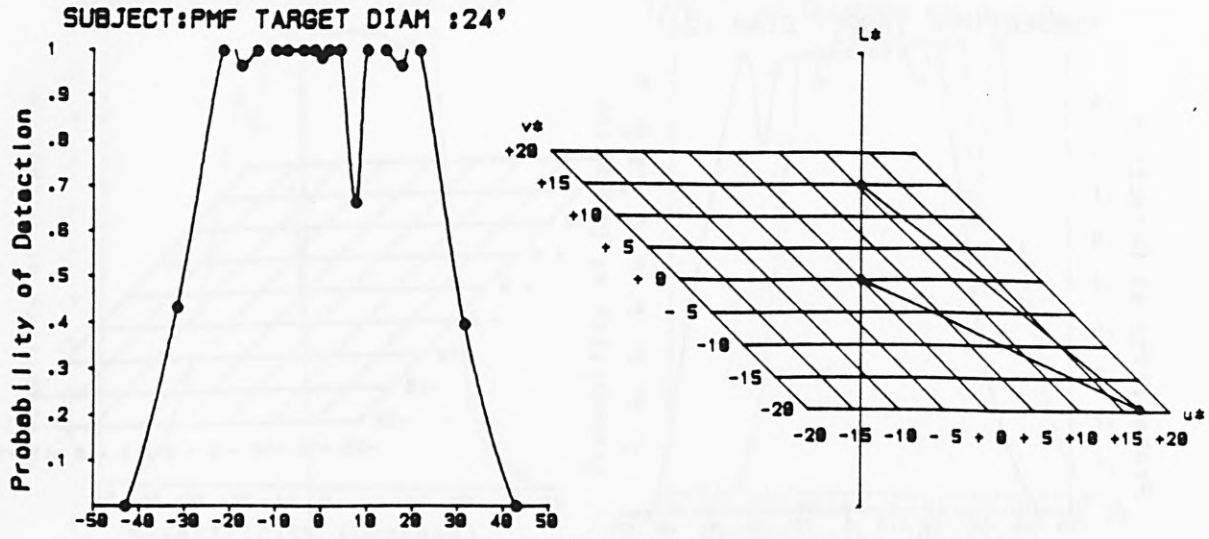

FIGURE 5.22

Visual lobe for a 24´ diameter stimulus for subject PMF and a plot showing the relation of the colour of the stimulus to that of its immediate surround, in L*U*V* uniform chromaticity space. This stimulus was then discarded as it was close in colour and lobe size to others.

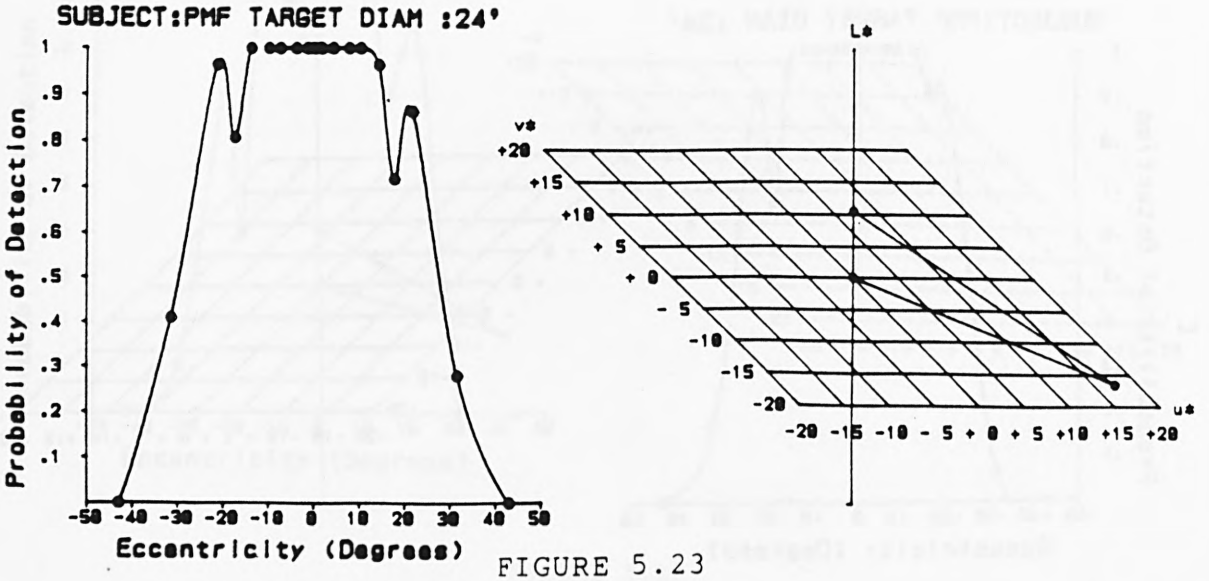

FIGURE 5.23

Visual lobe for a 24´ diameter stimulus for subject PMF and a plot showing the relation of the colour of the stimulus to that of its immediate surround, in L*U*V* uniform chromaticity space. This stimulus was then discarded as it was close in colour and lobe size to others.

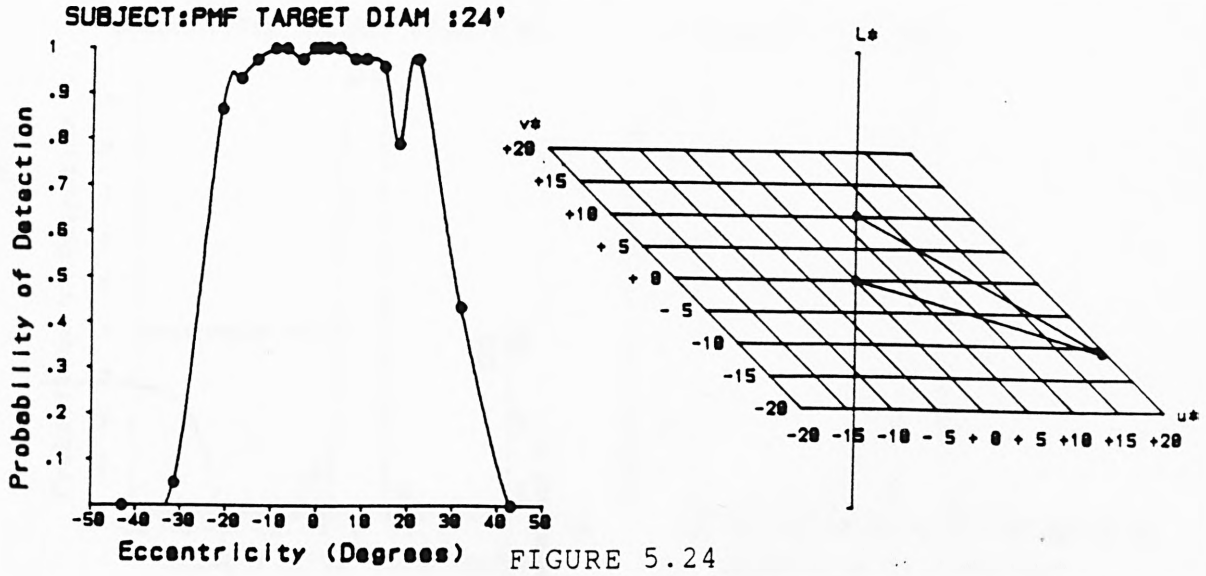

FIGURE 5.24

Visual lobe for a 24´ diameter stimulus for subject PMF and a plot showing the relation of the colour of the stimulus to that of its immediate surround, in L*U*V* uniform chromaticity space. This stimulus was then discarded as it was close in colour and lobe size to others.

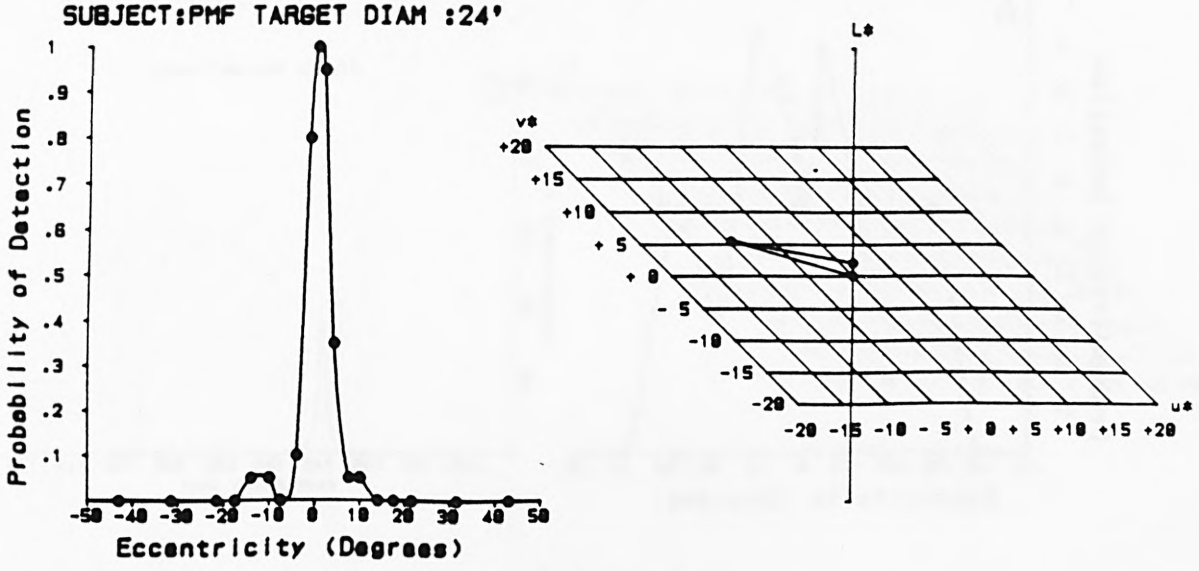

FIGURE 5.25

Visual lobe for a 24´ diameter stimulus for subject PMF and a plot showing the relation of the colour of the stimulus to that of its immediate surround, in L*U*V* uniform chromaticity space. This stimulus was then discarded as it was close in colour and lobe size to others.

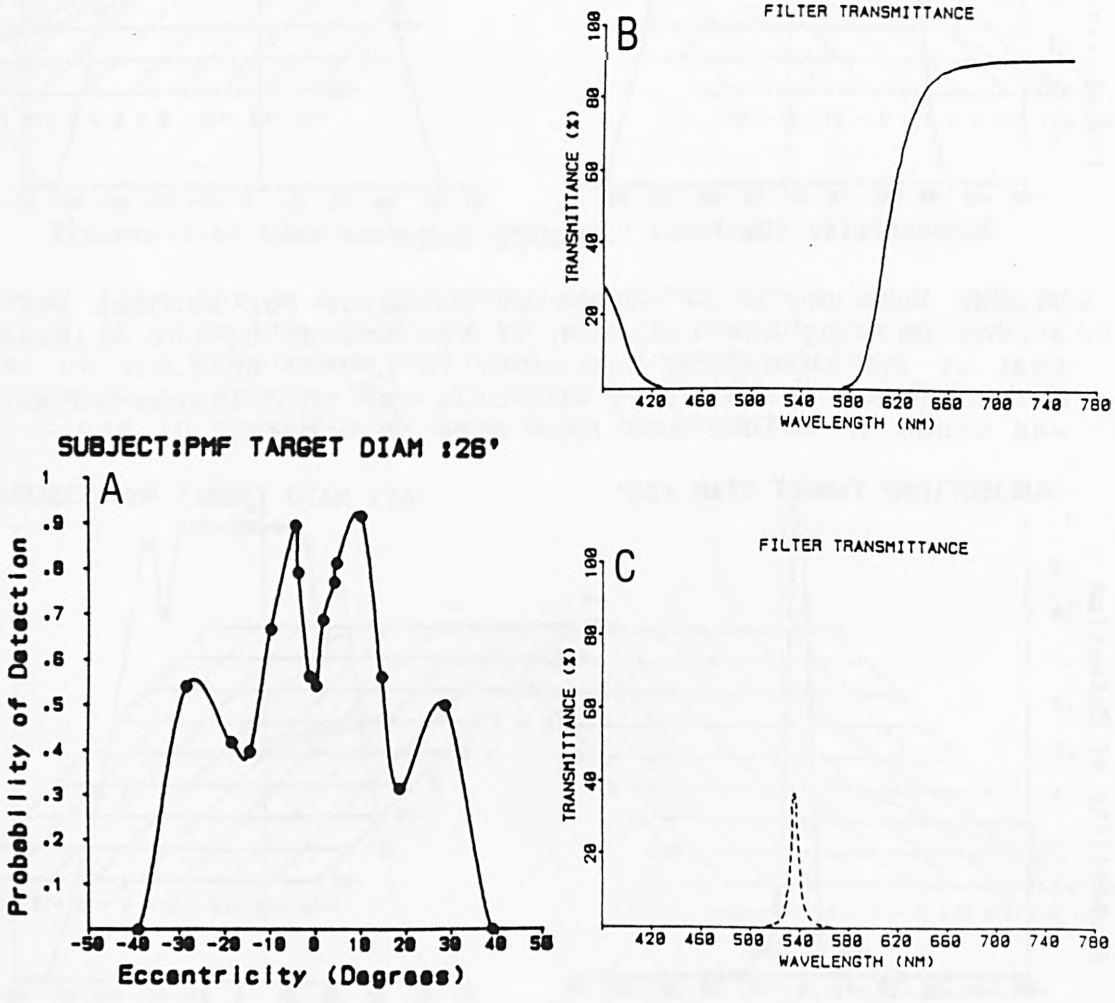

FIGURE 5.26

Visual lobe designed to emphasise rod response. Stimulus diameter:26'. Subject:PMF. A red background was projected, with a green stimulus superimposed. The spectral transmission curves of the filters used are shown alongside.

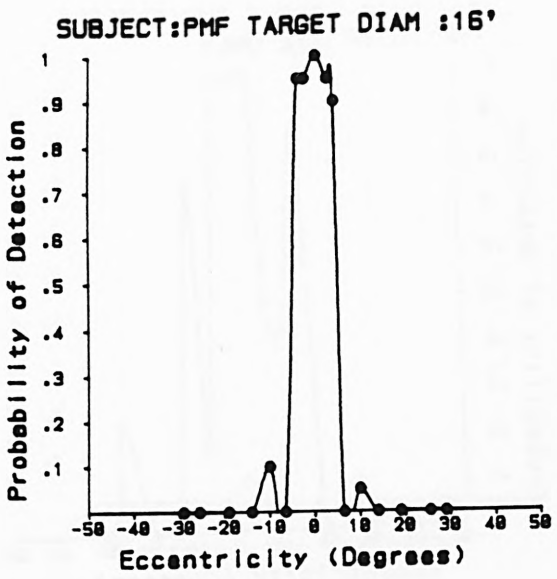

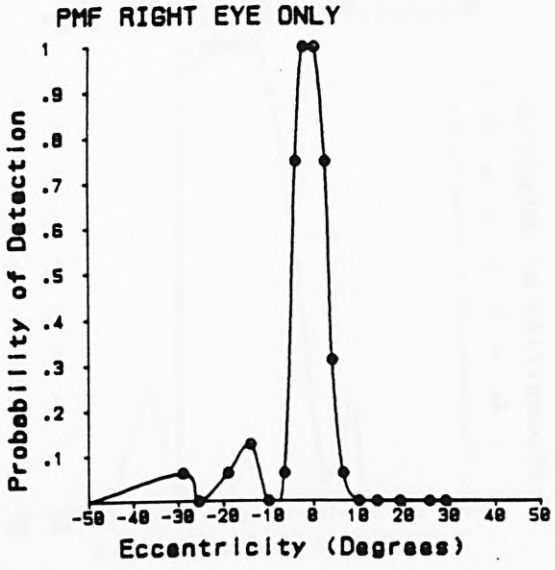

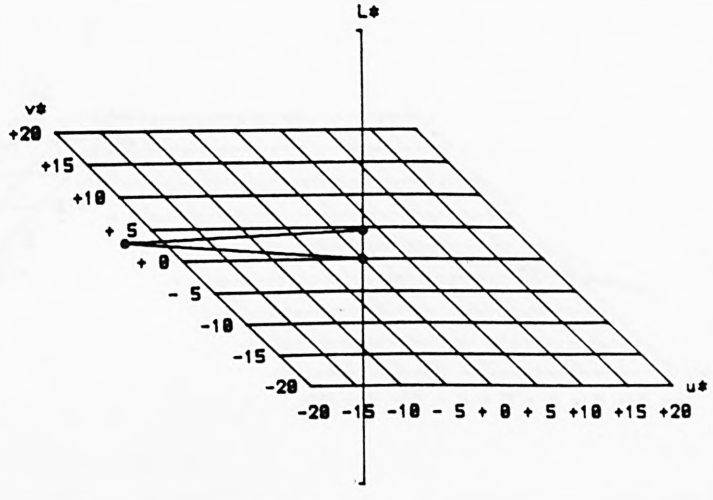

FIGURE 5.27
Visual lobes for the right eye only compared with similar ones observed binocularly. Stimulus diameter:16'. Subject:PMF. The fourth quadrant shows the relation of the colour of the stimulus to that of its immediate surround, in L* U* V* uniform chromaticity space.

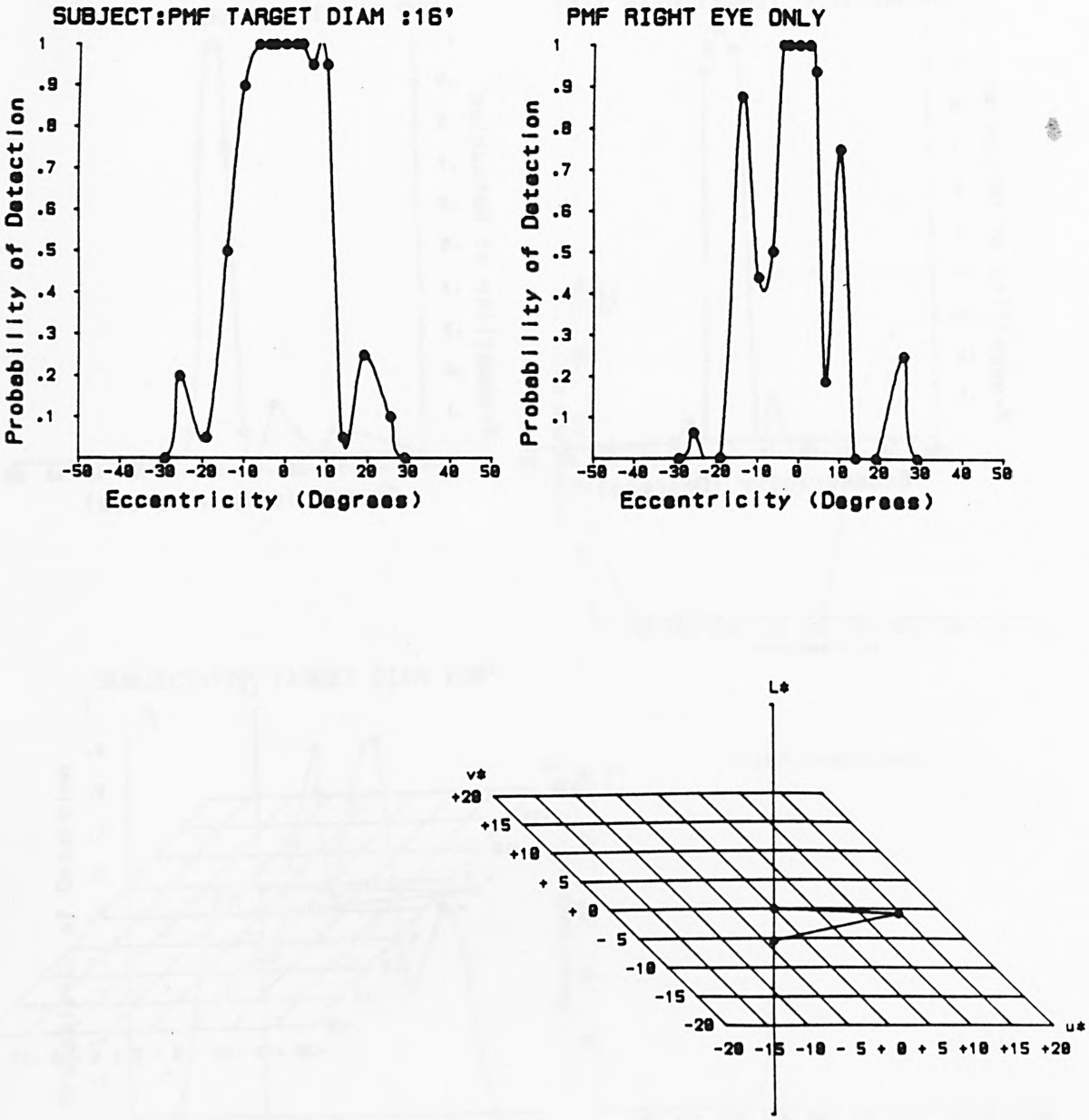

FIGURE 5.28
Visual lobes for the right eye only compared with similar ones observed binocularly. Stimulus diameter:16'. Subject:PMF. The fourth quadrant shows the relation of the colour of the stimulus to that of its immediate surround, in L* U* V* uniform chromaticity space.

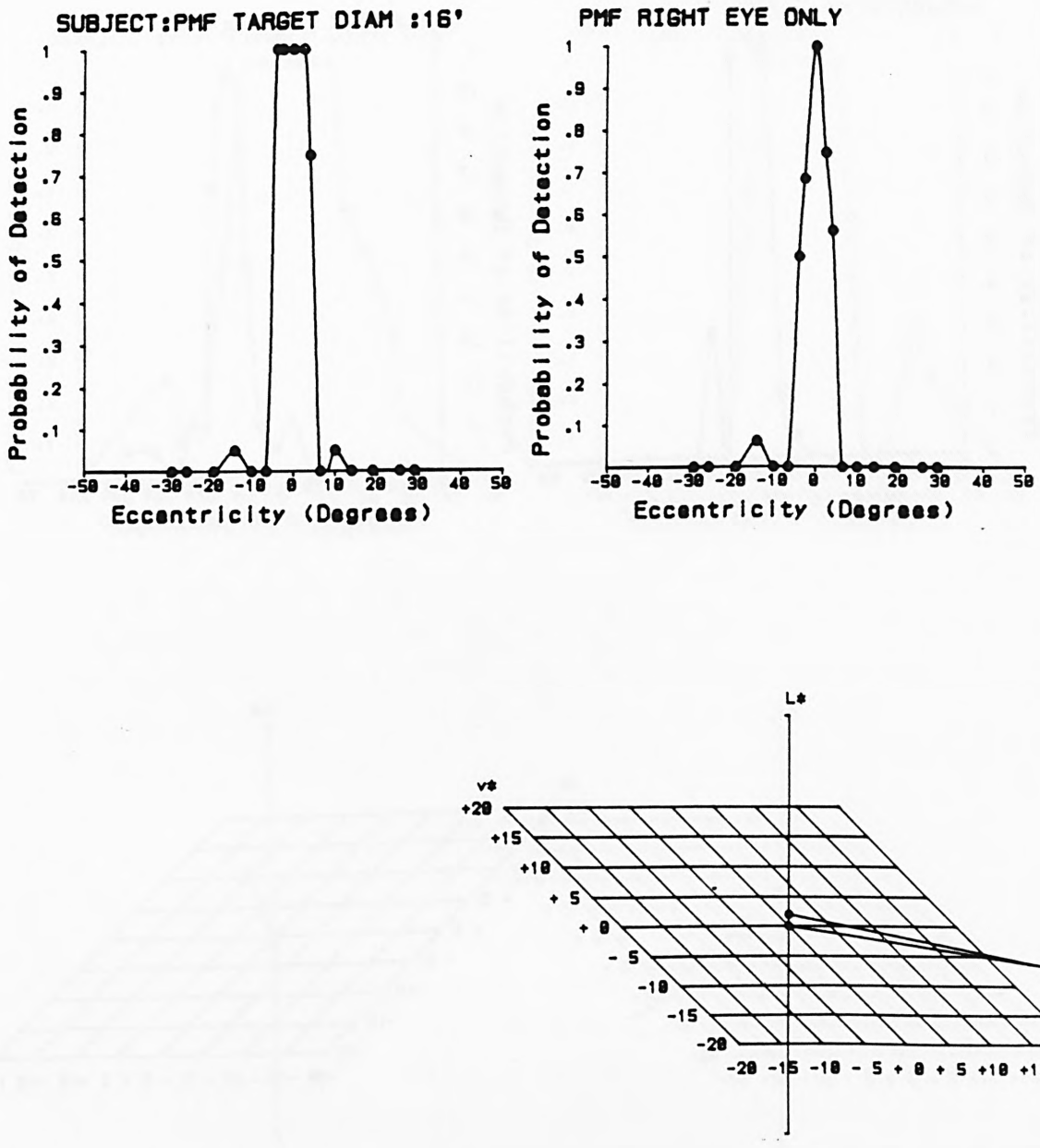

FIGURE 5.29
Visual lobes for the right eye only compared with similar ones observed binocularly. Stimulus diameter:16'. Subject:PMF. The fourth quadrant shows the relation of the colour of the stimulus to that of its immediate surround, in L* U* V* uniform chromaticity space.

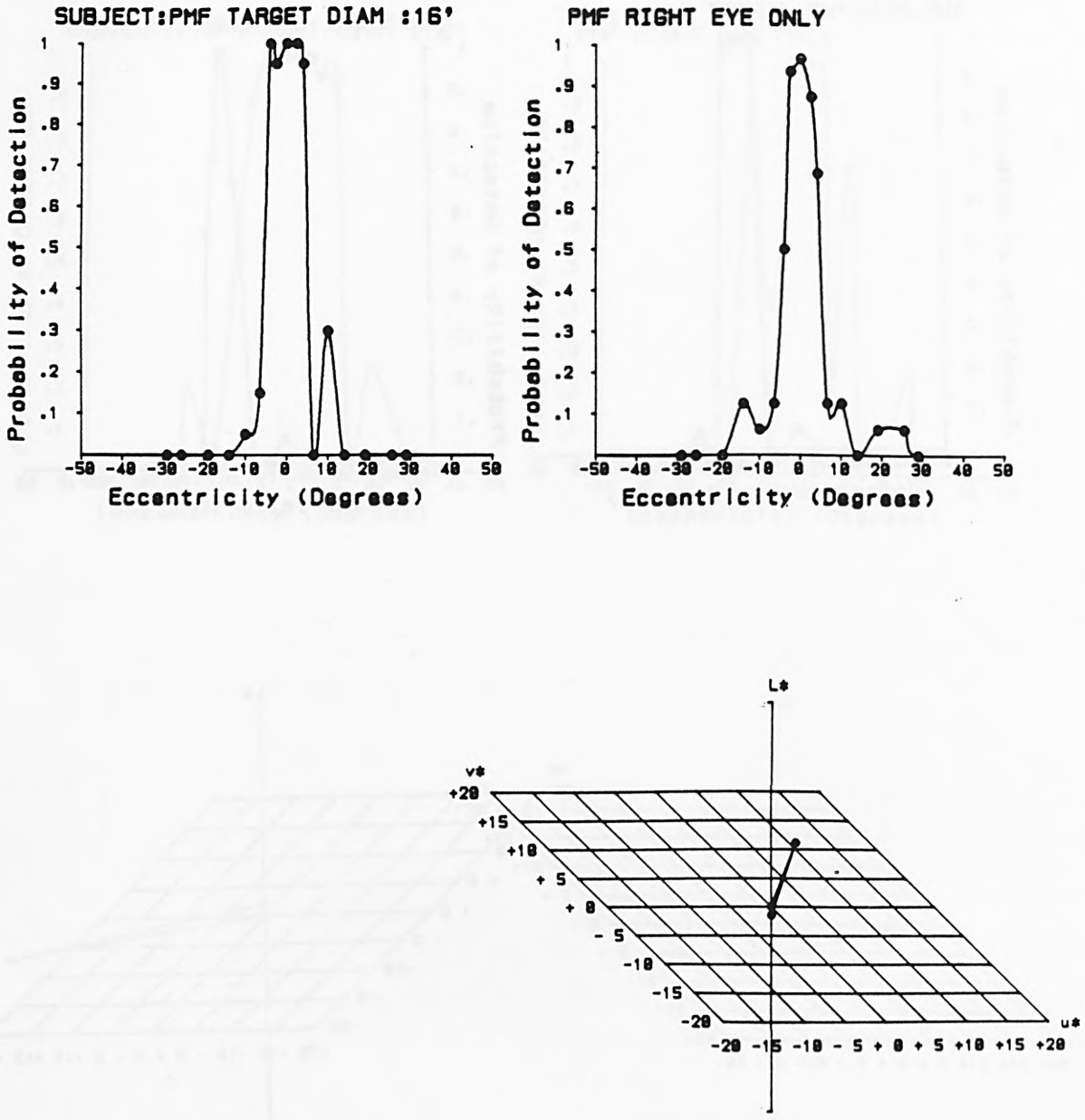

FIGURE 5.30
Visual lobes for the right eye only compared with similar ones observed binocularly. Stimulus diameter:16'. Subject:PMF. The fourth quadrant shows the relation of the colour of the stimulus to that of its immediate surround, in L* U* V* uniform chromaticity space.

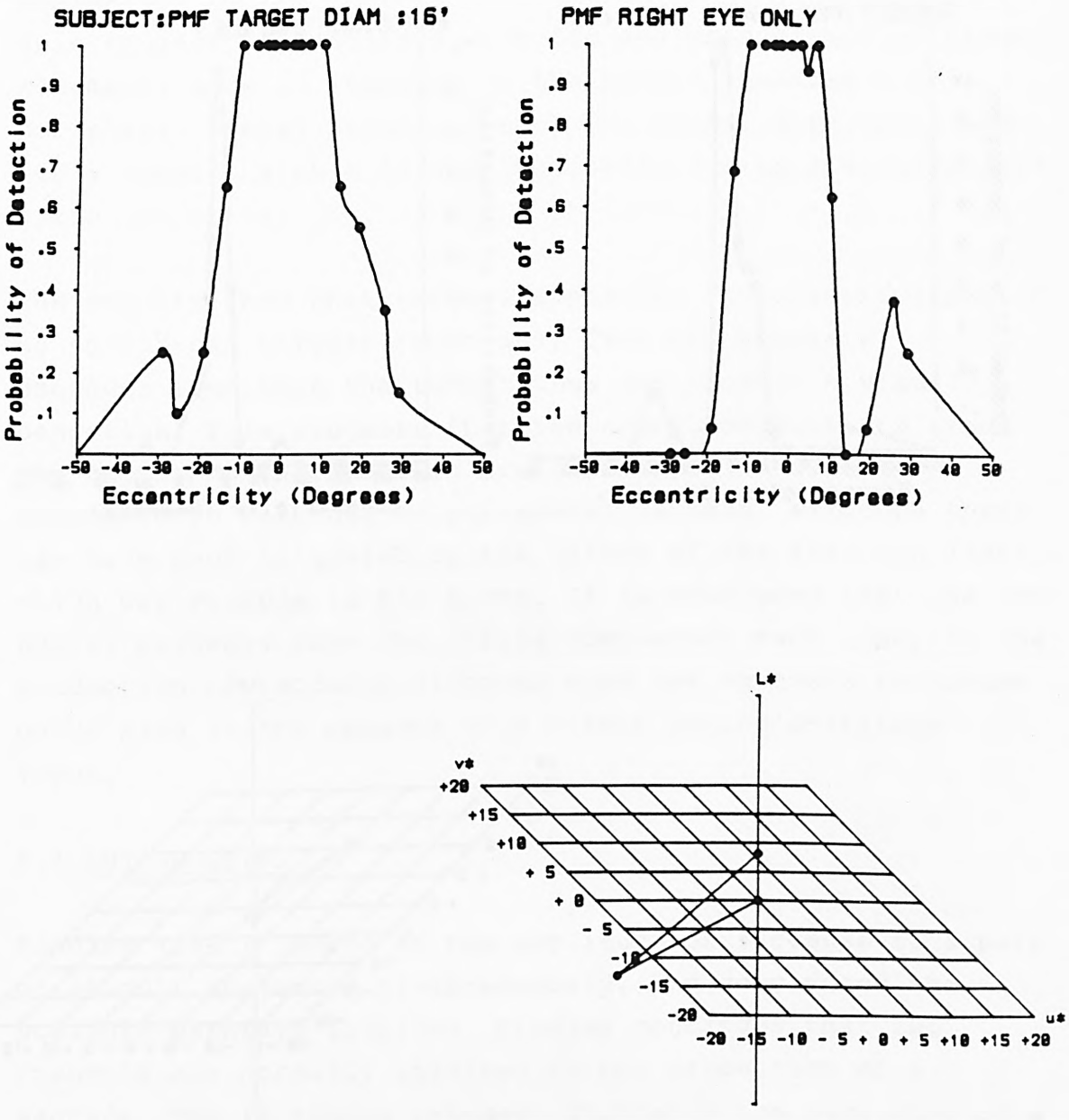

FIGURE 5.31
Visual lobes for the right eye only compared with similar ones observed binocularly. Stimulus diameter:16'. Subject:PMF. The fourth quadrant shows the relation of the colour of the stimulus to that of its immediate surround, in L* U* V* uniform chromaticity space.

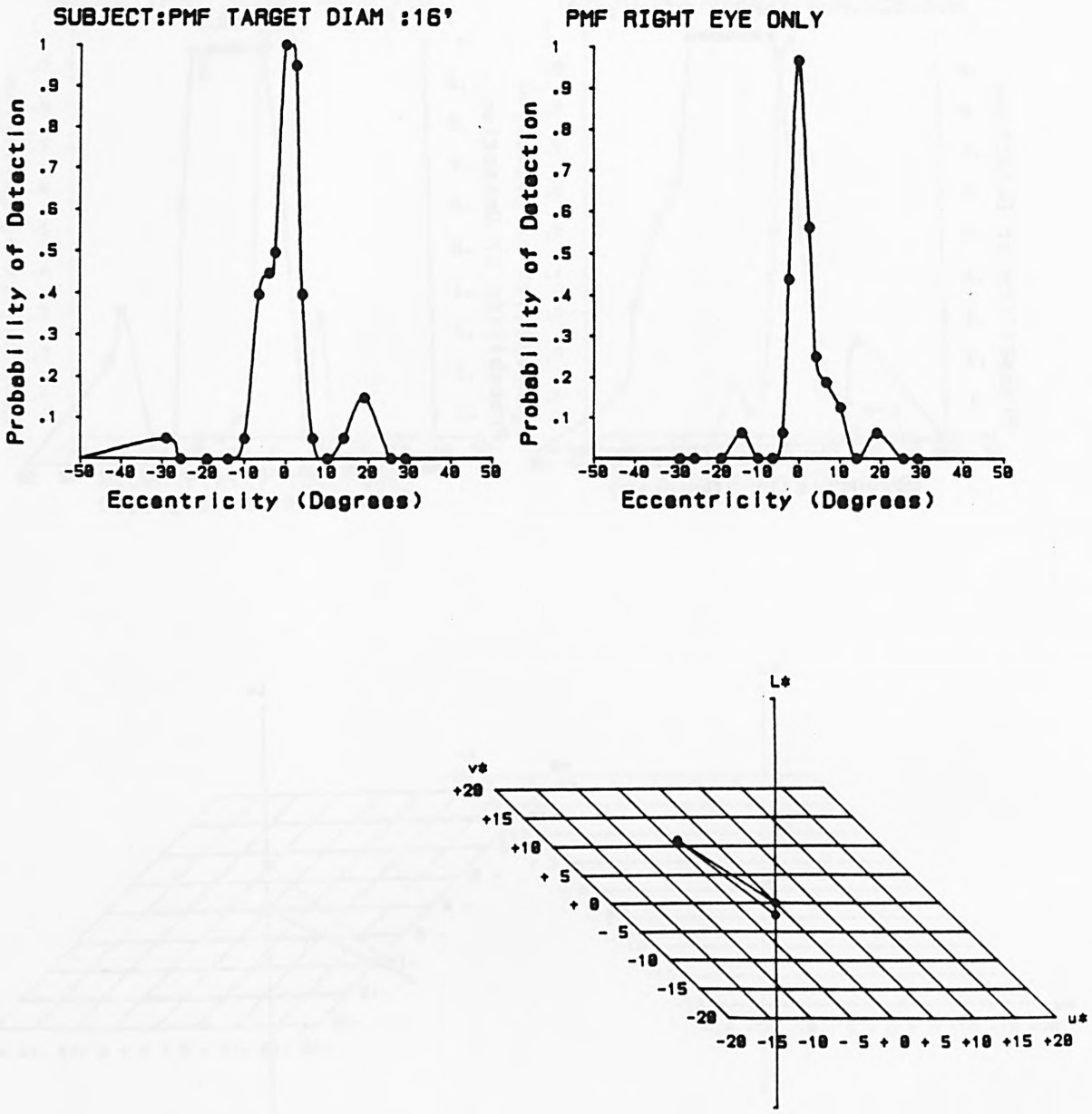

FIGURE 5.32
Visual lobes for the right eye only compared with similar ones observed binocularly. Stimulus diameter:16'. Subject:PMF. The fourth quadrant shows the relation of the colour of the stimulus to that of its immediate surround, in L* U* V* uniform chromaticity space.

EYE MOVEMENT RESPONSES TO BRIEFLY PRESENTED TARGETS.

SUMMARY

This chapter is concerned with the analysis of saccadic eye movements made in response to the sudden appearance of a peripheral visual stimulus, both for normal observers, and for a subject with a 'blind' hemifield due to a severed left optic radiation.

The results show that targets appearing at eccentricities of up to 15^{o} can trigger reasonably fast and accurate saccades even when the target does not produce a visual sensation. This suggests that the neural projections from the retina to the midbrain are sufficient to direct eye movements in response to peripheral targets, although these may have been triggered by the offset of the fixation light, which was visible at his fovea. It is concluded that the two neural pathways from the retina complement each other in the production of saccades although good eye movement responses occur even in the absence of a direct geniculo-striate input.

6.1 INTRODUCTION

Findlay (1982) looked at the amplitude of saccades to a pair of stimuli presented simultaneously, and considered the possible pathways involved. Findlay concludes that two channels are normally involved in the production of a saccade. One (a timing trigger) initiates the beginning of a saccade and determines its direction. The other concerns the spatial location of the target and determines its amplitude.

Findlay also reported that short latency saccades are made to the centre of gravity of the targets while saccades with longer latencies are directed progressively nearer to an individual target position (Findlay, 1982). These observations suggest that 'global' information is available earlier than more resolved information from the retina.

The distribution of latencies reported in these studies was continuous, but Fischer and Boch (1983) have shown that, in monkeys, under certain experimental conditions, saccades of extremely short latencies (100-150 ms) can be found. They termed these 'express-saccades' and more recently have demonstrated the existence of such saccades in human subjects (Fischer and Ramsperger, 1984). This group have also suggested that the express saccades are mediated via the superior colliculus (Boch, Fischer and Ramsperger, 1984).

The express saccades only occur when the visual system has been alerted to the imminent appearance of a stimulus by a cue such as the turning off of a fixation light. Ross and Ross (1980) studied the effect of a warning light onset and offset on the saccadic performance of human observers. They found the optimum warning condition was for a fixation light offset 100 ms to 300 ms before the stimulus appeared, though an onset warning had some effect on saccade latency. They suggest that the difference between onset and offset is due to the absence of any microsaccades at the moment the stimulus appears. They do not actually report a bimodal distribution of latencies, indeed they only report mean and standard deviation of latencies (mean: 220 ms to 280 ms, standard deviation: 20 ms to 30 ms).

Several studies have shown that patients who have lost part of the geniculo-striate pathway can nevertheless make appropriate saccades to targets imaged within the corresponding scotomas (Poppel, Held and Frost, 1973; Weiskrantz, Warrington, Sanders and Marshall,1974; Perenin and Jeannerod, 1978; Zihl, 1980). In these reports saccades have been shown to be made in the absence of conscious awareness of stimulation in the scotoma, although the status of this 'blindsight' phenomena has been questioned (Campion, Latto and Smith, 1983).

The studies mentioned above have, in general, been concerned to establish the existence of spatially appropriate saccades

following visual stimulation of the blind areas of the visual field, and have not analysed the properties of the responses in further detail. This chapter reports the results of an investigation of saccadic eye movements in a subject - 'GY' - with a blind hemifield caused by accidental damage to the left hemisphere. In spite of this damage which has resulted in a complete homonymous hemianopia with some macular sparing, earlier psychophysical investigations (Barbur, Ruddock and Waterfield, 1980) have shown that he can locate flashed targets, using verbal response or a pointer, when they are imaged on his blind hemifield and can discriminate the direction of movement of fast moving targets.

It is known from a recent VEP study (Ruddock, private communication) that GY's left striate cortex is completely inactive and this is consistent with complete degeneration of the left striate cortex as revealed in CT scans (Blythe, Bromley, Kennard and Ruddock (1986)). Tests on G's pupil light reflex yield normal results (see chapter 7). Barbur, Ruddock and Waterfield (1980) report that his perimeter plot shows no sensitivity to continously visible stationary stimuli in his right hemifield apart from an area within 3^{o} of the fovea.

6.2 METHODS.

The equipment and general methods used are described in chapter 2. The size of the stimuli and their luminances and contrasts are shown in table 6.1. A run would begin with 2 minutes adaptation, and each presentation would be preceded by a warning sound 2 to 4 seconds before the presentation sequence began. The exact time interval was randomly selected.

Experiment	background luminance cd/m^2	target luminance increment cd/m^2	log (contrast)	target diameter (degrees)
1 to 3	9.5	139	1.16	2
4	9.5	139	1.16	1
5	9.5	29 to 164	{ see .}	1
6	1.5 to 20.3	6.7 to 123	{table 6.6}	1

TABLE 6.1

6.3 EXPERIMENTAL RESULTS

The latencies and amplitudes of the saccadic responses to the stimulus patterns of each experiment are presented as a series of histograms in figures 6.6 to 6.35 at the end of the chapter. In these figures the ordinate is the relative frequency of the responses to that particular stimulus.

Three different sequences were used in these experiments:

Sequence 1. The fixation light was turned off as a signal that the stimulus was about to appear. 200 ms later, as suggested by Ross and Ross (1980), the stimulus appeared and the trace recording started. Under these circumstances one might expect the shortest latency saccades to appear. Although eye movement recording only continued for 600 ms, the stimulus remained visible on the screen until the subject acknowledged that he had seen it by pressing a response button.

Examples of GY's saccadic traces are included as figures 6.36 to 6.40. They appear normal in shape, often with a slight ballistic overshoot, and in the case of those to his blind hemifield, the first saccade is often followed by a corrective saccade to acquire the target accurately. This usually occurs within 200 ms of the start of the first saccade.

Sequence 2. The fixation light was turned off, and the stimulus appeared without any delay. The rest of the sequence was the same as sequence 1.

Sequence 3. The fixation light was turned off, and the stimulus appeared with no delay. However it remained visible for a period of 160 ms only. This time was selected as being shorter than any normal human saccade latency. Eye movement recording commenced only when the stimulus vanished.

The experiments were carried out, over a period of about six months, whenever the hemianopic subject was available. They were as follows:

EXPERIMENT 1.
A 2^{o} diameter disc stimulus was presented in one of six positions:

-15^{o}, -10^{o}, -5^{o}, $+5^{o}$, $+10^{o}$ and $+15^{o}$.

All three of the sequences described above were tested, and normal observers were used as controls. See figures 6.6 to 6.10, and table 6.7 in appendix 1.

In all three sequences it can be seen that there is a greater spread of saccade amplitudes and an increase in latency as stimulus eccentricity increases. This occurs for normal subjects as well as for the hemianope. In the case of GY his left hemifield saccades appear very accurate and closely grouped, but his blind hemifield saccades all have a wider spread in amplitude. The mean amplitude of his blind hemifield saccades is close to the stimulus position except for those to the $+15^{o}$ target, which he consistently undershoots. Perhaps this is not surprising since it is not uncommon to turn the head (if it is not restrained) in response to such a stimulus (See Bahill et al, 1973). In the histograms illustrating sequence 3 there are some saccades shown for all subjects with zero amplitude. This simply reflects the short time the stimulus was visible, which in some cases was insufficient to initiate a saccade.

Figures 6.1 and 6.2 show the relationship of mean saccade amplitude to stimulus position. For normal subjects, and for GY´s normal hemifield, the mean position lies near the stimulus position, indeed GY´s performance in his normal hemifield is more accurate than that of the normal observers. However in his blind hemifield the error increases with eccentricity. It is noteworthy that the error is less in the case of sequence 3, where he had the stimulus of target offset, as well as target onset. This is to be expected in the light of Barbur, Ruddock and Waterfield´s (1980) observation that he can respond to transient or moving stimuli in his blind hemifield, but not to temporally and spatially constant ones.

There is no evidence of a bimodal distribution of saccade latencies, such as might be expected if express saccades were occurring, except for sequence 3, where a more obvious explanation is that some saccades are a response to stimulus onset, and some are a response, about 160 ms later, to stimulus offset. GY´s blind hemifield saccade latencies were examined to see whether they formed a group that might be mediated by a faster or slower channel than the general population. In general his latencies seem to be similar to normal, their mean value being larger than normal. The only evidence for faster than normal processing is the short minimum latencies in response to a 200 ms advance warning cue (sequence 1), but this turns out to be misleading. In this sequence only there are a number of traces, for GY and for the controls, where the saccade starts early and in the wrong direction. It is reasonable to assume that these are triggered by the offset of the warning light alone. In figure 6.17 these saccades have been eliminated from the analysis, and with them, all suggestion of a faster than normal response.

In figures 6.3 the relation of the amplitude and latency of GY´s individual saccades is indicated. There is little sign that short latency saccades are either more or less accurate

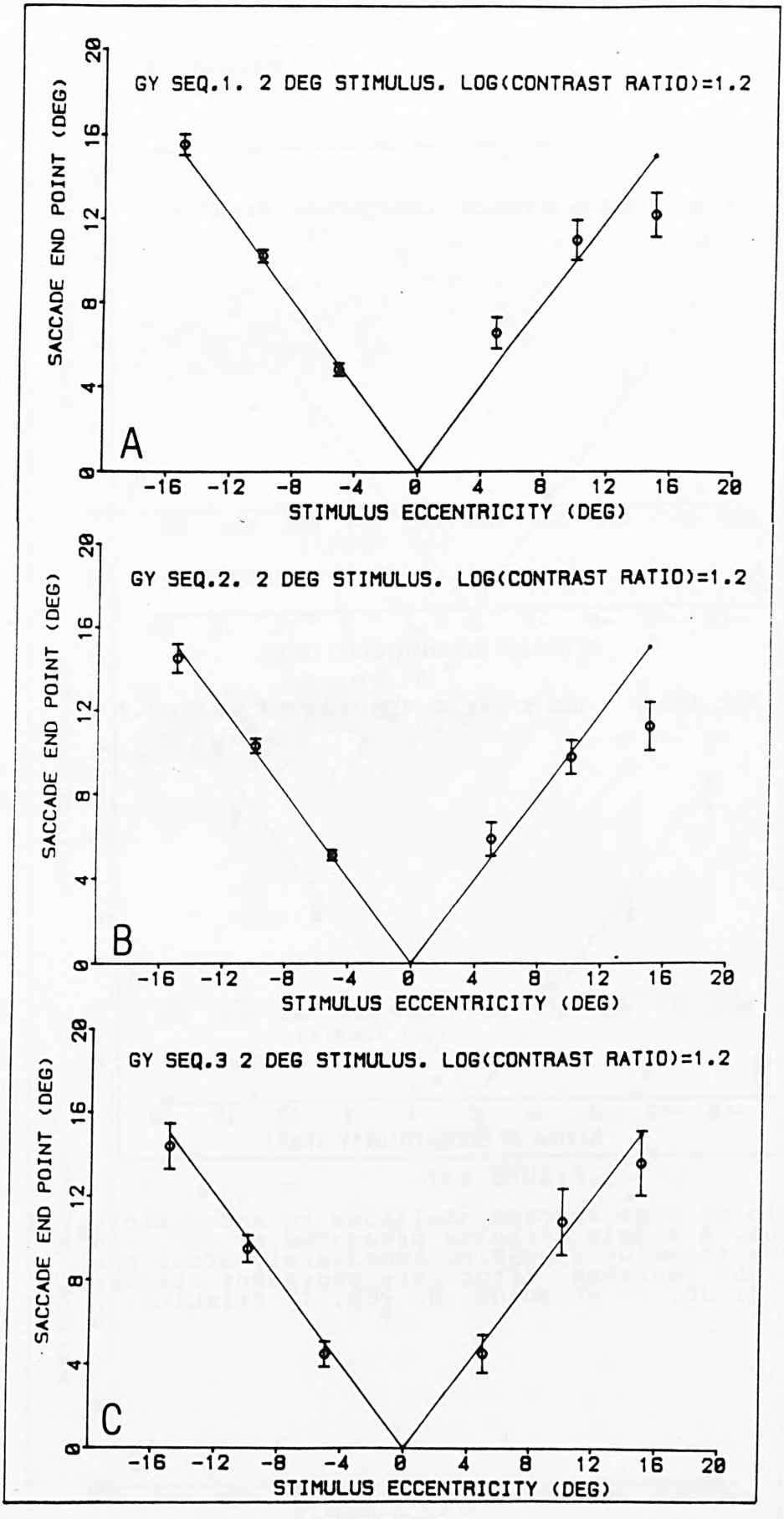

FIGURE 6.1

Relationship of mean saccade amplitude to eccentricity of the stimulus, for GY. A single 2° stimulus presented at +5°, +10° or +15°, the stimulus appearing 200 ms after the fixation light vanishes. Error bars represent standard deviation. A: sequence 1. B: sequence 2. C: sequence 3.

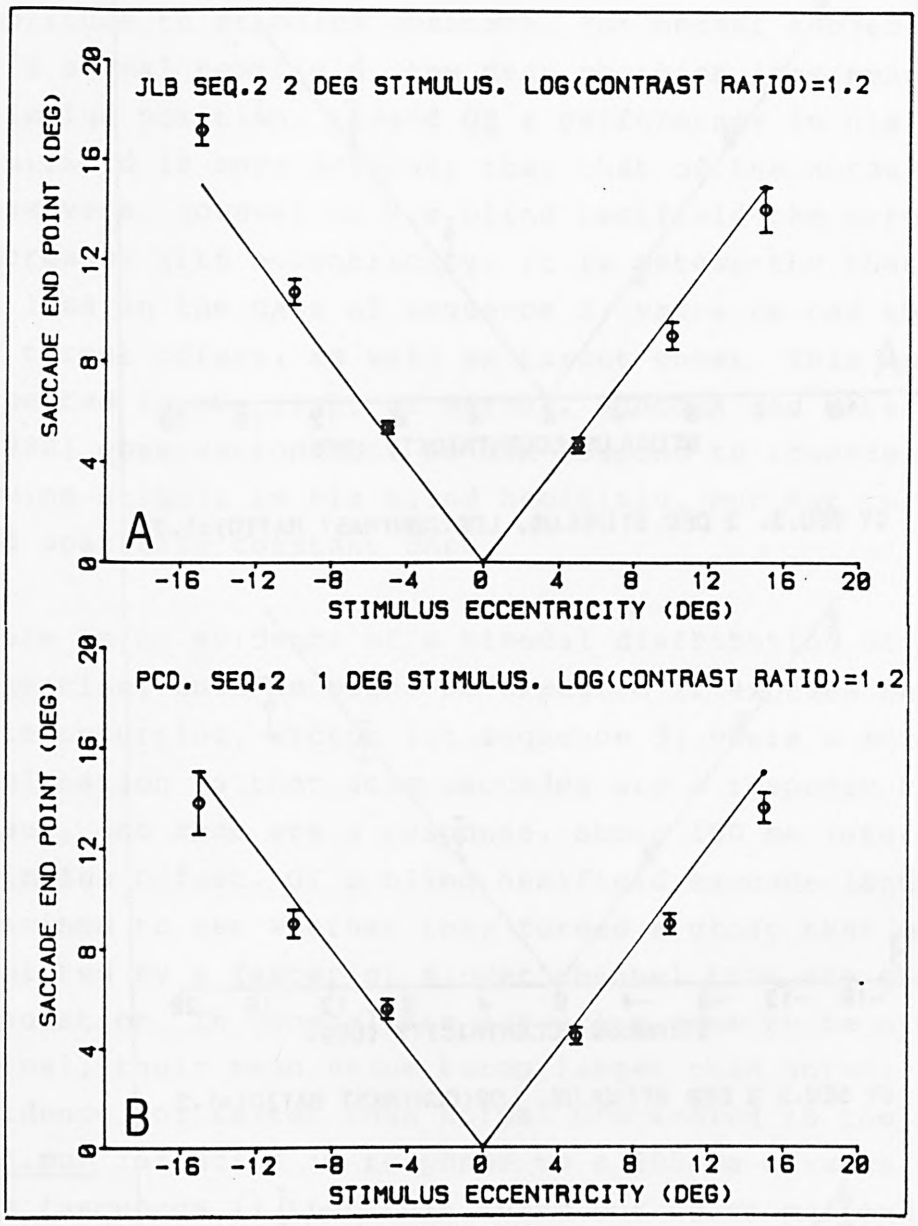

FIGURE 6.2

Relationship of mean saccade amplitude to eccentricity of the stimulus. A single stimulus presented at $\pm 5^{o}$, $\pm 10^{o}$ or $\pm 15^{o}$, the stimulus appearing immediately after the fixation light vanishes. Error bars represent standard deviation. A: JB, 2^{o} stimulus. B: PCD, 1^{o} stimulus.

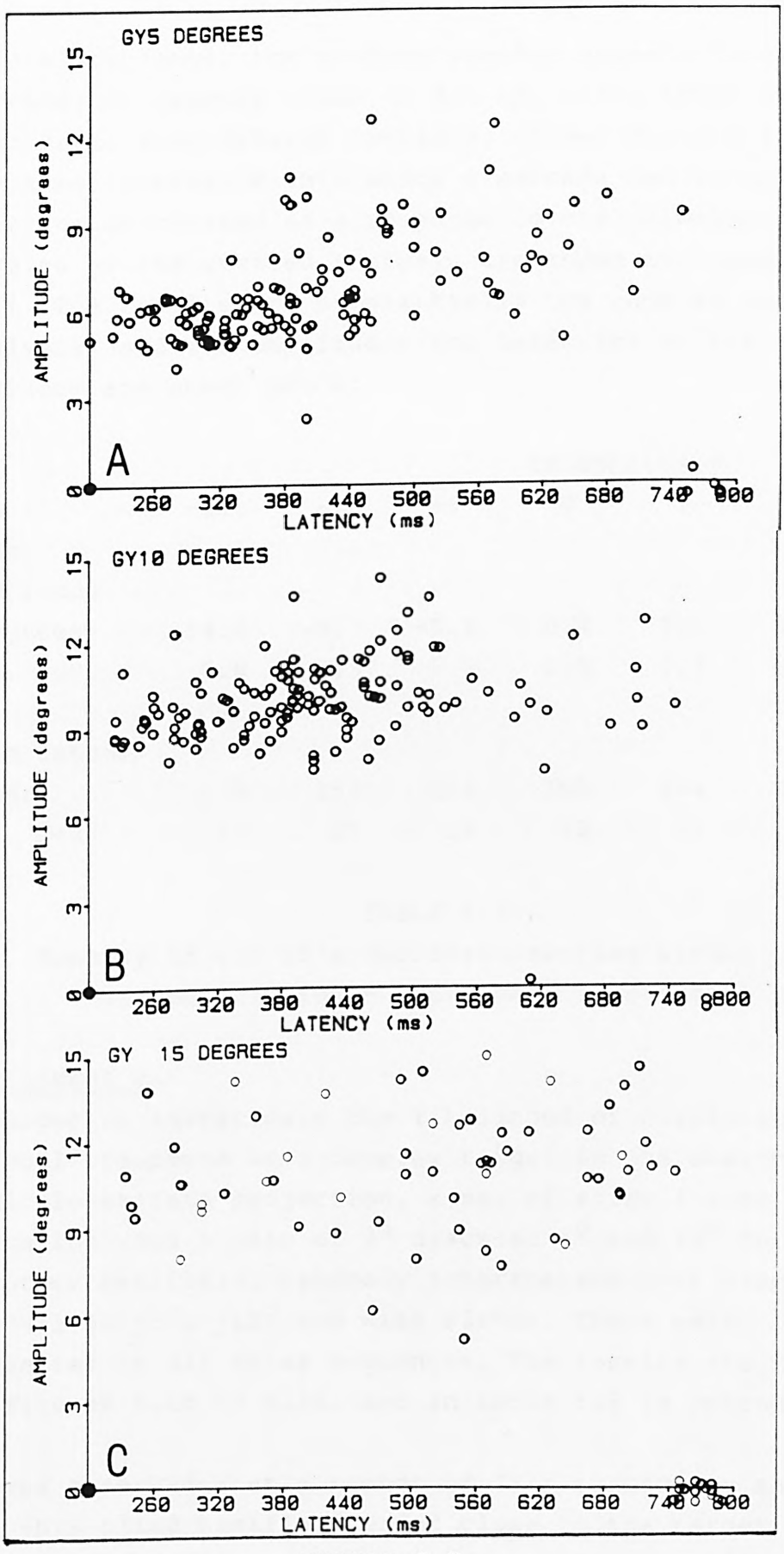

FIGURE 6.3

Correlation of individual saccade amplitudes with their latencies for GY, Sequence 2. Single 2° stimulus appearing immediately after the fixation light vanishes. A: stimulus at +5°. B: stimulus at +10°. C: stimulus at +15°.

than slower ones. the minimum scatter appears to occur for saccades of latency close to 320 ms. Since there are some inaccurate long delayed saccades, it was decided to amend the time interval within which a saccade had to occur in order to be classed as a response to the stimulus, and the results of the revised analysis are shown in figure 6.10 and 6.11. The results are substantially the same as the previous analysis, and the amplitudes and latencies of the remaining saccades are shown below.

	Eccentricity						
	-15	-10	-5	0	5	10	15
Mean Amplitude (degrees)	-14.0	-9.7	-5.1	0.4	5.1	8.9	10.2
Std. Dev.	0.8	0.5	0.4	1.5	0.7	0.9	1.8
Mean latency (ms)	273	253	254	306	294	288	282
Std. Dev.	31	25	19	12	37	39	36

TABLE 6.2

Summary of all GY's saccades starting within 350ms of the stimulus - experiment 1, sequence 2.

EXPERIMENT 2

In order to investigate the likelihood of obtaining a 'global' response to a complex target in the absence of a geniculo-striate projection, a set of stimuli were presented which included a pair of 2^{o} discs at 5^{o} and 10^{o} in one or other hemifield, randomly interspersed with single stimuli at $\pm 5^{o}$, $\pm 10^{o}$ and with blanks. These were presented in all three sequences. The results are summarised in figures 6.18 to 6.26, and in table 6.8 in appendix 1.

It was observed that a number of GY's corrective saccades into his blind hemifield ended close to the target location, although this did not always occur within the 600 ms of the recorded trace. Figure 6.21 shows a re-analysis of the data

shown in figure 6.20, which shows that a number of eye movements towards the pair of targets in his blind hemifield did eventually land near to one of the two targets.

Findlay has devised a Global Effect Parameter defined as follows:

$$G\ E\ P = \frac{(\text{double target amplitude} - 5^{o}\ \text{target amplitude})}{(10^{o}\ \text{target amplitude} - 5^{o}\ \text{target amplitude})}$$

Table 6.3, and indeed an inspection of the histograms, shows that this effect is small even for the normal observers. The mean level of GEP found in this experiment for normal observers is 16.6, compared with 17% to 21% found by Findlay (1982) for comparable target positions. This is probably because the structure of the stimuli used did not permit the usual requirement for the observer to detect some feature of both elements in the double target, thereby forcing him to acquire both targets as quickly as possible. For GY, the effect seems to be present for sequence 1, where the saccadic system is primed by an early warning, but reversed for sequence 2, and nonexistent for sequence 3. The experiment was repeated some time later (Experiment 4, and figure 6.38) with similar inconclusive results.

Sequence	Subject	Left hemifield	Right hemifield
1	GY	-17.9	28.6
1	PF	14.8	0.0
2	GY	-7.8	-17.2
2	PF	18.9	-5.0
2	JB	29.3	23.1
3	GY	55.6	2.4
3	PF	19.2	6.7
3	JB	33.3	25.9

TABLE 6.3

Global effect parameter for experiment 2

One interesting fact emerged: on GY's left hemifield, where his saccades were in general accurate and with low spread in amplitude, he consistently undershot: he saccaded to a point to the right of the inner of two targets. It is surmised that he had adopted a strategy like that described by Meienberg et al (1981) to keep both the targets well within his seeing hemifield.

EXPERIMENT 3

One might expect that if the amplitude of GY's blind hemifield saccades is processed by a faster (or indeed a different) channel than that he usually uses in his good hemifield, his response to a pair of rival stimuli, one in each hemifield, would differ from that of the controls. In this experiment (see figures 6.27 to 6.31 and table 6.9) the patterns presented included a pair of such rival stimuli, at + and -10^{o}, a single stimulus at $+10^{o}$, a single stimulus at -10^{o}, and a blank. Previous work with such stimuli by Findlay (1983) found longer latencies in such cases.

The normal subjects showed the longer latencies for bilateral targets that other workers have found. In this experiment they showed a marked preference to saccade to one particular side. The stimulus on this side was therefore reduced in intensity by a factor of ten: the result was unaltered. GY, as might be expected, always saccaded to the left target when rival targets were presented. The amplitude and latency of his saccades in this case were very close to those to a single target at the same eccentricity on his seeing side. He remarked that he was always aware of the rival target in his blind hemifield, but found it easier to look at the one in his good hemifield. It is noteworthy that he very rarely responded to the blank stimulus, whereas one might expect him to make an exploratory saccade into his blind hemifield in such cases.

EXPERIMENT 4

This was a repeat of experiment 2, but with 1^{o} targets, and with more precise calibration procedure. It was performed with sequence 2 only, that is, the fixation light was turned off and the stimulus appeared simultaneously, and the stimulus remained visible until the subject pressed the response button. The results are summarised in figure 6.32 and table 6.10, and show no global effect for either GY or the normal subject. The stimuli of experiment 5 were in fact combined with the pairs of stimuli presented in this experiment, so that 14 alternative patterns were equally likely to appear. The histograms for the six single stimuli have been plotted separately as figure 6.11, since they may be compared with experiment 1, sequence 2. The experimental conditions differ only in that this experiment used a 1^{o} target diameter.

EXPERIMENT 5

One criticism made by Campion, Latto and Smith (1983) of experiments on patients with homonymous hemianopias is that insufficient precautions were taken to avoid the possibility that the position of the stimulus was estimated from the amount of stray light reaching the patient's normal hemifield. In this experiment a set of stimuli at 10^{o} in either hemifield were included at four different luminances. The results (figures 6.33 and table 6.11) showed, as in experiment 1, that GY could saccade equally accurately to the 10^{o} stimulus at all luminances presented, whereas if he was responding to scattered light, one would expect the saccade amplitude to be related to the luminance of the stimulus. However, it is possible that he adopted a strategy of making a 10^{o} saccade when in doubt, or that he came to associate a given amount of stray light with a given target position, so the next experiment was designed to defeat such a strategy.

EXPERIMENT 6

Two sets of target slides were prepared in which the luminance of each spot was adjusted to be approximately proportional to the square of its eccentricity. The luminances of the projected stimuli were measured with an LMT meter, and are recorded in Table 6.5. The effect of scattered light in the retina is approximately proportional to luminance/(square of the angle) (Boynton and Clarke, 1964, Wyszecki and Stiles, 1967). This is illustrated in figure 6.4, where the data of Demott and Boynton (1958) are plotted as points, with a curve representing an inverse square law relationship. Thus with these stimuli the scattered light at the fovea from the six blind hemifield stimuli should be at one of two levels only, independent of eccentricity. These stimuli, together with similarly varied ones in the good hemifield and a blank, were presented to GY in the same way as before.

Since in this case the saccade amplitudes were of considerable interest, he was asked to press a response button when he had finally acquired each target, and his eye position was then recorded as a check on, and correction to, the eye movement monitor calibration. Since some spots had been reduced in luminance by a factor of 16, the background was also reduced, in different experimental runs, so as to reach a target contrast level above GY's threshold for his blind hemifield. The results are summarised in figures 6.34 and 6.35 and table 6.12, and are discussed in section 6.5.

6.4 GENERAL OBSERVATIONS.

The Haines eye tracker is fitted with direct indicators of analogue output, and it was notable that, during the course of setting up the instrument and calibration, GY made numerous brief saccades into his blind hemifield. These occurred about every second, but were completely suppressed when he was asked to fixate. They are presumably part of his normal strategy to maximise his knowledge of his visual surroundings.

GY was asked for his impressions of the stimuli presented in his blind hemifield at an eccentricity of 10^{o}, against a background of $10cd/m^2$. His replies are tabulated below.

Luminance of target- cd/m^2	Response to silent stimulus	Response to sound-cued stimulus
700 (approx) (against dark background)	localised change in the darkness level of the "emptiness"	
139	Sometimes aware of something moving up and down.	Always aware of something.
70	rarely aware of any stimulus at all	sometimes aware of something.
44	not aware of anything.	sometimes aware of something.
14	not aware of anything.	not aware of anything.

TABLE 6.4
GY's verbal responses to visual stimuli in his blind hemifield.

It will be seen from table 6.6 that GY saccades to such stimuli down to Log (contrast) values of .87, so that with a background luminance of 10 cd/m^2, his threshold target luminance for a 50% probability of saccade would be 74 cd/m^2.

In passing, it should be noted that GY is a very good observer. He rarely responds to a blank trial, and he keeps his head very still, so that frequent recalibrations of the eye tracker are not necessary. In the case of sequence 3,

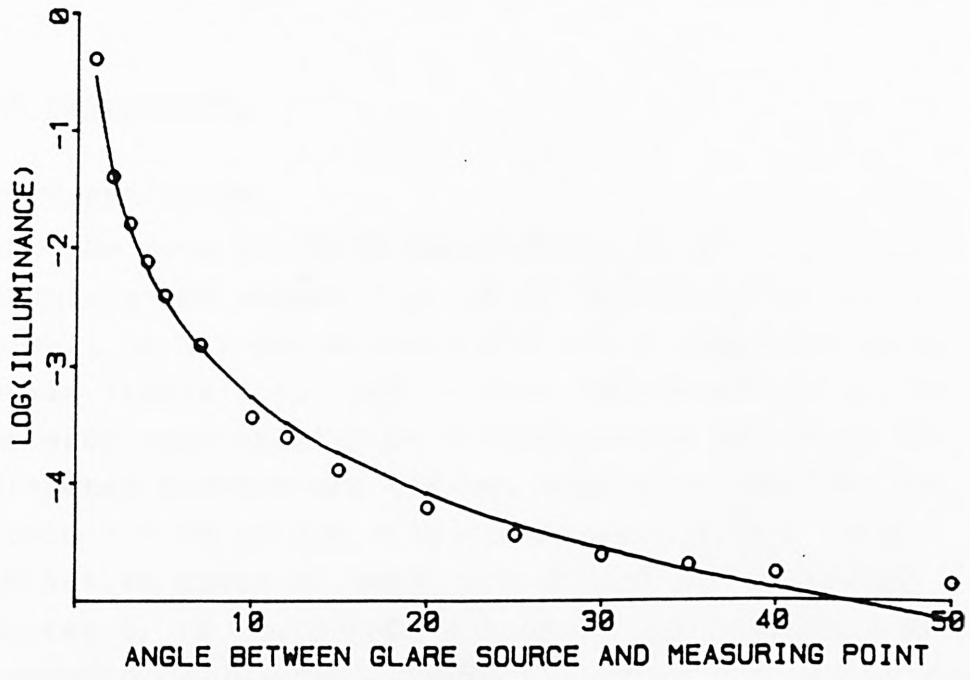

FIGURE 6.4

The relationship of log(illuminance) to the angle between the source of stray light and the measuring position. (Replotted from Demott and Boynton (1958).

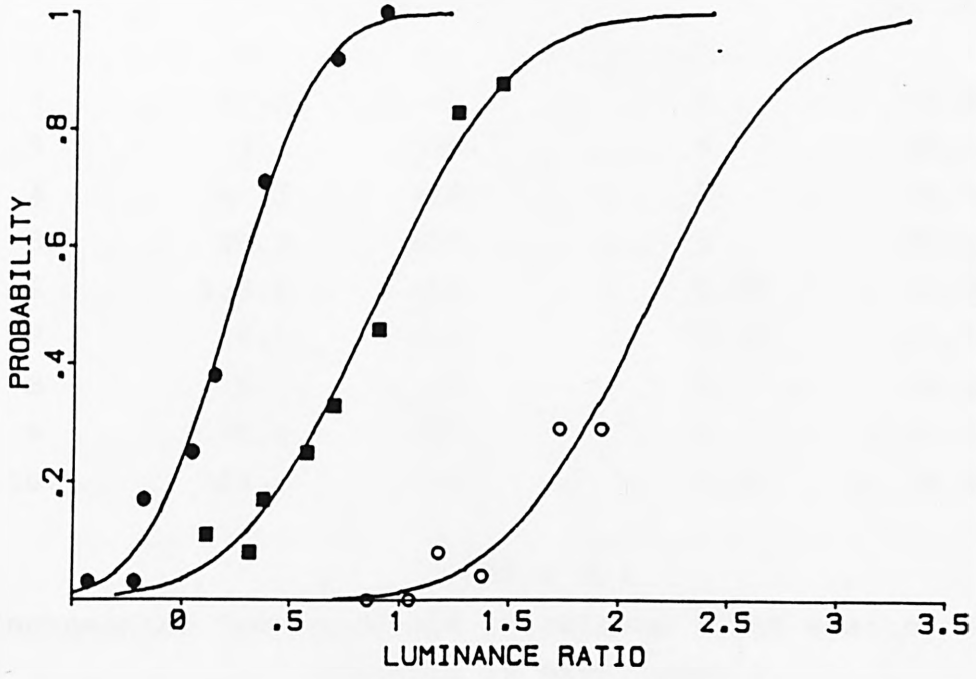

FIGURE 6.5

Probabilities of saccades to stimuli in GY's blind hemifield, plotted as a function of stimulus contrast for three stimulus positions. Filled circles: 5^{o} eccentricity, filled squares: 10^{o} eccentricity, open circles: 15^{o} eccentricity. The lines are cumulative gaussian curves fitted to the points as described in Chapter 2.

where the stimulus disappears before the saccade occurs, he seldom fails to make an appropriate saccade.

6.5 DISCUSSION.

SCATTERED LIGHT.

From the data of these experiments it was possible to calculate the probability of GY saccading to the 1^{o} stimuli in his blind hemifield for a range of contrast levels (table 6.6), and to plot "frequency of seeing" curves for each eccentricity as a function of contrast. The parameter plotted was the percentage of saccades which began within 350 ms of the stimulus appearing (for sequence 2). A cumulative gaussian curve was fitted (as described in chapter 2) to the points for each eccentricity, and a 50% threshold calculated. Figure 6.5 shows the points and the fitted frequency of seeing curves.

Target no.	cd/m^2	Eccentricity (degrees)	$100/E^2$	Scatter at fovea
1	0	-		
2	12.2	+5	4	48.8
3	7.4	+5	4	29.6
4	41.5	+10	1	41.5
5	26.2	+10	1	26.2
6	123.0	+15	0.44	54.7
7	79.0	+15	0.44	35.1
8	6.7	-5	4	26.8
9	25.3	-10	1	25.3
10	69.2	-15	0.44	30.8

TABLE 6.5
Incremental luminance and calculated light scatter for each stimulus in experiment 6.

Luminances		Log(contrast)	Probability of a saccade within 0.4 seconds
Background	Stimulus		
5° Eccentricity			
20.3	7.4	-0.43	0.03
20.3	12.2	-0.22	0.03
11.2	7.4	-0.18	0.17
11.2	12.2	0.04	0.25
5.3	7.4	0.14	0.38
5.3	12.2	0.36	0.71
1.5	7.4	0.69	0.92
1.5	12.2	0.91	1.00
(Calculated Threshold		0.21	0.50)
10° Eccentricity			
20.3	26.2	0.11	0.11
20.3	41.5	0.31	0.08
11.2	26.2	0.37	0.17
11.2	41.5	0.57	0.25
5.3	26.2	0.69	0.33
5.3	41.5	0.89	0.46
1.5	26.2	1.24	0.83
1.5	41.5	1.44	0.88
(Calculated Threshold		0.87	0.50)
15° Eccentricity			
20.3	79	0.59	0.03
20.3	123	0.78	0.00
11.2	79	0.85	0.00
11.2	123	1.04	0.00
5.3	79	1.17	0.08
5.3	123	1.37	0.04
1.5	79	1.72	0.29
1.5	123	1.91	0.29
(Calculated Threshold		2.12	0.50)

TABLE 6.6

Contrast Thresholds in GY's blind hemifield

The threshold rises steeply with eccentricity, so that at 15^{o} it is barely reached in the series of experiments using a 1^{o} diameter target. Hence it will be seen that GY's response to a 15^{o} stimulus is rarely large enough to produce an accurate saccade, except in the first three experiments, which used a 2^{o} target.

Where the stimuli are above threshold in this experiment, the saccades to his blind hemifield are accurate and had normal latencies (about 300 ms). In the case of 1^{o} diameter targets at 15^{o} eccentricity the threshold was not reached. Very few of such saccades were accurate or fast. The contrast thresholds required for normal subjects to make a saccadic response are examined in chapter 9, where it is concluded that this threshold is close to the psychophysical threshold.

The possibility that GY's blind hemifield saccades are due to some combination of good strategy and calculation made from the scattered light falling on his normal hemifield or macular region has to be considered. It seems improbable, since the background field was large, and the contribution of scattered light from the target to the retinal illuminance at the nearest non-scotoma area of his retina, between 1 and 11^{o} away, must be small. His performance in sequence 3, where the flash vanished before the saccade began, rules out the strategy of making a search saccade whenever no stimulus appeared in his normal hemifield.

If he were inferring the eccentricity of the target from the amount of scattered light reaching the macular area, his saccades in response to the twin targets in experiment 2 would be expected to undershoot, since the scattered light must be greater than for a single target at the nearer of the two positions.

Experiments 4 and 6 were carried out with more precise eye tracker calibration in order to confirm this point.
It seems reasonable to conclude that in experiment 6, GY's

saccades to his blind hemifield were not related to the amount of scattered light, since if this were the case, the mean saccade amplitude for the lower luminance stimulus at each eccentricity would differ from that for the higher luminance stimulus. In practice blind field stimulation produced saccades of accurate mean amplitude irrespective of stimulus luminance, provided the contrast of the stimulus was above the threshold for saccade generation at the eccentricity concerned. Where the stimulus contrast was below his threshold for visually guided eye movements he appears to adopt a strategy of saccading to a point where his experience leads him to expect the greatest probability of finding a stimulus. He distinguishes easily however between a blank trial (to which he makes no saccade) and a below threshold stimulus.

If he is deducing the stimulus position from the distribution of scattered light in his good hemifield, one would expect the extra signal processing to result in longer latencies for blind hemifield saccades. In many experiments his saccade latencies are no longer than in his normal hemifield.

NEURAL PATHWAYS

If neither the pattern nor the amount of light scatter can explain GY's ability to programme saccades to stimuli in his blind hemifield, one is driven to conclude that some ability to determine saccade endpoints must reside outside the striate cortex, although since the saccades have a greater spread, the corticular pathway appears to contribute greater accuracy to saccadic endpoint determination. As discussed in chapter 1, this is in line with lesion studies on monkeys. The absence of the express saccades found in monkeys (and in some studies of human subjects), or even of a bimodal distribution of saccade latencies, is more puzzling, although many saccade studies have not shown this feature.

THE GLOBAL EFFECT

It had been expected that, in the absence of processing via the visual cortex, the greater spatial summation of the midbrain pathway would increase the probability of the global effect when GY saccaded to pairs of targets in his blind hemifield. This was not the case, except for sequence 1. In this case, the priming of the saccadic system by the offset of the fixation light produced shorter latencies than in the other sequences. Findlay (1983) found that the global effect was greater for short latency saccades, so given that in sequence 2 and 3 for whatever reason GY produces relatively few short latencies, the lack of a global effect would follow. The mean global effect for the normal subjects (17%) was close to the lowest value found by Findlay (1982). Clearly the absence of cortical processing does not make either express saccades or the global effect inevitable.

6.6 CONCLUSIONS.

The results of a comparison of the accuracy and latency of the visually guided saccades of normal subjects with those of a hemianope are analysed, and compared to those to be expected from previous studies.

Examination of the distribution of latencies and amplitudes of saccades for normal subjects showed

1) accurate saccades for stimuli of eccentricity less than 10^{o}, and a tendency for the first saccade to undershoot to stimuli at 15^{o}.

2) a slight increase in latency as stimulus eccentricity increased.

3) a slight tendency for saccades to double target stimuli to land between the two, (Global effect).

4) no evidence of a bimodal population of saccade latencies, indicative of two alternative channels for saccade amplitude determination.

Examination of the hemianope's responses in his good hemifield showed completely normal saccadic behaviour, apart from a habit of undershooting the nearer of a pair of targets, with the effect that both were kept within his view.

Examination of his saccadic behaviour in his blind hemifield showed

5) that higher contrast is needed to trigger an accurate saccade than in his normal hemifield.

6) that provided this threshold is exceeded his saccades have normal latency.

7) with the same proviso his saccades have accurate mean amplitudes, but rather greater variability.

8) The likelihood that such saccades are mediated by scattered light reaching his normal hemifield has been shown to be very small.

9) He adopts a strategy of frequent searches of his blind hemifield when not required to fixate.

It is concluded that midbrain pathways can mediate at least the directional control of saccadic eye movements, and these are not necessarily particularly rapid. Optimum performance in eye movement control is observed only when the geniculo-striate pathway is also involved, and this suggests complementary parallel processing of the visual input.

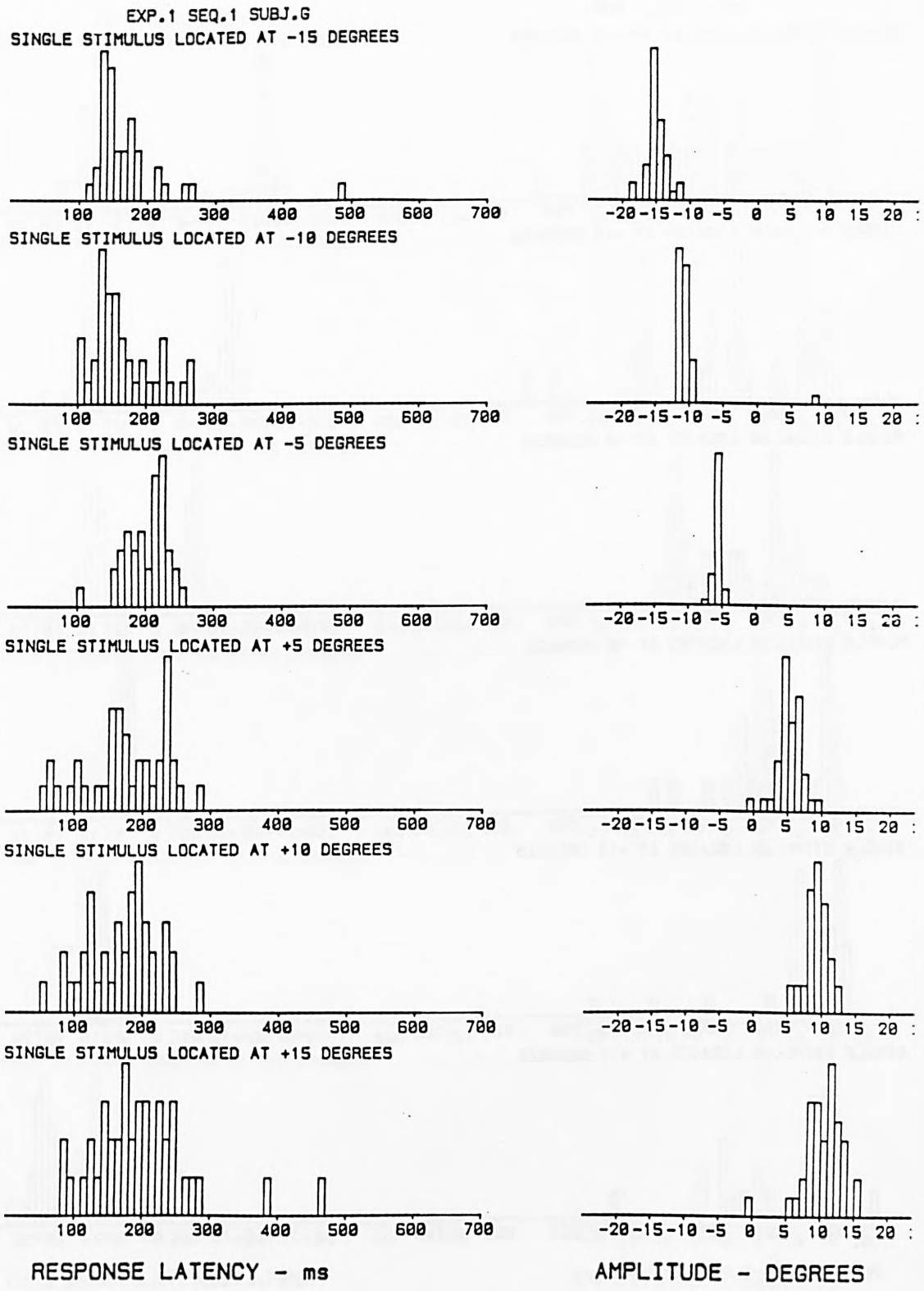

FIGURE 6.6

Distribution of latencies and amplitudes of saccades - GY. Experiment 1. A single 2° stimulus presented at + 5°, + 10° or + 15°, the stimulus appears 200 ms after the fixation light vanishes. (Sequence 1)

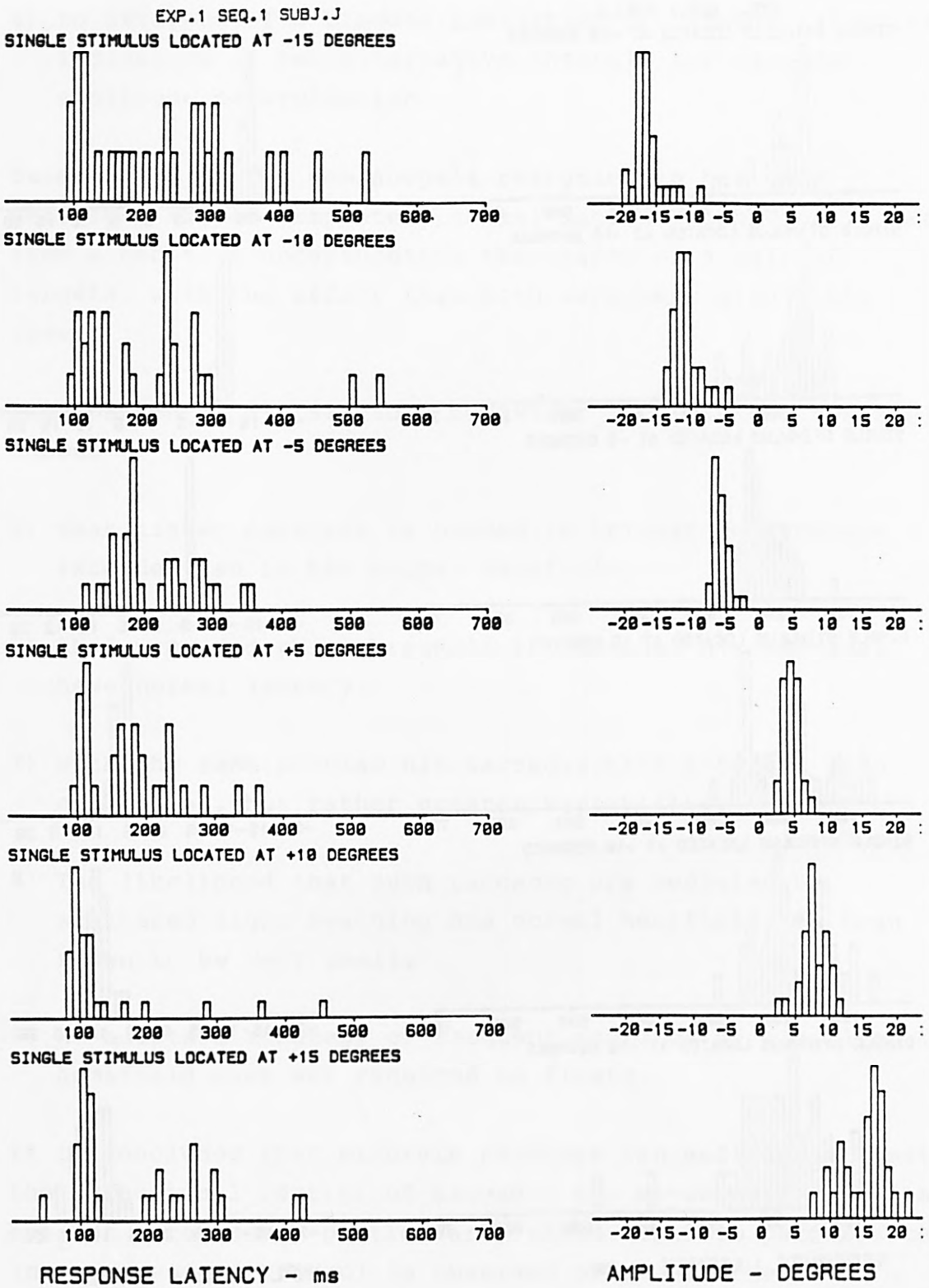

FIGURE 6.7

Distribution of latencies and amplitudes of saccades - JB. Experiment 1. A single 2° stimulus presented at + 5°, + 10° or + 15°, the stimulus appears 200 ms after the fixation light vanishes. (Sequence 1)

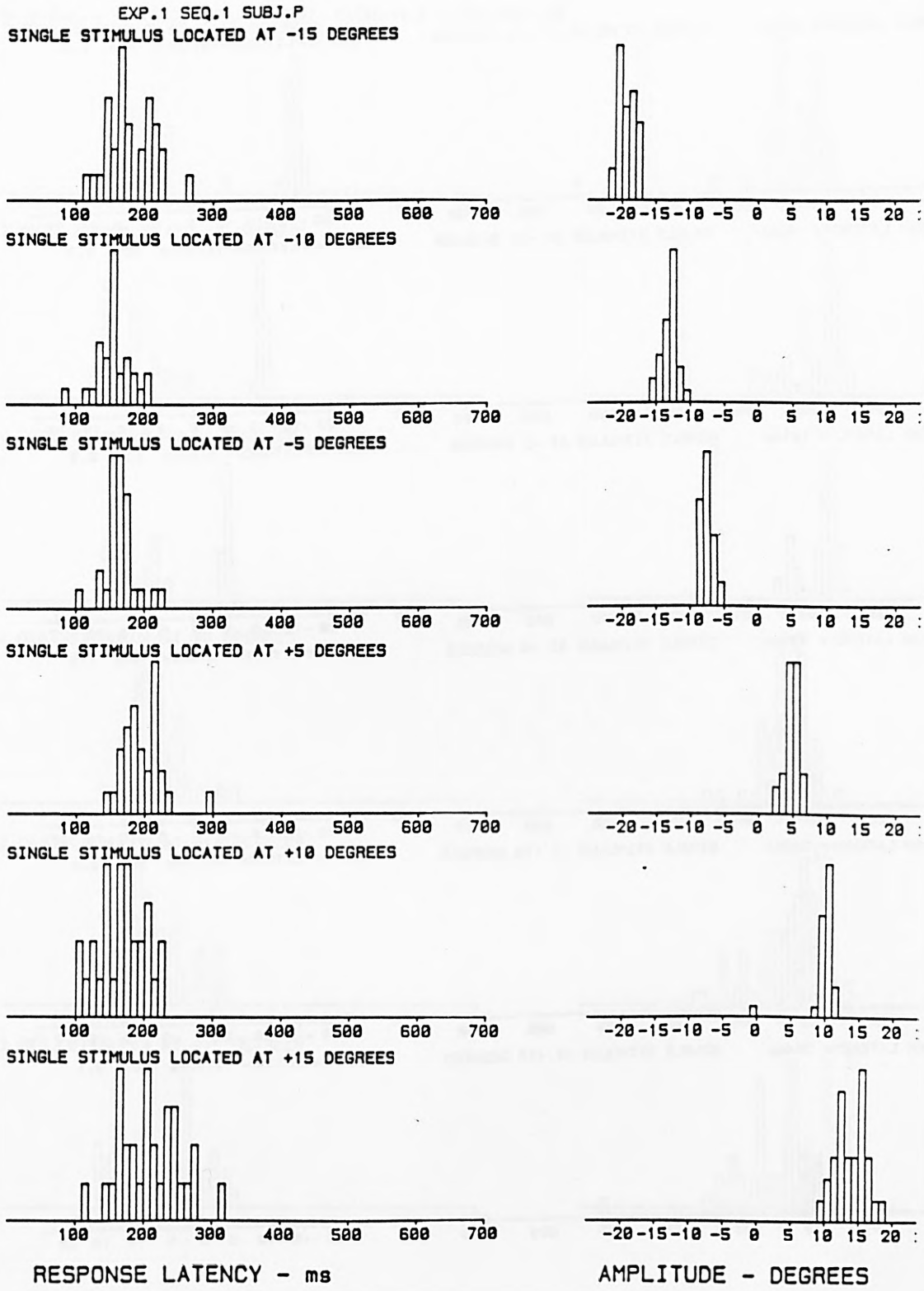

FIGURE 6.8

Distribution of latencies and amplitudes of saccades - PF. Experiment 1. A single 2° stimulus presented at + 5°, + 10° or + 15°, the stimulus appears 200 ms after the fixation light vanishes. (Sequence 1)

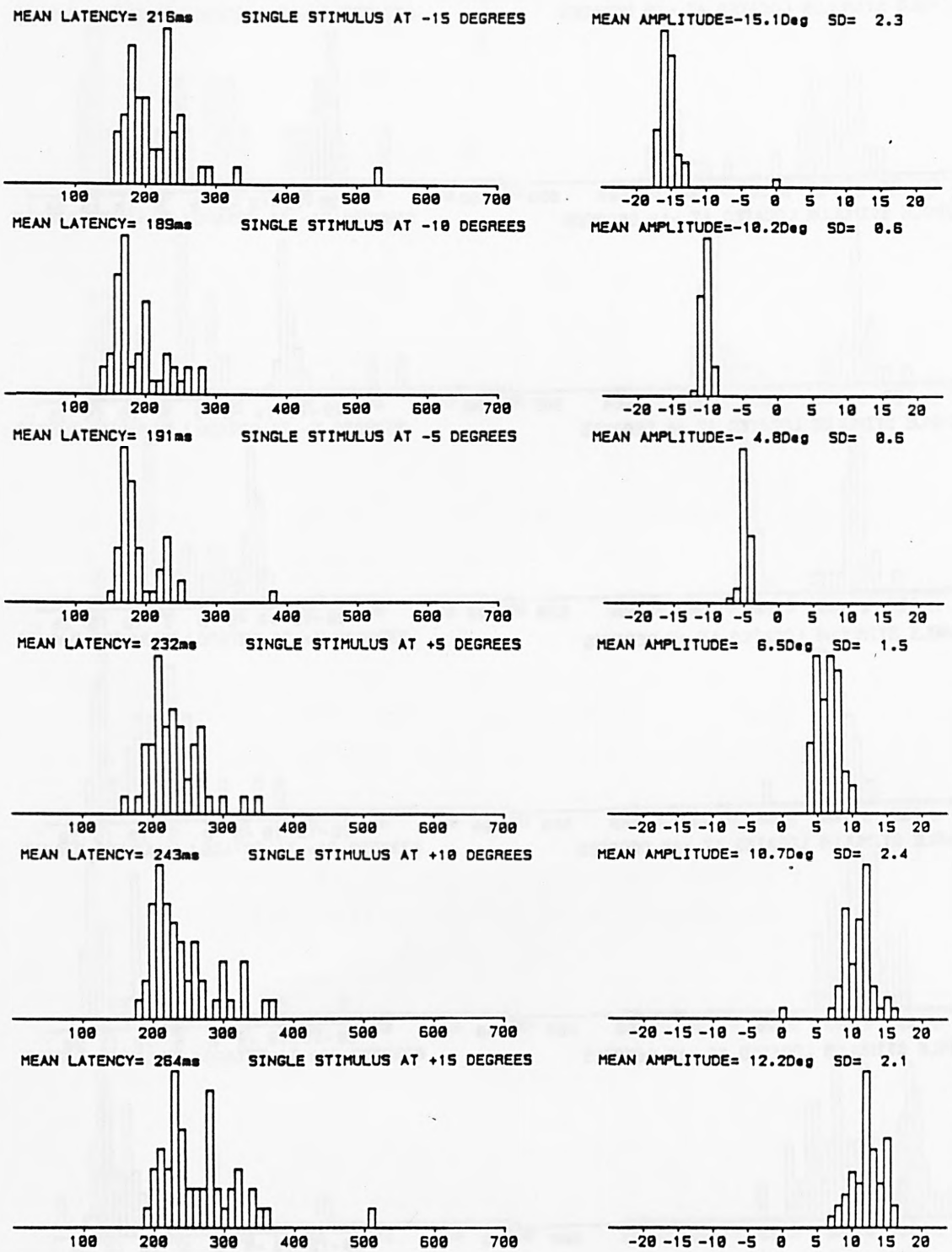

FIGURE 6.9

Distribution of latencies and amplitudes of saccades - GY Experiment 1. A single 2° stimulus presented at + 5°, + 10° or + 15°, the stimulus appearing immediately after the fixation light vanishes. (Sequence 2)

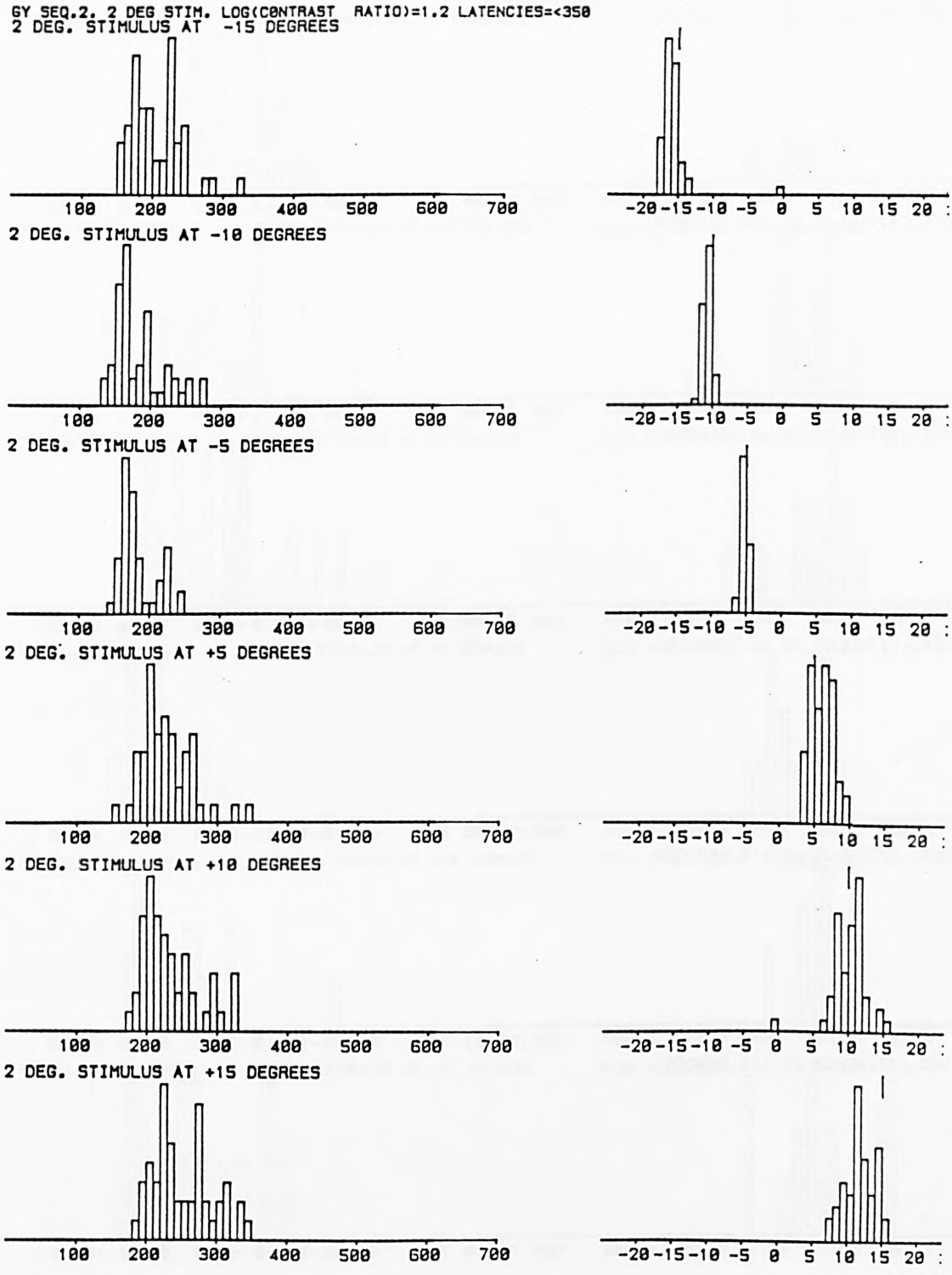

FIGURE 6.10

Distribution of latencies and amplitudes of saccades - GY Experiment 1. A single 2^{o} stimulus presented at $+ 5^{o}$, $+ 10^{o}$ or $+ 15^{o}$, the stimulus appearing immediately after the fixation light vanishes. (Sequence 2). In this revised analysis all saccades with latencies longer than 350 ms were ignored.

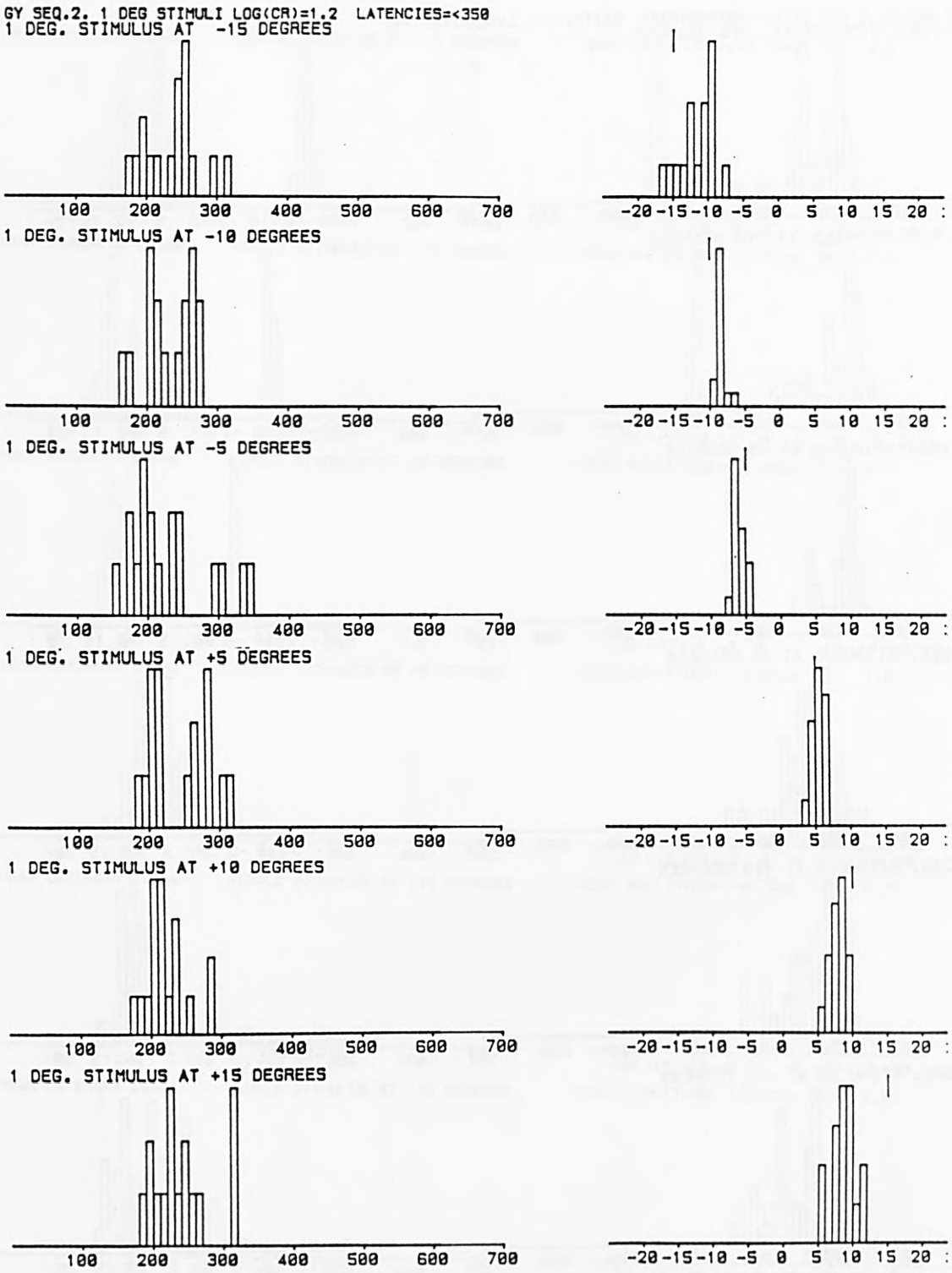

FIGURE 6.11

Distribution of latencies and amplitudes of saccades - GY Experiment 4. A single 1^{o} stimulus presented at $+ 5^{o}$, $+ 10^{o}$ or $+ 15^{o}$, the stimulus appearing immediately after the fixation light vanishes. (Sequence 2)

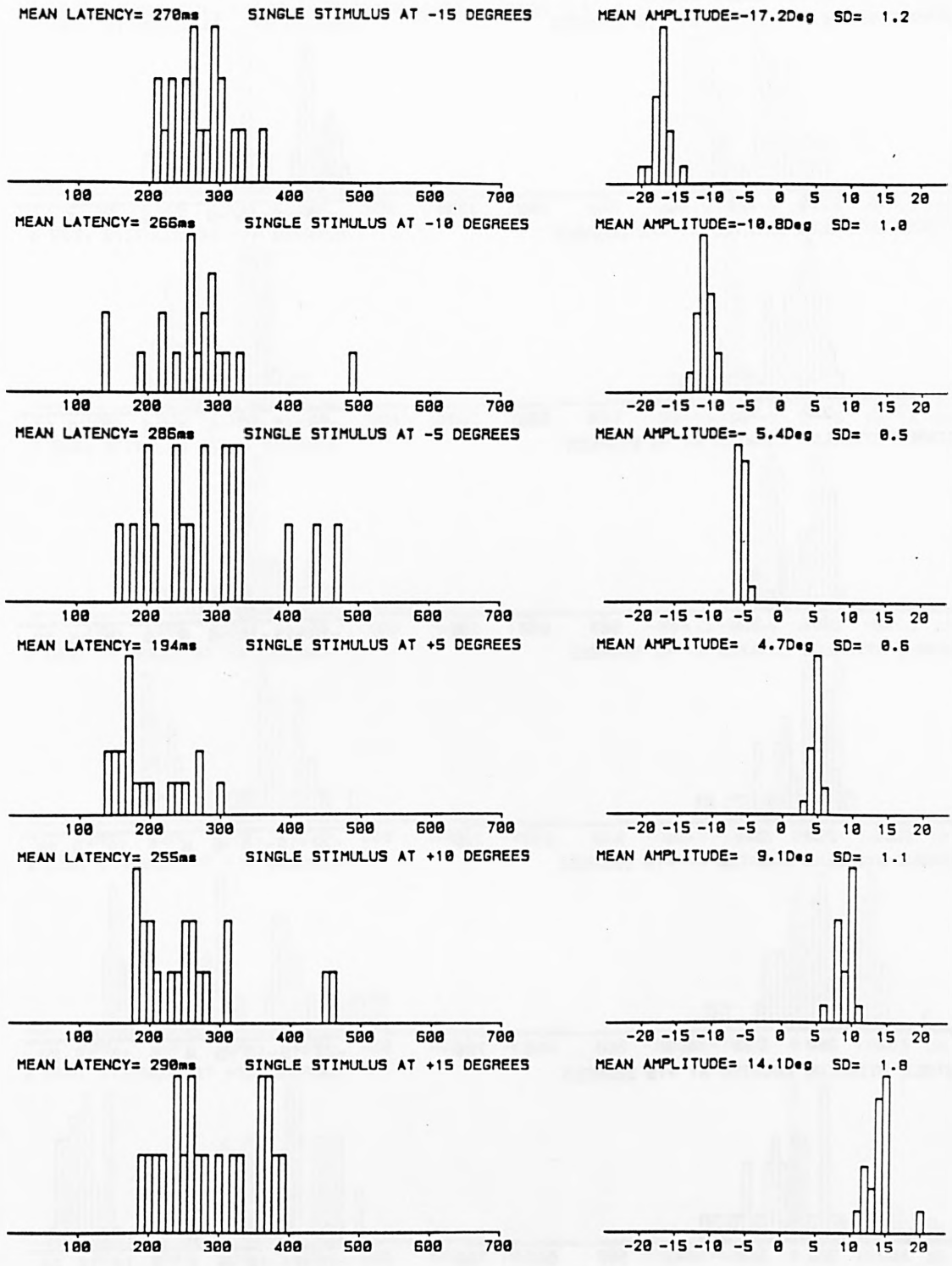

FIGURE 6.12

Distribution of latencies and amplitudes of saccades - JB Experiment 1. A single 2^{o} stimulus presented at $+ 5^{o}$, $+ 10^{o}$ or $+ 15^{o}$, the stimulus appearing immediately after the fixation light vanishes. (Sequence 2)

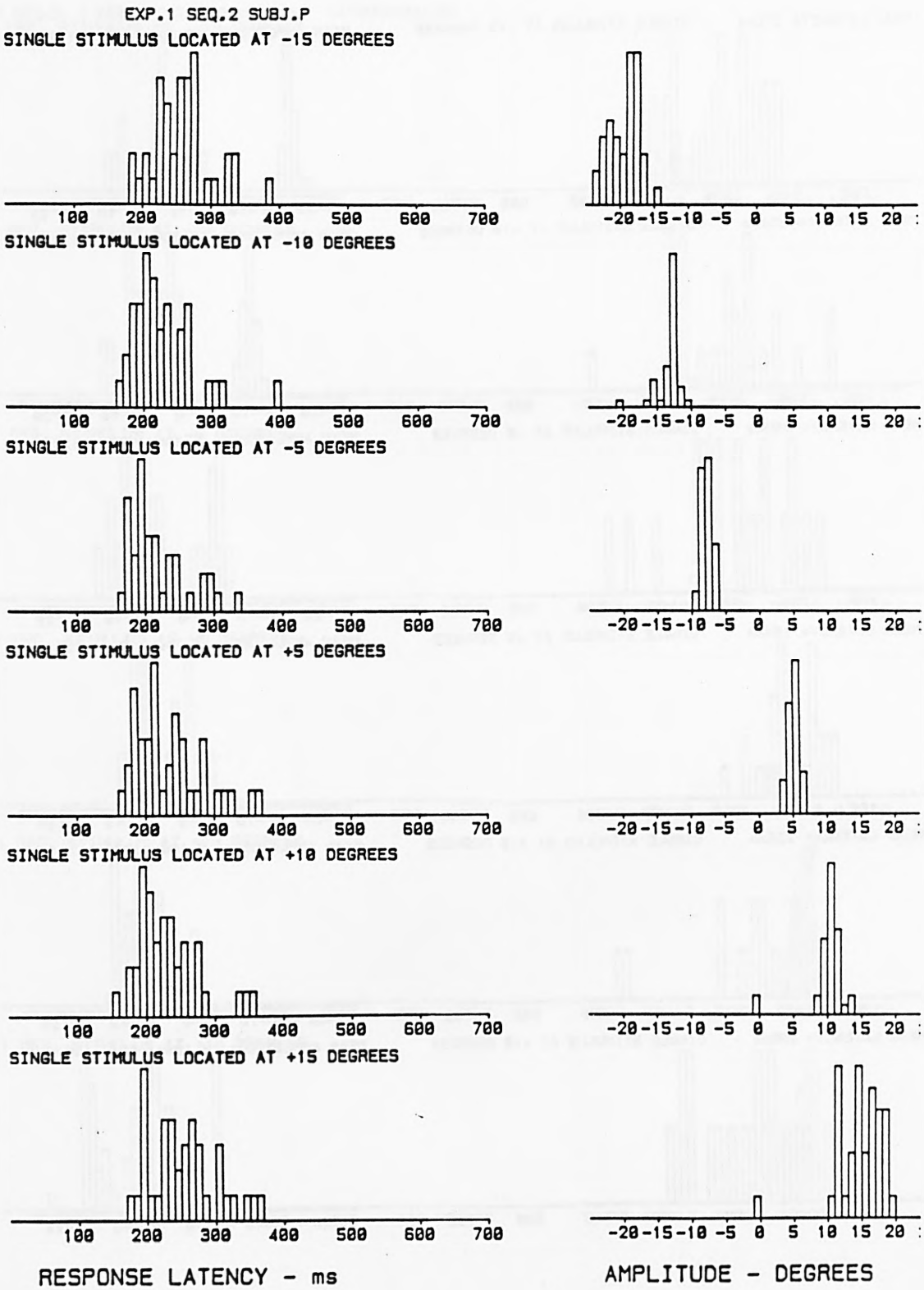

FIGURE 6.13

Distribution of latencies and amplitudes of saccades - PF Experiment 1. A single 2° stimulus presented at + 5°, + 10° or + 15°, the stimulus appearing immediately after the fixation light vanishes. (Sequence 2)

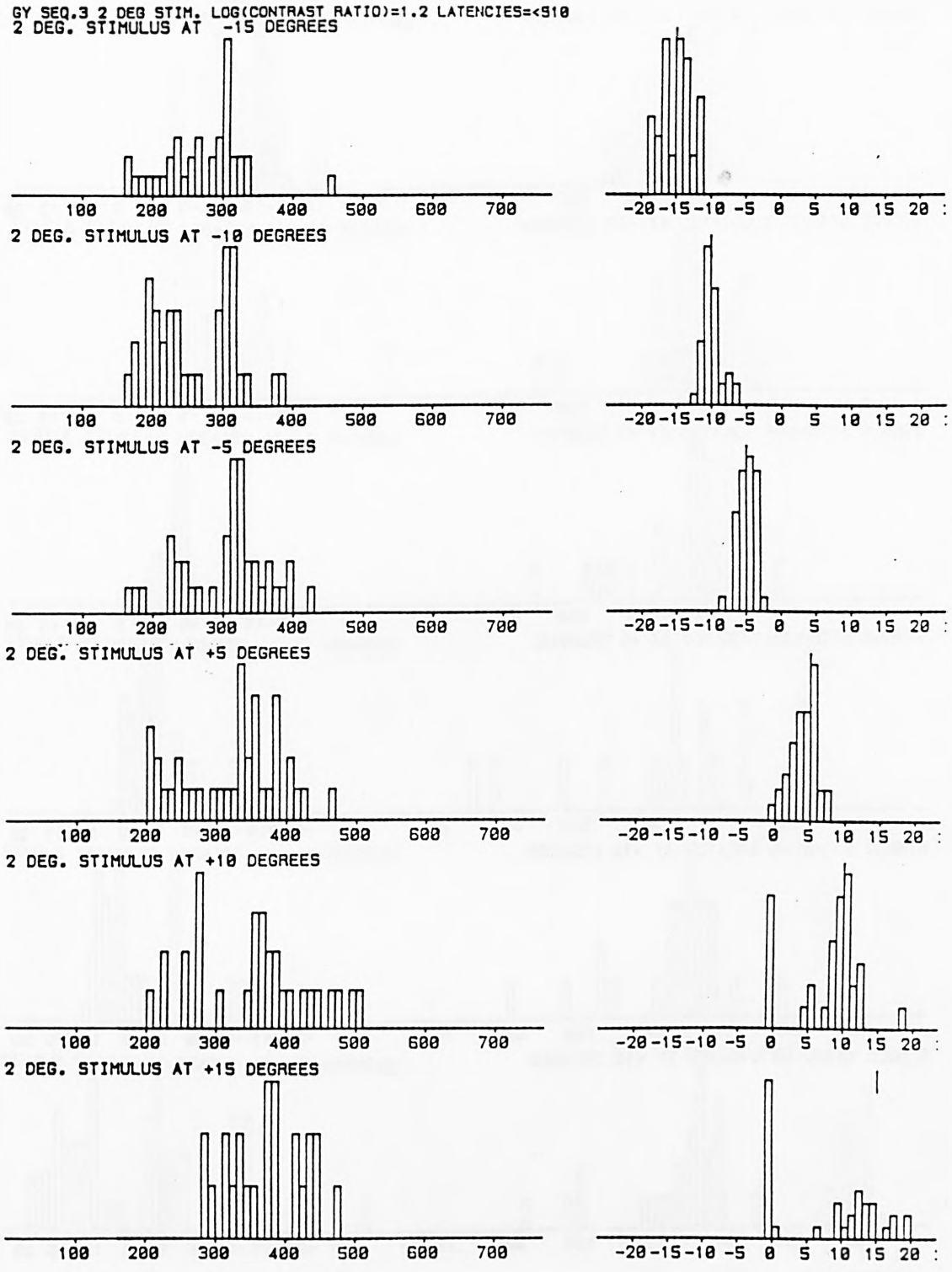

FIGURE 6.14

Distribution of latencies and amplitudes of saccades - GY Experiment 1. A single 2° stimulus presented at + 5°, + 10° or + 15°, the stimulus flashing on immediately after the fixation light vanishes, for 160 ms. (Sequence 3) In this analysis all saccades with latencies longer than 510 ms (i.e. 350 ms after the offset of stimulus) were ignored.

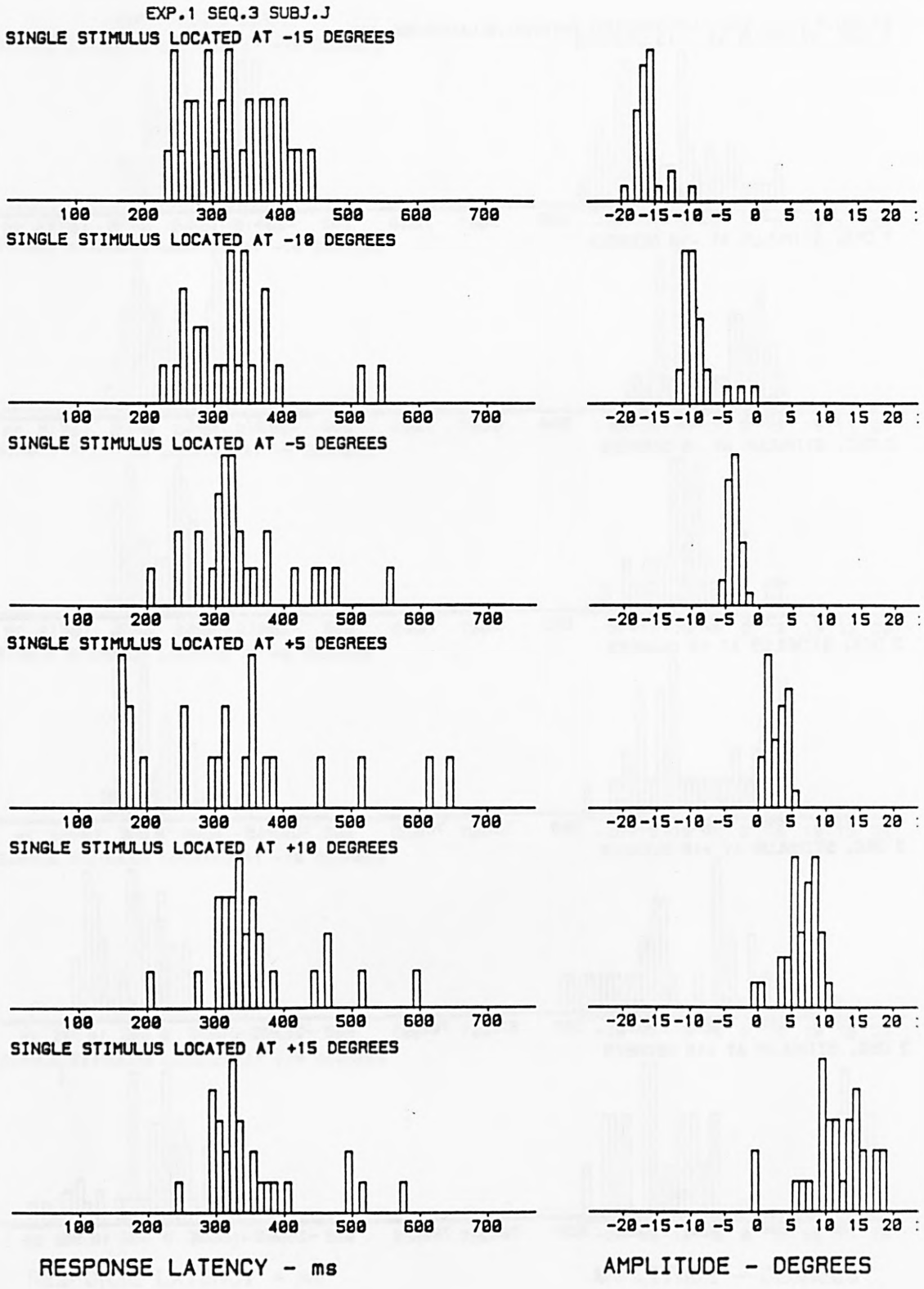

FIGURE 6.15

Distribution of latencies and amplitudes of saccades - JB Experiment 1. A single 2° stimulus presented at + 5°, + 10° or + 15°, the stimulus flashing on immediately after the fixation light vanishes, for 160 ms. (Sequence 3)

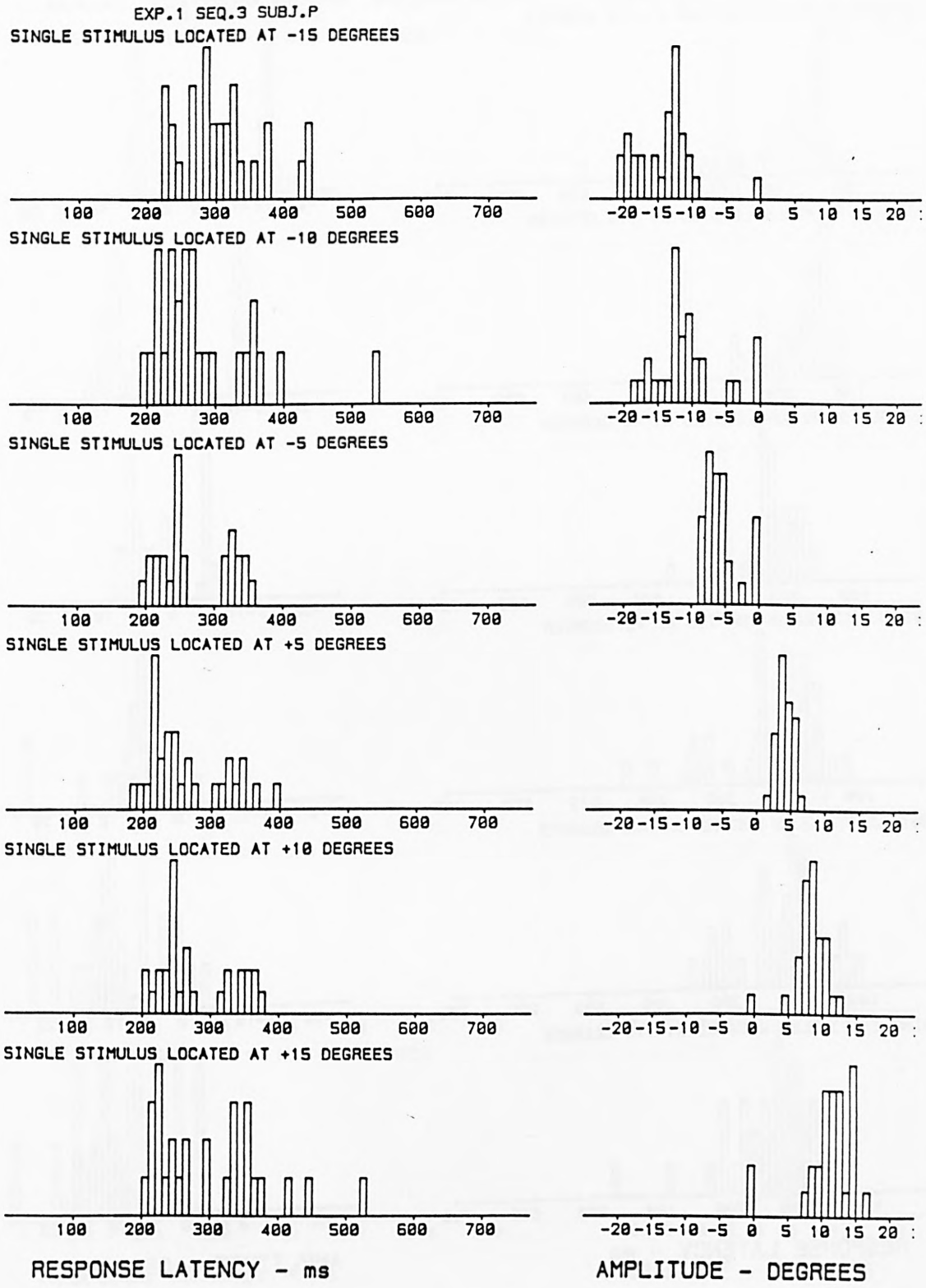

FIGURE 6.16

Distribution of latencies and amplitudes of saccades - PF Experiment 1. A single 2° stimulus presented at + 5°, + 10° or + 15°, the stimulus flashing on immediately after the fixation light vanishes, for 160 ms. (Sequence 3)

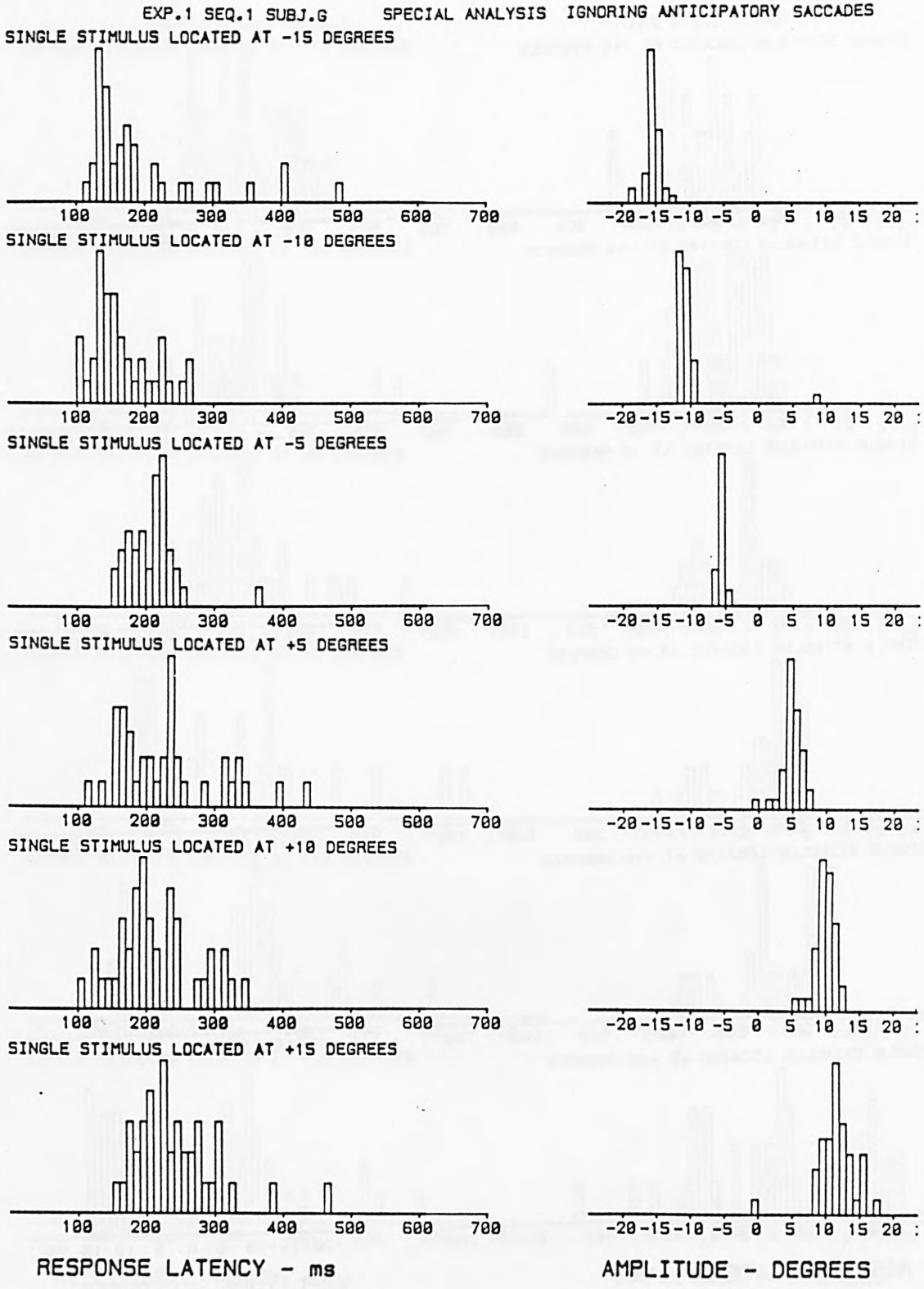

FIGURE 6.17

Distribution of latencies and amplitudes of saccades - GY. Experiment 1. A single 2° stimulus presented at + 5°, + 10° or + 15°, the stimulus appears 200 ms after the fixation light vanishes. (Sequence 1). The same set of eye movements as in figure 6.6, but ignoring anticipatory saccades.

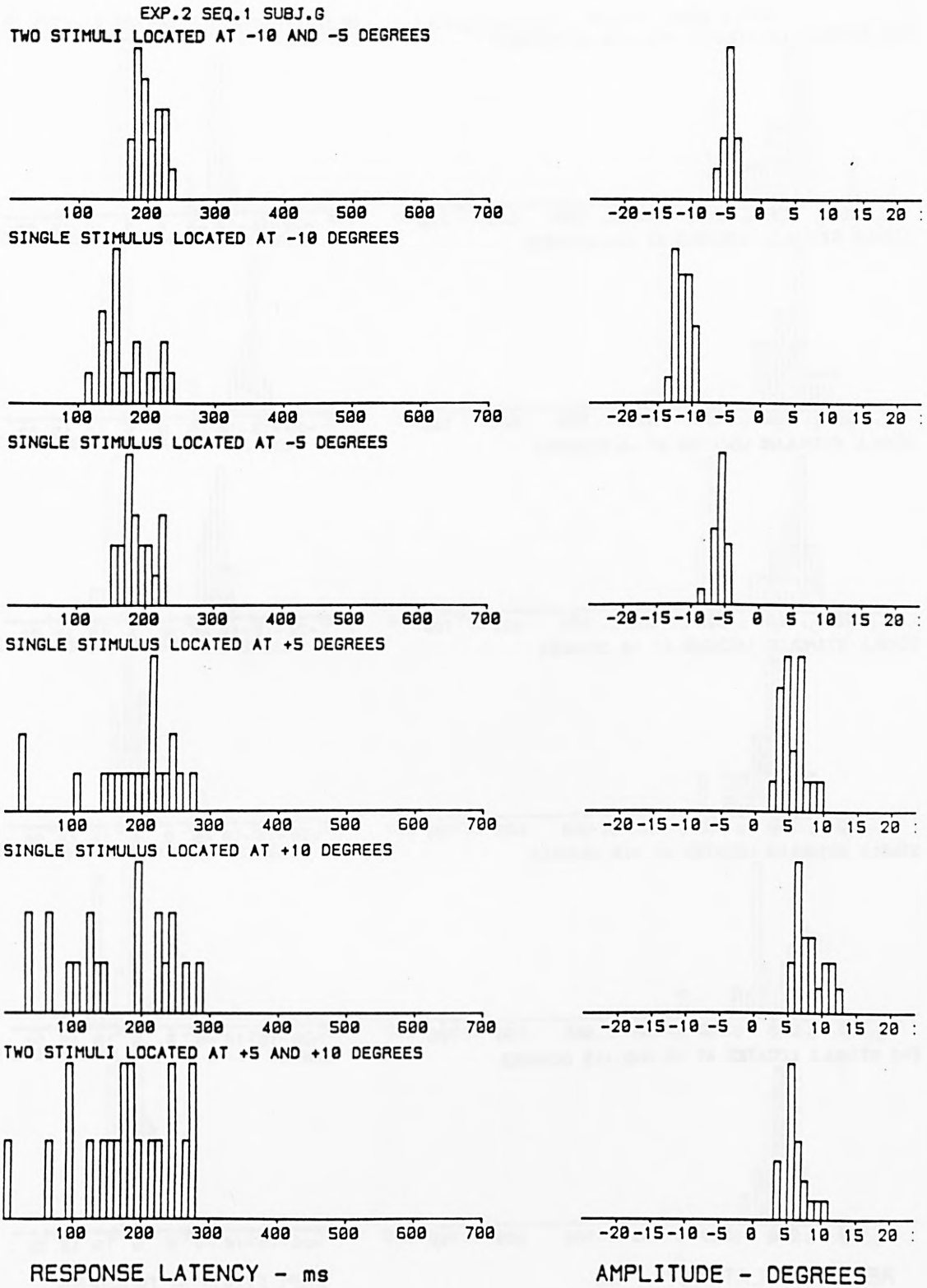

FIGURE 6.18

Distribution of latencies and amplitudes of saccades - GY. Experiment 2. A pair of 2^{o} stimuli presented at $+5^{o}$ and $+10^{o}$ or at -5^{o} and -10^{o} interspersed with single stimuli at $+5^{o}$ and $+10^{o}$. The stimulus appears 200 ms after the fixation light vanishes. (Sequence 1)

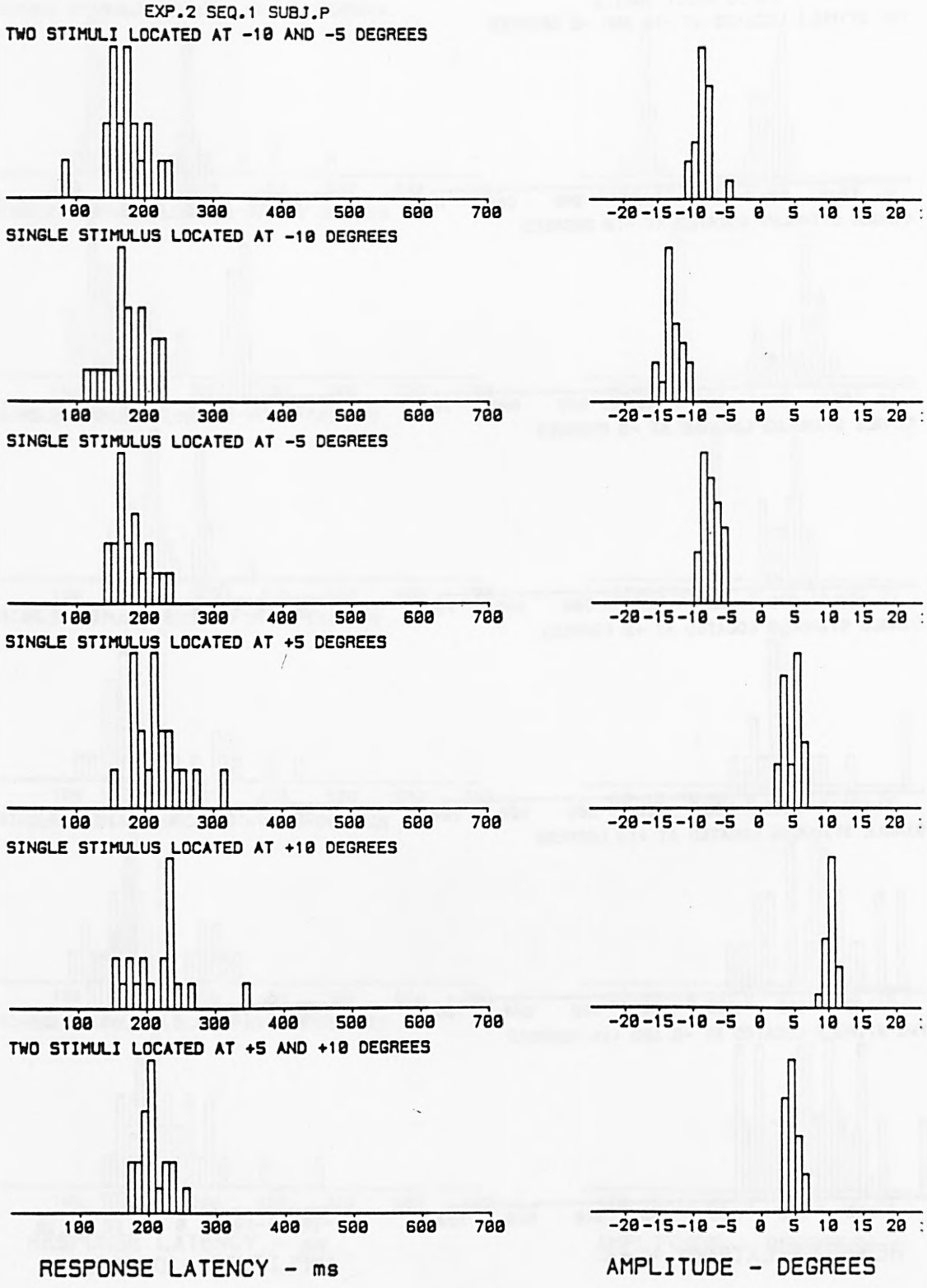

FIGURE 6.19

Distribution of latencies and amplitudes of saccades - PF. Experiment 2. A pair of 2^{o} stimuli presented at $+5^{o}$ and $+10^{o}$ or at -5^{o} and -10^{o} interspersed with single stimuli at $+5^{o}$ and $+10^{o}$. The stimulus appears 200 ms after the fixation light vanishes. (Sequence 1)

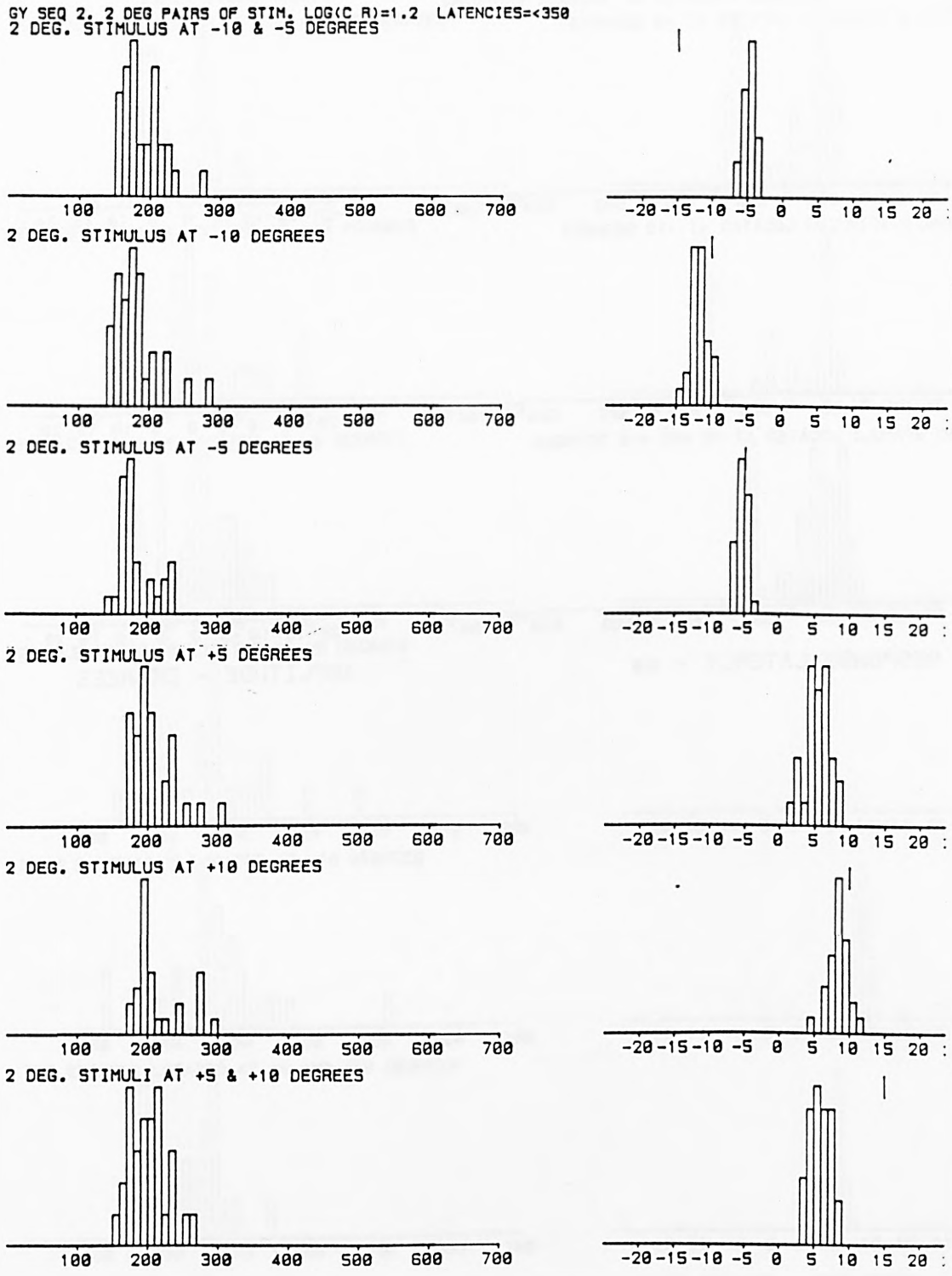

FIGURE 6.20

Distribution of latencies and amplitudes of saccades - GY. Experiment 2. A pair of 2^{o} stimuli presented at $+5^{o}$ and $+10^{o}$ or at -5^{o} and -10^{o} interspersed with single stimuli at $+5^{o}$ and $+10^{o}$. The stimulus appears immediately the fixation light vanishes. (Sequence 2). In this analysis all saccades with latencies longer than 350 ms were ignored.

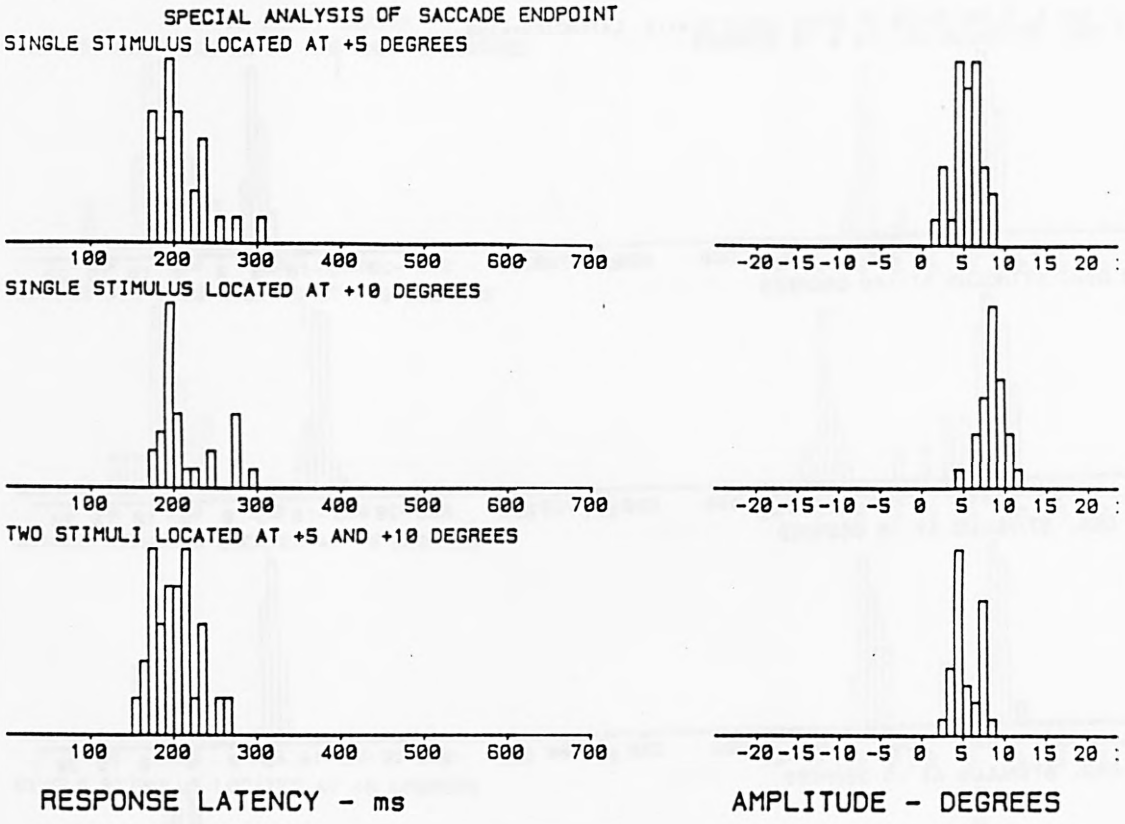

FIGURE 6.21

Distribution of latencies and amplitudes of saccades - GY. Experiment 2. A pair of 2° stimuli presented at +5° and +10° or at -5° and -10° interspersed with single stimuli at + 5° and + 10°. The stimulus appears immediately the fixation light vanishes. (Sequence 2). The same set of eye movements as figure 6.20, but analysed for the amplitude of the endpoint of the eye movement, 600 ms after the stimulus onset.

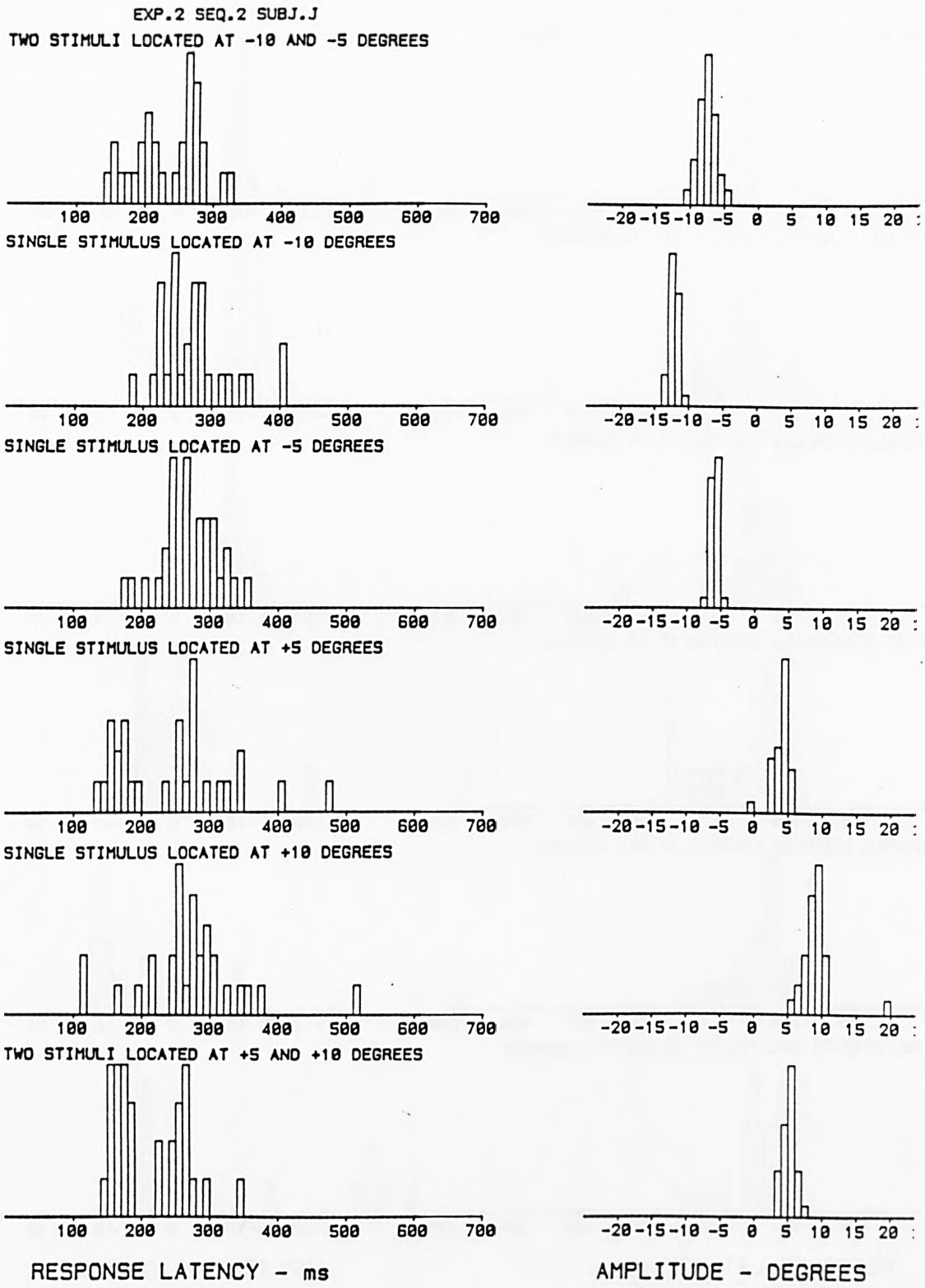

FIGURE 6.22

Distribution of latencies and amplitudes of saccades - JB. Experiment 2. A pair of 2^{o} stimuli presented at $+5^{o}$ and $+10^{o}$ or at -5^{o} and -10^{o} interspersed with single stimuli at $+5^{o}$ and $+10^{o}$. The stimulus appears immediately the fixation light vanishes. (Sequence 2).

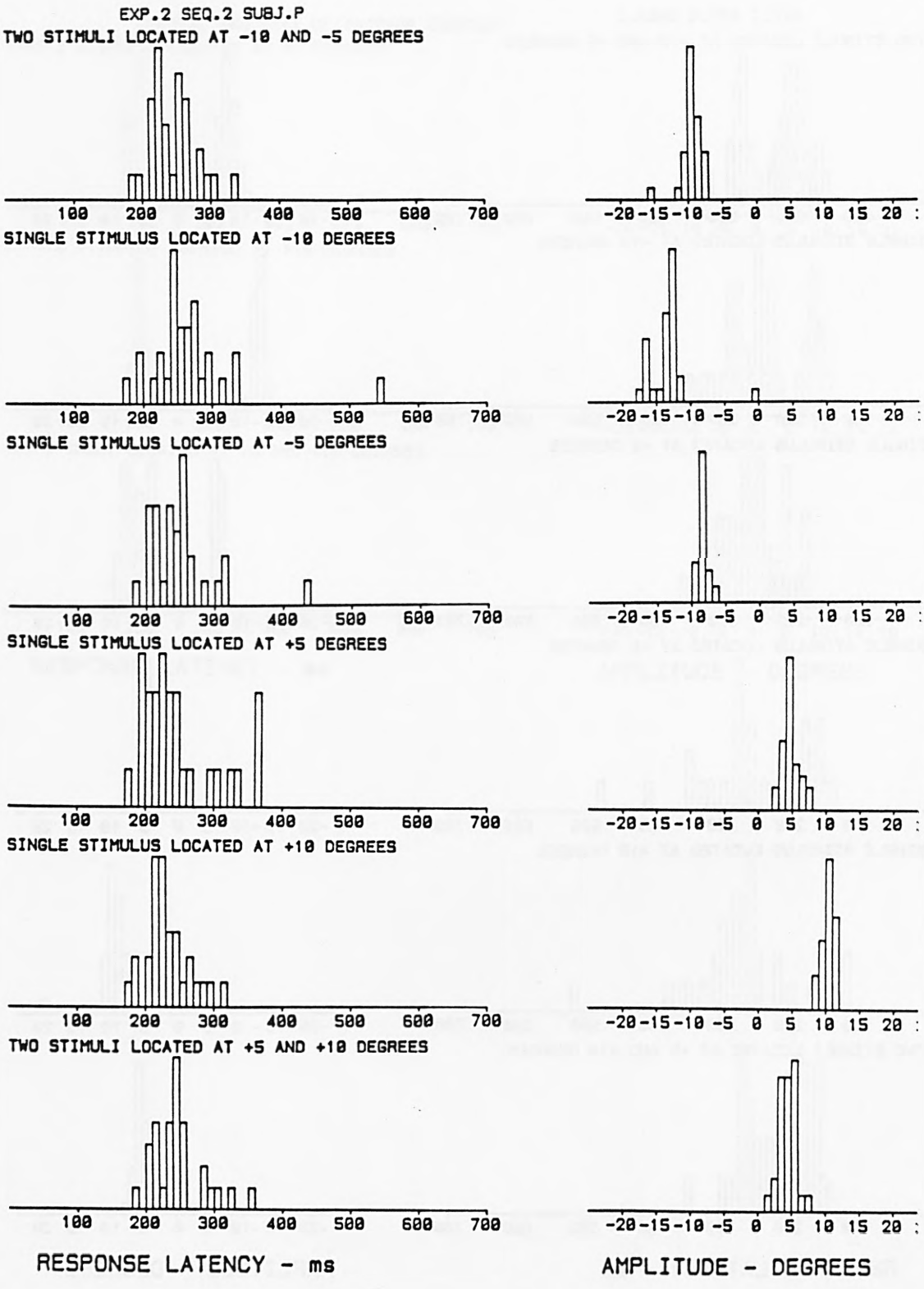

FIGURE 6.23

Distribution of latencies and amplitudes of saccades - PF. Experiment 2. A pair of 2^{o} stimuli presented at $+5^{o}$ and $+10^{o}$ or at -5^{o} and -10^{o} interspersed with single stimuli at $+5^{o}$ and $+10^{o}$. The stimulus appears immediately the fixation light vanishes. (Sequence 2).

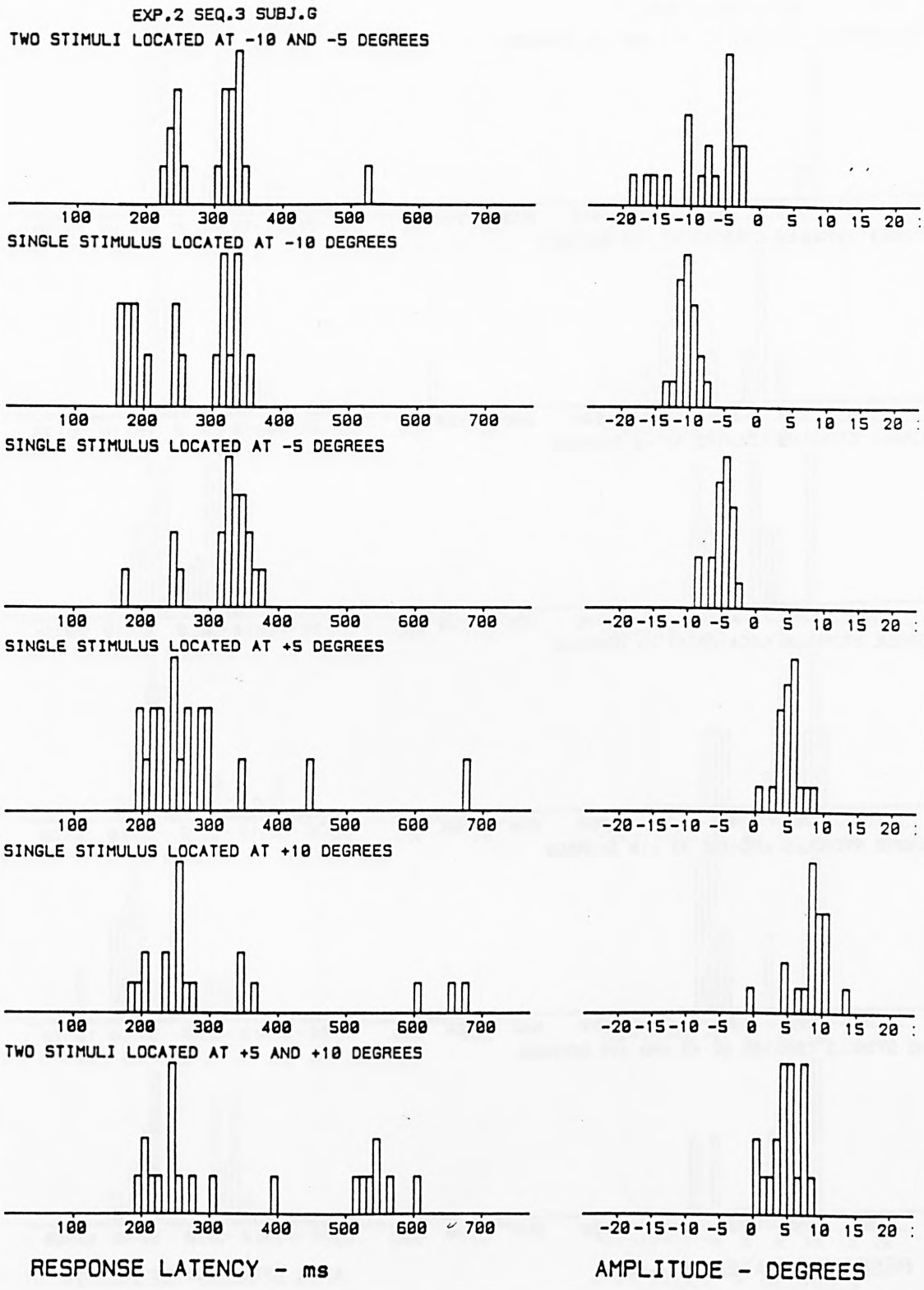

FIGURE 6.24

Distribution of latencies and amplitudes of saccades - GY. Experiment 2. A pair of 2^{o} stimuli presented at $+5^{o}$ and $+10^{o}$ or at -5^{o} and -10^{o} interspersed with single stimuli at $+5^{o}$ and $+10^{o}$. The stimulus flashes on immediately the fixation light vanishes, for 160 ms only. (Sequence 3).

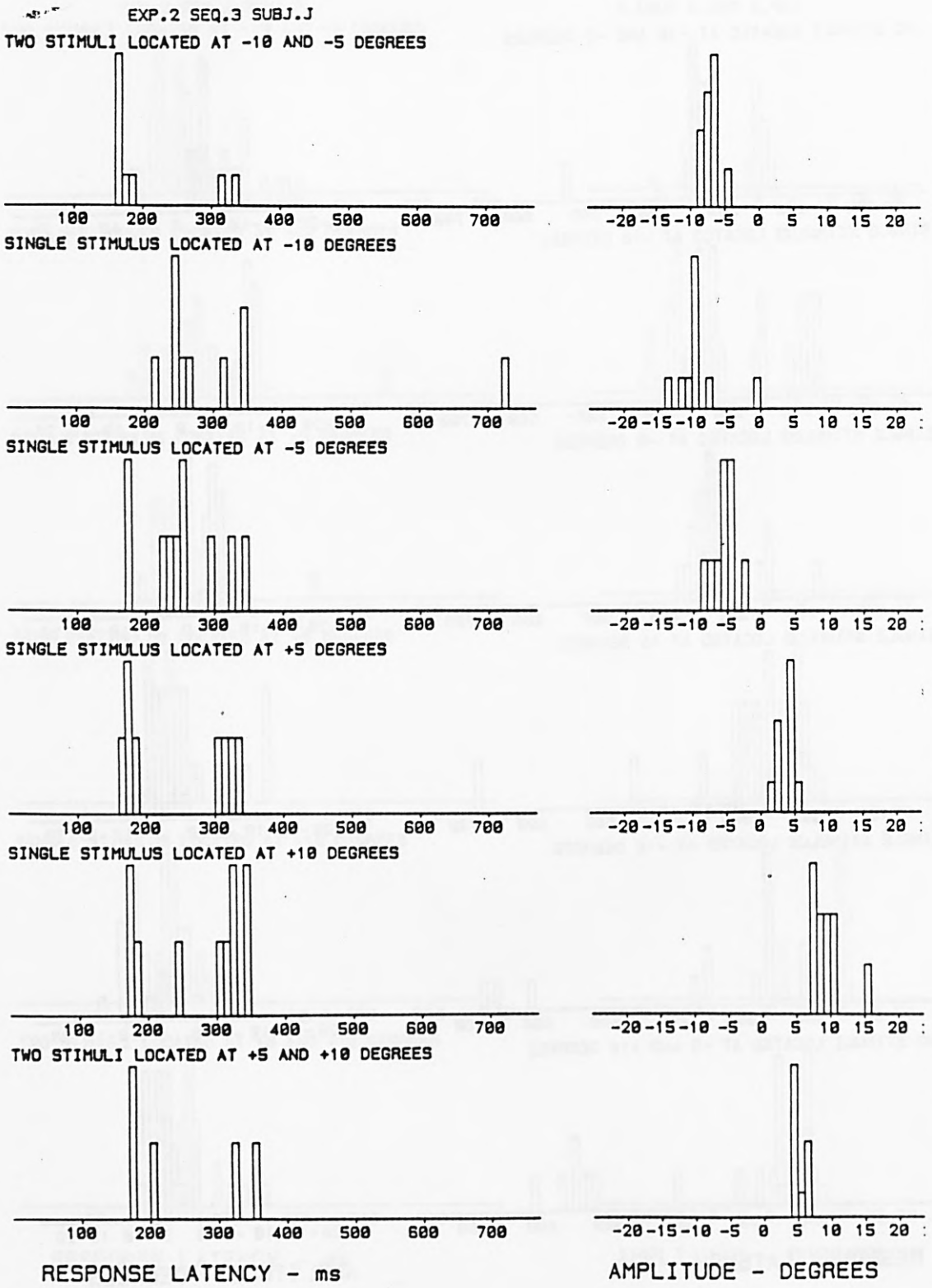

FIGURE 6.25

Distribution of latencies and amplitudes of saccades - JB. Experiment 2. A pair of 2^{o} stimuli presented at $+5^{o}$ and $+10^{o}$ or at -5^{o} and -10^{o} interspersed with single stimuli at $+5^{o}$ and $+10^{o}$. The stimulus flashes on immediately the fixation light vanishes, for 160 ms only.

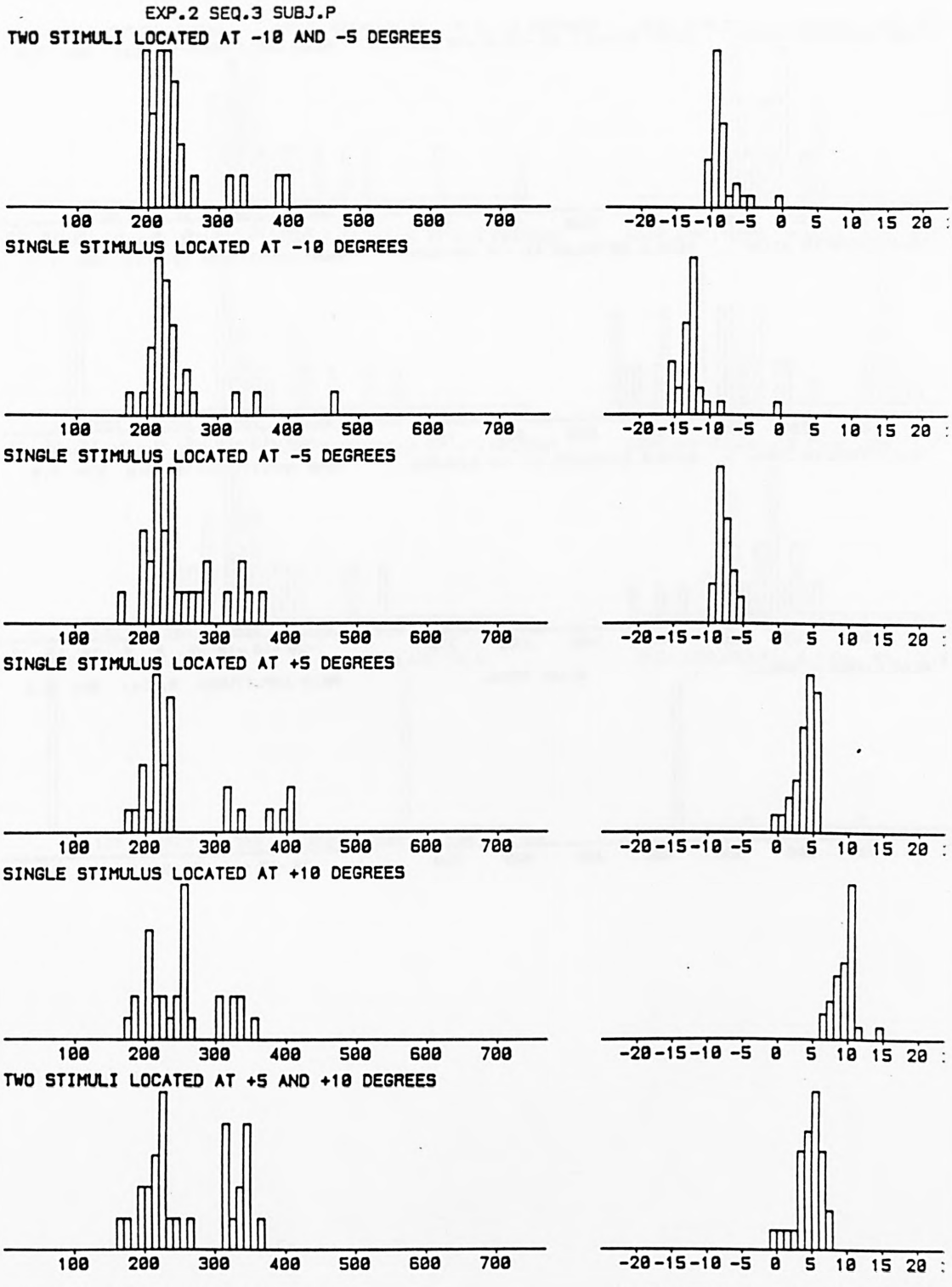

FIGURE 6.26

Distribution of latencies and amplitudes of saccades - PF. Experiment 2. A pair of 2° stimuli presented at +5° and +10° or at -5° and -10° interspersed with single stimuli at + 5° and + 10°. The stimulus flashes on immediately the fixation light vanishes, for 160 ms only.

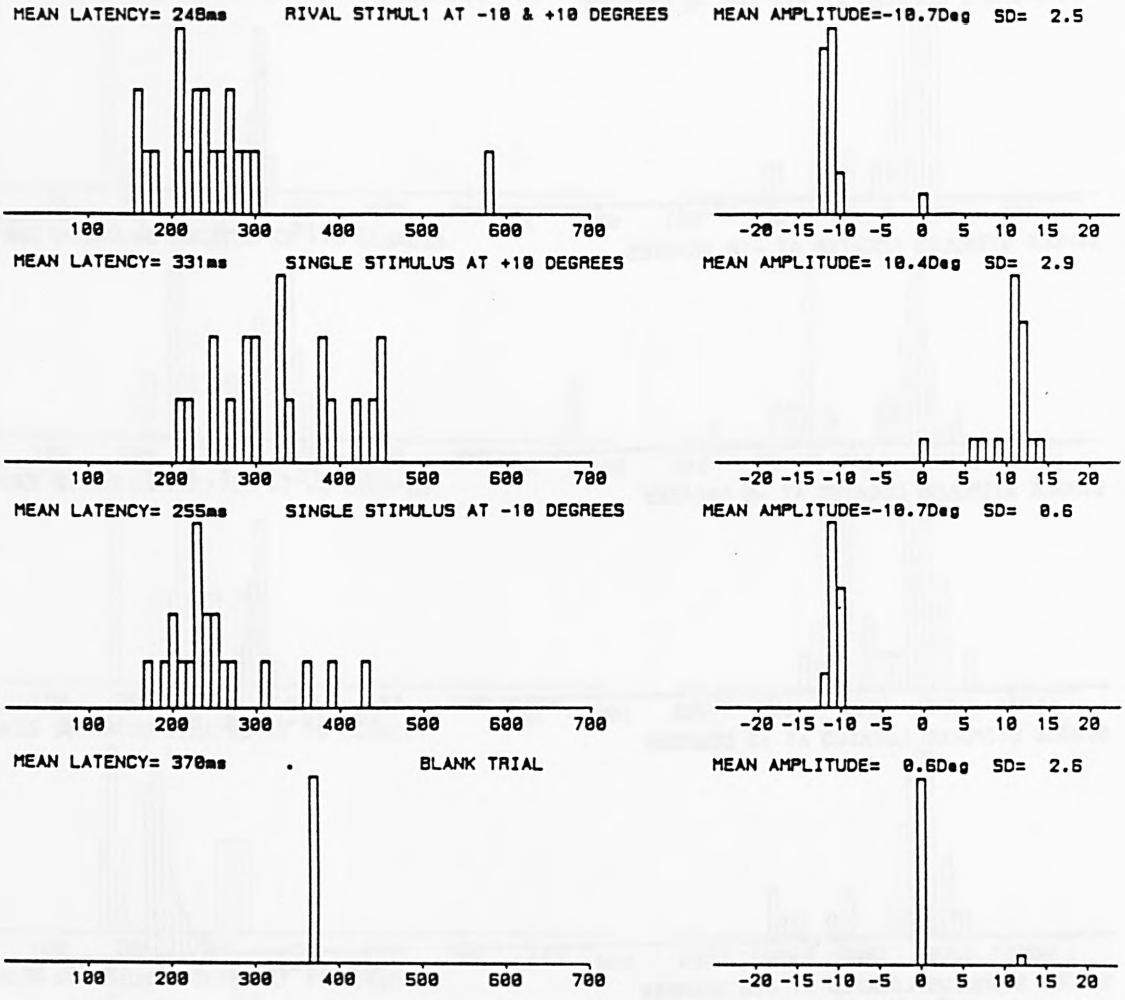

FIGURE 6.27

Distribution of latencies and amplitudes of saccades - GY. Experiment 3. A pair of 2^{o} stimuli presented at -10^{o} and $+10^{o}$ interspersed with single stimuli at $+10^{o}$ and with blank trials (no stimuli). The stimulus is presented immediately after the fixation light vanishes. (Sequence 2).

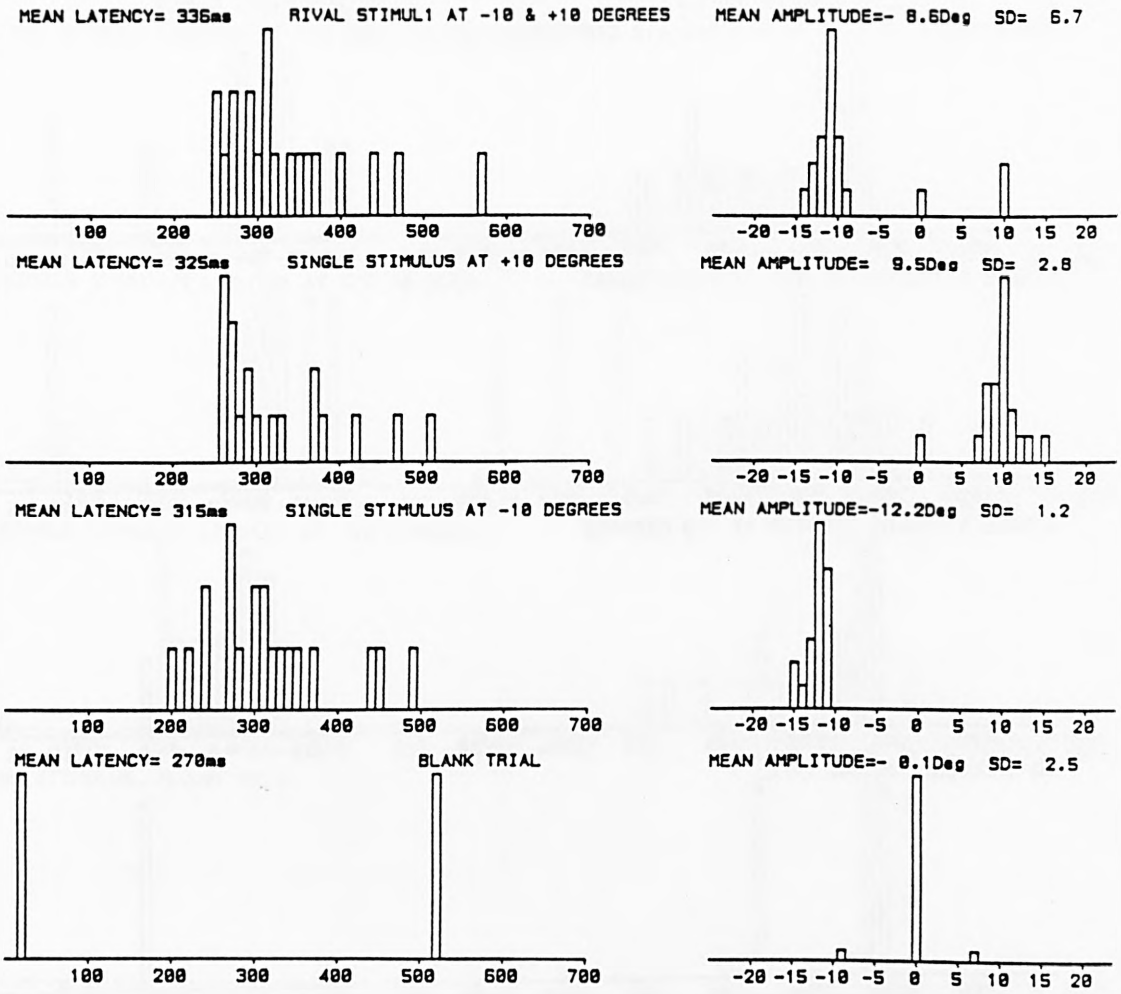

FIGURE 6.28

Distribution of latencies and amplitudes of saccades - JB. Experiment 3. A pair of 2^{o} stimuli presented at -10^{o} and $+10^{o}$ interspersed with single stimuli at $+ 10^{o}$ and with blank trials (no stimuli). The stimulus is presented immediately after the fixation light vanishes. (Sequence 2).

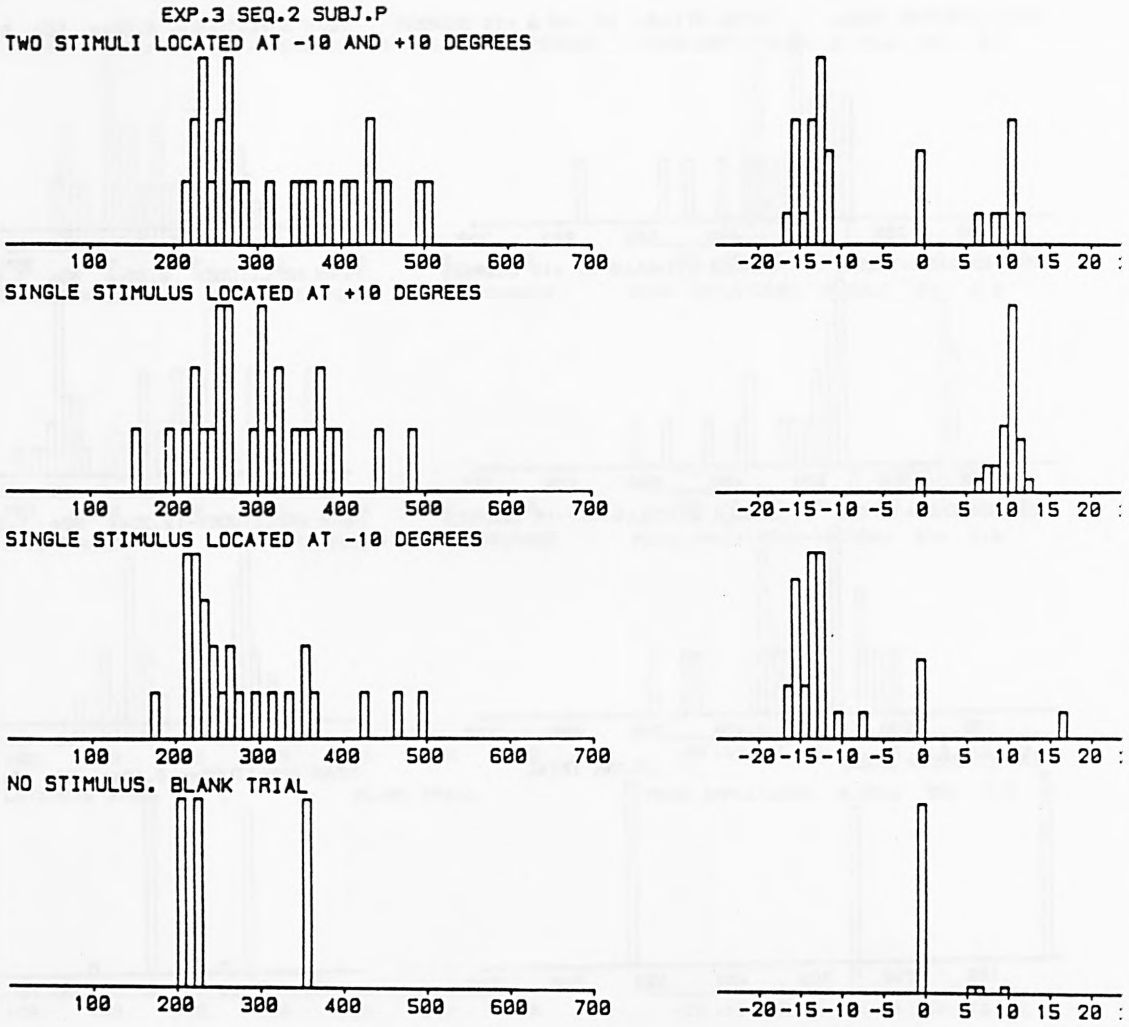

FIGURE 6.29

Distribution of latencies and amplitudes of saccades - PF. Experiment 3. A pair of 2^{o} stimuli presented at -10^{o} and $+10^{o}$ interspersed with single stimuli at $+10^{o}$ and with blank trials (no stimuli). The stimulus is presented immediately after the fixation light vanishes. (Sequence 2).

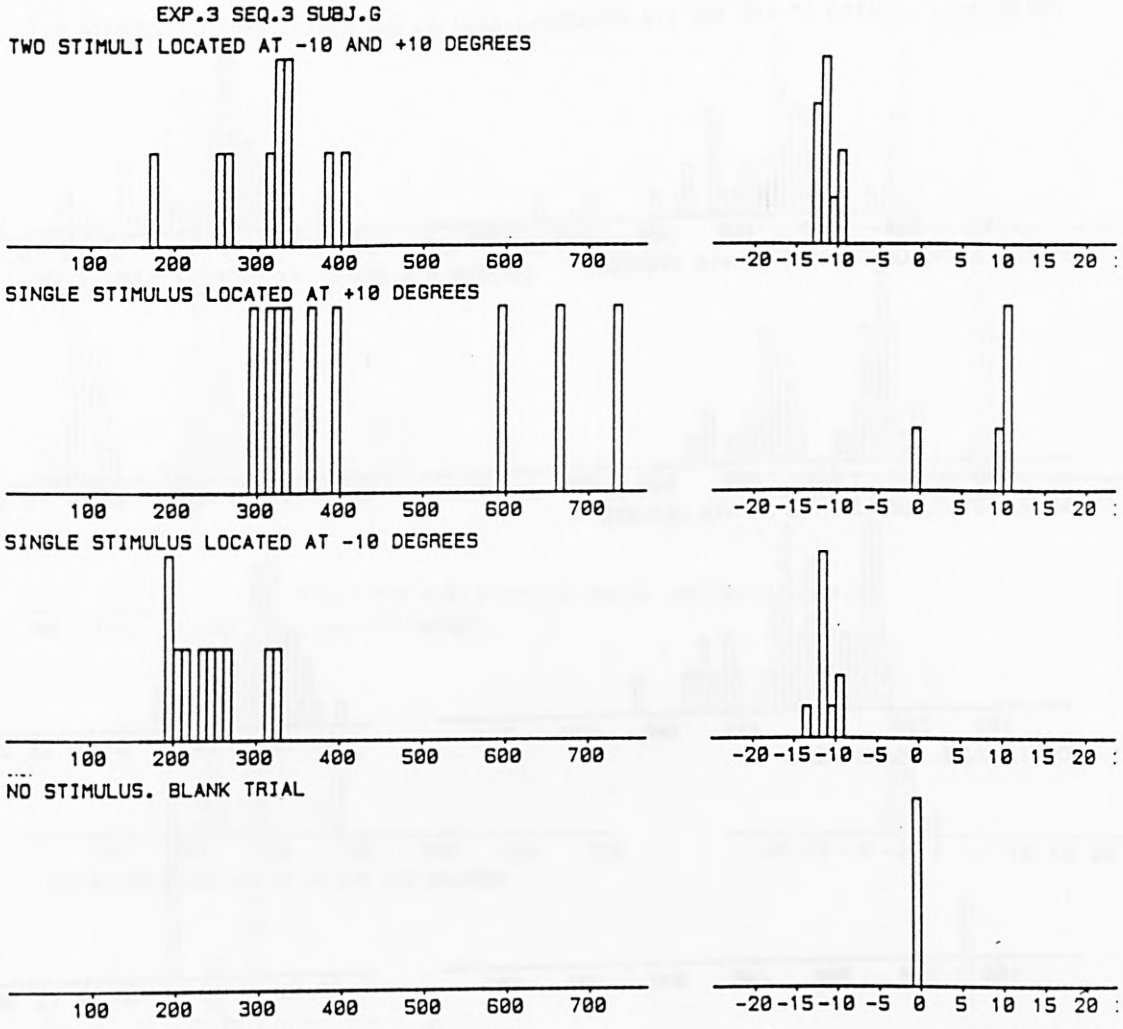

FIGURE 6.30

Distribution of latencies and amplitudes of saccades - GY. Experiment 3. A pair of 2^{o} stimuli presented at -10^{o} and $+10^{o}$ interspersed with single stimuli at $+10^{o}$ and with blank trials (no stimuli). The stimulus flashes on immediately the fixation light vanishes, for 160 ms only.

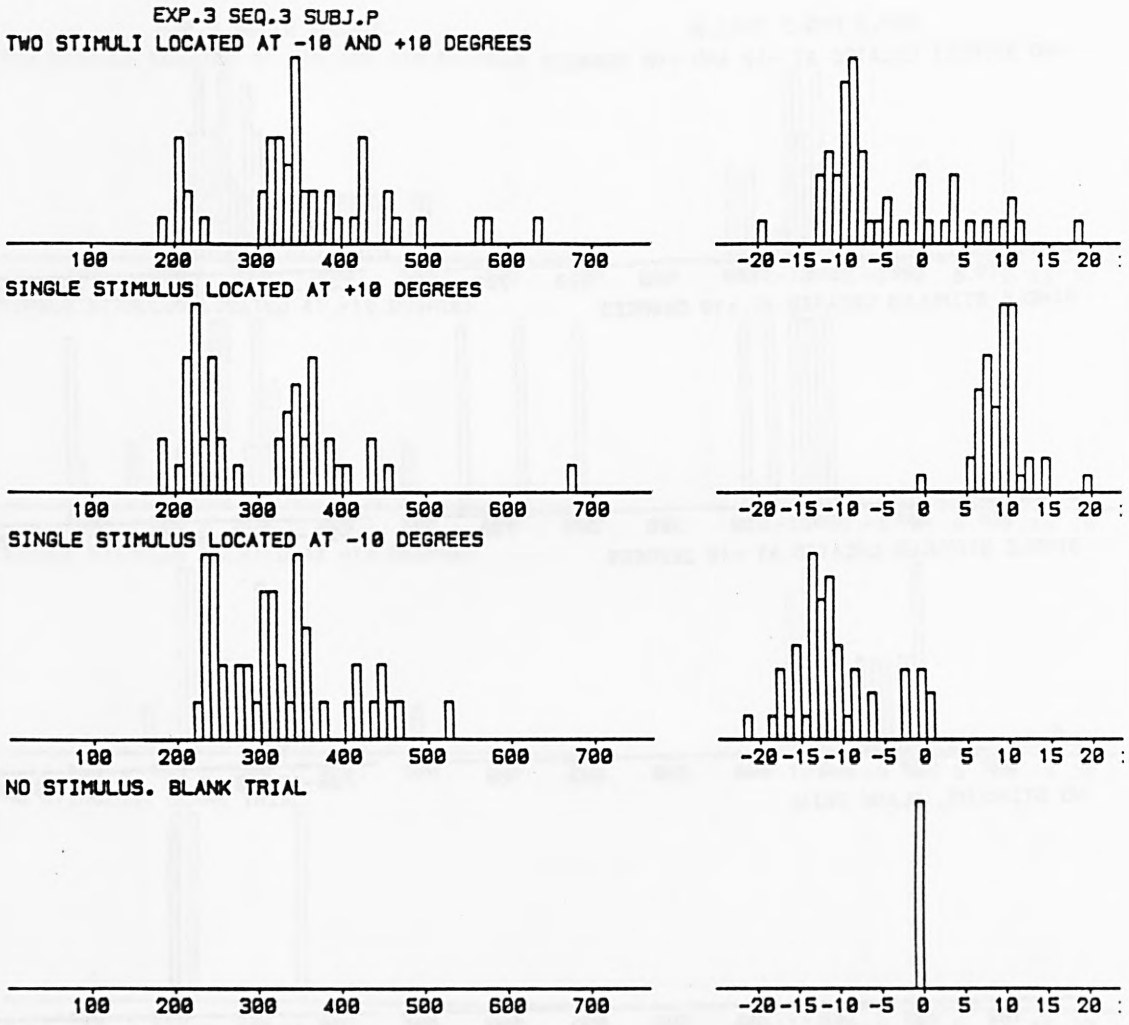

FIGURE 6.31

Distribution of latencies and amplitudes of saccades - PF. Experiment 3. A pair of 2^{o} stimuli presented at -10^{o} and $+10^{o}$ interspersed with single stimuli at $+10^{o}$ and with blank trials (no stimuli). The stimulus flashes on immediately the fixation light vanishes, for 160 ms only.

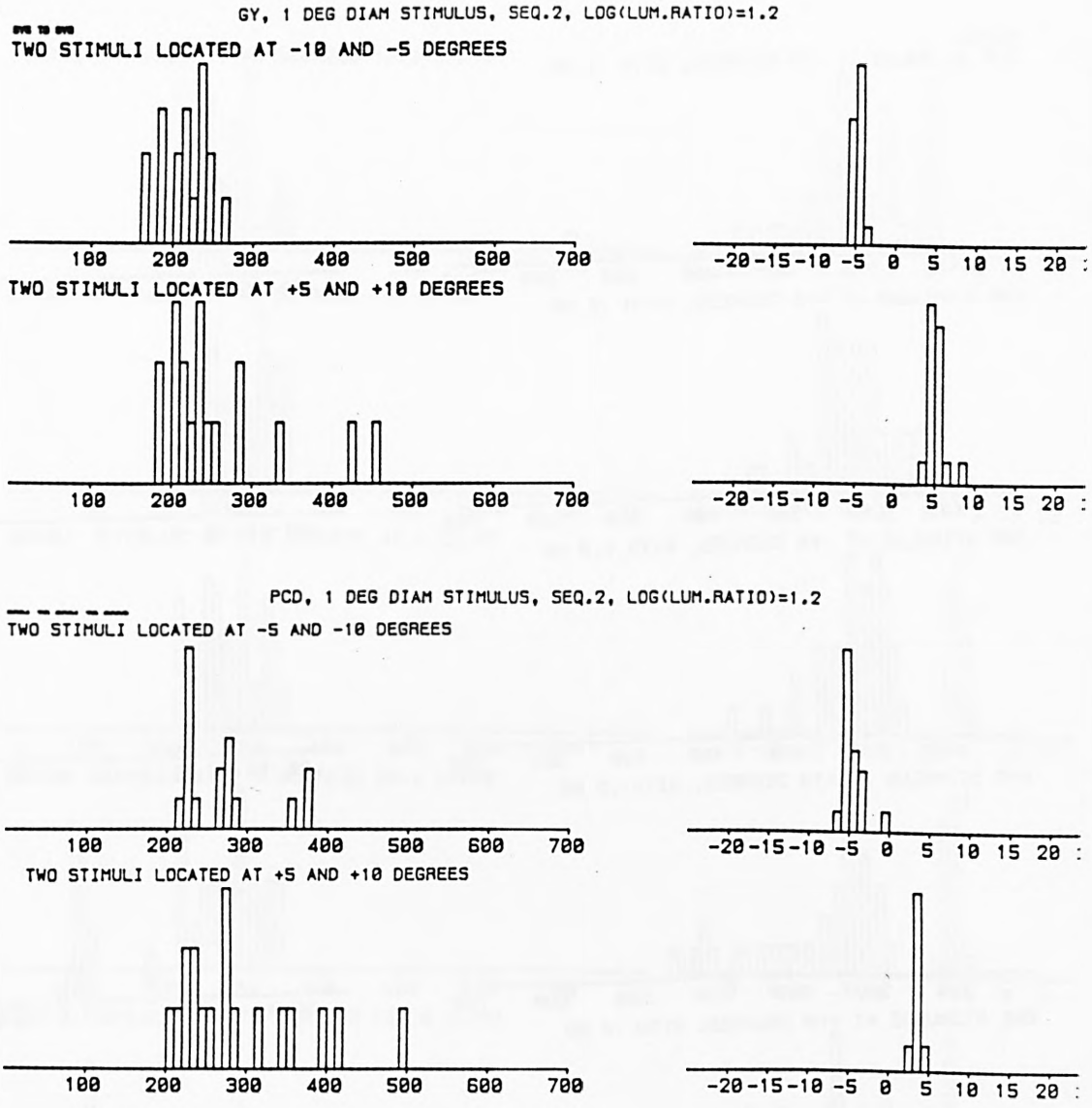

FIGURE 6.32

Distribution of latencies and amplitudes of saccades Experiment 4. A pair of 1° stimuli presented at +5° and +10° or at -5° and -10° interspersed with single stimuli at + 5° , + 10° and + 15°. The stimulus is presented immediately the fixation light vanishes. (Sequence 2). This is similar to experiment 2 (figure 6.20) but with smaller stimuli. Upper 2 pairs of histograms: GY. Lower 2 pairs: PCD.

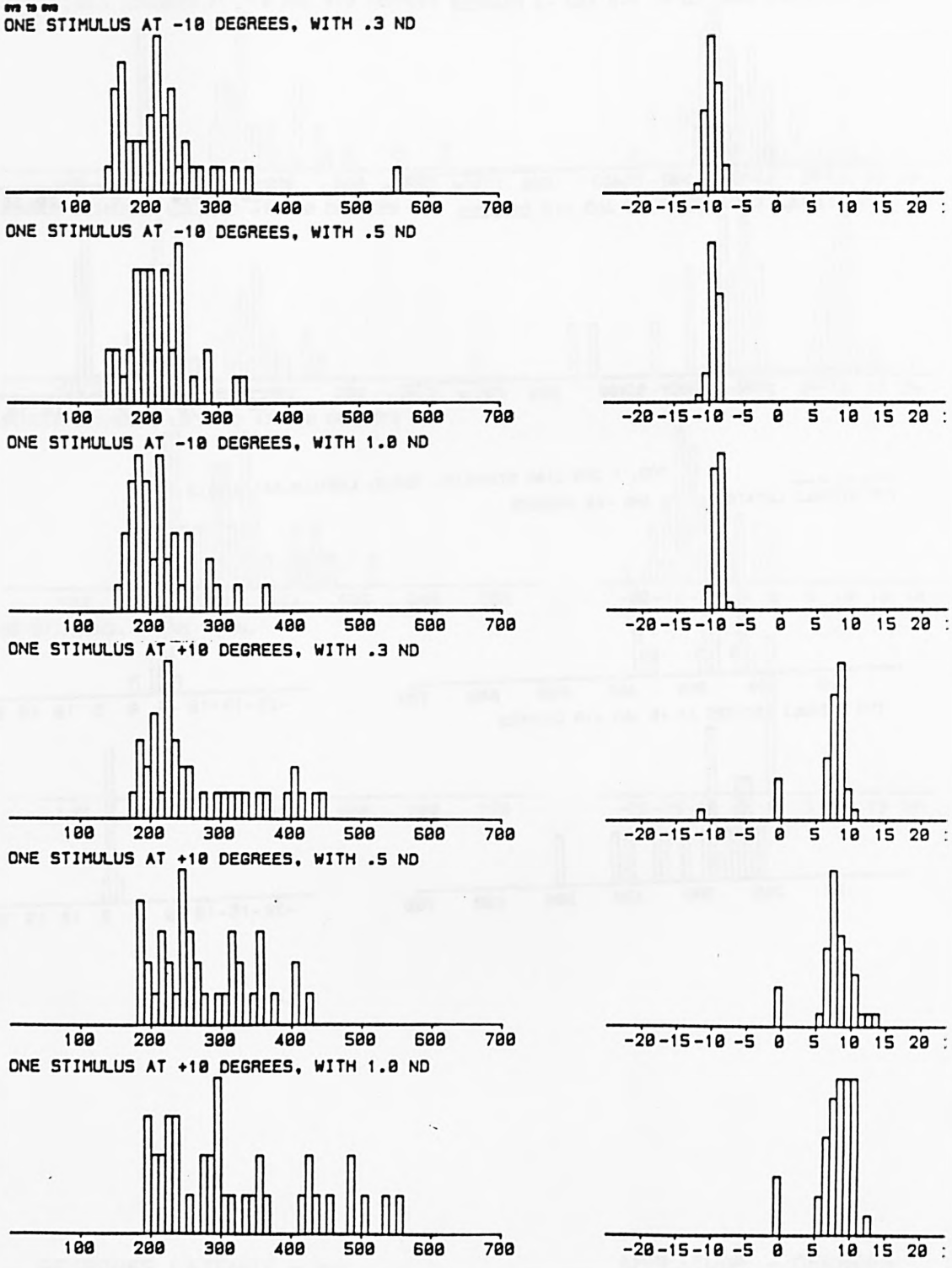

FIGURE 6.33

Distribution of latencies and amplitudes of saccades - GY. Experiment 5. Single stimuli presented at + 10^{o} at three different levels of luminance, (interspersed with the 11 stimuli of experiment 4). The stimulus is presented immediately the fixation light vanishes. (Sequence 2). A test for the effect of stray light.

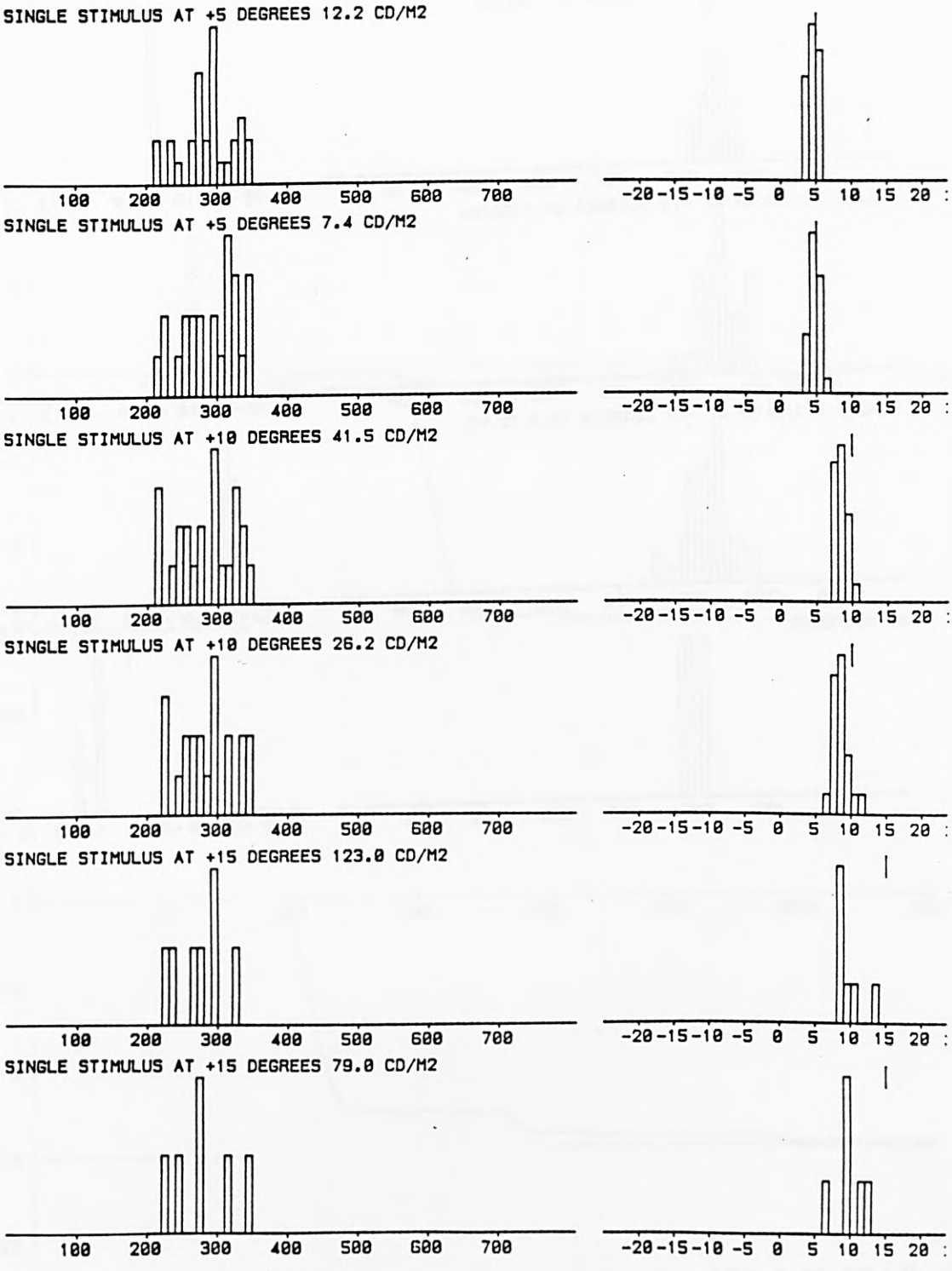

FIGURE 6.34

Distribution of latencies and amplitudes of saccades - GY. Experiment 6. Single stimuli presented at -5^{o}, -10^{o} and -15^{o} each at two levels of luminance, arranged to produce one of two levels of scattered light at the fovea. The stimulus is presented immediately the fixation light vanishes. (Sequence 2). A further test for the effect of stray light.

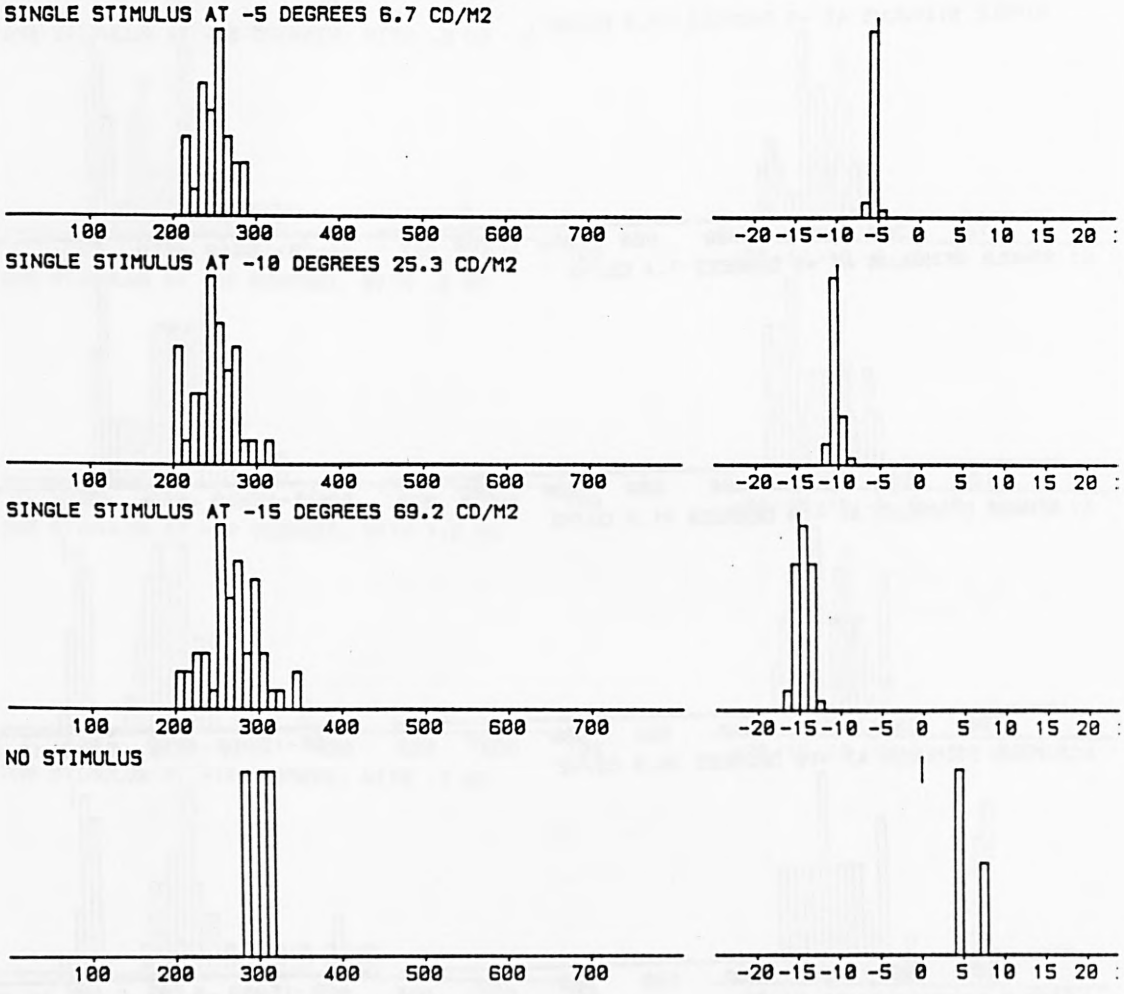

FIGURE 6.35

Distribution of latencies and amplitudes of saccades - GY. Experiment 6. Single stimuli presented at $+5^{o}$, $+10^{o}$ and $+15^{o}$ each at two levels of luminance, arranged to produce one of two levels of scattered light at the fovea. The stimulus is presented immediately the fixation light vanishes. (Sequence 2). This is a continuation of the previous figure.

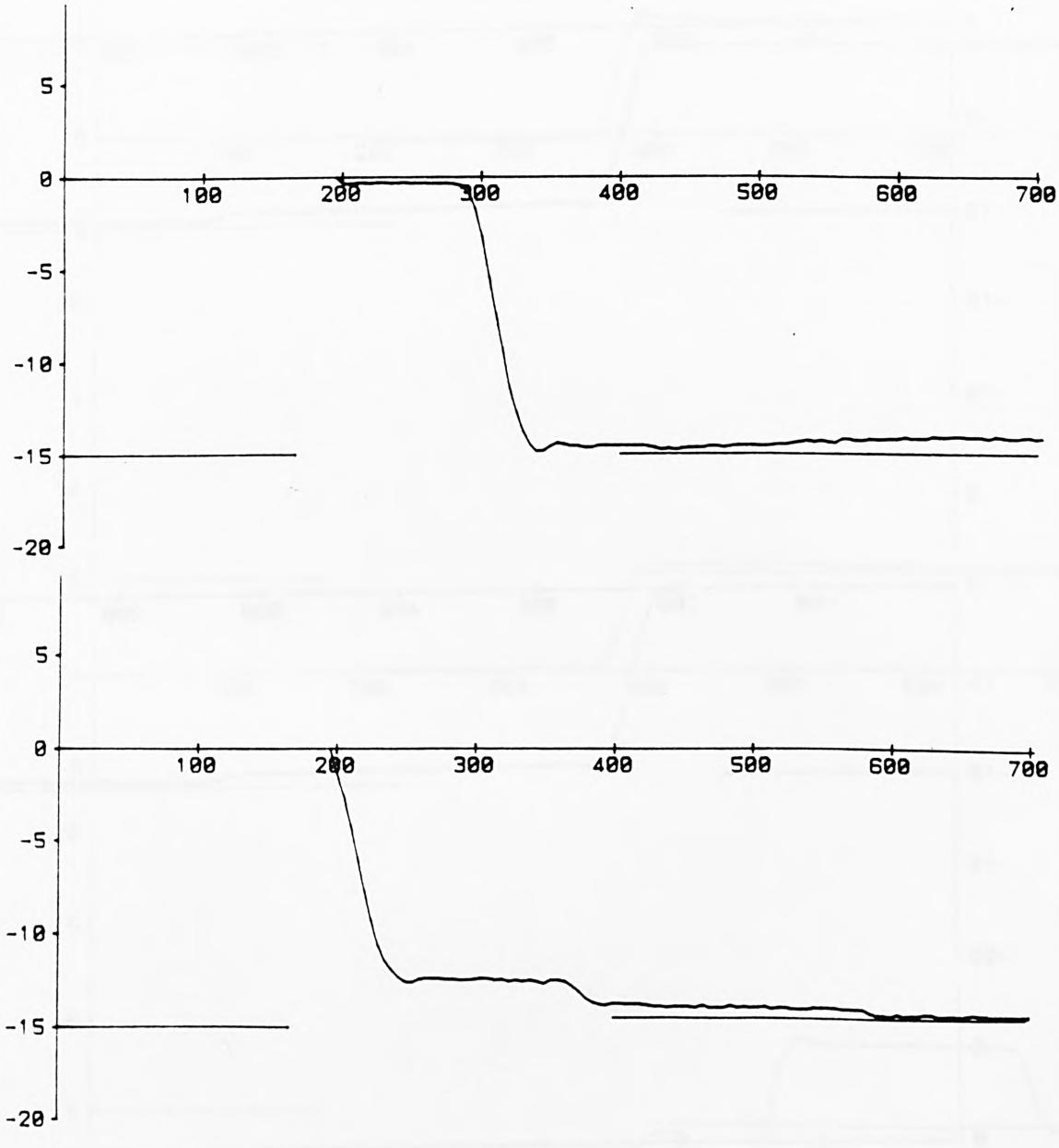

FIGURE 6.36

Examples of eye movement traces for GY, for stimulus position -15° (normal hemifield). Stimulus position is shown by the horizontal line at the left side of the graph, and final direction of gaze, when the target has been acquired, is shown by the horizontal line at the right side.

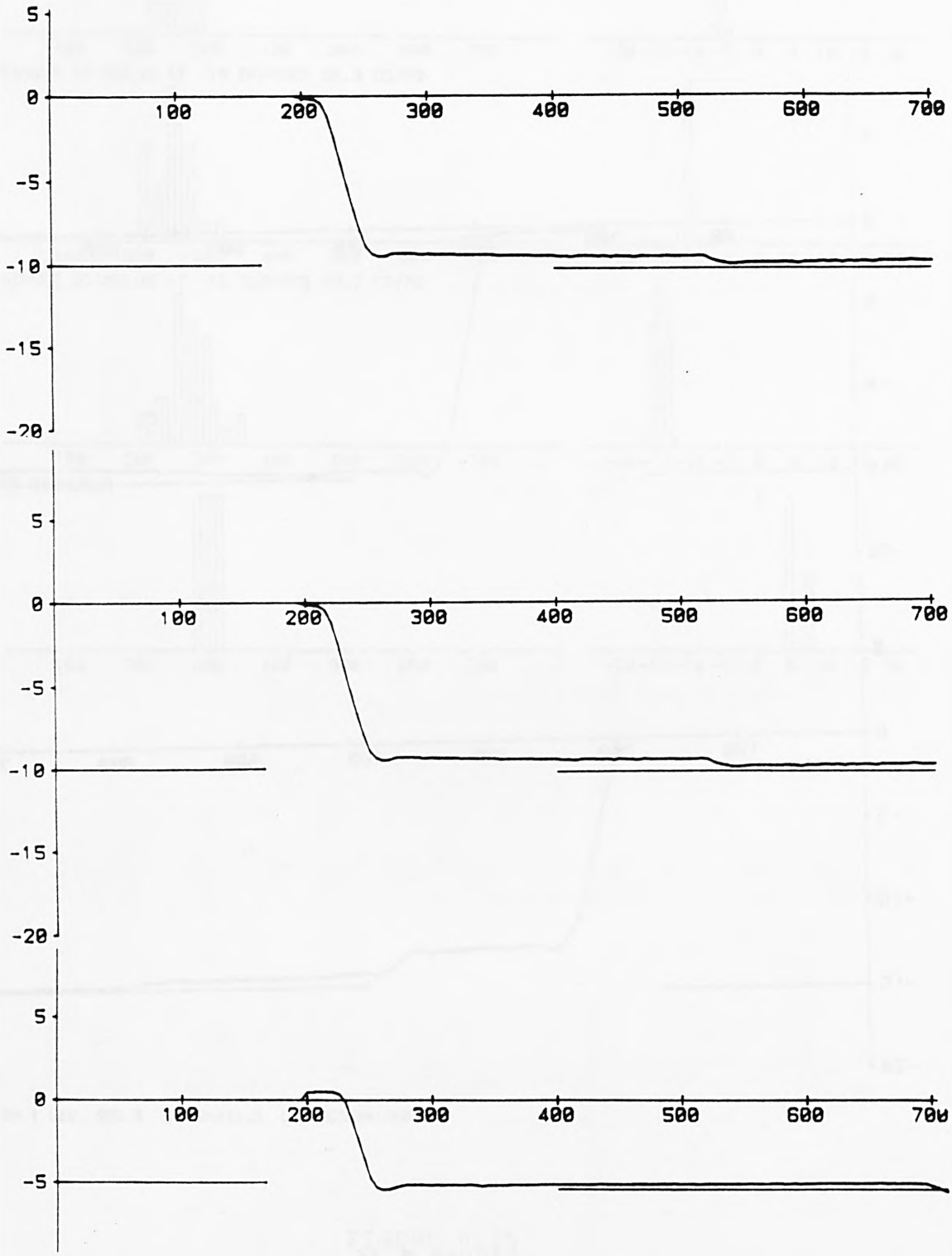

FIGURE 6.37

Examples of eye movement traces for GY, for stimulus position -10° and -5° (normal hemifield). Stimulus position is shown by the horizontal line at the left side of the graph, and final direction of gaze, when the target has been acquired, is shown by the horizontal line at the right side.

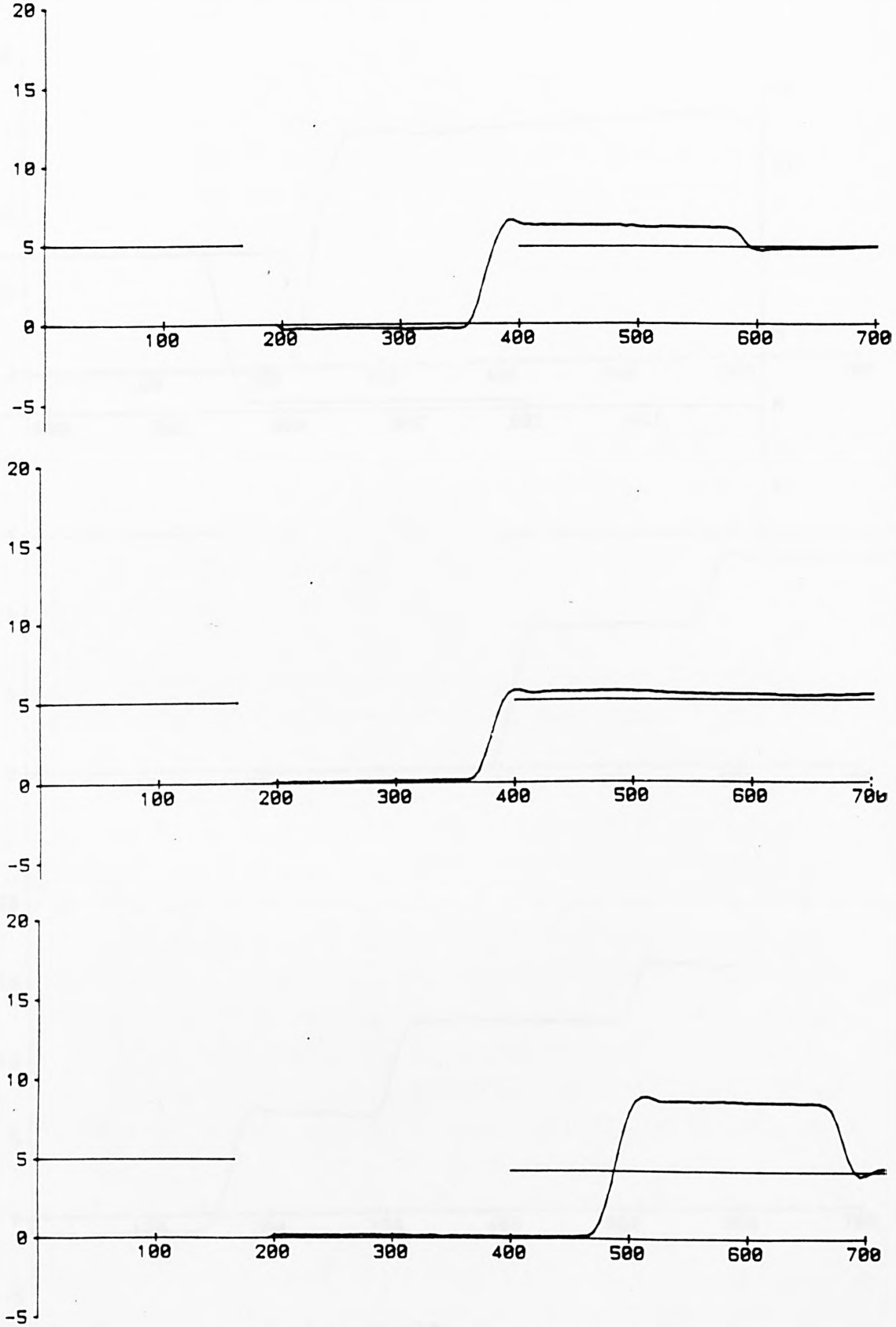

FIGURE 6.38

Examples of eye movement traces for GY, for stimulus position +5° (blind hemifield). Stimulus position is shown by the horizontal line at the left side of the graph, and final direction of gaze, when the target has been acquired, is shown by the horizontal line at the right side.

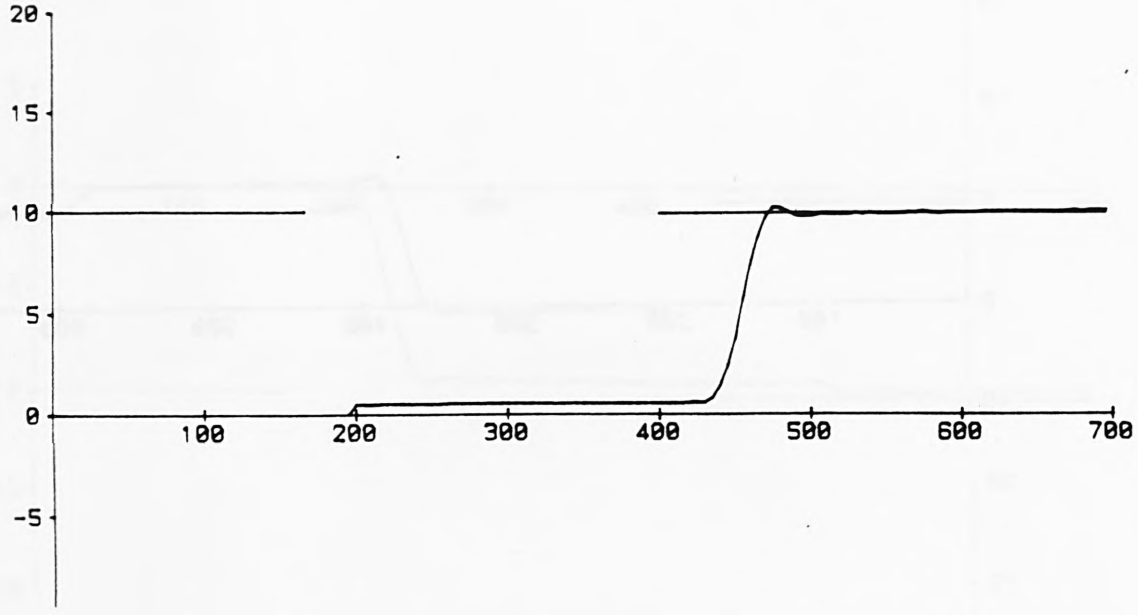

FIGURE 6.39

Example of eye movement trace for GY, for stimulus position $+10^{o}$ (blind hemifield). Stimulus position is shown by the horizontal line at the left side of the graph, and final direction of gaze, when the target has been acquired, is shown by the horizontal line at the right side.

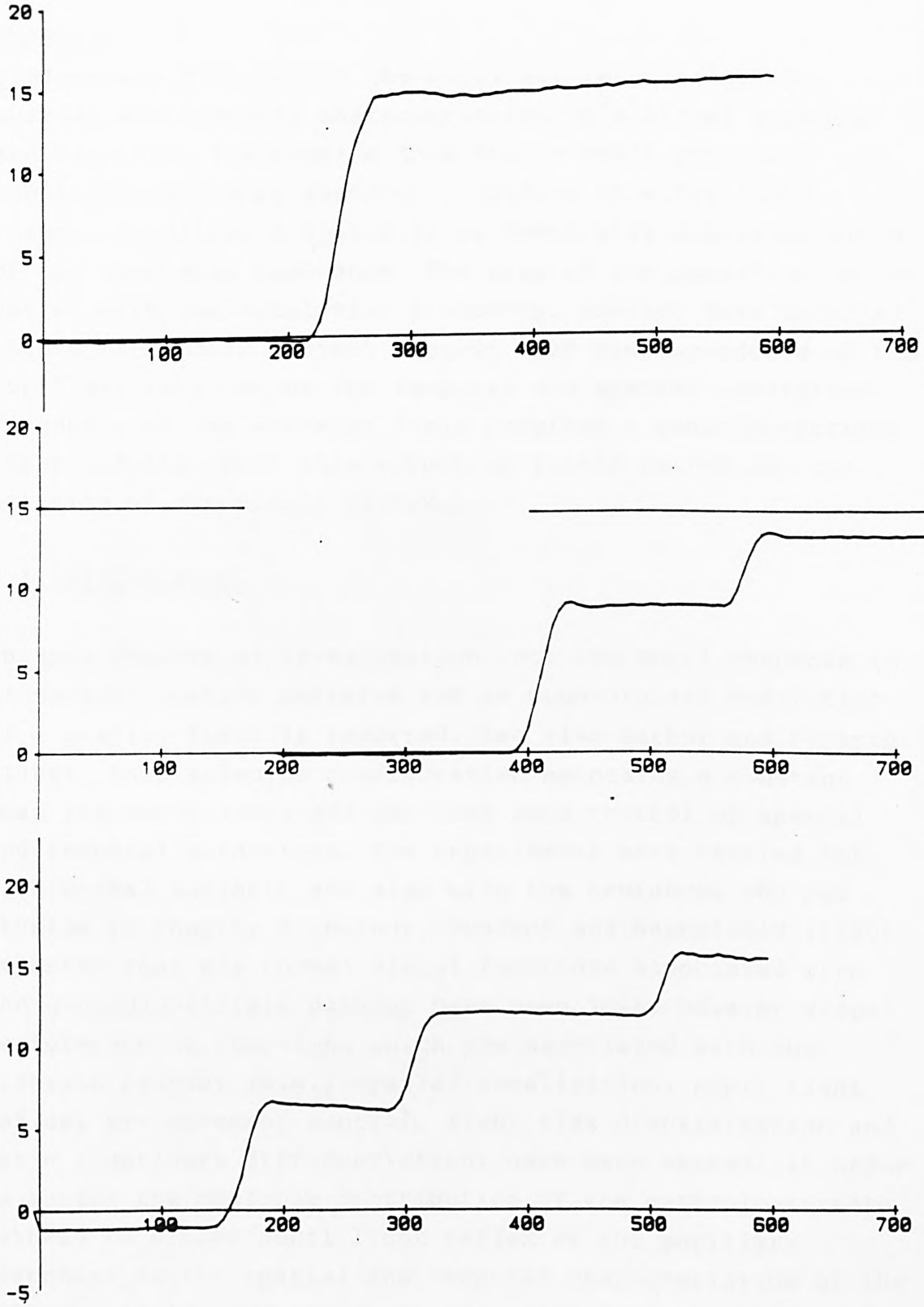

FIGURE 6.40

Examples of eye movement traces for GY, for stimulus position +15° (blind hemifield). Stimulus position is shown by the horizontal line at the left side of the graph, and final direction of gaze, when the target has been acquired, is shown by the horizontal line at the right side.

PUPIL RESPONSE TO A FLASH OR GRATING STIMULUS.

Summary

Preliminary findings on the pupillary response to the spatial and temporal characteristics of a visual stimulus are reported. The results show that a small pupillary constriction occurs whenever a uniform stimulus field changes to either a spatially or temporally modulated field of the same mean luminance. The size of the pupillary change varies with the modulation frequency. Similar data obtained with a hemianopic subject suggest that the dependence of the pupillary response on the temporal and spatial modulation frequency of the stimulus field requires a geniculo-striate input and therefore this effect is likely to reflect the activity of the visual cortex.

7.1 INTRODUCTION.

In this chapter an investigation into the pupil response to sinusoidal grating patterns and to counterphase modulation of a grating field is reported. See also Barbur and Forsyth (1986). This stimulus configuration maintains a constant mean luminance level and provides good control of spatial and temporal parameters. The experiments were carried out with normal subjects and also with the hemianope who was studied in Chapter 6. Barbur, Ruddock and Waterfield (1980) reported that his normal visual functions associated with the geniculo-striate pathway have been lost, however visual performance in functions which are associated with the midbrain pathway (e.g., spatial localisation, pupil light reflex, eye movement control, light flux discrimination and basic light/dark differentiation) have been spared. In order to assess the possible contribution of the geniculo-striate pathway to either pupil light reflex or the pupillary responses to the spatial and temporal characteristics of the stimulus field, dynamic pupil responses have been measured with the stimulus presented either in the foveal region, in the blind hemifield, or in the normal hemifield of a normal subject.

7.2 METHODS.

Pupil light-reflex responses to flashes of light of 250ms duration were measured for different stimulus eccentricities. The 2^{o} diameter test stimulus was presented foveally and at an eccentricity of 7^{o} on either side of fixation on a uniform background field of 20^{o} diameter. The specially contructed optical system mentioned in section 2.7 was used for this work.

The retinal illumination level of the test stimulus used in the pupil light-reflex experiment was 5.2 log trolands, and that of the background field was 2.5 log trolands. A red fixation spot of 0.3^{o} diameter was imaged in the centre of the field at an apparent distance of 0.8 m. This distance corresponds to the resting state of accommodation of the subject. For each measurement the pupil size was recorded for 15 seconds. The record was started 5 seconds before the onset of the test flash. Since automatic analysis of the pupil response data was not possible at the time when these experiments were carried out, single response traces were obtained with no averaging. Random pupil size fluctuations are therefore not eliminated, and thus give the measurements a noisy appearance, but the noise level does not mask the basic response pattern.

For the second experiment the stimulus was a rectangular field of 8.8^{o}x7.5^{o} which was presented either foveally or at an eccentricity of 8^{o} on either side of fixation. The stimulus was generated on a Tektronix 608 display unit by means of a raster-scan system operating at a frame rate of 200 Hz. The spatial and temporal modulation of the stimulus was restricted to a disc of 6^{o} diameter positioned in the centre of the rectangular pattern. The mean luminance of the stimulus field was 12.4 cd/m^{2} and showed insignificant variation with spatial frequency for contrast levels below 70%. The measurement method required the subject to fixate a circular spot while the test

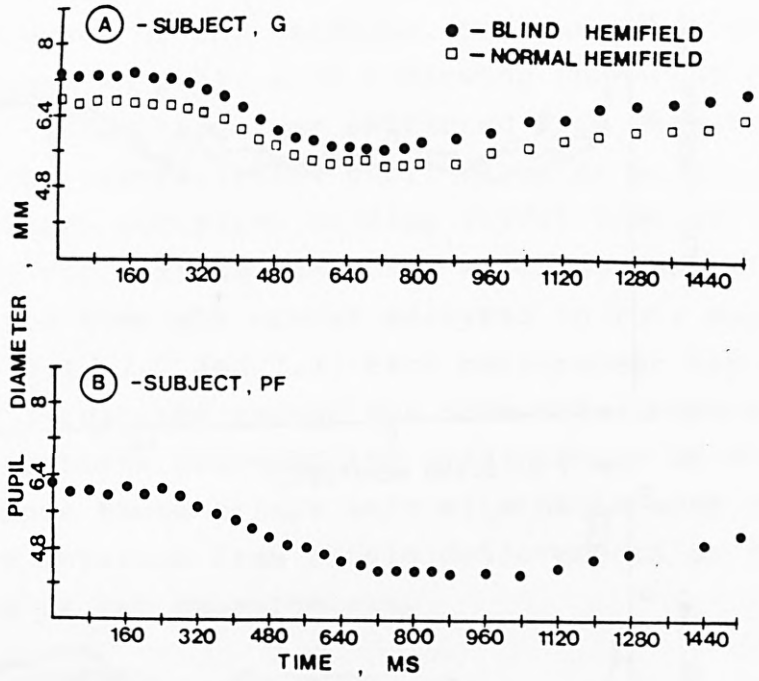

FIGURE 7.1

Pupil diameter changes in response to a test stimulus. plotted as a function of time from flash onset. (A) for subject GY, (filled circles: blind hemifield, open squares: normal hemifield). (B) for subject PF.

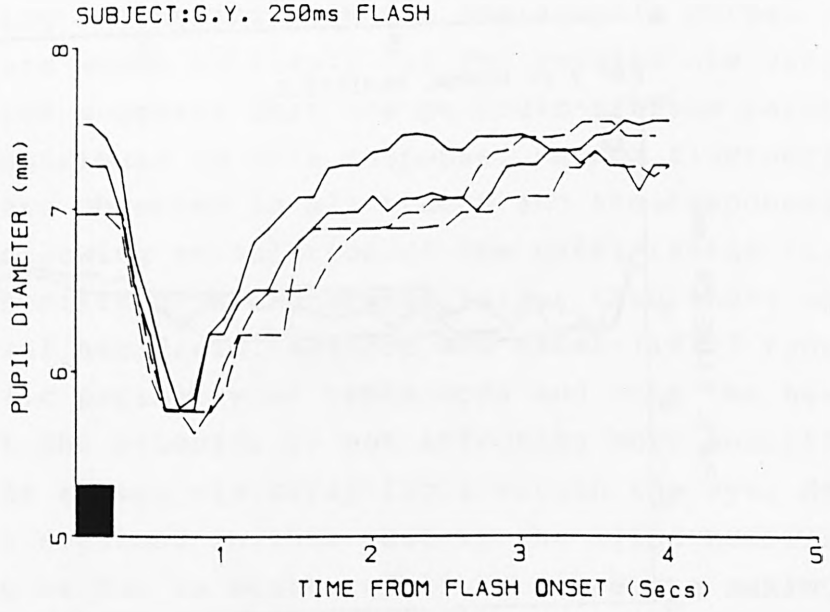

FIGURE 7.2

Pupil diameter changes in response to a flashed peripheral stimulus. plotted as a function of time from flash onset. Subject: GY. Solid lines: responses to stimuli at 7^{o} in his normal hemifield. Broken lines: responses to stimuli at 7^{o} in his blind hemifield. Background luminance: 2.55 log trolands, Target luminance: 5.24 log trolands. Target diameter: 2^{o}, Flash duration: 250 ms.

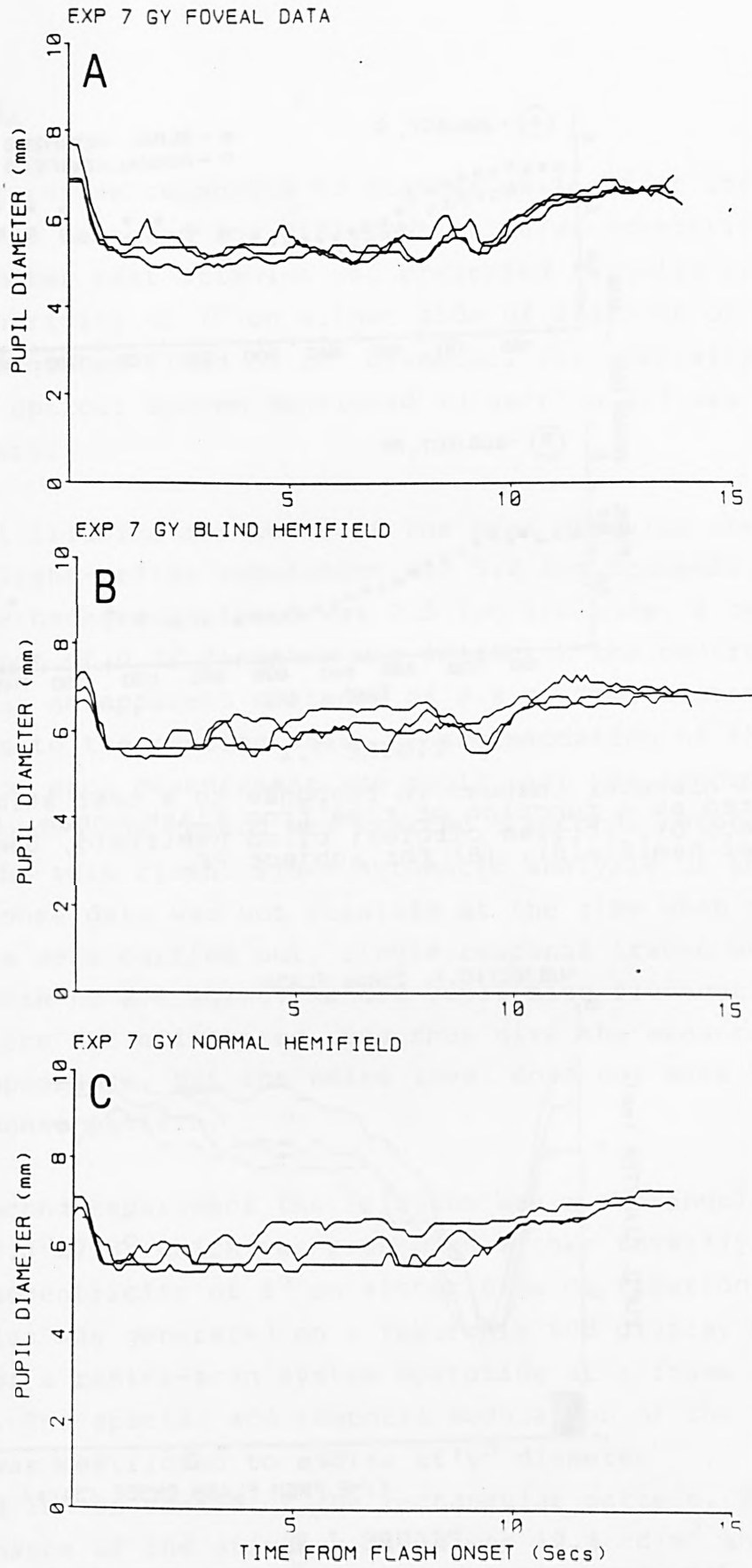

FIGURE 7.3

Pupil diameter changes in response to a continued stimulus. plotted as a function of time from stimulus onset, for GY. (A) Foveal data, (B) 7° in blind hemifield, (C) 7° in normal hemifield. Background luminance: 2.55 log trolands, Target luminance: 5.24 log trolands. Target diameter: 2°. Stimulus remained on throughout the recording period.

stimulus was imaged either foveally or in the periphery of the visual field. Measurement of pupil size began 5 seconds before the onset of the stimulus. The parameter of interest was the change in pupil area following the onset of stimulus modulation. This change was extracted from each trace by measuring the contralateral pupil diameter at stimulus onset and 0.9s after. According to Zinn (1972) this is close to the latency for maximum response, which agrees well with the findings from complete traces analysed in this experiment, see figure 7.1, 7.2 and 7.3. Each measurement represents the average of 3 readings except for some trials where large pupil fluctuations preceded the presentation of the test pattern. Since these trials were eliminated some of the data points were obtained from single measurements or represent the average of two measurements.

7.3 RESULTS.

A. LIGHT-REFLEX RESPONSE.

Dynamic response measurements when the test stimulus was presented either in the blind hemifield or at the corresponding eccentricity in the hemianope's normal hemifield are shown in figure 7.2 The results are very similar which suggests that the geniculo-striate pathway does not contribute to this response. Random fluctuations of the pupil are observed in all traces and the responses measured following stimulation of the nasal retina (i.e., the blind hemifield) are somewhat larger than those observed in the normal hemifield. Aulhorn and Harms (1972) report on pupillometric perimetry of hemianopes and note the need to ensure that the stimulus is not affecting more sensitive parts of the retina via stray light within the eye. However, the results obtained in this case in the blind hemifield are unlikely to be due to scattered light since the maximum pupil constriction with the flash in the blind hemifield is equal to or larger than that observed in the normal hemifield.

B. PUPIL RESPONSES TO SPATIO-TEMPORAL STIMULUS ATTRIBUTES.

The pupillary responses to the temporal counter-phase modulation of the stimulus field are shown in figure 7.4. The spatial frequency chosen for this measurement was 1.2 cycles/^{o} and the maximum modulation depth was 70%. The foveal measurements show that the maximum pupil constriction for this type of presentation occurs at temporal frequencies of the order of 6 to 8 cycles/sec. The mean luminance level of the stimulus remained constant for all modulation frequencies, and matched the uniform field when no stimulus was being presented. Hence, as was to be expected, no sinusoidal pupillary oscillation was observed at any frequency. The response curve obtained with counterphase modulation of the stimulus field resembles the shape of a threshold temporal sensitivity function obtained at about the same mean luminance level. The data of figure 7.4 show large random errors which are attributed to pupil fluctuations. Averaging would be required to reduce such errors, or the avoidance of stimulation at times when the pupil size was already varying. In spite of these fluctuations the results show a clear dependence of pupil response on modulation frequency and stimulus eccentricity and they also show the absence or the reduction of the observed effect when the stimulus was presented in the blind hemifield.

The results obtained when the uniform test field is changed to a vertically oriented sinusoidal grating of 70% contrast are shown in figure 7.5. In these measurements the stimulus was presented every 20 seconds and the spatial frequency was randomised. The results show that the percentage change in pupil area varies with the spatial frequency of the stimulus and is largest for foveal stimulus presentation. The effect is reduced and shifted to lower spatial frequencies when the stimulus is imaged in the normal hemifield and is absent or reduced to the level of random fluctuations for presentations in the blind hemifield.

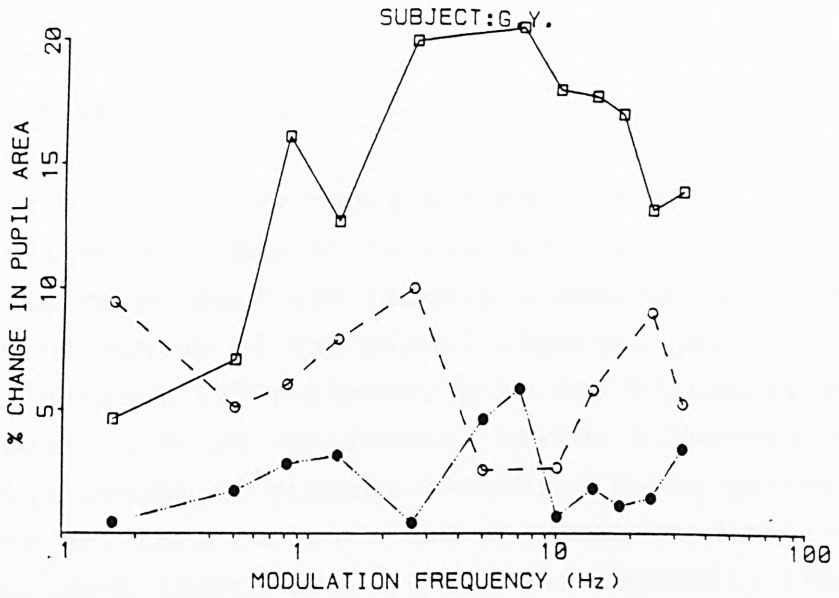

FIGURE 7.4

Pupillary responses by GY to counter-phase modulation of a 6° diameter disc stimulus generated in the centre of a rectangular field of the same luminance and dimensions - 8.8x7.5°. For each frequency the onset of stimulus modulation corresponded to zero amplitude and increased at the selected counterphase frequency to 70% modulation. The spatial frequency of the grating was 1.2 cycles/° and the mean luminance level of the display was 12.4cd/m^2 and remained constant throughout the experiment. The stimulus was presented either foveally (open squares), 8° in the blind hemifield (solid circles) or at the same eccentricity along the horizontal meridian in the normal hemifield (open circles).

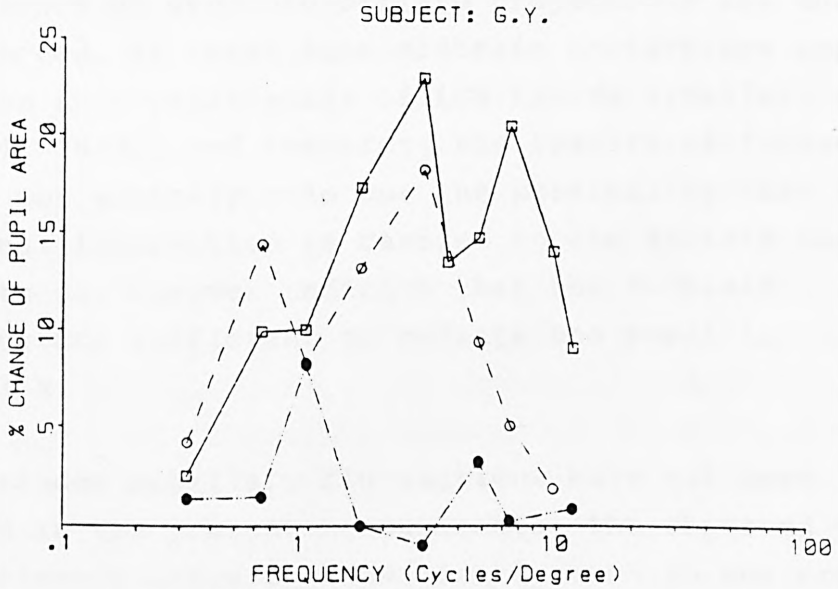

FIGURE 7.5

Pupillary responses by GY to a range of spatial frequencies of the test stimulus. The stimulus configuration was similar to that of figure 7.4, but stimulus onset consisted of the replacement of a uniform disc by a vertically oriented sinusoidal grating of equal mean luminance. Some data points represent single traces, but the majority of the points were obtained by averaging 2 or 3 traces. The data refer to foveal measurements (open squares), blind hemifield presentation (solid circles) and normal hemifield presentation (open circles).

7.4 DISCUSSION.

The constriction of the pupil following a rapid increase in retinal illuminance may be functionally important since its response is very rapid and immediate protection from extensive bleaching of the visual pigments can therefore be provided (Barlow, 1972; Alpern, Ohba and Birndorf,1974). A smaller pupil size in continuous, bright illumination reduces the amount of pigment bleaching under steady state conditions and this improves the absolute sensitivity of the eye during dark adaptation (Alpern and Campbell, 1962). The pupil reflex and basic light/dark differentiation are visual functions associated with the pretectal and accessory optic nuclei (Brindley, Gauthier-Smith and Lewin, 1969, Pasik and Pasik, 1973), and are mediated by fast conducting axons, connected to phasic ganglion cells (Stone, 1983). Stone also concludes that, in the cat, W-class ganglion cells project to the pretectum, and thence provide retinal input to the pupilloconstrictor reflex. The results of figures 7.1 to 7.3 which show that the pupil light reflex is quite normal even in the absence of geniculo-striate projections are therefore not unexpected. At least some midbrain projections appear to derive from axon collaterals of LGN fibres ((Weller, Kass and Wetzel, 1979), and therefore the results of figures 7.1 to 7.3 do not entirely rule out the possibility that the same retinal information is carried to the striate cortex. The results do, however indicate that the midbrain projections are sufficient to mediate the pupil light-reflex.

Although random pupillary fluctuations have not been eliminated in the present measurements, the observed effects are sufficiently large to show clearly even in the presence of noise. The size of the pupillary constrictions were found to vary with modulation depth both in the spatial and the temporal domain. The similarity between the foveal data of figures 7.2 and 7.3 and typical contrast sensitivity functions is also of interest. The largest pupillary restrictions are obtained when the stimuli are presented

foveally and they decrease with stimulus eccentricity. These pupillary changes are either absent or much reduced when the stimuli are presented in the blind hemifield of the hemianopic subject. The results are therefore consistent with previous findings which show that the hemianope cannot discriminate the structure of a stimulus imaged in his blind hemifield (Barbur, Ruddock and Waterfield, 1980). His threshold responses reveal extensive linear spatial summation and his cut off critical flicker frequency is extremely low. The results therefore suggest that the dependence of pupillary responses on the spatial and temporal modulation frequency of the stimulus reflect the activity of central mechanisms since they are either diminished or eliminated in the absence of the geniculo-striate projection. The type of stimulus attributes which generate the observed pupillary responses at a constant mean luminance level such as the spatial structure, temporal modulation frequency or a change in stimulus colour (Young and Alpern, 1980) are normally associated with geniculo-striate projections.

Other possibilities have been proposed to explain similar results obtained with uniform field modulation (Varju, 1964, Crawford, 1936), contrast reversal or alternation between a uniform field and a checkerboard pattern (Ukai, 1985, Slooter and van Norren, 1980), and alternating monochromatic stimuli at isoluminance (Young and Alpern, 1980). Although more detailed investigations are required in order to exclude alternative explanations the results of this investigation and the evidence obtained from some other studies (Ukai, 1985, Slooter and van Norren, 1980) suggest that central mechanisms are involved. If this is so then automatic pupillometry under controlled stimulus conditions could be used to investigate objectively the properties of central visual mechanisms involved in the processing of specific stimulus attributes.

MOTION PERCEPTION ACROSS THE VISUAL FIELD.

Summary.
Thresholds for the detection of target displacement and for the detection of a change in speed were made for speeds of from 0.1 to 50 degrees/second, for visual field positions out to 25°. A projection system was used for this purpose, utilising a servo-driven two-axis mirror. The displacement threshold function could generally be fitted by assuming that there was a constant threshold time for which the stimulus must be visible at all speeds and visual field positions. A minimum velocity discrimination threshold was found for foveal stimuli at a target velocity of about 3°/sec. At greater eccentricities the minimum threshold changed very little, but at higher or lower speeds the threshold increased with eccentricity. The results showed considerable random variation, probably due to the small stimulus size.

8.1 INTRODUCTION.

It has been suggested that displacement threshold measurement (measured using an oscillating grating) could form a valuable method of assessing neural dysfunction (Buckingham and Whittaker, 1986), particularly for patients with ocular opacities, indeed the equipment developed for the experiment reported in this chapter is already being put to clinical use. Furthermore such studies should provide information on how the nervous system analyses movement.

Studies of motion perception generally consist of a model of a proposed visual processing scheme, followed by a psychophysical or electrophysiological examination of responses to moving stimuli. The studies referred to below are in the first category.

One model, due to Reichardt (1961) is based on sensor units a certain span apart, linked by a time delay. Barlow and

Levick (1965) make use of this model in their study of direction sensing mechanisms.

Marr and Ullman (1981) proposed a model in which motion is detected as the rate of change (in time) of the second spatial derivative. Johnston and Wright (1985) present data which does not support this hypothesis, since the Lower Threshold of Motion (LTM) was found to be related to velocity rather than temporal frequency at a point.

Psychophysical and physiological studies have distinguished short range and long range motion mechanisms. Braddick (1974) distinguished a short range apparent motion process, occurring when the displacement of the stimulus was less than 15 minutes of arc (for a pattern within 5^{o} of the fovea), and found that this process must occur early in the visual pathway. Cavanagh et al (1985) in a similar experiment to Braddick's but exploring equiluminous red and green stimuli, found that motion was still perceptible at equiluminance, albeit over a more limited range of conditions. They also claim that only one motion mechanism is required to explain the full range of their results.

Mullen and Baker (1985) also studied motion detection at isoluminance, by examining the Motion After Effect. They found this to be present at all luminance ratios, at the velocity they studied (3.75^{o}/sec).

The above experiments are mostly concerned with the abilities of the fovea to detect motion. Van de Grind et al (1983) found that motion detection performance did not change out to an eccentricity of 48^{o} provided that the velocity and stimulus size were scaled by the cortical magnification factor. Tynan and Sekuler (1982) also examined motion processing performance, but in terms of reaction time and subjective matches of peripheral and foveal velocity. They found that perceived velocity decreases with eccentricity, but that this effect diminishes at high velocities.

McKee and Nakayama (1984) measured velocity discrimination at a range of eccentricities, and found that it was as precise in the periphery as at the fovea, at the optimum reference velocity for that eccentricity. This optimum velocity varied from 5^{o}/sec at the fovea to 30^{o}/sec at 40^{o} field angle. They point out that if the velocities are expressed as velocities across the cortex, the curves at all eccentricities coincide. Orban et al (1984) also measured differential velocity detection at the fovea, by a method that involved comparing the speed of a slit with a memory of the mean of several velocities. They found that speed discrimination followed a U-shaped function, with a minimum between 4^{o}/sec and 32^{o}/sec of about 6%, independent of contrast and of the duration of slit visibility. Orban et al (1985) found a similar set of curves relating velocity discrimination, reference velocity and eccentricity to those of McKee and Nakayama (1984), but did not confirm the proportionality to cortical magnification factor except for high contrast stimuli on the lower branch of the velocity-discrimination curve.

Barbur (1985) has proposed two models to cover the full range of perceptible stimulus velocity across the visual field. The models make use of the basic Barlow and Levick direction discriminator unit, but they differ from the Barlow and Levick model in that these schemes are also capable of speed discrimination. In the spatial coding model the signal from one receptive field is delayed by a single time delay before being compared, by a series of correlators, with the undelayed output of a series of increasingly remote receptive fields. This model may work both at very low speeds, using the longest available time delay, or in the high speed range, where the shortest possible delay time is used. In the multiple time delay model the signal from one receptive field is subjected to a series of increasing time delays before being compared by a series of correlators with the output of a single nearby receptive field. This scheme may provide a means of speed

and direction discrimination in an intermediate speed range.

Boulton (1986) also discusses the existence of two mechanisms for detecting motion, but he places the non-Reichardt mechanism in the periphery: beyond 35 og detection becomes a function of velocity, not displacement.

Van de Grind, Koenderink and van Doorn (1986) examined the distribution of motion detection thresholds across the temporal visual field, for a range of velocities. They found a critical velocity for maximum sensitivity to motion at each eccentricity, this velocity being related to the critical velocity at the fovea by the cortical magnification factor. Furthermore, speaking in terms of ´Reichardt detectors´ they found that for velocities lower than the critical one, the distance remained constant, and the time delay changed inversely with velocity, whereas for velocities higher than the critical one, the time delay remained constant, and the spans increased with velocity. This appears to fit in with the Barbur (1985) model, if one supposes that the range of the two motion detector systems meet at the critical velocity.

This chapter describes some experiments using similar stimuli to those used in the remainder of this project, and a wide range of stimulus velocities to test the validity of predictions based on the theoretical models mentioned above. It is hoped to be able to discriminate between the various models and to show how the organisation of the visual system for motion detection and speed discrimination changes with target eccentricity.

Displacement thresholds were measured foveally and out to an eccentricity of 20^{o}, for stimulus velocities from 0.1^{o}/sec to 50^{o}/sec. The stimulus was a small spot, 20 to 24 min arc in diameter, which was maintained at a contrast of 6.3 times the contrast threshold for that particular eccentricity, displacement and range of speeds.

One might expect that as velocity increases, the displacement threshold at any particular eccentricity would be proportional to velocity if the single time delay model is operative. For peripheral stimuli, a cortical magnification scaling factor should apply (Johnston and Wright,1985). As velocities decrease to the range where the multiple time delay scheme operates, one might expect a more or less constant displacement threshold at any one eccentricity, until one reaches the point where the stimulus remains within one receptive field throughout its appearance. At large eccentricities where the receptive fields are large, the delay times might be appropriately matched, so that the displacement threshold could be much the same in the periphery as at the fovea.

Ball and Sekuler (1980) found that reaction time to stimuli moving away from the fixation point was shorter than for motion towards fixation, however Mateef and Ehrenstein (1986) found shorter reaction times for centripetal motion. In the current experiments different eccentricities and directions (centrifugal and centripetal, but limited to the horizontal direction) were presented in random order in any one run, in order to avoid adaptation effects, or attention enhancement of sensitivity. Centripetal and centrifugal movements were recorded separately in order to evaluate any difference in threshold.

8.2 METHOD.

The equipment used was the projection set-up, with twin axis mirror drive, described in section 2.8. In order to cover the range of velocities of interest, it was necessary to use two different observer-to-screen distances.

Preliminary experiments (using PMF as subject) established the contrast threshold for a stimulus with a velocity in the middle of the range for each geometrical arrangement, for each of the eccentricities used, for a range of

displacements (or durations of exposure). These thresholds were measured with a .8 Neutral density filter in the stimulus beam, the neutral density being removed for subsequent displacement and velocity discrimination experiments in order to provide a stimulus .8 log units above threshold. Using this technique the contrast of the target remained approximately equally above threshold for all presentations, in spite of the non-uniformity of illumination referred to in section 2.8, and table 2.2. These preliminary determinations were not repeated for all observers, since the work described in Chapter 3 had established that PMF had similar contrast thresholds to the other observers. Figure 8.1 shows examples of the results obtained.

In figure 8.2 the contrast thresholds of figure 8.1A and 8.1B are replotted in the form used for presenting contrast thresholds in chapter 3, and compared with the thresholds made under the nearest comparable conditions. One cause of the lower thresholds measured in this experiment may be the use of the binocular viewing mode. One might expect a difference of log(1.4) in these thresholds (Home, 1978), which would account for over half the discrepancy.

8.3 RESULTS.

Figures 8.3 to 8.5 show displacement thresholds for a wide range of speeds, for three eccentricities and two observers. Figures 8.11 and 8.12 show similar thresholds for speeds up to 5^{o} for four observers. The experimental results are summarised in figure 8.13 and tabulated in appendix 1.

Velocity discrimination thresholds were measured for three observers over as wide a range as possible. Because of the need to allow for increments in speed of up to 100%, and also the need to allow for substantial decreases in speed, the starting speeds examined were restricted to the range 0.1^{o}/sec to 50^{o}/sec. Measurements were carried out at

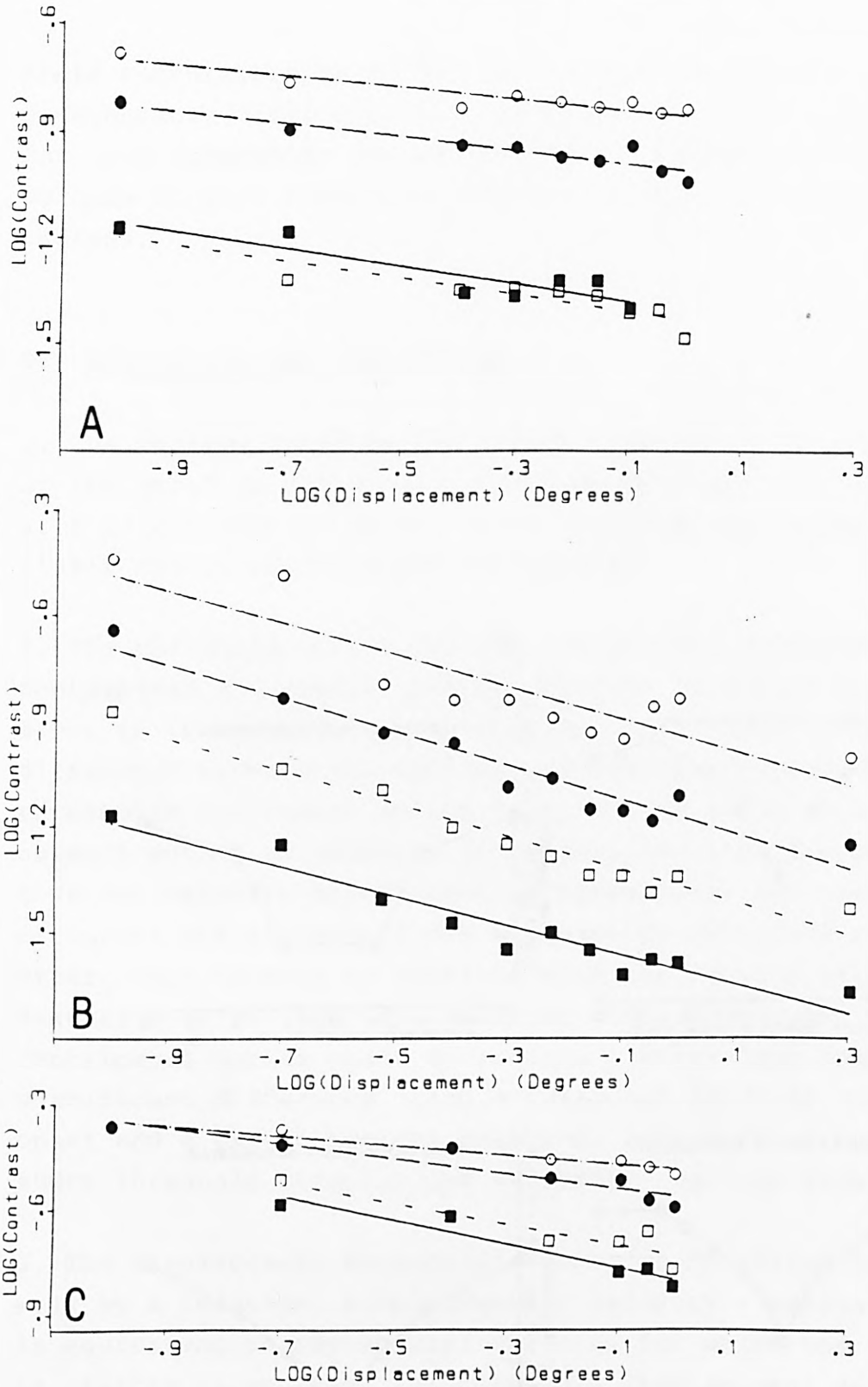

FIGURE 8.1

Examples of the lines fitted to log (contrast) thresholds plotted as a function of log (stimulus displacement), for a range of eccentricities. A: for a target velocity of 0.5^{o}/sec. B: for a target velocity of 3^{o}/sec. C: for a target velocity of 20^{o}/sec. Filled squares: foveal data, open squares: 5^{o} eccentricity, filled circles: 10 eccentricity, open circles: 20^{o} eccentricity. Subject: PMF.

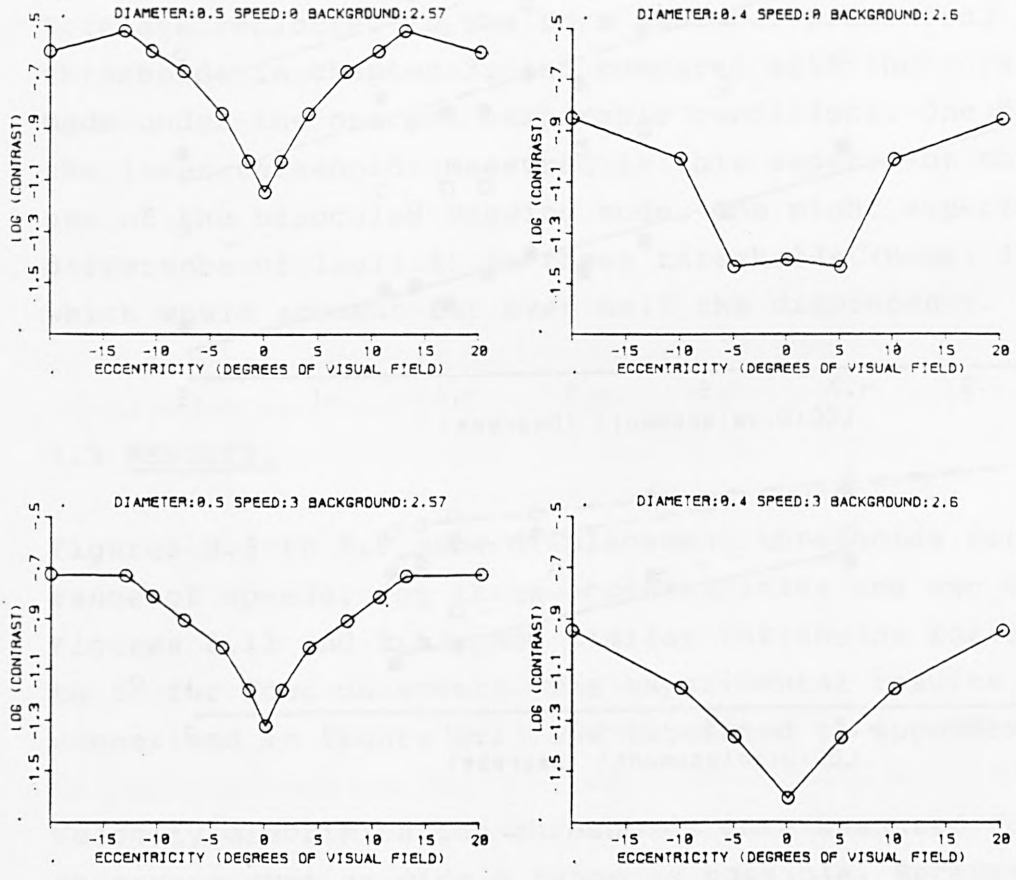

FIGURE 8.2

Plots of contrast thresholds vs eccentricity derived from the data of figure 8.1 (right column), and selected from the work described in chapter 3 (left column).

field eccentricities of 0^{o}, 10^{o} and 25^{o}. There was considerable difficulty in maintaining a constant criterion for this judgement, and at least three determinations had to be made of each threshold. Observers found this very tedious.

8.4 DISCUSSION AND CONCLUSIONS.

1. The minimum displacement thresholds of 1.5 to 2.6 minutes of arc shown in table 8.12 are comparable with the values of 1. 4 to 2.2 minutes of arc found by Legge and Campbell (1981) for an unstructured background.

2. The threshold curves for PMF are plotted separately for centripetal and centrifugal motion (see figures 8.8 and 8.9). In these experiments there is little consistent difference between the two sets of curves: displacement thresholds for inward motion tend to rise above those for outward motion as velocity increases, and the reverse is true for velocity discrimination thresholds, but the pairs of curves are all within one standard deviation of each other. This appears to conflict with the results of Ball and Sekuler's (1980) specific study of centrifugal and centripetal motion onset detection, however they found no significant difference using a threshold level of motion onset and a psychophysical response, only when using a supra-threshold stimulus and measuring reaction times.

3. The displacement threshold curves can be fitted rather well by a relation Displacement / velocity = constant. This is equivalent to saying that the time for which the stimulus is visible is constant for threshold displacement detection, and is what would be expected of a single time delay model. The time constant of the fitted lines was between 24 and 51 milliseconds (see table 8.1). The relation seems to hold down to speeds of 5^{o} or less. This is illustrated in figure 8.10. The curves shown were fitted as least squares straight lines on a linear scale, but have been shown on a

log velocity scale for convenience. The results for 25° eccentricity should be viewed with reservations: the fitting of the straight line is influenced by the very high threshold measured for a velocity of 50°/sec, and at this speed and eccentricity it was not possible to maintain the stimulus at the required contrast.

	Position in visual field (degrees)					
	0		10		25	
	R>L	L>R	R>L	L>R	R>L	L>R
Slope of line (ms)	30	21	28	36	27	52
Intercept (degrees)	.188	.157	.306	.146	.384	.036
correlation coeff.	.998	.991	.991	.998	.987	.992

TABLE 8.1

Time constant relating threshold displacement to target velocity (subject: PMF) L>R (target motion from left to right) implies a centripetal motion in this experiment.

4. The displacement threshold curves for the low velocity part of the range (foveal data) have been plotted on an expanded linear scale in figures 8.11 and 8.12. All subjects have a minimum foveal threshold for velocities close to 0.2°/sec. and most have little change in threshold between 2°/sec. and 4°/sec. A constant displacement threshold could be the result of a multiple time delay, single receptive field spacing scheme, operating in this speed range, as required by Barbur's two-mechanism model. For some observers there is evidence of a region of increasing displacement threshold at lower speeds, suggesting that, for speeds slower than those at which the longest time delay of the multiple time delay scheme operates, displacement must be detected by a single time delay, and a range of receptor spacings, but the evidence for this is slender. One may conclude that the degree of overlap of the postulated mechanisms varies from one individual to another.

5. The velocity discrimination curves show U shaped curves as described by Orban et al (1984 and 1985), with minima in

the velocity range 1^{o}/sec to 10^{o}/sec. However the minimum threshold discriminable velocity change in these experiments was about 30%, whereas other workers report values as low as 5%. Orban, de Wolf and Maes (1984) used a long vertical line of width 0.2^{o} as a stimulus, McKee, Silverman and Nakayama (1986) used a grating and van der Grind, van Doorn and Koenderink (1983) used a random dot pattern subtending at least 2^{o} (at the fovea), which may perhaps explain the difference, bearing in mind that the target in this experiment was a spot of diameter 17 minutes of arc.

The minimum threshold value of detectable velocity change showed little if any variation with visual field position, although the peripheral thresholds display too much variability to draw any reliable conclusions from this. Observers reported difficulty in detecting motion at the slower speeds in the periphery for these small targets, although the target was clearly visible, since it was subject to Troxler fading. It would be interesting to see if a larger target gives less variable and lower thresholds. Clearly, if the total displacement is such that the stimulus remains within one receptive field, no motion will be detected, so a steep rise in displacement threshold and in velocity discrimination threshold is to be expected at sufficiently low speeds, whatever model is considered.

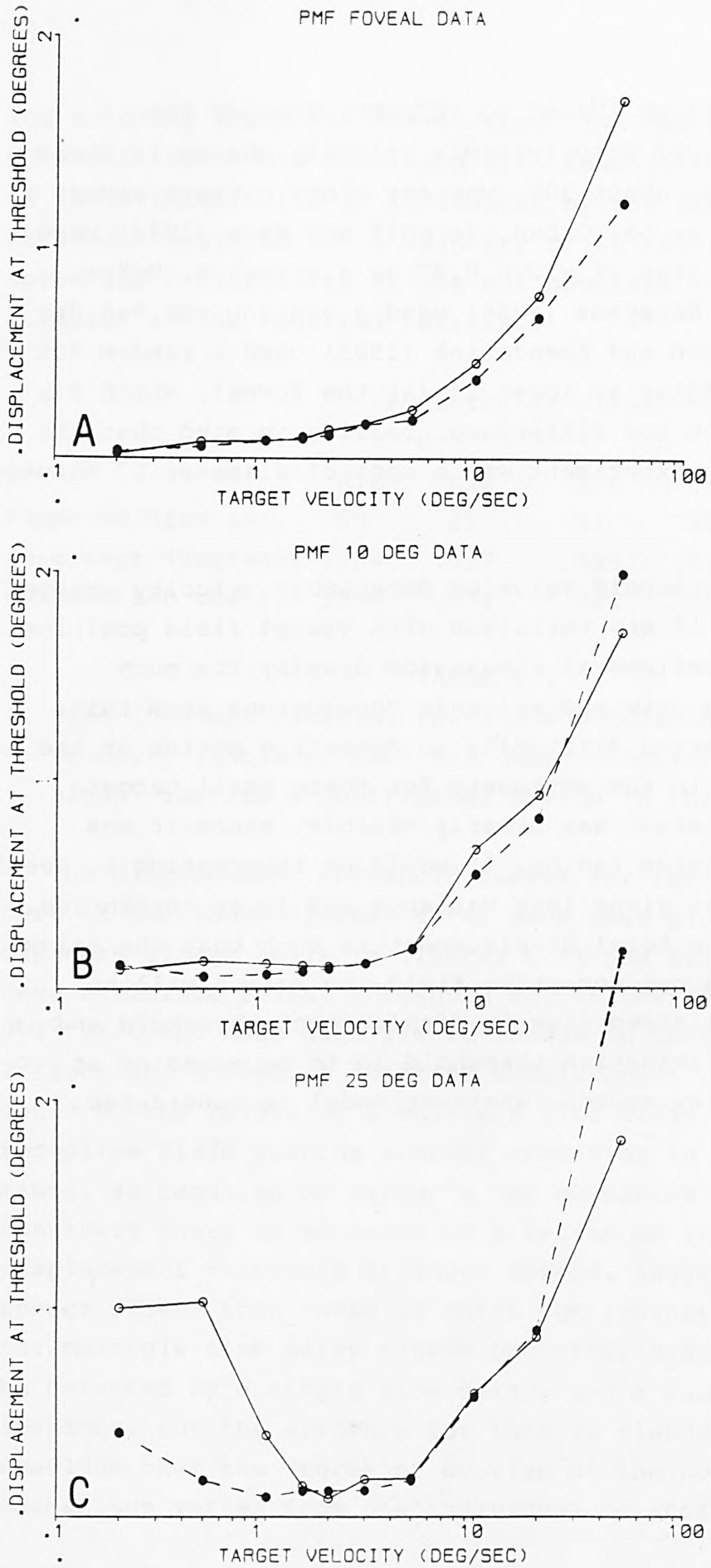

FIGURE 8.3

Displacement thresholds as functions of target velocity. Observer: PMF. Open circles: Right to left (centrifugal motion). Closed circles: Left to right (centripetal motion). A: Foveal data. B: 10° eccentricity. C: 25° eccentricity

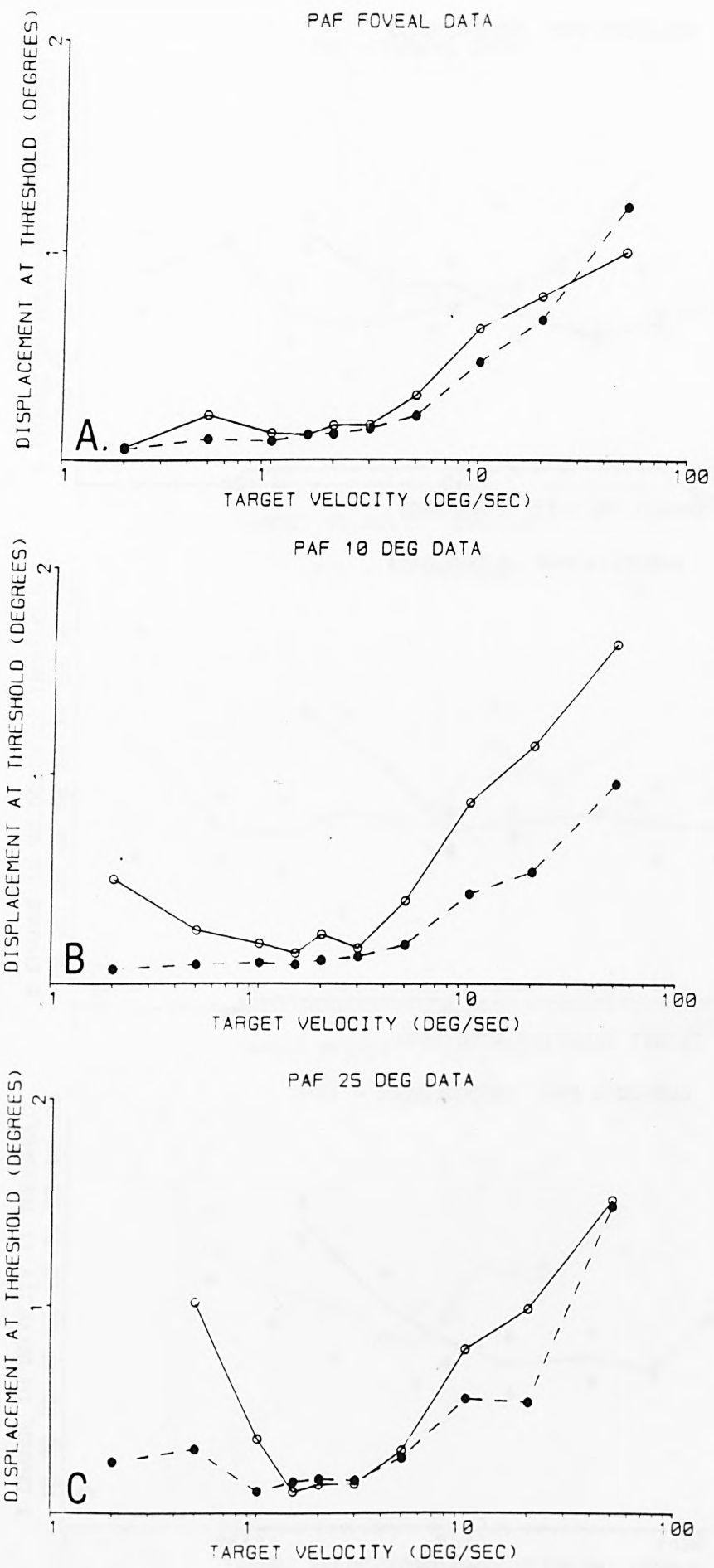

FIGURE 8.4

Displacement thresholds as functions of target velocity. Observer: PAF. Open circles: Right to left (centrifugal motion). Closed circles: Left to right (centripetal motion). A: Foveal data. B: 10° eccentricity. C: 25° eccentricity

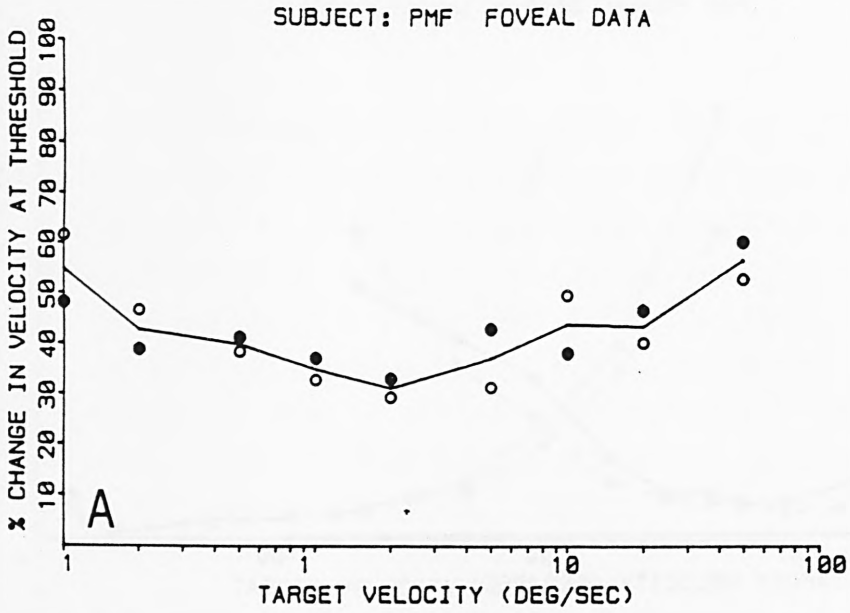

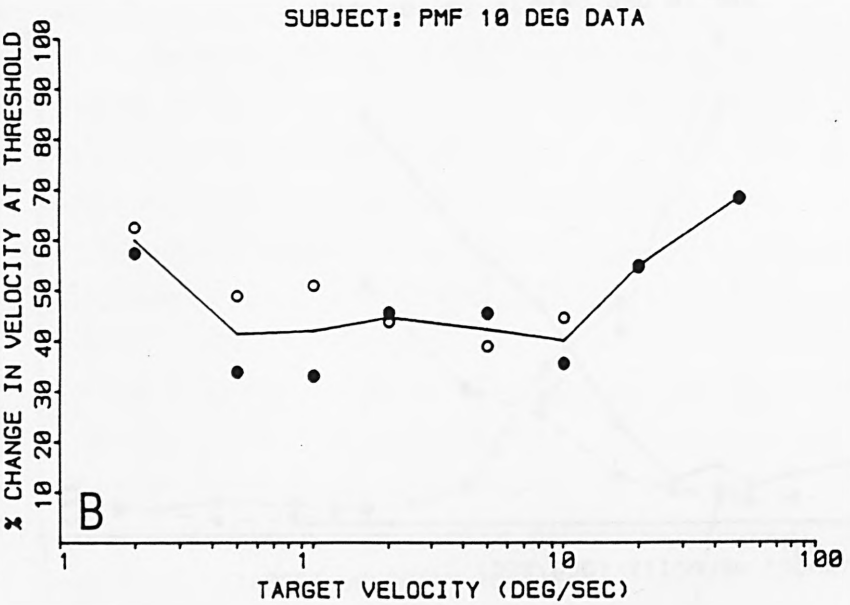

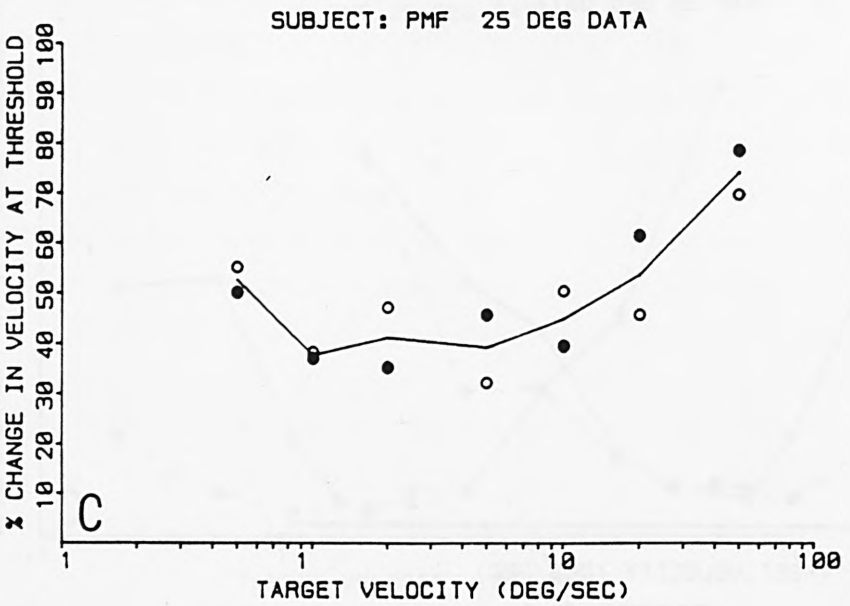

FIGURE 8.5

Velocity discrimination threshold as a function of target velocity. Observer: PMF. Open circles: increasing velocity, Closed circles: decreasing velocity. Solid line: Mean of increases and decreases. A: Foveal data. B: 10° eccentricity. C: 25° eccentricity.

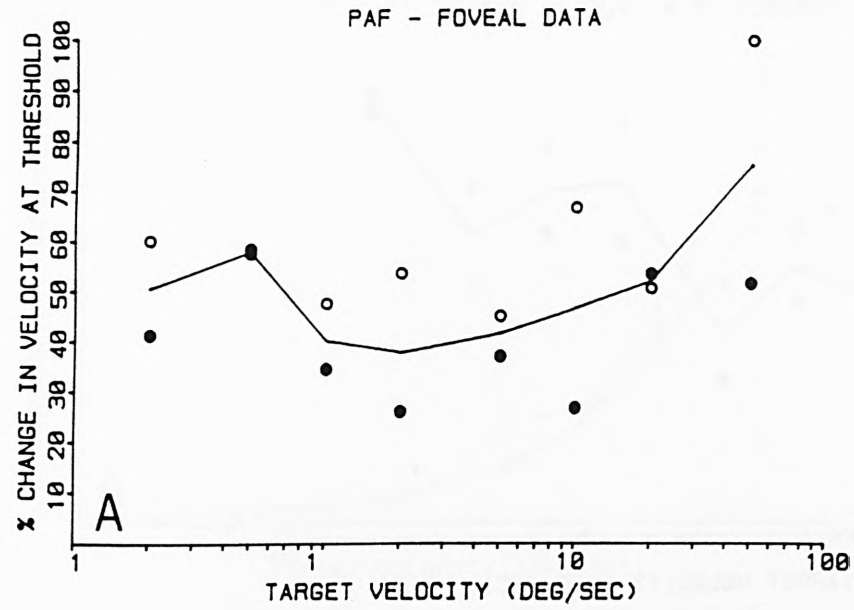

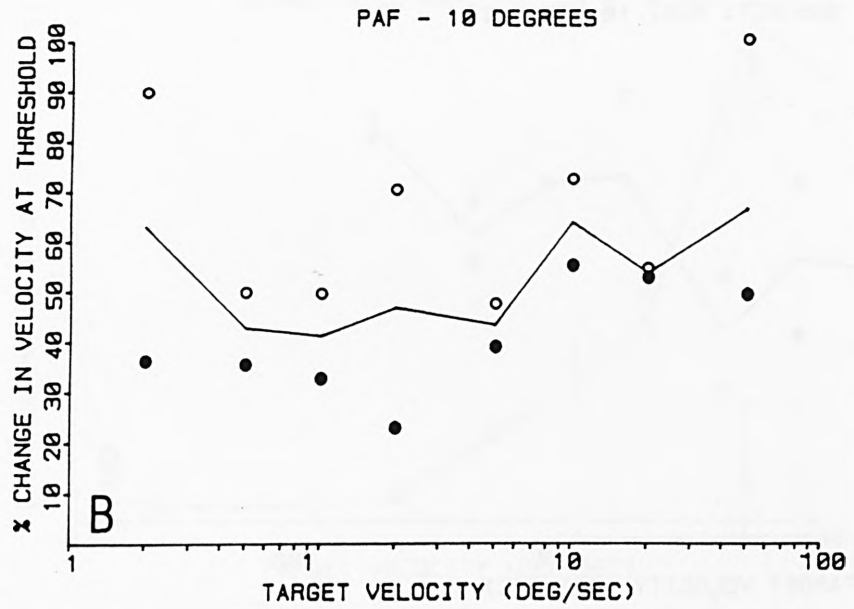

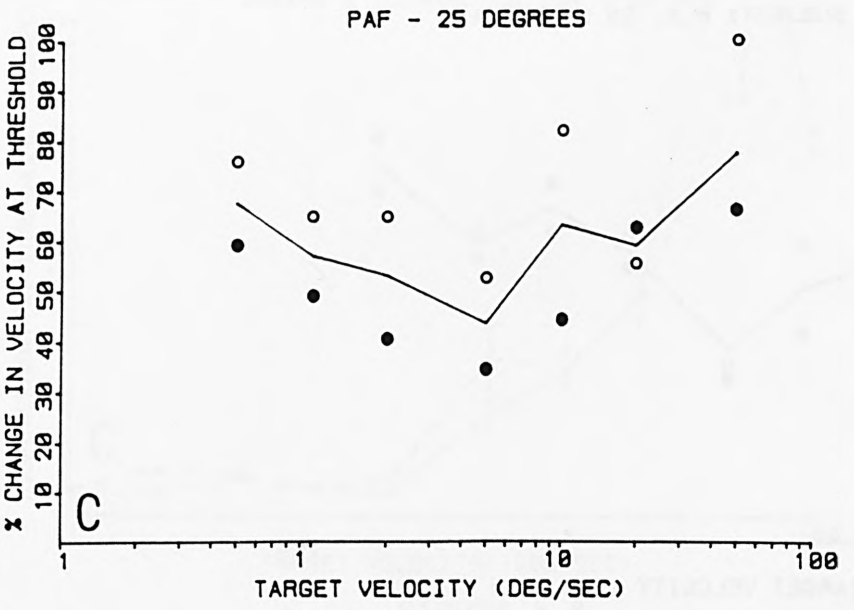

FIGURE 8.6

Velocity discrimination threshold as a function of target velocity. Observer: PAF. Open circles: increasing velocity, Closed circles: decreasing velocity. Solid line: Mean of increases and decreases. A: Foveal data. B: 10° eccentricity. C: 25° eccentricity.

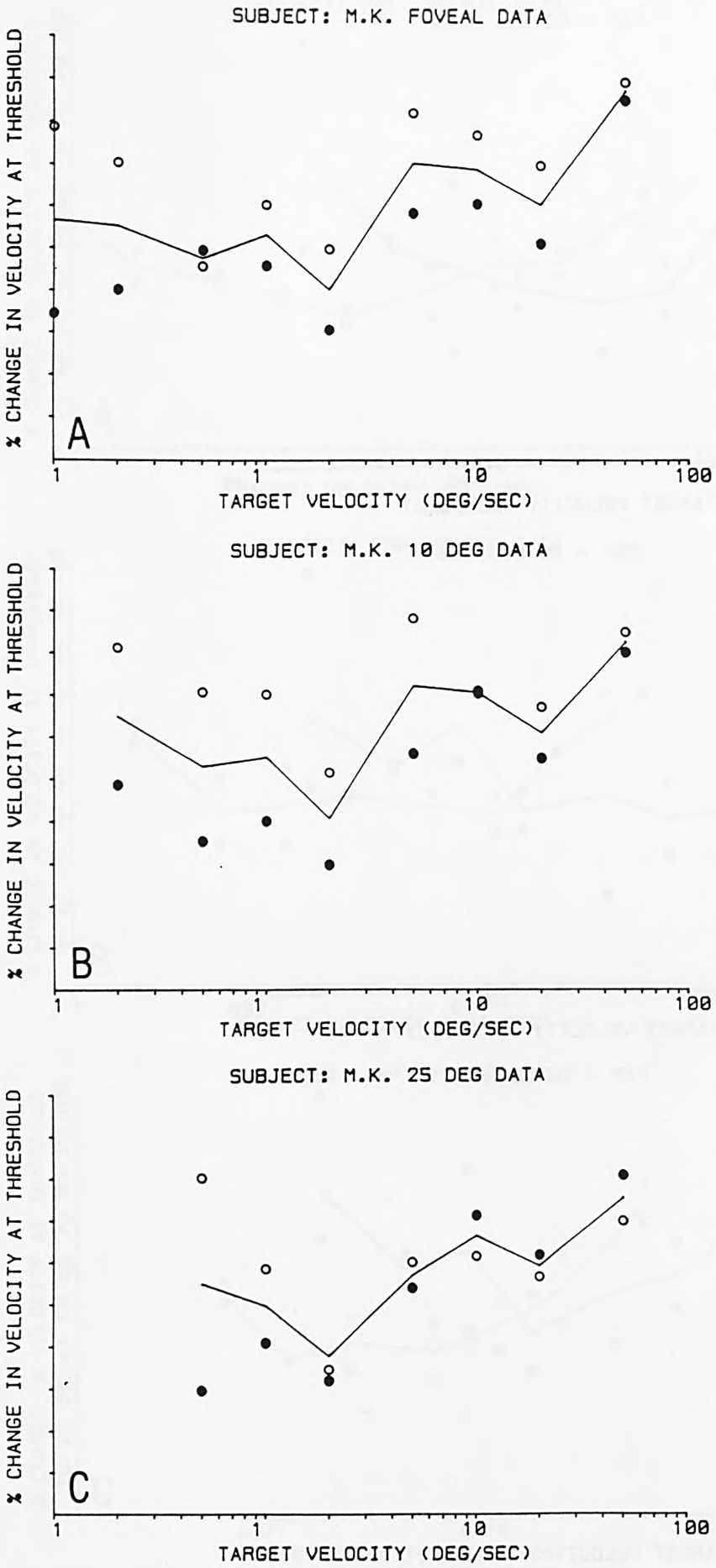

FIGURE 8.7

Velocity discrimination threshold as a function of target velocity. Observer: MK. Open circles: increasing velocity, Closed circles: decreasing velocity. Solid line: Mean of increases and decreases. A: Foveal data. B: 10° eccentricity. C: 25° eccentricity.

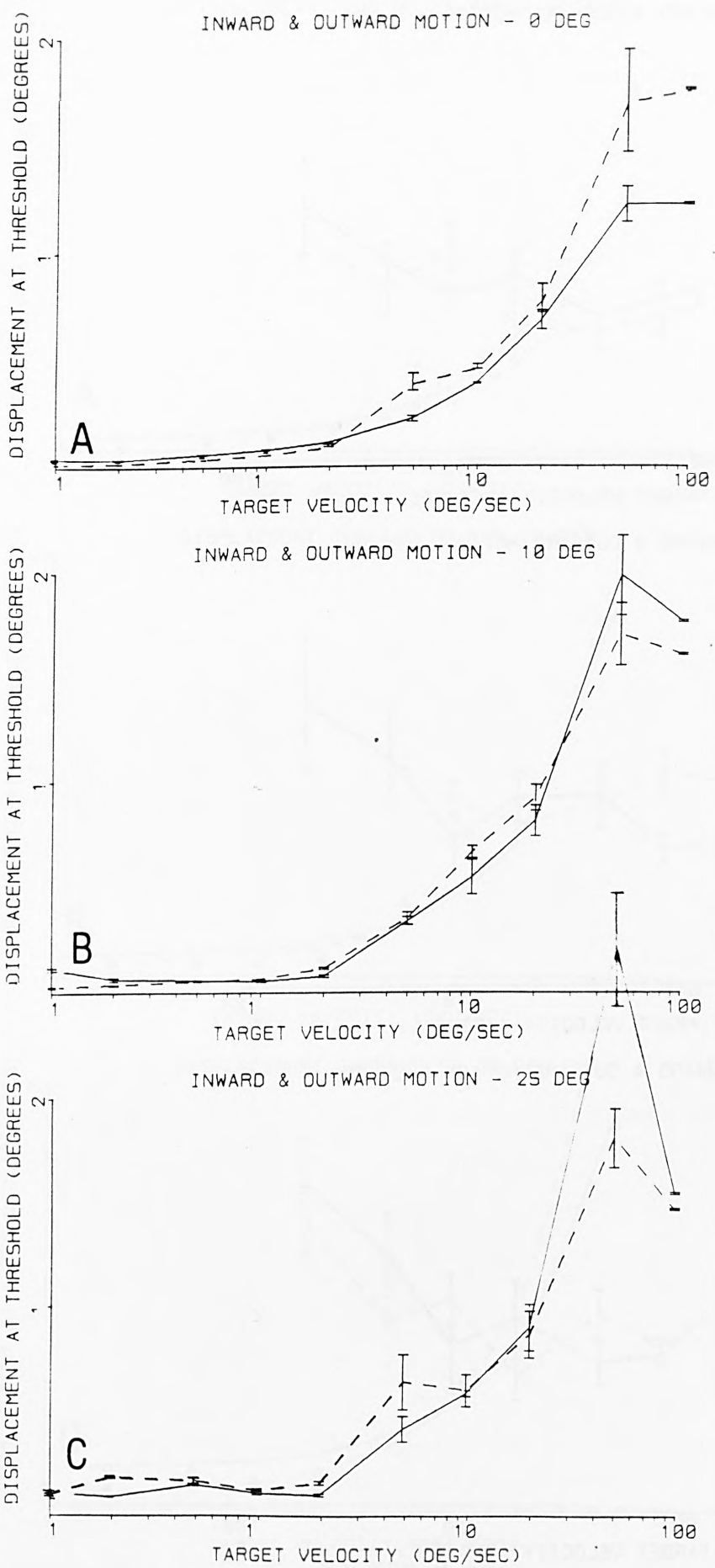

FIGURE 8.8

Displacement threshold as a function of target velocity. Observer: PMF. Solid line: Right to left (centrifugal motion). Broken line: Left to right (centripetal motion). Error bars represent estimated standard deviation. A: Foveal data. B: 10^{o} eccentricity. C: 25^{o} eccentricity.

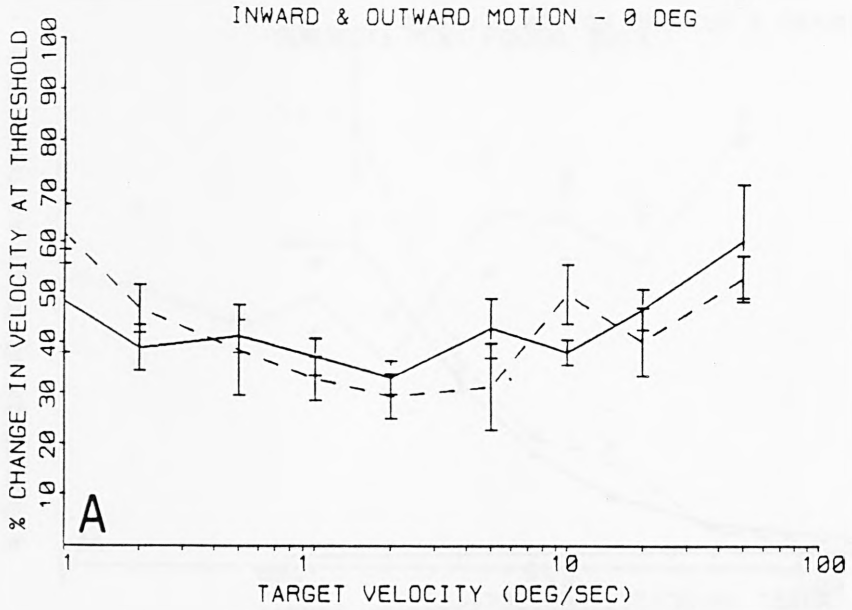

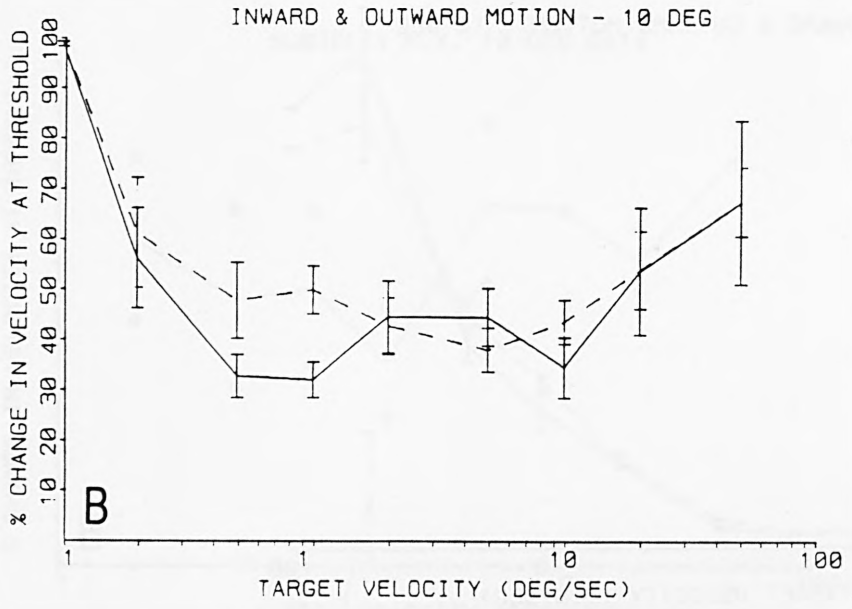

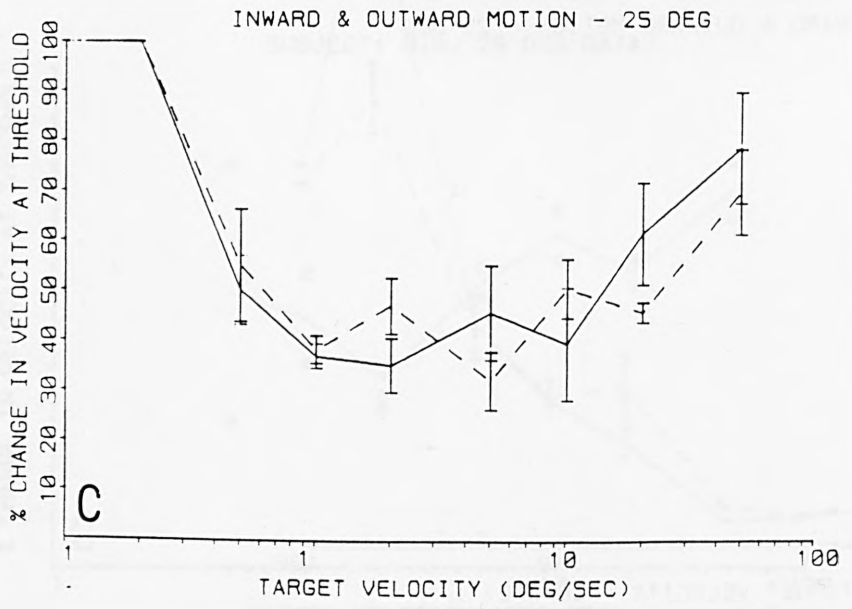

FIGURE 8.9

Velocity discrimination threshold as a function of target velocity. Observer: PMF. Solid line: Right to left (Centrifugal motion). Broken line: Left to right (centripetal motion). Error bars represent estimated standard deviation. A: Foveal data. B: 10° eccentricity. C: 25° eccentricity.

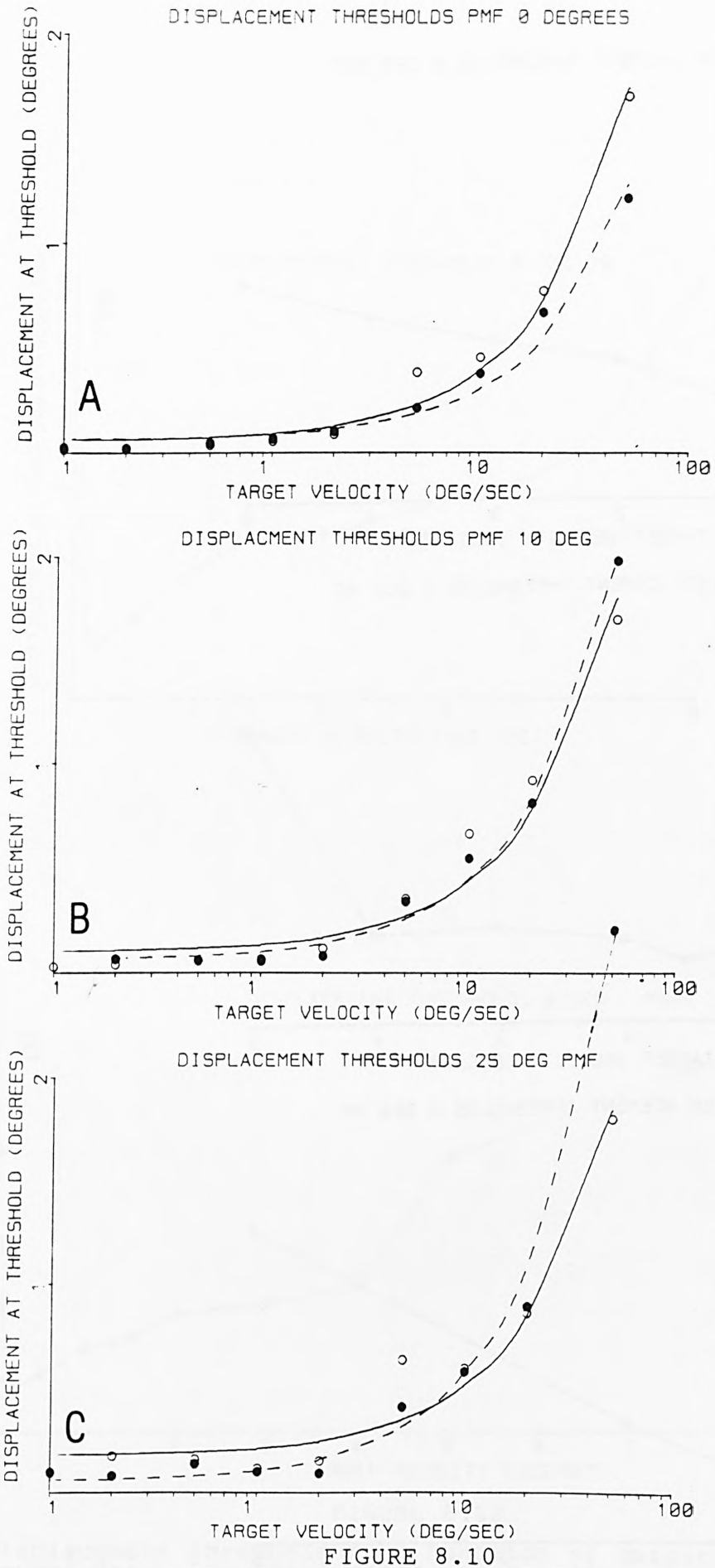

FIGURE 8.10

Displacement threshold as a function of target velocity. Observer: PMF. Open circles: Right to left (centrifugal motion). Closed circles: Left to right (centripetal motion). Solid line: Least squares fit to centrifugal points. Broken line: Least squares fit to centripetal points. A: Foveal data. B: 10° eccentricity. C: 25° eccentricity.

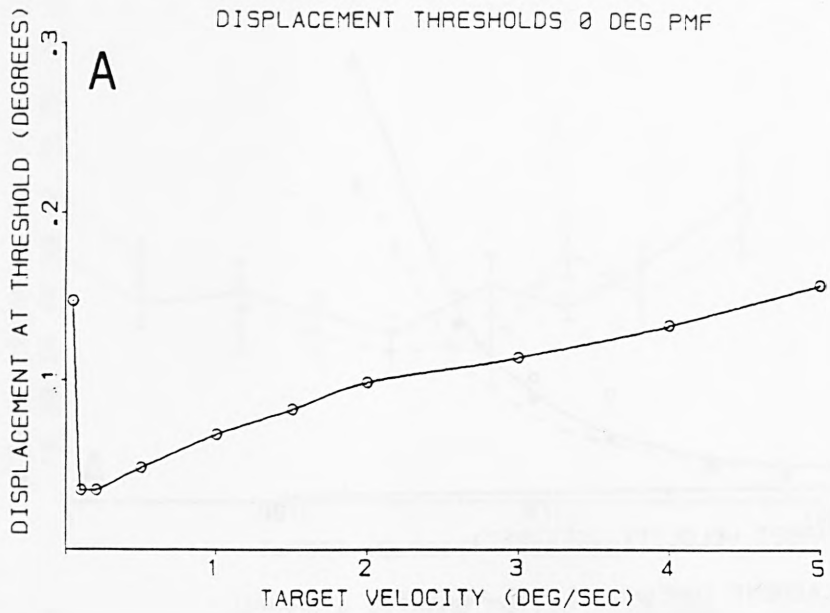

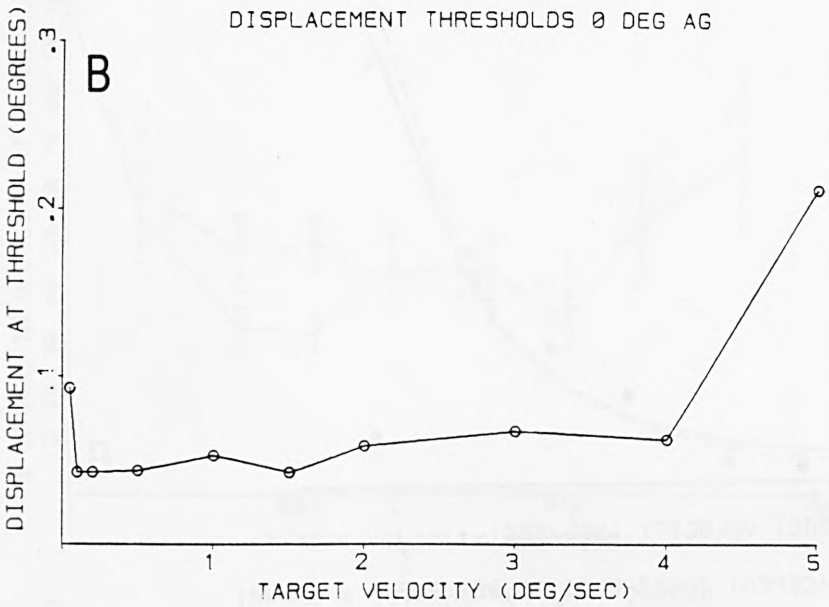

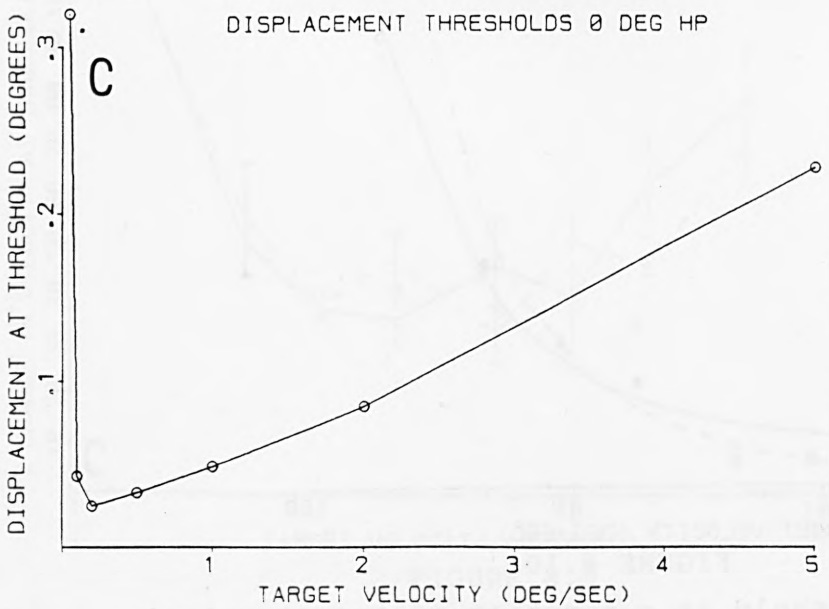

FIGURE 8.11

Displacement threshold as a function of target velocity. Foveal data. Low speed range using a linear scale. A: Subject PMF. B: Subject AG. C: Subject HP.

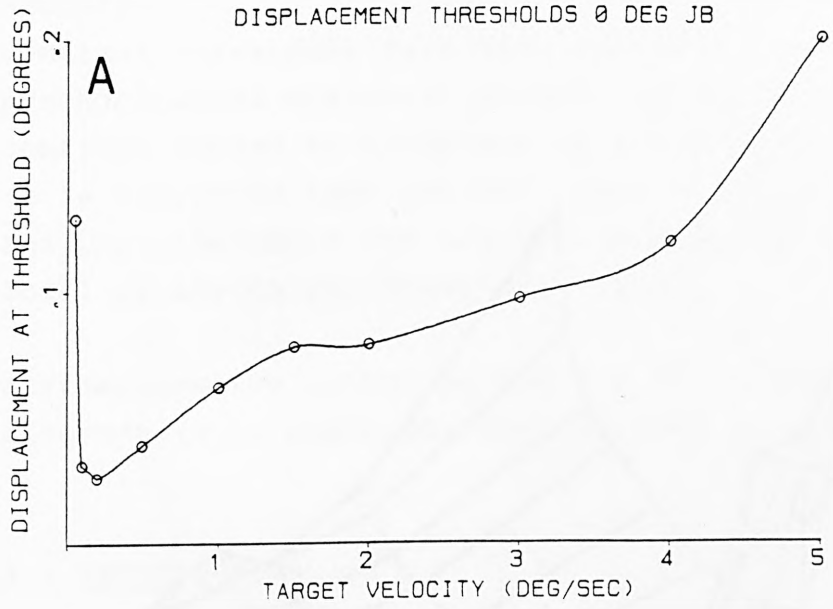

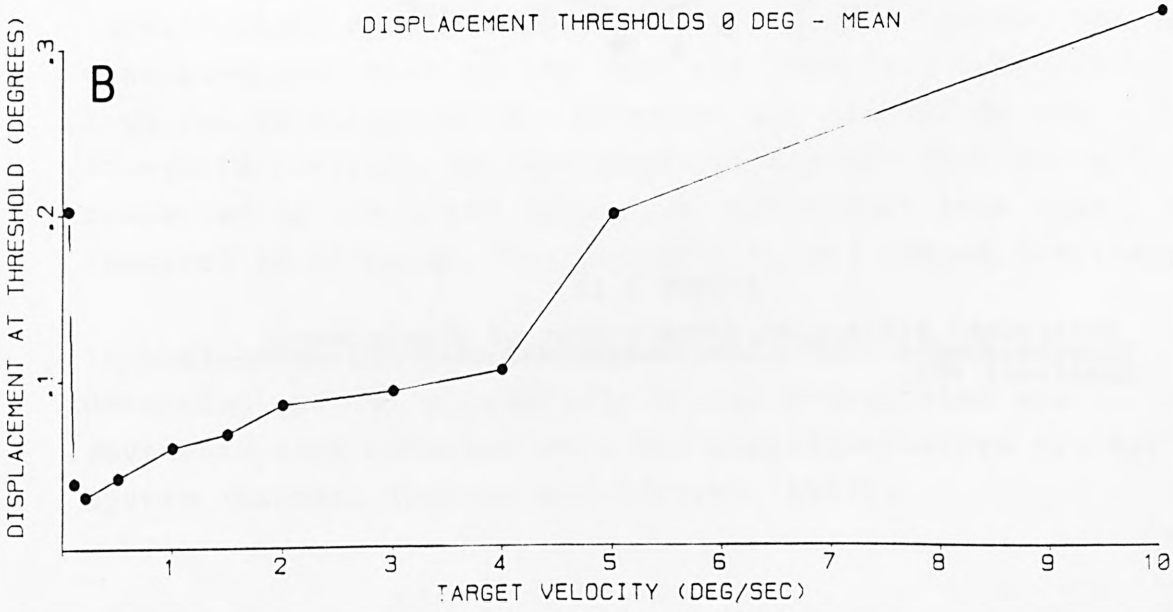

FIGURE 8.12

Displacement threshold as a function of target velocity. Foveal data. Low speed range using a linear scale. A: Subject JLB. B: Mean of four subjects.

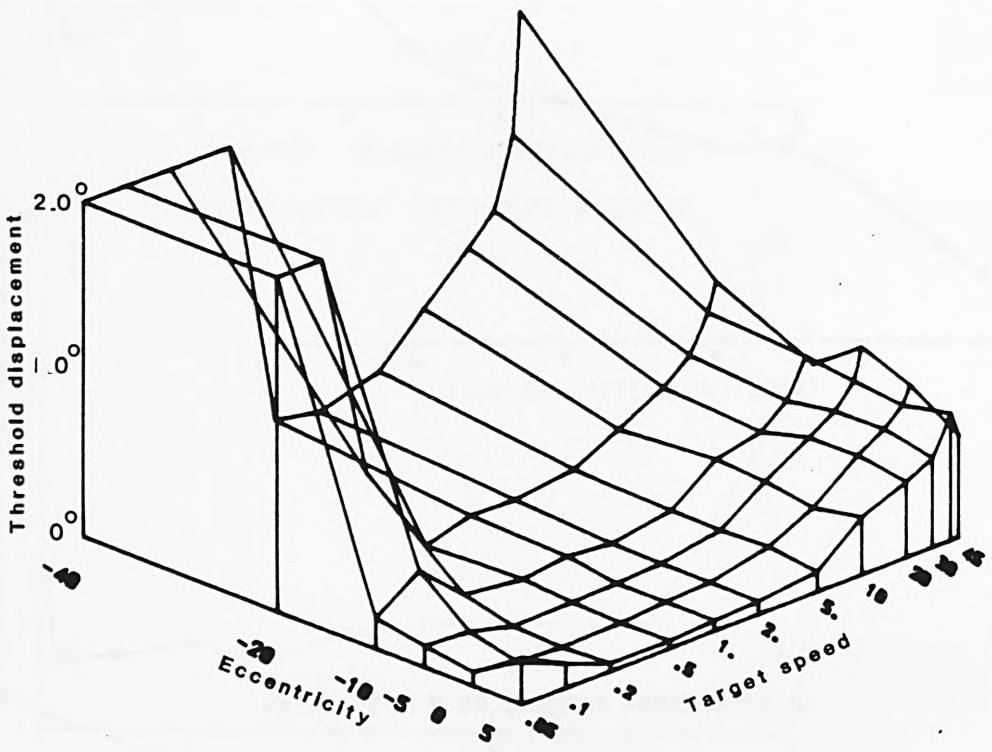

FIGURE 8.13

Orthogonal projection summary plot of Displacement threshold as a function of target velocity and eccentricity. Observer: PMF.

A COMPARISON OF THRESHOLDS FOR CONTRAST DETECTION AND EYE MOVEMENT RESPONSES.

Summary.
Contrast thresholds have been measured using a pyschophysical staircase method, and by determining the contrast needed to stimulate an accurate and timely saccade. It is concluded that the two types of threshold are close, and that therefore the use of the former procedure in a model of search performance is valid.

Furthermore the latter method may be useful as an alternative to psychophysical methods in some cases.

9.1 INTRODUCTION.

The validity of using the probability of detecting a peripheral stimulus whilst fixating on a fixed point as an indication of what would happen in a natural vision search procedure has been questioned in Chapter 1. In chapter 7 the saccadic responses of a hemianopic subject were investigated, for different target contrast levels. The data generated show that in his case the threshold contrast required to stimulate eye movement was similar to his threshold contrast for awareness of any stimulus being presented in his blind hemifield, but higher than that required to stimulate eye movement in his normal hemifield.

In this investigation comparison data for threshold detection and for appropriate stimulus-generated eye movements were obtained on a new pupillometer/eye tracker system (Barbur, Thomson and Forsyth, 1987).

9.2 METHOD.

A maxwellian view field of 20^{o} subtense was provided for this work. The stimulus subtense was 14 minutes of arc. The

stimulus for the psychophysical thresholds was presented, after an audible cue, for 330 ms. The stimulus duration for the saccadic threshold experiment was one second, in order to allow sufficient time for the eye to search for and acquire the target foveally. The eye movement was recorded for the whole of this second, so that the eye position when the target was eventually fixated could be compared with the position at the end of the first saccade.

The psychophysical threshold was determined by means of a staircase procedure with decreasing step sizes, the positions of the last five reversals being averaged to provide an estimate of 50% probability of detection (the third variant of the staircase procedure described in section 2.1). This procedure was carried out three times for each of three eccentricities, for two subjects. The results are shown in table 9.1.

The thresholds for saccadic response were determined for the same target positions, size and background luminance, by presenting the target at 5 luminances grouped around the psychophysical threshold, recording the time variation of pupil area, and classifying the resulting traces into two groups: those in which the first saccade was triggered by the stimulus and those where an accurate and timely saccade was not recorded.

The distribution of latencies usually shows a main peak which has diminished or dropped to zero by 500 ms (see figures 9.1 to 9.6). All saccades with longer latencies were excluded, as were all those with latencies of less than 100 ms. All traces which showed search type eye movements were also excluded, as well as all those with amplitudes outside a range $\pm$10% of the mean. The remainder were taken to be genuine saccades to the stimulus, and were used to calculate the probability of a stimulus-generated saccadic response. These probabilities are shown in table 9.2.

SUBJECT.... PMF COMMENTS....5 DEG. NASAL HEMIFIELD. RT EYE.

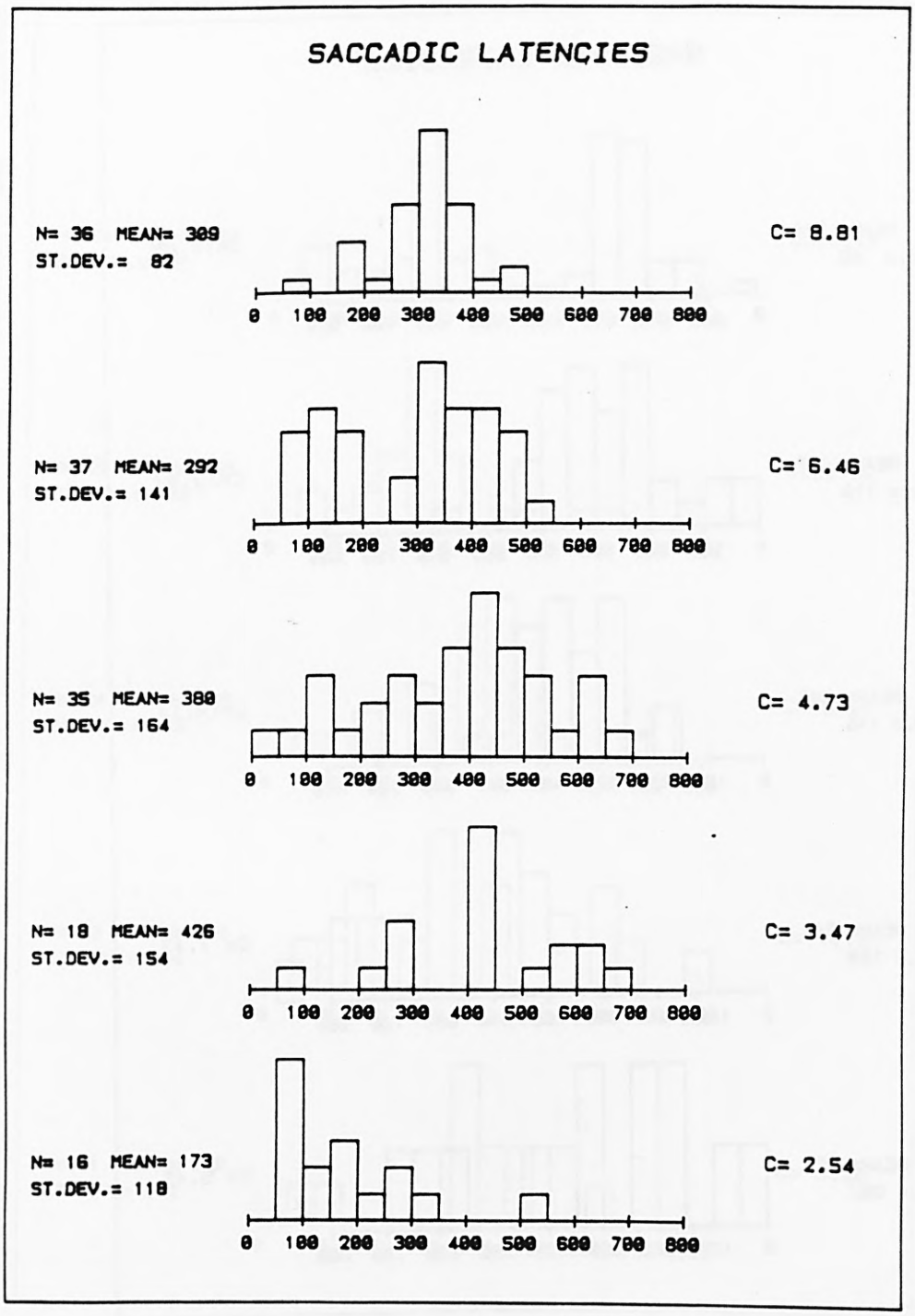

FIGURE 9.1

Distribution of saccade latencies for PMF in response to a 14′ stimulus at 5° eccentricity in the nasal hemifield of the right eye. Stimulus contrasts are shown to the right of each histogram. Stimulus duration: 330 ms. Background luminance: 3.87 log trolands.

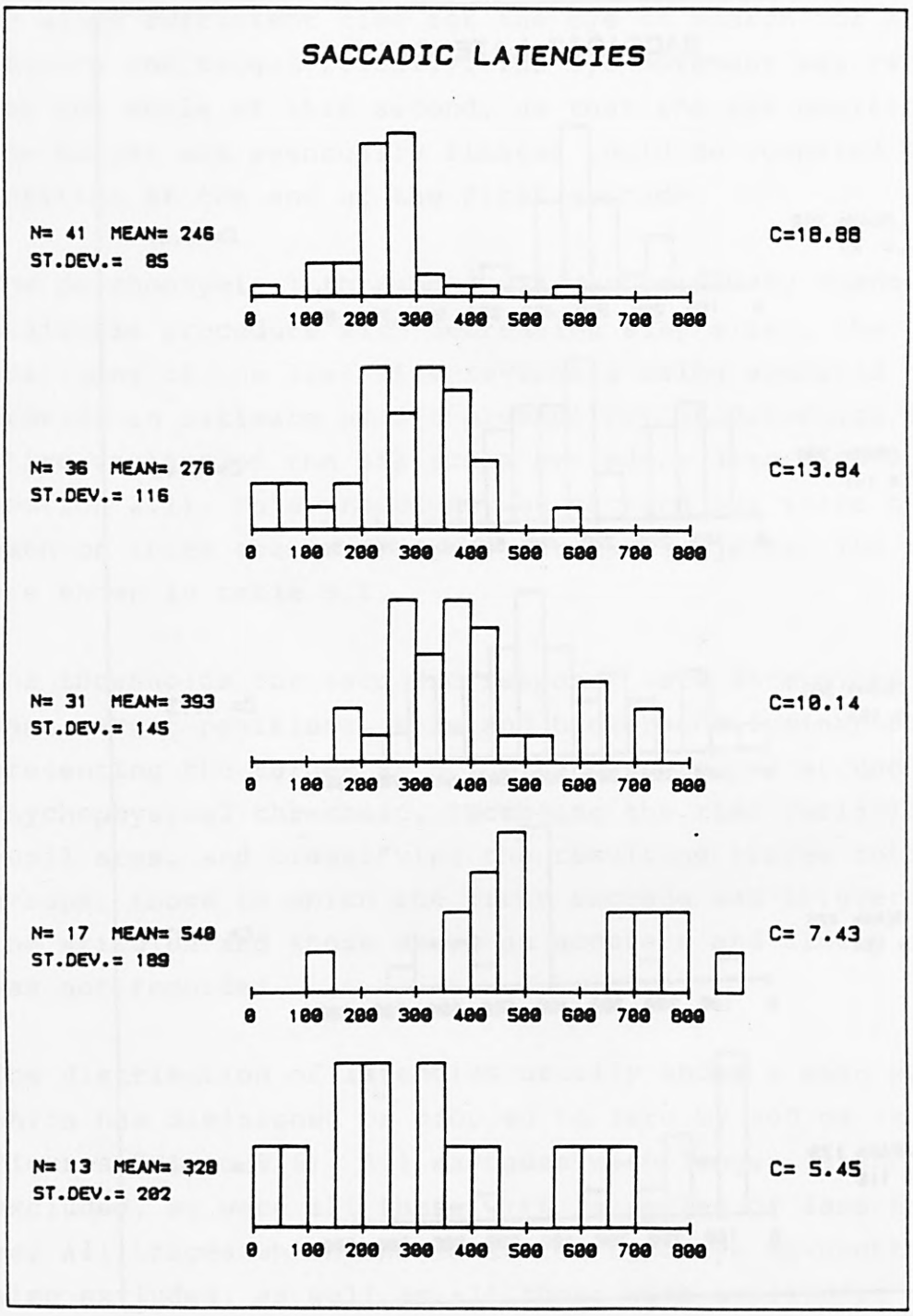

FIGURE 9.2

Distribution of saccade latencies for PMF in response to a 14′ stimulus at 10° eccentricity in the nasal hemifield of the right eye. Stimulus contrasts are shown to the right of each histogram. Stimulus duration: 330 ms. Background luminance: 3.87 log trolands.

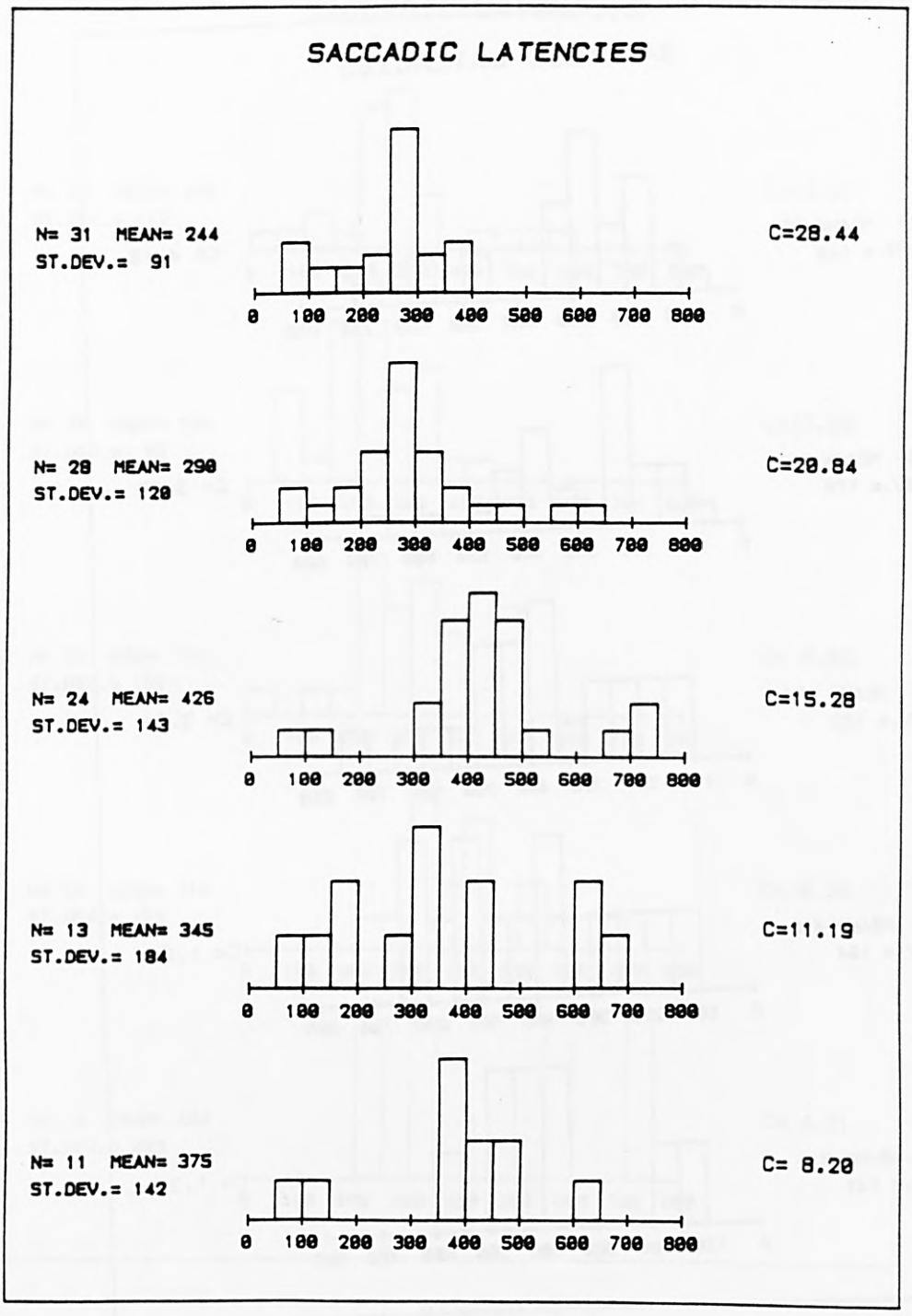

FIGURE 9.3

Distribution of saccade latencies for PMF in response to a 14′ stimulus at 15° eccentricity in the nasal hemifield of the right eye. Stimulus contrasts are shown to the right of each histogram. Stimulus duration: 330 ms. Background luminance: 3.87 log trolands.

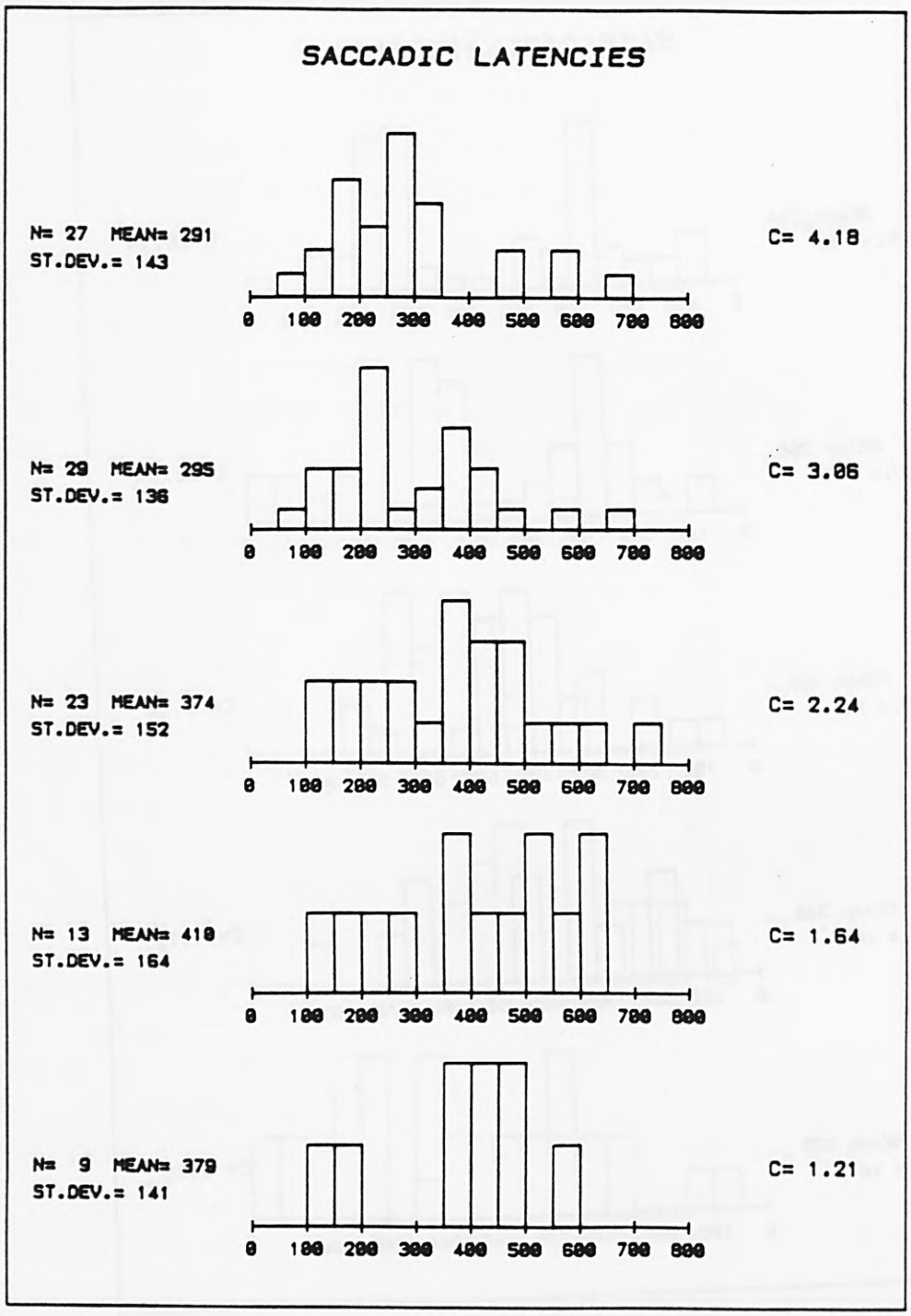

FIGURE 9.4

Distribution of saccade latencies for WDT in response to a 14′ stimulus at 5° eccentricity in the nasal hemifield of the right eye. Stimulus contrasts are shown to the right of each histogram. Stimulus duration: 330 ms. Background luminance: 3.87 log trolands.

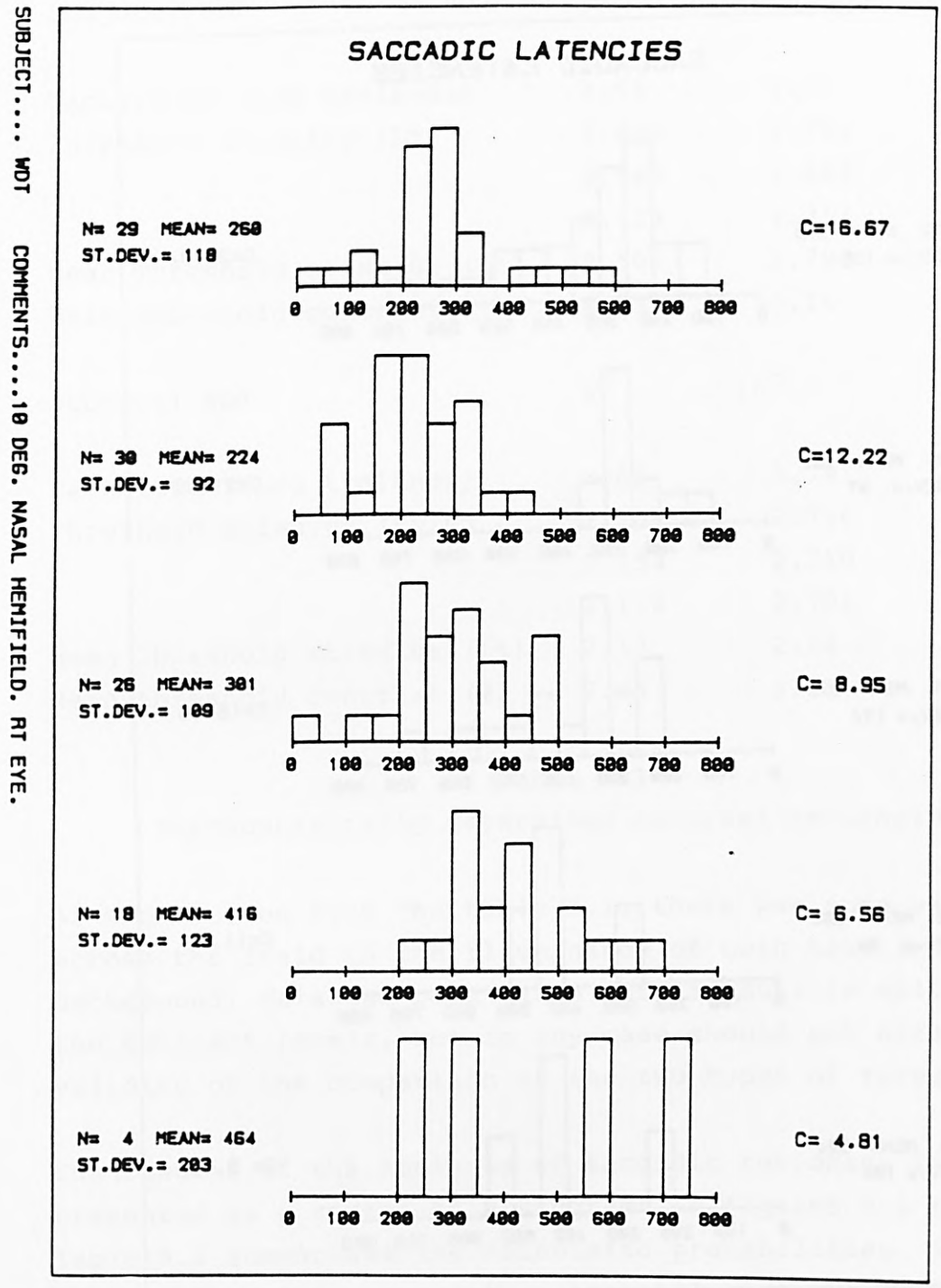

FIGURE 9.5

Distribution of saccade latencies for WDT in response to a 14′ stimulus at 10° eccentricity in the nasal hemifield of the right eye. Stimulus contrasts are shown to the right of each histogram. Stimulus duration: 330 ms. Background luminance: 3.87 log trolands.

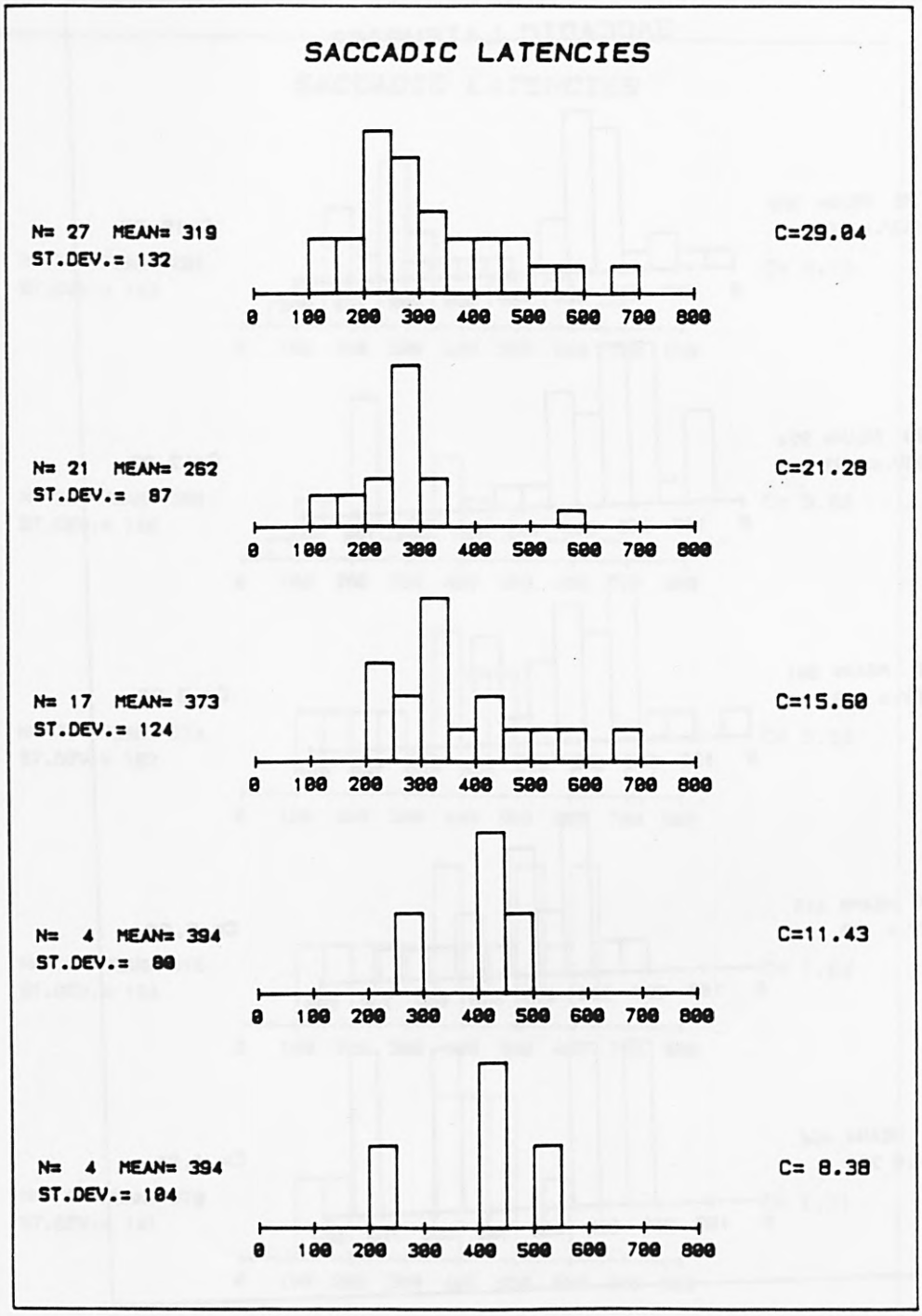

FIGURE 9.6

Distribution of saccade latencies for WDT in response to a 14′ stimulus at 15° eccentricity in the nasal hemifield of the right eye. Stimulus contrasts are shown to the right of each histogram. Stimulus duration: 330 ms. Background luminance: 3.87 log trolands.

9.3 RESULTS.

Subject: PMF	5°	10°	15°
Background (Log trolands)	3.83	3.79	3.75
Threshold Stimulus (Lt)	2.406	2.742	2.907
	2.586	2.886	2.907
	2.523	2.751	2.988
Mean Threshold stimulus (Lt)	2.505	2.796	2.934
Mean threshold contrast (%)	4.73	10.14	15.28

Subject: WDT	5°	10°	15°
Background (Log trolands)	3.83	3.79	3.75
Threshold Stimulus (Lt)	2.208	2.796	2.979
	2.154	2.710	2.844
	2.172	2.706	3.015
Mean Threshold stimulus (Lt)	2.18	2.74	2.94
Mean threshold contrast (%)	2.24	8.95	15.59

TABLE 9.1
Psychophysically determined contrast thresholds.

As can be seen from the table 9.1, there was some variation across the field in the illuminance of both test and background. This has been taken into account in calculating the contrast levels, but in any case should not affect the validity of the comparison of the two types of threshold.

The results of the analysis of saccadic responses is presented as a series of histograms in figures 9.1 to 9.6. Table 9.2 summarises the calculated probabilities. These were used to fit a cumulative probability curve to the set of five points, and calculate the contrast for 50% probability of response. Table 9.3 records the results of this procedure.

Subject:PMF	5°		10°		15°	
40 traces	contrast	prob.	contrast	prob.	contrast	prob.
	8.81	0.700	18.88	0.872	28.44	0.666
	6.46	0.538	13.84	0.737	20.84	0.462
	4.73	0.225	10.14	0.375	15.28	0.231
	3.47	0.100	7.43	0.125	11.19	0.050
	2.54	0.026	5.45	0.026	8.20	0.050

Subject:WDT	5°		10°		15°	
30 traces	contrast	prob.	contrast	prob.	contrast	prob.
	4.18	0.433	16.67	0.700	29.04	0.633
	3.06	0.266	12.22	0.633	21.28	0.533
	2.24	0.200	8.95	0.600	15.60	0.300
	1.64	0.133	6.56	0.333	11.43	0.100
	1.21	0.066	4.81	0.033	8.38	0.033

TABLE 9.2

Probability data for contrast required to make saccades.

Figures 9.7 and 9.8 show the probabilities of a saccadic response, and the curves fitted to them, and figure 9.9 repeats these curves, and shows the psychophysical thresholds. In table 9.4 these thresholds are compared with the psychophysical thresholds.

It can be seen that in all cases the saccadic threshold is slightly higher than the psychophysical one. The thresholds for the two observers are very close in the periphery, but WDT has lower thresholds near to the fovea. This could be due to the age difference between the two observers (PMF is 30 years older than WDT). Since receptive field sizes are so much larger in the periphery, the effect of light scatter on detection might well be less.

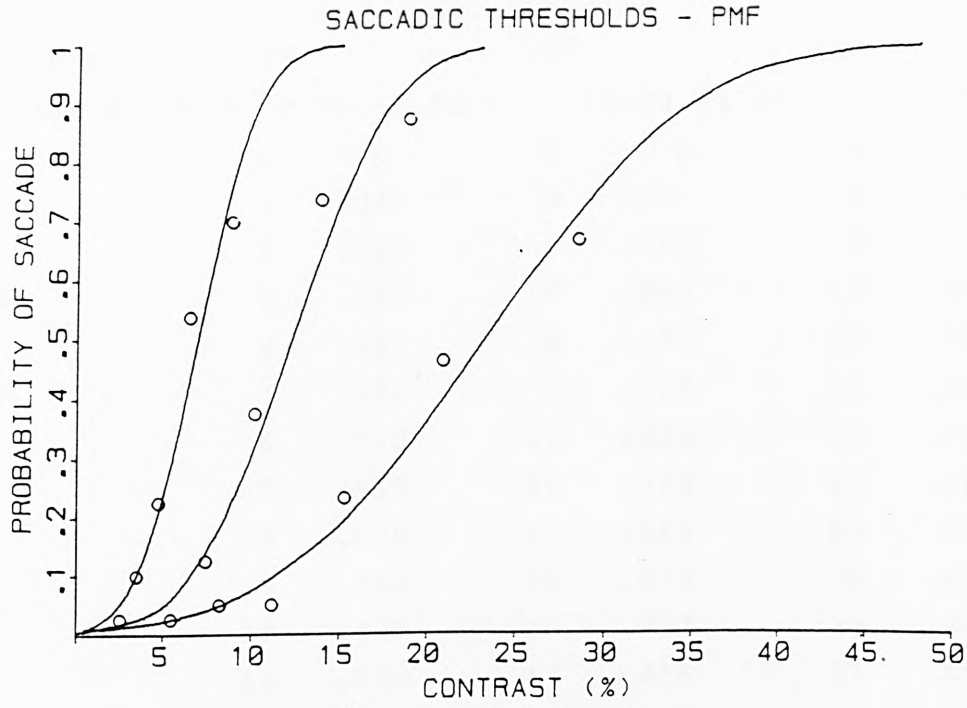

FIGURE 9.7

Probability of a saccade plotted against stimulus contrast. Observer: PMF. The lines represent cumulative probability curves fitted to the points. Leftmost curve: stimulus at 5°. Middle curve: stimulus at 10°. Rightmost curve: Stimulus at 15°.

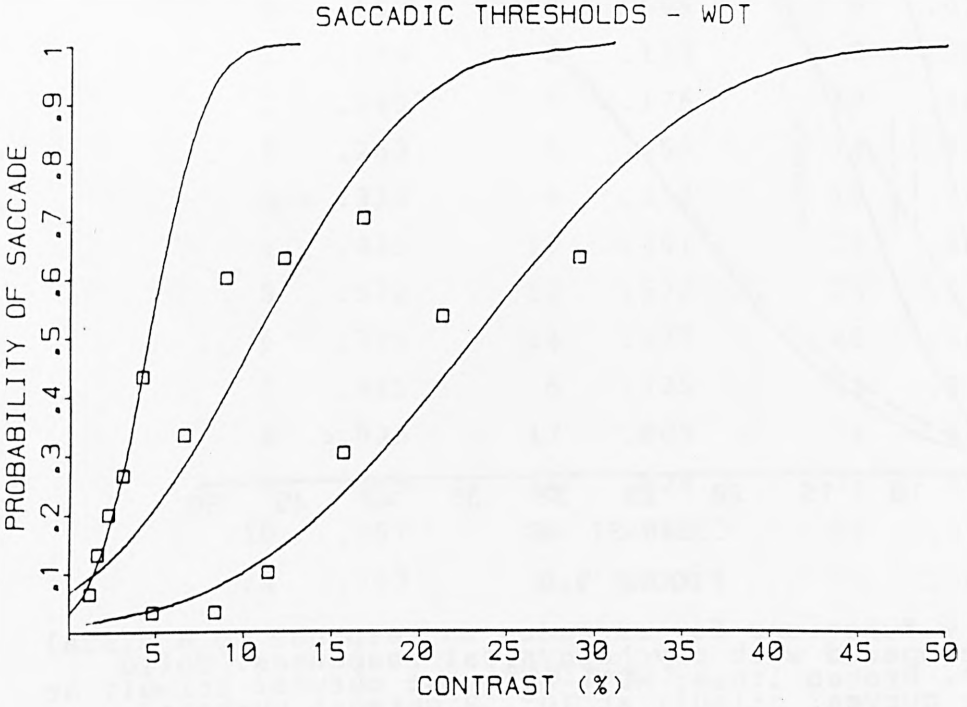

FIGURE 9.8

Probability of a saccade plotted against stimulus contrast. Observer: WDT. The lines represent cumulative probability curves fitted to the points. Leftmost curve: stimulus at 5°. Middle curve: stimulus at 10°. Rightmost curve: Stimulus at 15°.

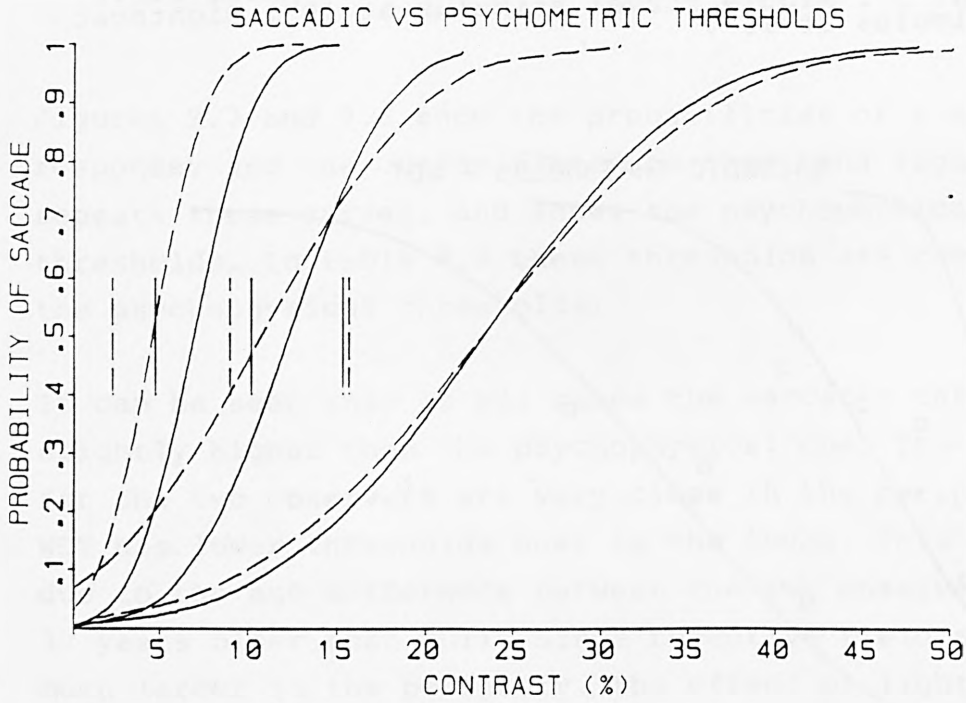

FIGURE 9.9

Probability functions for saccades in response to a visual stimulus compared with psychophysical responses. Solid lines: PMF. Broken lines: WDT. Leftmost curves: stimuli at 5^{o}. Middle curves: stimuli at 10^{o}. Rightmost curves: Stimuli at 15^{o}. The short vertical lines show the psychophysically determined contrast thresholds for the same stimuli.

Eccentricity

Subject:PMF	5°		10°		15°	
Mean Thrshld	6.90 ±2.70		12.23 ±4.45		23.25 9.22	
	C	p	C	p	C	p
	0	.005	0	.003	0	.006
	2	.035	4	.032	6	.031
	3	.074	6	.081	10	.075
	4	.141	8	.171	14	.158
	5	.241	9	.234	18	.285
	6	.370	11	.391	20	.362
	7	.515	12	.479	22	.446
	8	.659	13	.568	24	.532
	9	.782	14	.654	26	.617
	10	.875	15	.733	30	.768
	11	.936	17	.858	33	.855
	12	.971	20	.960	36	.917
	14	.996	23	.992	39	.956
					48	.996
Subject:WDT						
Mean Thrshld	4.55 ±2.45		10.70 ±7.20		23.17 ±10.34	
	C	p	C	p	C	p
	0	.032	0	.069	0	.016
	1	.074	2	.113	6	.048
	2	.149	4	.176	10	.101
	3	.263	6	.257	14	.188
	3.5	.334	8	.354	18	.308
	4	.411	10	.461	22	.455
	5	.572	12	.572	25	.570
	6	.722	14	.677	28	.680
	7	.841	15	.725	31	.776
	8	.920	17	.809	34	.853
	9	.965	21	.924	37	.910
	10	.987	24	.968	44	.978
	12	.999	31	.998	50	.995

TABLE 9.3

Probit Analysis of probabilities of saccades

	Eccentricity					
	5°		10°		15°	
	psycho.	sacc.	psycho.	sacc.	psycho.	sacc.
Subject:PMF	4.73	6.90	10.14	12.23	15.28	23.25
Subject:WDT	2.24	4.55	8.95	10.70	15.60	23.17

TABLE 9.4
Contrast thresholds (%)

9.4 CONCLUSIONS

It may be concluded that the two types of threshold are close, and the exact relationship depends on the definition selected for a saccadic response to the stimulus. Thus it seems reasonable to base search models on thresholds measured with a fixated eye, and conversely it would be possible to measure detection thresholds by means of eye movement measurements, where it is desirable to avoid some of the variability associated with psychophysical decision-making.

DISCUSSION AND CONCLUSIONS.

10.1 INTRODUCTION

Much previous work on search is summarised in Overington (1976 and 1982) and in Clare and Sinclair (1979). Foveal contrast thresholds for a range of target sizes from 3.6 to 121 minutes of arc and for a wide range of background luminances have been reported by Blackwell (1946). The relation of foveal to peripheral thresholds can be derived from Rovamo, Virsu and Nasanen (1978), and the influence of target velocity on contrast thresholds in the periphery has been studied by Koenderink et al (1978). Both these later studies state that M-scaling can be used to predict their findings. The effect of colour on the noticeability of a stimulus at the fovea can be predicted from a uniform colour space, and the relation of foveal colour discrimination to that in the periphery was reported by Noorlander, Koenderink et al (1983) to be predictable by M-scaling. Apart from Blackwell, this work was not done with simple disc targets. In terms of spatial and temporal frequency components discs which appear briefly and instantaneously are far from simple, so it is not easy to relate these studies directly. Where this can be done, the results of this study are broadly reconcilable with expectations based on previous findings.

In certain cases the results here reported are at odds with those of other workers, e.g., the effect of attention on visual thresholds, the level of threshold velocity discrimination, the absence of express saccades when a non-cortical visual pathway is invoked. It seems unlikely that these are the result of observer differences, and are more likely to be a consequence of the highly artificial nature of the stimuli used, or of some unremarked failure of, or difference in, the experimental procedure.

Some equipment has been built for this study which may be of use for further related work, in particular the

telespectroradiometer, the twin axis mirror drive system, with their associated software, and the software to record and analyse eye movements.

10.2 GENERAL OBSERVATIONS

Models of visual performance can be used both to predict performance in particular visual conditions, and to gain insights into the physiology underlying the performance. Both uses were envisaged in collecting the data of this study. The data can be used to incorporate into a predictive model in order to extend its use, and to confirm (or otherwise) the validity of other models.

To be useful in the first context, one aspires to the validity and reliability of the CIE standard observer data, or to Blackwells "Tiffany" experiments. To achieve this level requires more man years than were available in the current study, which had to be limited to far fewer observers and experimental repetitions, and hence far more variability from observer to observer and even within one observer's performance than is ideally desirable. One can nevertheless deduce some trends in the results, and some interesting functional relationships.

10.3 CONCLUSIONS RELATING TO SEARCH PERFORMANCE

The direct measurement of visual lobes appears to be less efficient, in terms of observers time, than the measurement of thresholds, followed by a prediction of the visual lobe for a given stimulus level, based on the appropriate psychometric function, or even on a generalised one. Such a procedure allows the generation of a range of lobes from one threshold function, and avoids the experimental variability inherent in measuring very low probabilities (chapter 3).

The threshold level of contrast at which observers respond

to a peripheral stimulus appears to be closely related to the level at which a saccade is triggered, so that it seems reasonable to use lobes or threshold functions derived from work with a fixated eye to indicate the likelihood of making the eye movement needed to place an image of a peripheral target on the fovea during visual search (chapter 9).

Experiments in which the stimulus appears or disappears suddenly are poor predictors of the stimulus level at which a continuously visible or gradually increasing level of stimulus will trigger an eye movement. Different ganglion cells and neural pathways may be involved and the threshold levels may differ (in the case of contrast thresholds) by up to 50% for a normal observer (chapter 3).

It has not proved possible to determine an optimum attention strategy for minimising detection thresholds: the effort of attempting to distribute one's attention away from the point of fixation may be counterproductive. The probability of detecting a peripheral stimulus declines markedly with fatigue. A large body of work suggests that prior knowledge of the properties of a visual stimulus does lower its detection threshold however, and more studies of the application of these findings might be fruitful (chapter 4).

As is well known the periphery (at about 20^{o} eccentricity) is more efficient at detecting low contrast stimuli than the fovea under scotopic conditions. This ability may extend into the photopic region in some conditions (chapter 5).

For stimuli near the threshold of detectability, chromatic contrast appears to add little to the probability of detection of a peripheral stimulus (chapter 5).

Results are given showing the variation in contrast threshold across the visual field as a function of target size and velocity (figures 3.4 and 3.5), and the way motion detection and speed discrimination vary with target velocity and visual field position (figure 8.3 to 8.17).

The ability of the periphery of the visual field to detect changes in target velocity is, for certain velocities, close to that of the fovea, but not actually better (chapter 8).

10.4 MODELS OF VISUAL FUNCTION.

The pupil light reflex is a well known response to a sudden increase in light flux on the retina, but a constriction also occurs when there is no change in total light flux, as in the case of a counterphase grating, or the replacement of a uniform area of illumination by a grating of the same mean luminance. The response to an increase in light flux occurred in the blind hemifield of a hemianopic subject, but not the latter responses, which suggests that the response to a pattern with no overall luminance change requires the mediation of the cortex.

Over a wide range of velocities, from 5^{o}/sec upwards, the threshold displacement for motion detection is proportional to the speed at which the target is moving, suggesting that in this range a model employing a single time delay of the Barlow and Levick type is appropriate. At speeds below 5^{o}/sec the displacement threshold is almost constant, suggesting that a series of different time delays must operate. At still lower speeds (the range differs from one observer to another), There is evidence of another region in which displacement is proportional to speed, but the function has a lower slope, suggesting a longer time delay.

The distribution of latencies and amplitudes of saccades for normal subjects showed a slight increase in latency as stimulus eccentricity increased, and a slight tendency for saccades to double target stimuli to land between the two.

The hemianope required higher target contrast for the generation of a saccade in his blind hemifield than in his normal hemifield, but provided this threshold is exceeded

saccades have accurate mean amplitudes, but rather greater variability.

The possibility that the goals of such saccades are mediated by scattered light reaching his normal hemifield is remote. It would appear that midbrain pathways can mediate saccadic eye movements, but the data obtained in this study do not suggest that these saccades are particularly rapid. Optimum saccade performance was observed only when the geniculo-striate pathway was also involved, and this suggests complementary parallel processing of the visual input.

APPENDIX 1

TABULATED EXPERIMENTAL DATA

Position of target on scale	Potentiometer voltage
20	2.38037
22	2.26190
24	2.14111
26	2.02150
28	1.90308
30	1.78467
32	1.65894
34	1.54419
36	1.42882
38	1.30493
40	1.18896
42	1.07056
44	0.95154
46	0.83557
48	0.71350

TABLE 2.3
Calibration of position potentiometer in chapter 3.

step no.	Log(P)	step no.	Log(P)	step no.	Log(P)
0	-2.70	130	-1.42	250	-0.173
10	-2.52	140	-1.30	260	-0.074
20	-2.52	150	-1.19	270	+0.025
30	-2.46	160	-1.09	280	+0.123
40	-2.35	170	-0.983	290	+0.229
50	-2.26	180	-0.873	300	+0.336
60	-2.19	190	-0.772	310	+0.448
70	-2.05	200	-0.663	320	+0.558
80	-1.96	210	-0.562	330	+0.663
90	-1.83	220	-0.465	340	+0.668
100	-1.74	230	-0.367	350	+0.667
110	-1.64	240	-0.270	360	+0.667
120	-1.52				

TABLE 2.4
Calibration of neutral density wedge

CONDITIONS				ECCENTRICITIES										
sze	spd	bkgnd	glimpse	-20	-13	-10.5	-7.5	-4	-1.5	0	1.5	4	7.5	10.5	13	20
Glimpse length series																
0.5	0	2.57	.11	2.162	2.223	2.082	1.982	1.841	1.660	1.399	1.228	1.720	1.720	1.841	1.982	1.921
0.5	0	2.57	.33	2.095	2.022	2.137	1.930	1.762	1.494	1.425	1.595	1.695	1.856	1.809	2.084	1.843
0.5	0	2.57	.66	2.162	1.982	2.082	1.921	1.740	1.519	1.338	1.580	1.600	1.740	1.740	1.660	1.841
0.5	0	2.57	.99	2.022	1.982	2.042	1.901	1.660	1.338	1.379	1.519	1.580	1.660	1.740	1.901	1.901
Target size series																
0.5	0	4.17	.33	3.605	3.544	3.605	3.464	3.223	3.082	2.740	3.162	3.162	2.982	3.303	3.363	3.363
1.4	0	4.17		3.363	3.363	3.404	3.223	2.982	2.901	2.399	3.022	2.982	3.082	3.082	3.223	2.961
2.6	0	4.17		3.223	3.162	3.223	3.022	2.841	2.841	2.781	2.841	2.921	3.042	2.982	2.982	3.022
4.0	0	4.17		3.082	2.921	3.162	3.082	2.981	2.901	2.801	2.901	2.982	3.022	3.022	2.921	3.022
5.5	0	4.17		3.162	3.022	3.223	3.162	3.022	2.841	2.801	2.841	2.901	2.921	2.841	3.022	3.022
0.5	3	4.17		3.491	3.419	3.492	3.251	3.110	2.978	2.744	2.973	3.070	3.158	3.134	3.288	3.182
1.4	3	4.17		3.223	3.162	3.270	3.075	2.968	2.807	2.559	2.747	2.934	2.935	2.941	3.095	2.981
2.6	3	4.17		3.082	3.082	3.223	3.042	2.982	2.660	2.660	2.600	2.901	2.901	2.901	2.841	2.921
4.0	3	4.17		3.162	3.022	3.022	3.022	2.801	2.600	2.801	2.419	2.801	2.901	2.841	2.901	2.901
5.5	3	4.17		3.042	3.022	3.162	3.022	2.841	2.660	2.801	2.740	2.982	3.042	2.841	2.841	2.982

50% PROBABABILITY THRESHOLDS

CONDITIONS				ECCENTRICITIES										
Size	spd	bkgnd	runs	-20	-13	-10.5	-7.5	-4	-1.5	0	1.5	4	7.5	10.5	13	20
1.4	0	4.17	1	2.961	3.223	3.363	3.223	3.082	2.921	2.740	2.982	2.982	3.082	3.082	3.223	3.162
1.4	3	4.17	1	3.082	2.982	2.982	2.982	2.901	2.580	2.600	2.740	2.921	3.022	2.982	3.082	2.921
0.133	0	4.17	1	4.409	4.167	4.167	3.745	3.544	3.363	3.162	3.544	3.544	3.605	3.846	4.409	4.248
0.133	3	4.17	1	3.966	3.745	3.786	3.544	3.303	3.162	2.982	3.162	3.363	3.404	3.605	3.866	3.605

50% PROBABILITY THRESHOLDS (GRADUAL APPEARANCE OF TARGET)

TABLE 3.3

Summary of contrast thresholds results- in log(retinal illuminance) of target at threshold. Glimpse length series, target size series and gradual appearance trial.Subject: PMF

CONDITIONS				ECCENTRICITIES												
sze	spd	bkgnd	runs	-20	-13	-10.5	-7.5	-4	-1.5	0	1.5	4	7.5	10.5	13	20
1.4	0	4.17	3	3.363	3.296	3.303	3.263	3.015	2.988	2.734	2.995	3.075	3.049	2.988	3.223	2.961
1.4	1	4.17	2		3.333	3.363	3.162	3.002	2.821	2.539	2.851	3.002	3.082	3.082	3.333	
1.4	3	4.17	3	3.223	3.162	3.270	3.075	2.968	2.807	2.559	2.747	2.934	2.935	2.941	3.095	2.981
1.4	0	2.57	4	1.602	1.711	1.727	1.626	1.576	1.430	1.339	1.445	1.440	1.556	1.445	1.510	1.609
1.4	1	2.57	2		1.700	1.790	1.660	1.620	1.379	1.258	1.419	1.519	1.589	1.479	1.660	
1.4	3	2.57	3	1.544	1.568	1.601	1.568	1.454	1.340	1.139	1.300	1.400	1.420	1.374	1.548	1.404
0.5	0	4.17	5	3.611	3.545	3.697	3.524	3.387	3.150	3.014	3.231	3.315	3.271	3.279	3.473	3.377
0.5	1	4.17	2		3.535	3.645	3.544	3.223	2.911	2.781	3.122	3.192	3.293	3.383	3.504	
0.5	2	4.17	2	3.544	3.454	3.575	3.454	3.223	2.912	2.821	3.092	3.192	3.223	3.192	3.434	3.082
0.5	3	4.17	4	3.464	3.459	3.479	3.258	3.117	2.997	2.746	2.992	3.112	3.142	3.127	3.262	3.162
0.5	0	2.57	3	2.095	2.022	2.137	1.930	1.762	1.494	1.425	1.595	1.695	1.856	1.809	2.084	1.843
0.5	1	2.57	2	2.082	2.002	2.042	1.851	1.791	1.580	1.268	1.580	1.710	1.801	1.751	1.912	1.901
0.5	3	2.57	2	1.841	1.942	1.951	1.700	1.550	1.334	1.248	1.439	1.560	1.620	1.560	1.731	1.841

50% PROBABILITY THRESHOLDS

CONDITIONS				ECCENTRICITIES												
Size	spd	bkgnd	runs	-20	-13	-10.5	-7.5	-4	-1.5	0	1.5	4	7.5	10.5	13	20
0.133	0	4.17	1	4.308	4.107	4.348	4.107	3.404	3.544	2.982	3.223	3.605	3.745	3.745	4.167	4.107
0.133	3	4.17	1	4.027	3.926	3.926	3.544	3.464	3.223	2.921	3.164	3.363	3.404	3.605	3.987	4.107
0.133	0	2.57	1	2.926	2.544	2.966	2.162	2.223	1.841	1.660	1.801	2.022	2.303	2.162	2.363	2.464
0.133	3	2.57	1	2.544	2.303	2.363	2.223	1.901	1.740	1.600	1.600	2.022	2.082	2.223	2.404	2.223
0.033	0	4.17	2	5.077	5.549	5.549	5.087	4.253	4.263	3.921	4.826	5.097	4.635	5.258	5.479	4.755
0.033	3	4.17	1	5.549	5.308	5.308	4.866	4.605	4.404	3.901	4.363	4.605	4.926	5.248	5.549	5.308
0.033	0	2.57	2	4.185	3.863	3.688	3.643	3.040	2.879	2.592	2.864	3.281	3.673	3.512	4.024	4.075
0.033	3	2.57	1	3.926	3.685	3.544	3.303	2.982	2.901	2.660	2.921	3.022	3.223	3.464	3.846	3.846

TABLE OF 50% PROBABILITY THRESHOLDS - OBSERVER D.T.

0.133	0	4.17	1	4.308	4.167	4.167	4.027	3.987	3.544	2.982	3.363	3.605	3.786	3.866	4.107	4.107
0.133	3	4.17	1	4.027	3.846	3.987	3.605	3.404	2.982	2.982	3.042	3.303	3.605	3.605	4.308	3.745
0.033	0	4.17	1	5.549	5.549	5.409	5.549	5.549	4.786	4.042	4.866	5.308	5.549	5.409	5.409	5.489
0.033	3	4.17	1	4.605	5.409	5.348	5.348	5.107	4.605	4.162	4.464	4.786	4.926	5.027	5.489	4.966

50% PROBABILITY THRESHOLDS

TABLE 3.4

Summary of contrast thresholds results- in log(retinal illuminance) of target at threshold. target velocity series. Diameters: 0.033^{o}, 0.133^{o}, 0.5^{o} & 1.4^{o}. Subject: PMF Diameters: 0.033^{o} and 0.133^{o}. Subject: WDT.

CONDITIONS					ECCENTRICITIES										
Size	spd	bkgnd	times presented	target illum.	-14	-10.5	-7.5	-4	-1.5	0	1.5	4	7.5	10.5	14
1.4	0	4.17	30	2.97	.07	.00	.10	.33	.70	.97	.77	.37	.13	.10	.03
1.4	1	4.17	20	2.97	.00	.05	.10	.20	.95	1.00	.80	.10	.10	.20	.00
1.4	3	4.17	20	2.97	.05	.10	.15	.40	.85	1.00	.95	.55	.30	.40	.05
1.4	0	2.57	30	1.37	.03	.03	.10	.20	.27	.90	.53	.10	.07	.10	.07
1.4	1	2.57	20	1.37	.00	.00	.10	.10	.60	1.00	.65	.25	.10	.20	.05
1.4	3	2.57	20	1.37	.00	.05	.15	.10	.85	.95	.90	.60	.25	.20	.10
0.5	0	4.17	40	3.15	.00	.00	.00	.15	.68	1.00	.80	.20	.03	.08	.00
0.5	1	4.17	20	3.15	.10	.00	.00	.20	.80	1.00	.90	.35	.05	.10	.05
0.5	2	4.17	10	3.15	.00	.00	.10	.30	.90	1.00	1.00	.30	.20	.20	.00
0.5	3	4.17	20	3.15	.00	.00	.15	.65	1.00	1.00	1.00	.80	.40	.45	.00
0.5	0	2.57	20	1.57	.00	.00	.00	.15	.40	1.00	.60	.15	.05	.00	.00
0.5	1	2.57	20	1.57	.00	.00	. 5	.05	.55	1.00	.95	.15	.00	.00	.00
0.5	3	2.57	20	1.57	.00	.00	.00	.40	.95	1.00	1.00	.55	.30	.25	.00
0.5	0	2.57	20	1.57	.00	.00	.00	.15	.40	1.00	.60	.15	.05	.00	.00
0.5	0	2.57	10	1.65	.00	.00	.00	.10	.80	1.00	.90	.30	.10	.10	.10
0.5	0	2.57	10	1.70	.00	.00	.10	.40	.80	1.00	1.00	.70	.20	.00	.10
0.5	1	2.57	20	1.57	.00	.00	.05	.05	.55	1.00	.95	.15	.00	.00	.00
0.5	1	2.57	20	1.65	.05	.00	.10	.20	.90	1.00	.90	.60	.30	.00	.00
0.5	3	2.57	20	1.57	.00	.00	.00	.40	.95	1.00	1.00	.55	.33	.25	.00
0.5	3	2.57	10	1.65	.00	.00	.30	.70	1.00	1.00	1.00	.60	.70	.40	.00
0.5	3	2.57	10	1.70	.00	.00	.30	.90	1.00	1.00	1.00	1.00	.80	.70	.00

VISUAL LOBE PROBABILITIES (for P.M.F.)

CONDITIONS					ECCENTRICITIES										
Size	spd	bkgnd	times presented	target illum	-14	-10.5	-7.5	-4	-1.5	0	1.5	4	7.5	10.5	14
1.4	0	4.17	10	3.02	.00	.00	.00	.20	.70	1.00	.90	.10	.10	.20	.00
1.4	3	4.17	10	3.02	.00	.80	.90	.40	1.00	1.00	1.00	.90	.30	.30	.30
0.5	0	4.17	10	3.15	.00	.00	.00	.30	.70	1.00	1.00	.00	.00	.00	.00
0.5	2	4.17	10	3.15	.20	.20	.40	.40	.50	.60	.90	.80	.90	.00	.10
0.5	3	4.17	20	3.15	.05	.50	.40	.55	.65	.75	.80	1.00	.35	.35	.45

TABLE OF VISUAL LOBE PROBABILITIES
(With gradual rise and fall of target illuminance)

TABLE 3.5

Summary of Visual lobe results- in terms of probability of detection of target, for a range of values of target log(retinal illuminance), i.e. a range of contrast levels. Diameters: 0.5^{o} and 1.4^{o}. Subject: PMF

	Relative contrast									
	0.0	0.2	0.4	0.6	0.8	1	1.2	1.4	1.6	1.8	2.0
Prob:	0.019	0.048	0.106	0.202	0.338	0.500	0.662	0.798	0.894	0.952	0.981
s=0.48											

	log(contrast)									
	-0.70	-0.40	-0.22	-0.10	0.0	+0.08	+0.15	+0.20	+0.26	+0.30
Prob:	0.0	0.010	0.096	0.286	0.500	0.679	0.805	0.885	0.933	0.962
s=0.17										

TABLE 3.6

Probability data to fit Blackwell (1946) figure. (s is the standard deviation of the normal curve required to produce the fitted slope to the cumulative curve)

	Eccentricity (degrees)						
	20	13	10.5	7.5	4	1.5	0
0.033^{o} n=6							
log (contrast)	0.917	1.316	1.192	0.703	0.482	0.321	-0.255
Standard Dev.	0.604	0.095	0.144	0.441	0.411	0.293	0.009
0.133^{o} n=4							
log (contrast)	-0.003	-0.123	-0.264	-0.470	-0.711	-0.882	-1.219
standard dev.	0.104	0.095	0.280	0.265	0.091	0.150	0.030
0.5^{o} n=18							
log (contrast)	-0.653	-0.596	-0.657	-0.760	-0.844	-1.003	-1.182
standard dev.	0.135	0.222	0.231	0.181	0.102	0.106	0.123
1.4^{o} n=14							
log (contrast)	-1.063	-0.928	-1.001	-0.985	-1.089	-1.165	-1.319
standard dev.	0.198	0.147	0.196	0.116	0.105	0.083	0.193

TABLE 3.7

Mean log (c) thresholds for target size series. Subject: PMF. Speed 0
(Mean of left and right hemifields, and two background luminances)
standard deviations are population estimates from n values.

	Eccentricity (degrees)					
	20	14	7.5	4	1.5	0
M	0.959	1.24	2.31	3.44	5.25	7.75
$1/M^2$	4.120	2.465	0.710	0.320	0.138	0.0631
log $(1/M^2+K)$	1.560	1.337	0.796	0.450	0.083	-0.255
log $(1/M^2+K)$	0.615	0.392	-0.149	-0.495	-0.862	-1.200

TABLE 3.8

Mean log (c) thresholds for target size series. Predicted from Rovamo's "M"

	Eccentricity (degrees)						
	20	13	10.5	7.5	4	1.5	0
speed=0^{o}/sec							
log (contrast)	-0.639	-0.589	-0.640	-0.725	-0.831	-1.003	-1.151
speed=1^{o}/sec							
log (contrast)	-0.579	-0.632	-0.665	-0.748	-0.892	-1.072	-1.346
speed=3^{o}/sec							
log (contrast)	-0.793	-0.772	-0.841	-0.940	-1.036	-1.180	-1.373

TABLE 3.9

Mean log (c) thresholds for target speed series. Subject: PMF. Diam:0.5
(Mean of left and right hemifields, and two background luminances)

	Eccentricity (degrees)												
	-20	-13	-10.5	-7.5	-4	-1.5	0	1.5	4	7.5	10.5	13	20
Diameter:0.5°. Speed:0°/sec. Subject:PMF Mean of n measurements													
Mn	-0.713	-0.464	-0.637	-0.627	-0.861	-1.013	-1.182	-0.993	-0.827	-0.780	-0.677	-0.710	-0.593
SD	0.134	0.170	0.308	0.218	0.117	0.105	0.138	0.131	0.109	0.173	0.198	0.244	0.156
n	6	7	9	9	9	9	9	9	9	9	9	8	5
Diameter:1.4°. Speed:0°/sec. Subject:PMF Mean of n measurements													
Mn	-1.079	-0.928	-0.919	-0.922	-1.074	-1.175	-1.319	-1.155	-1.105	-1.040	-1.083	-0.928	-1.048
SD	0.301	0.215	0.249	0.124	0.101	0.091	0.208	0.087	0.122	0.093	0.111	0.092	0.162
n	3	6	7	6	7	7	7	7	7	7	7	7	3

TABLE 3.10
Mean log (contrast) thresholds for two levels of background retinal illuminance

	Eccentricity (degrees)										
	-13	-10.5	-7.5	-4	-1.5	0	1.5	4	7.5	10.5	13
Diameter:0.5°. Speed:0°/sec. Subject:PMF Log(contrast)=-1 (-0.97 to -1.02)											
Mn	0.000	0.075	0.050	0.238	0.800	1.000	0.675	0.137	0.130	0.130	0.025
SD	-	0.089	0.053	0.192	0.193	-	0.249	0.119	0.035	0.046	-
n	8	8	8	8	8	8	8	8	8	8	8
Diameter:0.5°. Speed:3°/sec. Subject:PMF Log (contrast)=-1											
Mn	0.000	0.350	0.350	0.675	1.000	1.000	0.975	0.525	0.075	0.000	0.000
SD	-	0.238	0.191	0.171	-	-	0.050	0.150	0.096	-	-
Diameter:1.4°. Speed:0°/sec. Subject:PMF Log(contrast)=-1.2											
Mn	0.067	0.150	0.083	0.200	0.650	0.933	0.483	0.200	0.117	0.017	0.050
SD	0.052	0.138	0.075	0.210	0.217	0.082	0.483	0.200	0.117	0.040	0.084
n	8	8	8	8	8	8	8	8	8	8	8

TABLE 3.11
Visual lobes for two levels of background retinal illuminance

	Eccentricity (degrees)										
	-13	-10.5	-7.5	-4	-1.5	0	1.5	4	7.5	10.5	13
Diameter:0.5°. Speed:0°/sec. Subject:PSB Log (contrast)=-1.03											
Mn	0.074	0.483	0.667	0.817	0.843	0.960	0.733	0.381	0.148	0.017	0.024
SD	0.125	0.397	0.273	0.172	0.150	0.064	0.327	0.300	0.100	0.041	0.058
n	6	6	6	6	6	6	6	6	6	6	6
Diameter:0.5°. Speed:3°/sec. Subject:PSB Log (contrast)=-1.36											
Mn	0.000	0.170	0.633	0.833	0.967	0.800	0.733	0.333	0.063	0.063	0.024
n	3	3	3	3	3	3	3	3	3	3	3

TABLE 3.12
Visual lobes for one levels of background retinal illuminance

	Eccentricity (degrees)												
	-20	-13	-10.5	-7.5	-4	-1.5	0	1.5	4	7.5	10.5	13	20
sigma=0.1 log(contrast)=-0.4													
	0.000	0.001	0.000	0.138	0.942	1.000	1.000	1.000	0.942	0.138	0.000	0.001	0.000
sigma=0.15 log(contrast)=-0.4													
	0.001	0.015	0.013	0.234	0.852	0.993	1.000	0.993	0.852	0.234	0.013	0.015	0.001
sigma=0.2 log(contrast)=-0.4													
	0.008	0.052	0.047	0.293	0.784	0.967	0.999	0.967	0.784	0.293	0.047	0.052	0.008
sigma=0.1 log(contrast)=-0.6													
Mn	0.000	0.000	0.000	0.001	0.334	0.954	1.000	0.954	0.334	0.001	0.000	0.000	0.000
sigma=0.15 log (contrast)=-0.6													
	0.000	0.000	0.000	0.020	0.387	0.869	0.999	0.869	0.387	0.020	0.000	0.000	0.000
sigma=0.2 log(contrast)=-0.6													
	0.000	0.004	0.004	0.061	0.415	0.800	0.988	0.800	0.415	0.061	0.004	0.004	0.000

TABLE 3.13
Predicted probability lobe based on mean right and left threshold data for two luminance levels, for a range of values of sigma. Diameter:0.133°. Speed:0°/sec Subject:PMF.

	Eccentricity (degrees)																				
	-15	-13	-11.5	-10	-8.5	-7	-5.5	-4	-3	-2	-1	0	1	2	3	4	5.5	7	8.5	10	11.5	13	15
speed:0°/sec.																							
	0	0	.024	.048	.215	.191	.167	.262	.548	.952	1	.905	.310	.262	.095	.072	0	.024	0	.024	0	0	0
	-	-	-	-	.120	.173	.141	.229	.355	.116	-	.074	.277	.229	.173	.078	-	-	-	-	-	-	-
speed:3°/sec.																							
	.036	.358	.929	.893	.893	.893	.786	.893	1	1	1	1	1	.893	.893	.786	.571	.250	.107	0	0	.107	0
	.072	.083	.083	.072	.072	.072	.083	.072	-	-	-	-	-	.137	.072	.143	.116	.215	.137	-	-	.137	-

TABLE 3.14
27 point lobe diameter:0.5° log(contrast)=-1 Subject:PMF

	Eccentricity (degrees)			
	-10.000	-4.000	4.000	10.000
rnd first	3.675	3.430	3.255	3.370
cued second	4.125	3.550	3.450	3.456
rnd first	3.725	3.475	3.360	3.385
cued second	4.050	3.588	3.450	3.550
rnd first	3.650	3.370	3.300	3.400
cued second	4.013	3.400	3.345	3.430
rnd first	3.769	3.531	3.431	3.430
cued second	4.200	3.580	3.544	3.513
cued first	3.630	3.430	3.200	3.288
rnd second	3.700	3.400	3.330	3.400
cued first	3.694	3.475	3.330	3.338
rnd second	3.700	3.494	3.450	3.513
cued first	3.675	3.445	3.288	3.438
rnd second	3.875	3.644	3.350	3.513
cued first	3.675	3.388	3.313	3.385
rnd second	3.950	3.513	3.420	3.494
mean	3.819	3.482	3.364	3.431
standard dev	0.188	0.080	0.088	0.072

TABLE 4.3

Effect of attention and fatigue. Target log(retinal illuminance) PMF speed: 0.

	Eccentricity (degrees)			
	-10.000	-4.000	4.000	10.000
rnd first	3.880	3.700	3.550	3.500
cued second	3.860	3.740	3.540	3.600
cued first	3.760	3.600	3.475	3.483
rnd second	3.800	3.680	3.480	3.560
rnd first	4.000	3.740	3.480	3.580
cued second	4.067	3.800	3.400	3.575
cued first	3.720	3.600	3.400	3.500
rnd second	3.880	3.760	3.525	3.625
rnd first	3.800	3.640	3.457	3.500
cued second	4.075	3.600	3.400	3.480
cued first	3.667	3.700	3.480	3.467
rnd second	3.875	3.740	3.625	3.675
rnd first	3.733	3.666	3.500	3.617
cued second	3.940	3.633	3.453	3.583
cued first	3.760	3.600	3.460	3.433
rnd second	3.900	3.725	3.625	3.675
mean	3.857	3.683	3.491	3.553
standard dev	0.120	0.065	0.069	0.075

TABLE 4.4

Effect of attention and fatigue. RMF speed: 0

	Eccentricity (degrees)			
	-10.000	-4.000	4.000	10.000
rnd first	3.700	3.500	3.400	3.275
cued second	3.680	3.700	3.450	3.375
cued first	3.600	3.440	3.380	3.340
rnd second	3.675	3.575	3.375	3.450
rnd first	3.540	3.560	3.340	3.420
cued second	3.625	3.480	3.550	3.450
cued first	3.560	3.420	3.400	3.320
rnd second	3.600	3.570	3.380	3.360
rnd first	3.540	3.400	3.300	3.340
cued second	3.580	3.580	3.475	3.460
cued first	3.560	3.440	3.375	3.160
rnd second	3.680	3.400	3.340	3.325
rnd first	3.640	3.540	3.340	3.340
cued second	4.000	3.580	3.500	3.420
cued first	3.500	3.540	3.300	3.300
rnd second	3.625	3.480	3.350	3.300
mean	3.632	3.513	3.391	3.352
standard dev	0.114	0.082	0.071	0.078

TABLE 4.5

Effect of attention and fatigue. RMF speed: 3

	Eccentricity (degrees)			
	-10.000	-4.000	4.000	10.000
cued first	3.467	3.067	2.960	3.000
rnd second	3.580	3.200	2.925	3.060
rnd first	3.680	3.200	3.040	3.000
cued second	4.100	3.180	3.040	3.000
rnd first	3.550	3.180	3.025	3.040
cued second	4.000	3.100	2.917	3.060
cued first	3.467	2.967	2.940	3.040
rnd second	3.525	3.200	3.025	3.125
rnd first	3.660	3.100	3.075	3.025
cued second	4.067	3.240	3.020	3.150
cued first	3.500	3.060	2.940	3.080
rnd second	3.580	3.180	3.080	3.080
rnd first	3.540	3.217	3.017	3.133
cued second	3.680	3.210	3.060	3.083
cued first	3.500	3.250	3.000	3.083
rnd second	3.650	3.310	3.100	3.167
mean	3.659	3.166	3.010	3.070
standard dev	0.210	0.086	0.058	0.053

TABLE 4.6

Effect of attention and fatigue. JLB speed: 0

Ecc.	slide 4	slide 5	slide 6	slide 7	slide 8	slide 9	slide 10
-43.0	0.000	0.000	0.000	0.000	0.000	0.000	0.000
-31.5	0.000	0.300	0.033	0.066	0.000	0.233	0.433
-21.5	0.210	1.000	0.033	0.866	0.366	0.633	1.000
-17.5	0.000	0.933	0.033	0.900	0.133	0.733	0.966
-14.0	0.050	1.000	0.000	1.000	0.500	0.833	1.000
-10.0	0.600	1.000	0.266	1.000	1.000	1.000	1.000
-7.5	0.860	1.000	0.100	1.000	1.000	1.000	1.000
+4.0	1.000	1.000	1.000	1.000	1.000	1.000	1.000
-1.5	1.000	1.000	1.000	1.000	1.000	1.000	1.000
0	1.000	1.000	1.000	1.000	1.000	1.000	0.983
+1.5	1.000	1.000	1.000	1.000	1.000	1.000	1.000
+4.0	1.000	1.000	0.966	1.000	1.000	1.000	1.000
+7.5	1.000	1.000	0.133	1.000	1.000	0.966	0.666
+10.0	0.694	1.000	0.900	1.000	1.000	1.000	1.000
+14.0	0.210	0.966	0.000	0.966	0.600	0.733	1.000
+17.5	0.033	0.800	0.000	0.666	0.166	0.533	0.966
+21.5	0.050	1.000	0.000	0.900	0.200	0.933	1.000
+31.5	0.000	0.566	0.000	0.166	0.000	0.133	0.400
+43.0	0.000	0.000	0.000	0.000	0.000	0.000	0.000

Ecc.	slide 11	slide 12	slide 14	slide 16	slide 17	slide 18
-43.5	0.000	0.000	0.000	0.000	0.000	0.000
-31.5	0.000	0.000	0.000	0.000	0.000	0.000
-21.5	0.000	0.000	0.000	0.000	0.000	0.000
-17.5	0.000	0.000	0.000	0.050	0.000	0.000
-14.0	0.050	0.000	0.050	0.000	0.000	0.050
-10.0	0.050	0.100	0.100	0.050	0.300	0.000
-7.5	0.000	1.000	0.300	0.100	0.000	0.000
-4.0	1.000	1.000	1.000	1.000	0.950	0.950
-1.5	1.000	1.000	1.000	1.000	1.000	1.000
0	1.000	1.000	1.000	1.000	1.000	1.000
+1.5	1.000	1.000	1.000	1.000	1.000	1.000
+4.0	1.000	1.000	0.950	0.950	1.000	1.000
+7.5	0.000	1.000	0.850	0.400	0.100	0.000
+10.0	0.000	0.400	0.100	0.350	0.650	0.400
+14.0	0.000	0.000	0.000	0.000	0.000	0.000
+17.5	0.000	0.000	0.000	0.000	0.000	0.050
+21.5	0.000	0.000	0.050	0.050	0.050	0.000
+31.5	0.000	0.000	0.050	0.000	0.000	0.000
+43.0	0.000	0.000	0.000	0.000	0.000	0.000

PROBABILITIES OF DETECTION: TRAY 1. 36mm LENS. SUBJECTS NAME; PMF

TABLE 5.3

Probabilities of detection.
Target diameter: 24 minutes of arc. Subject: PMF.

Ecc.	slide 1	slide 2	slide 3	slide 4	slide 5	slide 6	slide 7
-43.5	0.000	0.000	0.000	0.000	0.000	0.000	0.200
-31.5	0.031	0.110	0.410	0.050	0.075	0.000	0.900
-21.5	0.025	0.878	0.964	0.866	0.000	0.000	1.000
-17.5	0.031	0.864	0.807	0.933	0.000	0.000	1.000
-14.0	0.031	1.000	1.000	0.975	0.025	0.050	1.000
-10.0	0.000	1.000	1.000	1.000	0.125	0.050	1.000
-7.5	0.025	0.950	1.000	1.000	0.100	0.000	1.000
-4.0	0.587	1.000	1.000	0.975	1.000	0.100	1.000
-1.5	0.937	1.000	1.000	1.000	1.000	0.800	1.000
0	0.925	1.000	1.000	1.000	0.988	1.000	1.000
+1.5	0.600	1.000	1.000	1.000	1.000	0.950	1.000
+4.0	0.331	1.000	1.000	1.000	0.976	0.350	1.000
+7.5	0.275	1.000	1.000	0.975	0.200	0.050	1.000
+10.0	0.162	1.000	1.000	0.975	0.575	0.050	1.000
+14.0	0.000	0.825	0.964	0.958	0.075	0.000	1.000
+17.5	0.031	0.792	0.717	0.791	0.000	0.000	1.000
+21.5	0.056	1.000	0.864	0.975	0.000	0.000	1.000
+31.5	0.000	0.328	0.278	0.433	0.000	0.000	0.950
+43.5	0.000	0.000	0.000	0.000	0.000	0.000	0.200

Ecc.	slide 8	8 defocus	8 bright adapting field
-43.5	0.000	0.000	0.000
-31.5	0.221	0.100	0.100
-21.5	0.839	1.000	0.700
-17.5	0.781	0.900	0.400
-14.0	0.969	1.000	1.000
-10.0	1.000	1.000	1.000
-7.5	0.969	1.000	0.900
-4.0	1.000	1.000	1.000
-1.5	1.000	1.000	1.000
0	1.000	1.000	1.000
+1.5	1.000	1.000	1.000
+4.0	1.000	1.000	1.000
+7.5	1.000	1.000	1.000
+10.0	1.000	1.000	1.000
+14.0	0.969	1.000	0.700
+17.5	0.969	0.600	0.800
+21.5	1.000	1.000	0.800
+31.5	0.196	0.300	0.000
+43.5	0.030	0.000	0.000

PROBABILITIES OF DETECTION: TRAY 2. 36mm LENS. SUBJECTS NAME; PMF

TABLE 5.4

Probabilities of detection.
Target diameter: 24 minutes of arc. Subject: PMF.
includes lobes showing the effects of defocussing and mismatched background.

Ecc.	slide 4	slide 5	slide 6	slide 7	slide 8	slide 9	slide 10
-29.0	0.000		0.000		0.050	0.000	
-25.5	0.000		0.000		0.000	0.200	
-19.0	0.000		0.000		0.000	0.050	
-14.0	0.200		0.000		0.000	0.500	
-10.0	0.350		0.100		0.750	0.900	
-6.5	0.450		0.000		0.800	1.000	
-4.0	1.000		0.950		1.000	1.000	
-2.5	1.000		0.950		1.000	1.000	
0	1.000		1.000		1.000	1.000	
+2.5	1.000		0.950		1.000	1.000	
+4.0	1.000		0.900		1.000	1.000	
+6.5	0.650		0.000		0.850	0.950	
+10.0	0.650		0.050		0.900	0.950	
+14.0	0.100		0.000		0.100	0.050	
+19.0	0.000		0.000		0.000	0.250	
+25.5	0.000		0.000		0.000	0.100	
+29.0	0.000		0.000		0.000	0.000	

Ecc.	slide 11	slide 12	slide 14	slide 16	slide 17	slide 18
-29.0	0.000	0.000	0.000	0.000	0.000	0.000
-25.5	0.000	0.000	0.000	0.000	0.000	0.000
-19.0	0.000	0.000	0.000	0.050	0.000	0.000
-14.0	0.050	0.000	0.000	0.000	0.000	0.000
-10.0	0.000	0.000	0.000	0.050	0.050	0.050
-6.5	0.000	0.000	0.050	0.050	0.150	0.000
-4.0	1.000	1.000	1.000	0.800	1.000	0.950
-2.5	1.000	1.000	1.000	0.800	0.950	1.000
0	1.000	1.000	1.000	1.000	1.000	1.000
+2.5	1.000	1.000	0.950	0.900	1.000	1.000
+4.0	0.750	0.950	0.700	0.450	0.950	1.000
+6.5	0.000	0.100	0.200	0.050	0.000	0.000
+10.0	0.050	0.000	0.000	0.200	0.300	0.100
+14.0	0.000	0.000	0.000	0.000	0.000	0.000
+19.0	0.000	0.000	0.000	0.000	0.000	0.000
+25.5	0.000	0.000	0.000	0.000	0.000	0.000
+29.0	0.000	0.000	0.000	0.000	0.000	0.000

PROBABILITIES OF DETECTION: TRAY 1. 55mm LENS. SUBJECTS NAME; PMF

Ecc.	slide 1	slide 2	slide 5	slide 7	slide 8
-29.0	0.050	0.250	0.050	0.909	0.000
-25.5	0.000	0.100	0.100	1.000	0.250
-19.0	0.000	0.250	0.000	0.800	0.050
-14.0	0.000	0.650	0.050	1.000	0.850
-10.0	0.050	1.000	0.300	1.000	1.000
-6.5	0.400	1.000	0.400	1.000	0.950
-4.0	0.450	1.000	0.950	1.000	1.000
-2.5	0.500	1.000	1.000	1.000	1.000
0	1.000	1.000	1.000	1.000	1.000
+2.5	0.950	1.000	1.000	1.000	1.000
+4.0	0.400	1.000	0.950	1.000	1.000
+6.5	0.050	1.000	0.100	0.900	1.000
+10.0	0.000	1.000	0.600	1.000	0.950
+14.0	0.050	0.650	0.000	1.000	0.800
+19.0	0.150	0.550	0.000	0.900	0.350
+25.5	0.000	0.350	0.050	0.900	0.200
+29.0	0.000	0.150	0.000	0.900	0.150

PROBABILITIES OF DETECTION: TRAY 2. 55mm LENS SUBJECTS NAME; PMF

TABLE 5.5

Probabilities of detection.
Target diameter: 16 minutes of arc. Subject: PMF.

Ecc.	slide 4	slide 6	slide 8	slide 9	slide 11	slide 12	slide 14
-29.0	0.000	0.000	0.000	0.187	0.000	0.000	0.000
-25.5	0.000	0.000	0.000	0.812	0.000	0.000	0.000
-19.0	0.000	0.000	0.000	0.062	0.000	0.000	0.000
-14.0	0.000	0.062	0.062	0.187	0.000	0.000	0.000
-10.0	0.562	0.062	0.875	1.000	0.000	0.187	0.000
-6.5	0.875	0.125	1.000	1.000	0.937	0.562	0.062
-4.0	1.000	1.000	0.937	1.000	1.000	1.000	1.000
-2.5	1.000	1.000	1.000	1.000	1.000	1.000	1.000
0	1.000	1.000	1.000	1.000	1.000	1.000	1.000
+2.5	1.000	1.000	1.000	1.000	1.000	1.000	0.937
+4.0	1.000	1.000	1.000	1.000	0.937	1.000	0.937
+6.5	0.812	0.062	0.937	0.937	0.562	0.062	0.000
+10.0	1.000	0.062	1.000	0.937	0.000	0.000	0.000
+14.0	0.000	0.000	0.125	0.875	0.000	0.000	0.062
+19.0	0.000	0.000	0.000	0.312	0.000	0.000	0.000
+25.5	0.000	0.000	0.000	0.437	0.000	0.000	0.000
+29.0	0.000	0.000	0.000	0.062	0.000	0.000	0.000

	TRAY 1 WDT		TRAY 2 WDT		TRAY 1 GY	
Ecc.	slide 17	slide 18	slide 1	slide 2	slide 4	Slide 8
-29.0	0.000	0.000	0.000	0.125	0.000	0.000
-25.5	0.000	0.000	0.000	0.812	0.062	0.000
-19.0	0.000	0.000	0.125	0.375	0.000	0.000
-14.0	0.062	0.000	0.000	0.750	0.062	0.125
-10.0	0.437	0.125	0.000	1.000	0.150	0.285
-6.5	0.375	0.500	0.625	1.000	0.250	1.000
-4.0	1.000	0.687	0.812	1.000	0.500	0.875
-2.5	1.000	0.937	1.000	1.000	0.812	1.000
0	0.968	1.000	1.000	1.000	0.787	0.932
+2.5	1.000	1.000	1.000	1.000	1.000	0.642
+4.0	1.000	1.000	1.000	1.000	0.000	0.000
+6.5	0.312	0.000	0.000	1.000	0.000	0.000
+10.0	0.625	0.000	0.062	1.000	0.000	0.000
+14.0	0.000	0.000	0.000	0.875	0.000	0.000
+19.0	0.000	0.000	0.000	0.250	0.000	0.000
+25.5	0.000	0.000	0.000	0.687	0.000	0.000
+29.0	0.000	0.000	0.000	0.187	0.000	0.000

PROBABILITIES OF DETECTION: TRAY 1. 55mm LENS. SUBJECTS NAME; WDT

Slide	Area of lobe
Tray 1	
4	21.419
6	11.805
8	24.058
9	37.185
11	14.871
12	13.073
14	10.713
17	16.743
18	11.717
Tray 2	
1	12.950
2	42.947

SUMMARY OF LOBES

55mm Lens. Subjects name; WDT

TABLE 5.6

Probabilities of detection.
Target diameter: 16 minutes of arc. Subject: WDT.

Ecc.	slide 6	slide 9	slide 1	slide 11	slide 2	slide 17
-29.0	0.062	0.000	0.000	0.000	0.000	0.000
-25.5	0.000	0.062	0.000	0.000	0.000	0.000
-19.0	0.062	0.000	0.000	0.000	0.062	0.000
-14.0	0.125	0.875	0.062	0.062	0.687	0.125
-10.0	0.000	0.437	0.000	0.000	1.000	0.062
-6.5	0.062	0.500	0.000	0.000	1.000	0.125
-4.0	0.750	1.000	0.062	0.500	1.000	0.500
-2.5	1.000	1.000	0.437	0.687	1.000	0.937
0	1.000	1.000	0.968	1.000	1.000	0.968
+2.5	0.750	1.000	0.562	0.750	1.000	0.875
+4.0	0.312	0.937	0.250	0.562	0.937	0.687
+6.5	0.062	0.187	0.187	0.000	1.000	0.125
+10.0	0.000	0.750	0.125	0.000	0.625	0.125
+14.0	0.000	0.000	0.000	0.000	0.000	0.000
+19.0	0.000	0.000	0.062	0.000	0.062	0.062
+25.5	0.000	0.250	0.000	0.000	0.375	0.062
+29.0	0.000	0.000	0.000	0.000	0.250	0.000

PROBABILITIES OF DETECTION: TRAY 1. 55mm LENS. SUBJECTS NAME; PMF Right eye only

TABLE 5.7

Probabilities of detection. Target diameter: 16 minutes of arc. Subject:PMF. Right eye only.

26' diameter Green target, .084 cd/m

Ecc.	Red background, 6.1 cd/m.
-39.0	0.000
-28.5	0.541
-18.5	0.416
-14.0	0.749
-10.0	0.666
-4.5	0.895
-4.0	0.791
-1.5	0.562
0	0.541
+1.5	0.687
+4.0	0.770
+4.5	0.812
+10.0	0.916
+14.0	0.666
+18.5	0.312
+28.5	0.312
+39.0	0.000

PROBABILITIES OF DETECTION:

SUBJECTS NAME; PMF

TABLE 5.8

Probabilities of detection. 26' target designed to enhance rod response.

Standard set of stimuli. Sequence 1.

	-15	-10	-5	+5	+10	+15
Subject: G						
Amplitude	-14.5	-10.3	-5.1	5.9	9.8	11.2
std. dev.	1.4	0.7	0.5	1.6	1.6	2.3
Av. Latency	174	171	207	180	175	201
min. Latency	110	100	100	50	50	80
Subject: J						
Amplitude	-15.7	-10.1	-5.2	5.1	8.2	15.2
std. dev.	2.2	1.9	1.1	1.1	1.9	3.2
Av. Latency	236	216	223	183	139	188
min. Latency	90	90	110	90	80	90
Subject: P						
Amplitude	-18.9	-12.5	-6.9	5.3	10.6	14.4
std. dev.	1.2	1.1	0.8	1.0	0.7	2.2
Av. Latency	183	161	170	201	172	214
min. Latency	110	80	100	140	90	100
					Sequence 2	
Subject: G						
Amplitude	-15.5	-10.2	-4.8	6.5	11.0	12.2
std. dev.	1.0	0.6	0.6	1.5	1.9	2.1
Av. Latency	216	189	191	232	242	264
min. Latency	150	130	140	150	170	180
Subject: J						
Amplitude	-17.2	-10.8	-5.4	4.7	9.1	14.1
std. dev.	1.2	1.0	0.5	0.6	1.1	1.8
Av. Latency	270	266	286	194	255	290
min. Latency	200	130	150	130	170	180
Subject: P						
Amplitude	-18.8	-12.6	-7.3	5.6	11.1	15.6
std. dev.	2.1	1.6	0.8	0.8	1.1	2.5
Av. Latency	262	232	223	240	234	257
min. Latency	180	160	160	160	150	170
					Sequence 3	
Subject: G						
Amplitude	-14.4	-9.5	-4.5	4.5	10.8	13.6
std. dev.	2.2	1.3	1.2	1.8	3.2	3.1
Av. Latency	269	263	305	329	380	410
min. Latency	160	160	160	200	180	200
Subject: J						
Amplitude	-15.4	-8.4	-3.2	3.2	7.5	11.6
std. dev.	1.8	2.4	0.9	1.4	1.9	4.3
Av. Latency	330	335	343	331	362	359
min. latency	230	220	200	160	200	240
Subject: P						
Amplitude	-14.1	-11.4	-6.0	4.5	9.1	12.4
std. dev.	3.4	3.5	1.5	1.1	1.7	2.2
Av. Latency	310	285	275	267	282	303
min. Latency	220	190	190	180	200	200

TABLE 6.7

Summary of saccade amplitudes and latencies. Experiment 1. (6 single 2° stimuli)

Pairs of stimuli 5 degrees apart.					Sequence 1	
	-10 &-5	-10	-5	+5	+10	+5 & +10
Subject: G						
Amplitude	-4.2	-10.8	-5.2	5.9	8.7	6.7
Std. dev.	0.8	1.1	0.9	1.7	2.0	1.7
Av. Latency	206	175	193	191	167	180
min. Latency	170	110	150	100	20	0
Subject: P						
Amplitude	-7.8	-12.4	-7.0	5.1	10.8	5.1
std. dev.	1.2	1.3	1.2	1.2	0.7	0.9
Av. Latency	178	179	185	223	221	211
min. Latency	80	110	140	150	150	170
					Sequence 2	
Subject: G						
Amplitude	-4.3	-11.2	-4.8	5.9	8.8	5.4
std. dev.	0.8	1.1	0.7	1.7	1.6	1.4
Av. Latency	194	186	189	212	229	206
min. Latency	150	140	140	170	170	150
Subject: J						
Amplitude	-7.1	-11.6	-5.4	4.4	9.6	5.6
std. dev.	1.3	0.6	0.6	1.2	2.2	0.9
Av. Latency	239	279	275	250	276	217
min. Latency	140	180	170	130	110	140
Subject: P						
Amplitude	-8.9	-13.2	-7.9	5.2	10.8	4.9
std. dev.	1.4	1.7	0.7	1.2	0.9	1.2
Av. Latency	251	271	254	252	238	252
min. Latency	180	170	180	170	170	180
					Sequence 3	
Subject: G						
Amplitude	-7.5	-9.9	-4.5	5.2	9.3	5.3
std. dev.	4.7	1.3	1.5	1.6	2.1	2.2
Av. Latency	311	264	322	286	324	359
min. Latency	220	160	170	190	180	190
Subject: J						
Amplitude	-6.5	-9.5	-5.0	4.2	10.0	5.7
std. dev.	1.1	1.6	1.6	1.2	2.2	0.9
Av. Latency	208	325	258	252	279	252
min. Latency	160	210	170	160	170	170
Subject: P						
Amplitude	-8.3	-12.5	-7.3	4.5	10.0	5.2
std. dev.	1.5	1.5	1.0	1.4	1.5	1.9
Av. Latency	243	244	251	256	255	268
min. Latency	190	170	160	170	170	160

TABLE 6.8

Summary of saccade amplitudes and latencies. Experiment 2. (Pairs of stimuli, 5^{o} apart)

Rival stimuli in opposite hemifields, presented simultanously

	-10 &+10	+10	-10	Sequence 2 Blank
Subject: G				
Amplitude	-11.3	11.0	-10.7	0.6
std. dev.	0.7	1.9	0.6	2.6
Av. Latency	248	332	255	370
min. Latency	150	200	160	370
Subject: J				
Amplitude	-8.6	9.5	-12.2	-0.1
std. dev.	6.7	2.8	1.2	2.5
Av. Latency	336	325	315	270
min. Latency	240	250	190	-
Subject: P				
Amplitude	-5.5	10.2	-10.8	0.7
std. dev.	10.3	2.2	6.7	2.3
Av. Latency	332	306	286	266
min. Latency	210	150	170	200
				Sequence 3
Subject: G				
Amplitude	-10.8	10.8	-10.7	0
std. dev.	1.0	0.5	1.1	0
Av. Latency	317	452	250	-
min. Latency	170	290	200	-
Subject: P				
Amplitude	-8.7&+8.4	9.8	-11.6	-
std. dev.	2.8 4.8	2.5	4.0	-
Av. Latency	358	307	328	-
min. Latency	180	180	220	-

Summary of differences in latency between left and right hemifield responses for sequence 2

	+ & -5	+ & -10	+ & -15
Subject: G			
Diff. in Av. Latencies Exp.1	41	54	48
Diff. in Av. Latencies Exp.2	23	43	
Diff. in Av. Latencies Exp.3		77	
std. dev. of latencies Exp.1	36/37	35/45	57/55
std. dev. of latencies Exp.2	25/30	31/51	
std. dev. of latencies Exp.3		65/74	
Subject: J			
Diff. in Av. latencies Exp.1	-82	-11	+20
Diff. in Av. latencies Exp.2	-25	-3	
Diff. in Av. latencies Exp.3		+10	
std. dev. of latencies Exp.1	81/47	71/77	39/63
std. dev. of latencies Exp.2	42/82	51/74	
std. dev. of latencies Exp.3		74/73	

TABLE 6.9

Summary of saccade amplitudes and latencies. Experiment 3. (Rival stimuli in both hemifields, presented simultaneously)

Summary of Eye Movement tests on P.C.D on 16th and 17th May 1985.

Stimulus No.	Description	Amplitude(deg.) Mean	S.D.	Latency(ms) Mean	S.D.
1	-15 degrees	-13.8	2.5	352	93
2	-10 degrees	-9.0	1.1	315	43
3	-5 degrees	-5.6	0.8	304	64
4	+5 degrees	+4.5	0.7	295	65
5	+10 degrees	+9.0	0.8	339	68
6	+15 degrees	+13.6	1.2	353	70
2	-10 deg 164cd/m^2	-9.0	1.1	315	43
9	-10 deg 90cd/m^2	-10.0	1.5	307	53
10	-10 deg 62cd/m^2	-9.7	1.7	317	57
11	-10 deg 29cd/m^2	-9.3	1.7	288	55
5	+10 deg 164cd/m^2	+9.0	0.8	339	68
12	+10 deg 90cd/m^2	+8.6	0.9	326	83
13	+10 deg 62cd/m^2	+8.4	0.7	306	55
14	+10 deg 29cd/m^2	+8.7	0.8	342	64
7	2 Stimuli at -10 & -15	-9.4	1.3	302	32
8	2 Stimuli at +10 & +15	+8.7	2.4	315	77
7	2 Stimuli at -5 & -10	-4.4	0.9	272	51
8	2 Stimuli at +5 & +10	+4.0	0.4	297	77

Summary of Eye Movement tests on G.Y. on 1st and 2nd May 1985.

Stimulus No.	Description	Amplitude(deg.) Mean	S.D.	Latency(ms) Mean	S.D.
1	-15 degrees	-12.0	1.9	243	43
2	-10 degrees	-8.1	0.6	229	47
3	-5 degrees	-5.2	0.5	219	45
4	+5 degrees	+5.6	1.2	260	74
5	+10 degrees	+8.5	1.3	258	64
6	+15 degrees	+9.2	1.7	279	75
2	-10 deg 164cd/m^2	-8.1	0.6	229	47
9	-10 deg 90cd/m^2	-8.8	0.9	227	70
10	-10 deg 62cd/m^2	-8.7	0.7	220	40
11	-10 deg 29cd/m^2	-8.5	0.6	220	44
5	+10 deg 164cd/m^2	+8.5	1.3	258	64
12	+10 deg 90cd/m^2	+8.4	0.9	275	79
13	+10 deg 62cd/m^2	+9.0	1.8	278	66
14	+10 deg 29cd/m^2	+9.1	1.6	324	103
7	2 Stimuli at -10 & -15	-8.0	0.7	216	29
8	2 Stimuli at +10 & +15	+8.8	1.9	263	82
7	2 Stimuli at -5 & -10	-4.3	0.5	219	27
8	2 Stimuli at +5 & +10	+5.6	1.0	262	74

TABLE 6.10

Summary of saccade amplitudes and latencies. Experiments 4 and 5. (Stimuli at a range of luminance levels, interspersed with pairs of stimuli, 5^{o} apart)

Statistical summary of all runs in this experiment.

	Eccentricity of stimulus									
	-15°	-10°	-5°	0°	5°	5°	10°	10°	15°	15°
Luminance inc. (cd/m°)	79	26.2	7.4	-	12.2	7.4	41.5	26.2	123	79
Bkgrnd 20.3										
Latency ms	314	285	287	630	482	569	491	511	558	535
Std. Dev.	51	46	34	115	59	95	81	94	73	75
Amplitude $^{\circ}$	-13.8	-9.8	-5.5	3.4	7.4	8.4	9.9	9.4	9.7	103
Std. Dev.	0.9	0.6	1.2	4.4	1.6	1.9	1.2	0.9	2.0	14
Bkgrnd 11.5										
Latency ms	283	259	258	600	485	525	487	483	575	690
Std. Dev.	15	17	12	128	97	139	103	106	115	0
Amplitude $^{\circ}$	-13.6	-10.0	-5.2	4.8	6.2	8.2	10.2	9.6	8.0	100
Std. Dev.	0.7	0.4	0.4	5.2	1.3	0.8	1.6	1.4	2.0	0
Bkgrnd 5.3										
Latency ms	288	258	255	618	384	417	400	416	581	561
Std. Dev.	34	28	21	104	67	104	67	77	115	123
Amplitude $^{\circ}$	-13.9	-9.5	-5.0	2.5	5.5	6.3	9.3	9.3	10.6	113
Std. Dev.	0.7	0.5	0.3	4.0	0.9	1.5	0.9	1.1	0.7	21
Bkgrnd 1.5										
Latency ms	254	236	266	495	286	317	309	320	392	391
Std. Dev.	39	20	53	190	35	85	75	100	149	160
Amplitude $^{\circ}$	-14.3	-9.9	-5.2	2.4	5.0	5.1	9.4	9.2	11.4	105
Std. Dev.	0.9	0.5	0.4	4.7	0.7	0.6	1.3	1.3	2.0	18
Bkgrnds 11.2-1.5 All latencies <350ms										
Latency ms	273	253	254	306	293	296	286	289	278	285
Std. Dev.	31	25	19	12	35	39	40	37	32	40
Amplitude $^{\circ}$	-14.0	-9.7	-5.1	0.4	5.0	5.2	8.9	8.9	10.1	103
Std. Dev.	0.8	0.5	0.4	1.5	0.7	0.7	0.8	1.1	1.7	18

TABLE 6.11

Summary of saccade amplitudes and latencies. Experiment 6. (Stimuli adjusted to produce two levels of scattered light at the fovea, for a range of contrast levels)

contrast threshold data - Motion experiment

Summary of wedge positions at threshold contrast

0.5 degrees/sec		eccentricities		
Displacement	20 degrees	10 degrees	5 degrees	fovea
.1	47	361	628	807
.2	115	426	745	818
.4	171	460	768	956
.5	126	464	762	964
.6	155	486	771	928
.7	166	494	779	928
.8	154	458	818	990
.9	180	516	811	[920]
1.0	202	542	876	[840]
spot luminance	3.6	9.1	10.0	14.1
	15.1	21.3	24.8	28.8

3.0 degrees/sec		eccentricities		
Displacement	20 degrees	10 degrees	5 degrees	fovea
.1	190	353	540	779
.2	230	513	674	846
.3	481	593	723	969
.4	518	616	808	1024
.5	517	717	845	1084
.6	559	696	873	1046
.7	593	767	915	1086
.8	606	770	917	1142
.9	535	793	955	1108
1.0	548	738	918	1114
2.0	648	844	988	1181
spot luminance		9.7		
backgnd luminance		15.5		

20 degrees/sec		eccentricities		
Displacement	20 degrees	10 degrees	5 degrees	fovea
.1	4	4	[243]	[250]
.2	2	38	155	212
.4	38	40	234	234
.6	63	105	286	[420]
.8	64	108	287	356
.9	79	154	262	348
1.0	94	170	348	389
spot luminance	4.35	5.2		
backgnd luminance	9.88	10.61		

TABLE 8.2

Relation of contrast thresholds to target velocity for a range of visual field positions - least squares fitted line. (These figures were used to insert wedge positions for each displacement into look-up tables in the computer program. They have been converted to log(contrast) terms in figure 8.1 for ease of comparision with earlier data.

	Eccentricity (degrees)					
File	-25		-10		0	
	R>L	L>R	R>L	L>R	R>L	L>R
.1	0.095±.03	0.099±.03	0.029±.01	[0.113±.01]	0.015±.00	0.025±.01
.2	0.177±.01	0.080±.01	0.038±.02	0.064±.00	0.018±.00	0.023±.00
.5	0.160±.03	0.139±.01	0.055±.01	0.058±.01	0.036±.00	0.047±.01
1	0.117	0.101±.02	0.065±.01	0.054±.01	0.055±.06	0.067±.01
2	0.153±.02	0.093±.01	0.115±.01	0.079±.01	0.087±.01	0.100±.01
5	0.634±.26	0.409±.12	0.352±.06	0.339±.04	0.383±.08	0.211±.03
10	0.594±.15	0.579±.03	0.662±.06	0.545±.16	0.454±.02	0.377±.01
20	0.860±.22	0.892±.22	0.920±.12	0.811±.14	0.776±.13	0.673±.09
50	1.800±.28	2.715±.54	1.697±.30	1.980±.38	1.708±.48	1.219±.17
99	1.459	1.535	1.603	1.761	1.908	1.219

TABLE 8.3
Displacement threshold (degrees). Subject: PMF Summary

	Eccentricity (degrees)		
File	-25	-10	0
.1	0.097 ±0.025	0.071 ±0.47	0.020 ±0.007
.2	0.109 ±0.087	0.051 ±0.051	0.021 ±0.021
.5	0.150 ±0.150	0.057 ±0.005	0.041 ±0.007
1	0.109 ±0.040	0.060 ±0.060	0.061 ±0.008
2	0.123 ±0.123	0.097 ±0.022	0.094 ±0.094
5	0.522 ±0.522	0.345 ±0.345	0.297 ±0.109
10	0.587 ±0.099	0.604 ±0.126	0.416 ±0.045
20	0.876 ±0.199	0.866 ±0.134	0.725 ±0.725
50	2.258 ±0.632	1.837 ±0.344	1.464 ±0.419
99	1.459		

TABLE 8.4
Displacement threshold (degrees) , combined right to left and left to right. Subject: PMF

	Eccentricity (degrees)		
Speed	-25	-10	0
0.1	0.702	0.252	0.947
0.2	0.747	0.494	0.875
0.2	3.810	0.744	0.944
0.5	0.992	1.078	0.818
1	1.343	1.609	0.961
10	1.027	1.102	1.150
20	1.028	0.962	1.004
20	0.777	0.851	0.822
50	0.950	0.910	1.408

TABLE 8.5
Ratio of (R>L)/(L>R) for runs where foveal ratio is close to unity

	Eccentricity (degrees)						
File	-25		-10		0		
	R>L	L>R	R>L	L>R	R>L	L>R	
.1	-	0.349±.01	0.045±.01	0.080±.01	0.023±.01	0.020±.01	*
.2	1.000 -	0.406±.13	0.092±.06	0.114±.01	0.023±.00	0.035±.00	
.5	0.780±.57	0.177±.05	0.103±.05	0.059±.01	0.079±.03	0.056±.01	
1	0.395±.12	0.097±.01	0.121±.03	0.068±.01	0.085±.02	0.085±.01	
1.5	0.151±.02	0.126±.02	0.110±.01	0.082±.01	0.095±.01	0.103±.01	
2	0.089±.03	0.126±.02	0.106±.01	0.094±.02	0.134±.03	0.110±.01	
3	0.183±.01	0.129±.01	0.119±.01	0.120±.02	0.165±.03	0.163±.01	
5	0.186±.04	0.176±.01	0.193±.01	0.189±.02	0.231±.05	0.183±.03	
10	0.375±.01	0.327±.04	0.221±.25	0.193±.18	0.299±.03	0.298±.05	*

TABLE 8.6
Displacement threshold, Subject:PMF 12/8/86 Summary
* These estimates of Standard Deviation obtained from Mean Displacement*(1-exp(LSD), where exp(LSD) is the figure quoted in the raw data as Standard Deviation.

	Eccentricity (degrees)					
speed	-25		-10		0	
	R>L	L>R	R>L	L>R	R>L	L>R
.2	-	0.253±.09	0.497±.11	0.069±.01	0.064±.02	0.055±.01
.5	1.014±.24	0.313±.11	0.255-	0.091±.03	0.215±.12	0.102±.02
1	0.360±.01	0.108±.03	0.191±.05	0.101±.02	0.129±.05	0.093±.02
1.5	0.107±.02	0.155±.02	0.145±.00	0.091±.02	0.120±.02	0.122±.02
2	0.140±.03	0.168±.02	0.235±.05	0.113±.02	0.164±.03	0.124±.01
3	0.143±.04	0.160±.03	0.171±.00	0.131±.00	0.166±.05	0.151±.08
5	0.302±.22	0.268±.01	0.397±.10	0.187±.09	0.308±.14	0.210±.03
10	0.443	0.443	0.337	[0.163]	0.193	0.288
5	1.419±.03	0.374±.13	0.736±.23	0.412±.02	0.678±.25	0.373±.07
10	0.787±.08	0.553±.06	0.864±.12	0.430±.07	0.628±.09	0.468±.05
20	0.979±.04	0.535±.01	1.139±.16	0.536±.02	0.785±.17	0.672±.05
50	1.501±.20	1.471±.12	1.628±.18	0.956±.28	0.994±.32	1.210±.21

TABLE 8.7
Displacement Threshold Subject:PAF Summary.

	Eccentricity (degrees)		
speed	-25	-10	0
SPD.2A1		6.07	0.89
SPD.2A2		10.96	1.18
SPD1A3	4.88	1.33	0.90
SPD1.5A2	0.873	1.6	0.943
SPD2A3	.804	1.944	1.029
SPD3A1'	.972	1.295	0.990
SPD5A2	1.080	2.492	1.099
SPD10A2	1.629	1.963	1.100
SPD20A2	1.862	2.065	0.939
SPD50A1	1.088	1.395	0.940

TABLE 8.8
Displacement threshold (degrees). Subject PAF. R>L/L>R for runs where foveal ratio is in range .8 to 1.2

	Eccentricity				
Speed	-20	-10	-5	0	+5
0.1	1.257	0.669	0.156	0.040	0.077
0.2	1.860	0.132	0.043	0.034	0.048
0.5	0.043	0.068	0.050	0.044	0.047
1.0	0.128	0.082	0.052	0.072	0.037
1.5	0.120	0.075	0.057	0.083	0.062
2	0.179	0.117	0.077	0.101	0.072
3	0.216	0.109	0.103	0.114	0.074
4	0.158	0.164	0.127	0.133	0.082

TABLE 8.9
Displacement threshold (degrees). Slow speed range. PMF

	Eccentricity				
Speed	-20	-10	-5	0	+5
0.05	-	-	0.093	0.129	0.604
0.1	-	-	0.140	0.031	0.119
0.2	-	-	0.043	0.026	0.044
0.5	-	-	0.065	0.039	0.042
1.0	0.283	0.127	0.066	0.062	0.075
1.5	0.259	0.150	0.103	0.079	0.085
2	0.238	0.157	0.086	0.081	0.087
3	0.308	0.248	0.118	0.097	0.098
4	0.284	0.216	0.139	0.119	0.108

TABLE 8.10
Displacement threshold (degrees). Slow speed range. JLB

	Eccentricity (degrees)				
Speed	-20	-10	-5	0	+5
0.05	-	-	1.815	0.093	0.489
0.1	-	1.975	0.157	0.043	0.138
0.2	-	0.147	0.055	0.043	0.050
0.5	0.197	0.095	0.060	0.044	0.061
1.0	0.144	0.088	0.076	0.053	0.051
1.5	0.174	0.099	0.071	0.043	0.067
2	0.203	0.121	0.080	0.059	0.067
3	0.228	0.112	0.089	0.068	0.086
4	0.304	0.191	0.110	0.063	0.107

TABLE 8.11
Displacement threshold (degrees). Slow speed range. AG

	Eccentricity (degrees)				
Speed	-20	-10	-5	0	+5
0.05	0.475	0.401	1.375	0.417	0.217
0.1	1.928	0.163	0.060	0.025	0.095
0.2	0.363	0.066	0.051	0.025	0.033
0.5	0.096	0.075	0.045	0.033	0.044
1.0	0.102	0.086	0.056	0.049	0.059
2	0.222	0.133	0.096	0.085	0.106
5	0.347	0.321	0.276	0.228	0.277

TABLE 8.12
Displacement threshold (degrees). Slow speed range. HP

File	Eccentricity (degrees) -25		-10		0	
	R>L	L>R	R>L	L>R	R>L	L>R
+.1					94.24	63.22
+.2			96.74	65.82	83.15	57.33
+.5	91.01	69.57	81.15	60.06	59.09	32.07
+1	78.51	43.44	75.48	64.66	55.33	64.81
+2	39.83	29.19	51.06	51.71	63.70	35.51
+5	54.83	65.39	83.56	92.41	84.11	79.59
+10	58.57	64.37	75.80	64.24	74.27	69.08
+20	42.87	69.81	64.81	69.09	85.65	53.38
+50	69.75	100.00	73.33	96.12	95.69	82.87
-.1					50.68	18.24
-.2			61.93	35.33	43.87	36.13
-.5	21.87	37.48	22.09	48.63	49.46	49.24
-1	40.18	38.74	41.69	38.30	51.44	40.04
-2	31.29	32.64	24.20	35.29	30.40	30.85
-5	47.64	60.50	48.83	61.04	55.54	60.95
-10	60.59	81.72	62.67	78.78	55.15	65.78
-20	63.26	59.94	55.03	54.59	50.65	51.37
-50	75.18	86.12	88.50	71.46	80.24	89.85

TABLE 8.13
Velocity discrimination (percentage). Summary. Subject: MK

speed	Eccentricity (degrees) -25	-10	0
+.1	100	100	78.73 ± 21.93
+.2	100	81.28 ± 21.86	70.24 ± 18.26
+.5	80.29 ± 18.76	70.61 ± 21.56	45.58 ± 19.11
+1	58.59 ± 25.97	70.07 ± 11.65	60.07 ± 28.96
+2	34.51 ± 14.15	51.38 ± 27.70	49.61 ± 20.31
+5	60.11 ± 14.90	87.98 ± 7.20	81.85 ± 11.99
+10	61.47 ± 17.80	70.02 ± 17.50	76.68 ± 18.45
+20	56.34 ± 26.40	66.96 ± 22.92	69.52 ± 22.22
+50	69.75	84.73 ± 16.11	89.28 ± 9.07
-.1	100	100	34.46 ± 22.94
-.2	100	48.63 ± 25.35	40.00 ± 11.77
-.5	29.67 ± 12.34	35.36 ± 16.63	49.35 ± 3.72
-1	40.92 ± 6.62	40.00 ± 15.80	45.74 ± 11.65
-2	31.97 ± 9.01	29.75 ± 9.41	30.63 ± 13.07
-5	54.07 ± 15.04	55.96 ± 16.38	58.25 ± 7.82
-10	71.15 ± 13.15	70.72 ± 11.18	60.47 ± 16.50
-20	61.57 ± 13.90	54.81 ± 13.01	51.01 ± 7.82
-50	80.65 ± 8.98	79.98 ± 18.46	85.04 ± 9.20

TABLE 8.14
Velocity Discrimination (percentage). M.K. Summary combining left and right motion

File	Eccentricity (degrees) -25		-10		0	
	R>L	L>R	R>L	L>R	R>L	L>R
+.1					56.70	65.96
+.2			76.49	60.68	43.54	33.56
+.5	72.92	54.53	55.47	33.87	23.11	39.33
+1	35.32	40.65	56.15	38.22	25.64	36.14
+2	49.54	43.91	50.58	57.57	27.46	34.58
+5	35.25	33.61	42.27	35.18	36.60	38.56
+10	57.56	44.57	50.55	38.17	56.64	39.73
+20	44.88	73.53	66.43	75.88	30.34	48.02
+50	76.88	98.37	76.29	98.15	45.83	78.84
-.1					66.47	30.37
-.2			48.64	54.23	49.72	44.20
-.5	37.27	45.73	42.52	34.00	53.86	43.16
-1	41.38	33.47	45.61	28.14	40.16	38.34
-2	44.66	26.57	36.86	33.51	31.66	31.83
-5	29.18	58.80	35.86	55.95	26.55	47.67
-10	43.37	34.43	38.80	33.04	42.90	36.94
-20	46.46	49.14	43.61	33.65	50.61	45.68
-50	62.61	58.82	60.83	38.83	59.98	41.80

TABLE 8.15
Velocity discrimination (percentage). Summary. Subject: PMF

File	Eccentricity (degrees) -25		-10		0	
	R>L	L>R	R>L	L>R	R>L	L>R
.1					61.58±12	48.17±21
.2			62.56±22	57.45±20	46.63±47	38.88±9
.5	55.10±23	50.13±14	48.99±15	33.94±9	38.49±18	41.24±7
1	38.35±6	37.06±5	50.92±10	33.18±7	32.90±9	37.24±7
2	47.10±11	35.24±11	43.72±11	45.54±14	29.56±9	33.21±7
5	32.22±12	45.70±19	39.07±9	45.57±12	31.58±17	43.11±12
10	50.47±12	39.50±22	44.67±9	35.61±12	49.77±12	38.34±5
20	45.67±4	61.33±20	55.02±16	54.76±25	40.47±13	46.85±8
50	69.75±17	78.59±22	68.56±14	68.49±33	52.91±9	60.32±23

TABLE 8.16
Velocity discrimination (percentage). Increases and decreases combined. Subject PMF

speed	Eccentricity (degrees) -25	-10	0
.2		1.19	0.998
		0.80	1.03
.5	1.96	1.10	1.04
1	1.27	1.56	1.06
2	0.95	0.80	1.00
	0.96	0.77	1.00
	1.32	0.97	1.03
10	2.17	1.84	0.95
	1.19	1.50	1.00
20	0.85	1.07	1.02
	1.16	1.32	1.04
	0.86	1.17	1.07

TABLE 8.17
Ratio of (R>L)/(L>R) for runs where foveal ratio is close to unity PMF

	Eccentricity (degrees)		
Speed	-25	-10	0
+.1	-	-	61.33
-.1	-	-	48.42
+.2	-	68.58	38.55
-.2	-	51.43	46.96
+.5	63.73	44.67	31.22
-.5	41.50	38.26	48.51
+1	37.99	47.19	30.89
-1	37.43	36.88	39.25
+2	46.72	54.08	31.02
-2	35.62	35.19	31.75
+5	34.43	38.73	37.58
-5	43.99	45.91	37.11
+10	51.07	44.36	48.19
-10	38.90	35.92	39.92
+20	59.21	71.16	39.18
-20	47.80	38.63	48.15
+50	87.63	87.22	62.34
-50	60.72	49.83	50.89

TABLE 8.18
Velocity discrimination (percentage). Right to left and left to right combined. Subject: PMF.

0.1	-	-	1.27
0.2	-	1.33	1.10
0.5	1.54	1.17	0.64
1	1.01	1.28	0.79
2	1.31	1.54	0.98
5	0.78	0.84	1.01
10	1.31	1.23	1.21
20	1.24	1.84	0.81
50	1.44	1.75	1.22

TABLE 8.19
Velocity discrimination. Ratio of increases/decreases. Subject: PMF.

	Eccentricity (degrees)		
speed	-25	-10	0
21	-	-	54.88
0.2	-	60.01	42.76
0.5	52.62	41.47	39.87
1	37.71	42.04	35.07
2	41.17	44.64	31.39
5	39.21	42.32	37.35
10	44.99	40.14	44.06
20	53.51	54.90	43.67
50	74.18	68.53	56.62

TABLE 8.20
Velocity discrimination. (percentage). Mean thresholds for each velocity. Subject: PMF

	Eccentricity (degrees)					
speed	-25		-10		0	
	R>L	L>R	R>L	L>R	R>L	L>R
+.2			100	79.60	61.68	58.75
+.5	98.14	53.79	64.82	34.45	57.97	57.31
+1	90.02	65.96	51.67	46.93	55.44	82.73
+2	44.19	86.87	57.92	82.53	49.20	378.17
+5	61.00	44.10	45.63	49.02	57.24	33.93
+10	66.49	97.74	72.75	71.65	70.40	62.81
+20	53.61	56.95	56.35	52.48	62.41	38.89
+50	100	100	100	100	100	100
-.2			57.81	14.40	45.40	37.25
-.5	71.47	46.80	31.82	38.94	61.98	55.11
-1	32.62	65.50	35.53	29.52	41.82	21.90
-2	36.91	44.05	21.46	24.29	33.24	19.05
-5	26.18	42.42	37.32	40.42	35.18	36.02
-10	30.38	57.96	38.56	71.35	16.72	36.84
-20	64.15	60.75	40.92	64.20	57.17	49.98
-50	56.18	75.91	68.33	30.22	39.30	64.03

TABLE 8.21
Velocity Discrimination (percentage). PAF Summary

	Eccentricity (degrees)		
speed	-25	-10	0
+.2	100	89.80	60.21
+.5	75.97	49.64	57.64
+1	64.95	49.30	69.09
+2	64.95	70.22	63.68
+5	52.55	47.33	49.92
+10	82.12	72.20	66.61
+20	55.28	54.42	50.65
+50	100	100	100
-.2	100	36.11	41.33
-.5	59.13	35.38	58.55
-1	49.06	32.52	31.86
-2	40.48	22.87	26.14
-5	34.30	38.87	35.60
-10	44.17	54.96	26.78
-20	62.45	52.56	53.58
-50	66.04	49.27	51.66

TABLE 8.22
Velocity Discrimination (percentage). Summary combining left and right motion. Subject: PAF.

	Eccentricity (degrees)					
speed	-25/-30		-10		0	
	R>L	L>R	R>L	L>R	R>L	L>R
+.2	98.6±2	74.6±42	80.7±22	54.3±30	34.4±7	36.7±16
+.5	67.5±35	46.1±14	57.3±5	50.1±12	27.7±5	25.9±5
+1	74.5±33	32.4±15	53.7±19	50.9±13	33.0±13	27.0±5
+2	73.4±38	29.0±16	46.7±16	43.6±22	43.2±11	18.4±5
+5	53.5±18	35.2±9	49.1±16	32.8±15	26.6±12	23.8±13
+10	48.9±17	47.0±9	74.1±12	49.0±14	33.5±15	37.1±11
+20	62.4±14	75.9±12	75.7±17	78.5±9	39.0±17	36.1±22
+30	67.0±17	95.7±8	67.5±20	93.4±9	55.2±31	47.3±7
-.2	99.6±1	100	78.3±13	84.6±24	34.1±9	30.0±4
-.5	74.6±21	50.8±35	20.6±8	22.6±4	32.3±4	41.3±2
-1	37.9±12	31.2±31	29.5±8	20.2±7	33.9±4	38.3±3
-2	29.8±11	32.0±13	25.2±11	22.3±8	27.2±9	33.8±9
-5	48.2±14	19.5±4	42.3±15	30.9±4	32.1±5	35.9±1
-10	52.5±6	27.6±12	40.0±12	32.2±6	35.4±5	39.6±8
-20	45.4±2	32.5±7	39.2±5	28.9±8	53.5±6	46.5±2
-30	53.3±2	43.1±14	52.1±4	40.3±5	58.3±7	51.3±3

TABLE 8.23

Velocity Discrimination (percentage). Subject: PMF 21/4/86 Summary

	Eccentricity (degrees)					
speed	-25		-10		0	
	R>L	L>R	R>L	L>R	R>L	L>R
.2	99.0	82.2	79.5±16	69.4±29	34.3±8	33.4±11
.5	69.0	47.4	39.0±20	36.3±17	30.2±5	33.6±9
1	50.4	38.5	43.4±20	37.8±19	33.4±10	32.1±7
2	44.5	31.0	35.1±17	32.1±19	34.6±12	26.7±11
5	50.8±15	27.4±11	45.7±15	31.9±10	29.4±8	29.8±11
10	50.0±13	33.4±12	54.9±23	41.4±15	31.8±8	36.2±7
20	53.9±13	54.2±25	57.4±23	53.7±28	46.2±14	41.3±15
30	61.1±14	73.1±30	61.0±17	70.6±29	50.8±17	49.0±6

TABLE 8.24

Velocity discrimination (percentage). Increases and decreases combined. Subject:PMF

APPENDIX 2

INTERFACE CIRCUIT DIAGRAMS

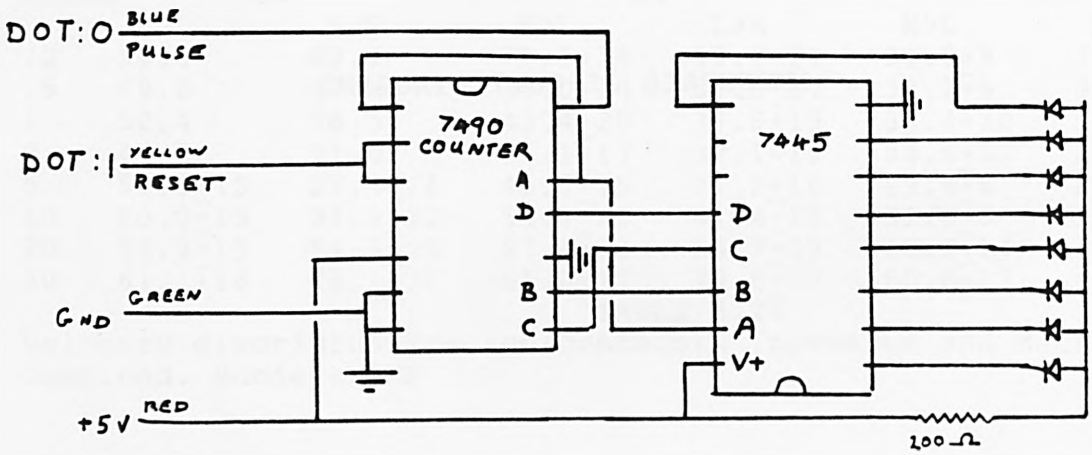

DRIVER FOR LIGHT EMMITTING DIODES

A train of TTL pulses is transmitted by the computer, and counted by the 7490 IC. The BCD output of the counter is used to set a multiplexer so that only one LED has a low resistance path to ground. The small amount of power required for the two IC's is drawn from the computer. If all LED's are to be turned off, a train of 9 pulses is sent.

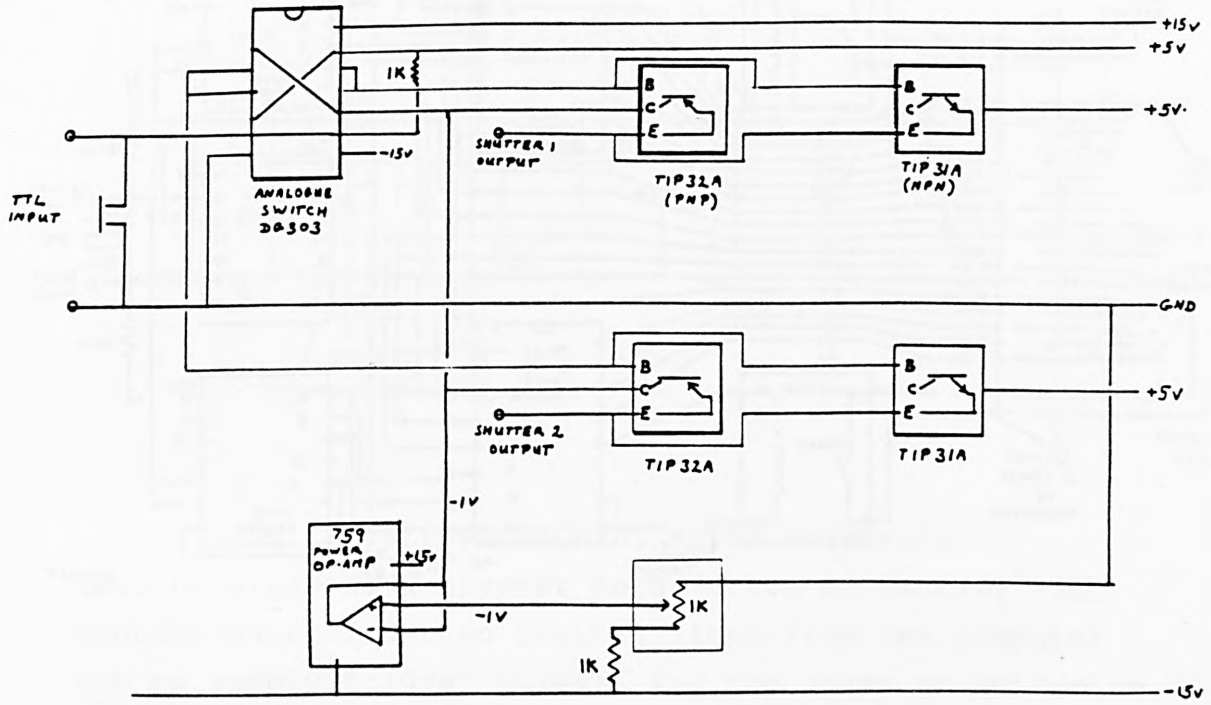

DUAL SHUTTER DRIVE

The shutter pen motor requires +5v to open and -1v to close. The power supply available can provide +5v and ±15v, so the -15v line was used (via a power op-amp) to provide the -1v.

The TTL signal from the computer was used directly to trigger the dual analogue switch, which in turn switched on the appropriate pair of power transistors. Thus in either state one shutter is open and the other closed, and the current load is kept constant, and within the capacity of the supply.

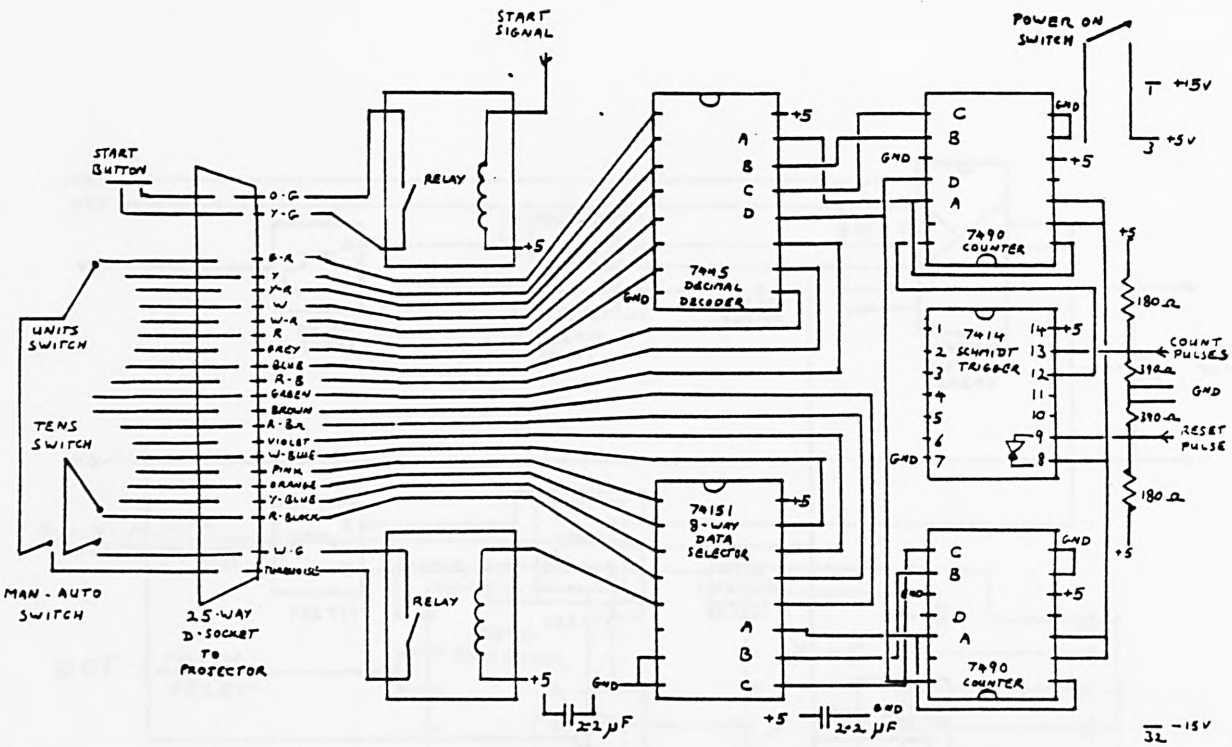

CAROUSEL PROJECTOR INTERFACE

The projector has a "units" switch and a "tens" switch. When a circuit is completed through both via the external 25-way lead, the tray rotation motor stops. The interface allows the circuit to be completed via the two thumbwheel switches (in the manual position), or via the multiplexers (in the auto position). The tray rotation may be started manually via the start button, or by a digital TTL signal from line 'C'.

Line 'B' resets the counters and line 'A' provides a train of pulses corresponding to the slide position required. The maximum number of slides that can be handled is 79.

The Schmidt trigger is necessary to condition the TTL signal from the computer so as to avoid spurious counts due to electrical noise. The relays serve to isolate the computer and counting circuit from the projector.

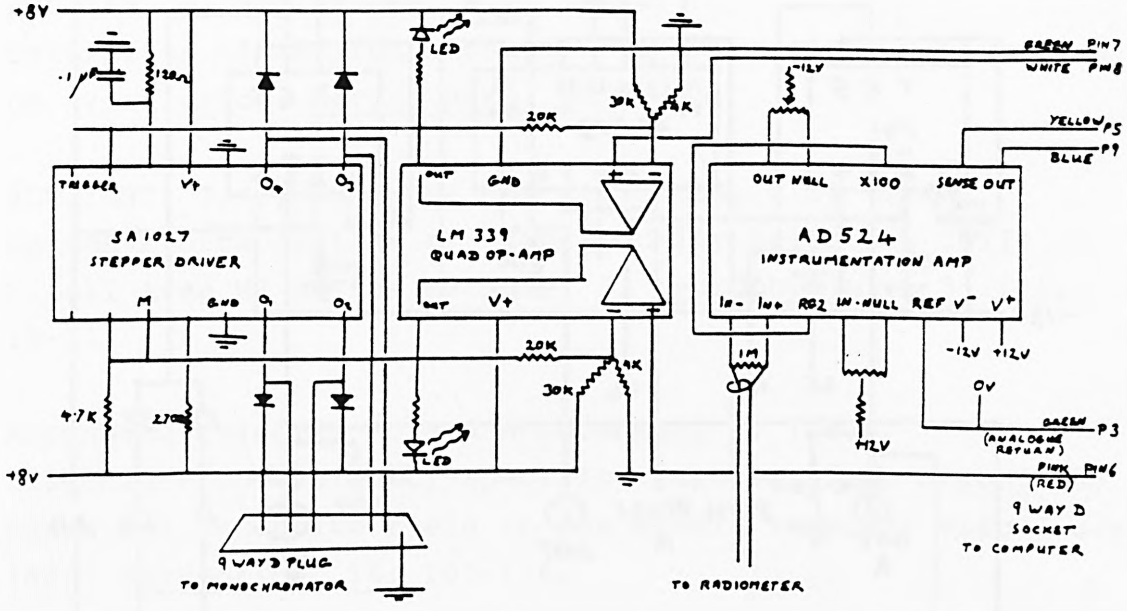

TELESPECTRORADIOMETER INTERFACE

This consists of a stepper motor drive to control the monochromator from two digital lines from the computer - one to supply trigger pulses, and the other to determine direction of rotation - and an amplifier to convert the 100 ma signal from the radiometer to a 10v signal suitable for the analogue input to the Macsym 150.

The TTL outputs from the computer have to be fed to the stepper drive IC via operational amplifiers , which also provide current for the indicating LED´s. The interface unit also includes an encapsulated power supply for the amplifier, and simple DC supply for the stepper motor.

The yellow and blue leads to the computer are connected at the computer end of the lead only, in order to sense the output voltage of the amplifier and correct for any losses in the rather long cable.

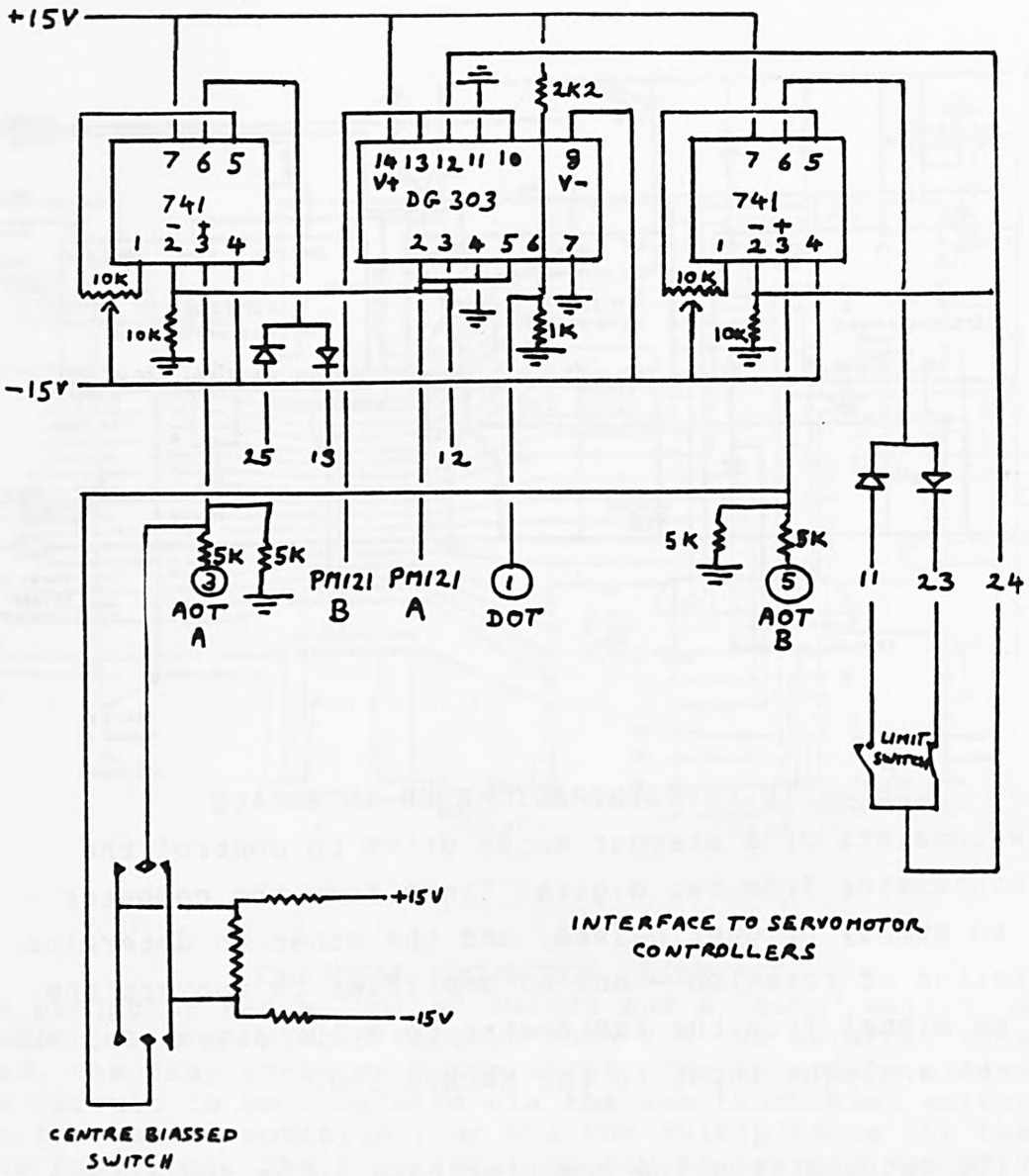

INTERFACE TO SERVO CONTROLLERS (PM121) FOR MIRROR CONTROL
Op-amps are provided to isolate the computer from the controllers, and limit switches are arranged so that when one is opened the motor can only be driven away from the limit. A digital line is provided to hold the signal to the servo controllers at ground, to avoid any possibility of creep of the motors. Both motors are stopped or enabled by the same digital signal.

REFERENCES AND BIBLIOGRAPHY

ABEL, L.A., TROOST, B.T., and DEL'OSSO, L.F. (1983)
The effects of age on normal saccadic characteristics and their variability. Vision Res., 23: 33-37.

AGUILAR, M. and STILES, W.S. (1954)
Saturation of the rod mechanism of the retina at high levels of stimulation. Optica Acta, 1: 59-65.

ALBRIGHT, T.D., DESIMONE, R. and GROSS, C.G. (1984)
Columnar Organisation of Directionally Selective Cells in Visual Area MT of the Macaque. J. Neurophysiol., 51 (1): 16-31.

ALLMAN, J. MIEZIN, F. and MCGUINNESS, E. (1985)
Direction- and velocity-specific responses from beyond the classical receptive field in the middle temporal visual area (MT). Perception, 14: 105-126.

ALPERN, M. and CAMPBELL,F.W. (1962)
The spectral sensitivity of the consensual light reflex. J. Physiol. Lond., 165: 478-507.

ALPERN, M., OHBA, N. and BIRNDORF, L. (1974)
Can the response of the iris to light be used to break the code of the second cranial nerve? In Pupillary dynamics and behaviour. Ed. Janisse, M.P. (New York: Plenum Press).

ANDERSON, S.J. and BURR, D.C. (1985)
Spatial and temporal selectivity of the human motion detection system. Vision Res, 25 (8): 1147-1154.

ANON. (1975)
First Interprofessional Standard for Visual Field Testing. (U.S.A.: National Academy of Sciences).

AULHORN, and HARMS, (1972)
Visual Perimetry. In Handbook of Sensory Physiology, VII/4: Visual Psychophysics. Ed. Jameson, D. and Hurvich, L.M. (Berlin: Springer-Verlag).

BAHILL, T.A., ADLER, D. and STARK, L. (1973)
Most naturally occurring human saccades have magnitudes of 15 degrees or less. Invest. Ophth., 14 (6): 468-469.

BAKER JR, C.L. and BRADDICK, O.J. (1985)
Eccentricity-dependent scaling of the limits for short-range apparent motion perception. Vision Res., 25 (6): 803-812.

BALL, K. and SEKULER, R. (1980)
Human vision favours centrifugal motion. Perception, 9:317-325.

BALL, K. and SEKULER, R. (1981)
Cues reduce direction uncertainty and enhance motion detection. Perception and Psychophysics 30 (2):119-128.

BARBUR, J.L., RUDDOCK, K.H. and WATERFIELD, V.A. (1980)
Human visual responses in the absence of the geniculo-calcarine projection. Brain, 103:905-928.

BARBUR, J.L. (1985)
Speed discrimination and its relation to involuntary eye movements in human vision. Neuroscience Letters, 54:7-12.

BARBUR, J.L., FINDLAY,J.M. and FORSYTH,P.M. (1985)
Pattern of saccadic eye movement responses associated with mid-brain projections in human vision. Proc. Physiol. Soc. 14-15 June 1985 J. Physiol., 367:38p

BARBUR,J.L. and FORSYTH, P.M. (1986)
Can the pupil response be used as a measure of the visual input associated with the geniculostriate pathway. Clin. Vision Sci., 1 (1): 107-111.

BARBUR, J.L., DUNN, G.M. and WILSON, J.A. (1986)
The perception of moving comets at high retinal illuminance levels: a rod cone interaction effect.
Biological Cybernetics: (in press)

BARBUR,J.L., THOMSON, W.D. and FORSYTH,P.M. (1987)
A new system for the simultaneous measurement of pupil size and two-dimensional eye movements.
(Submitted to: Clin. Vis. Res.).

BARLOW, H.B. (1972)
Dark and Light adaptation: Psychophysics. In: Handbook of Sensory Physiology, Vol VII/4 Springer, Berlin.

BARLOW, H.B. and LEVICK, W.R. (1965)
The mechanism of directionally sensitive units in Rabbit's retina. J. Physiol., 178: 477-504.

BARTLESON, C.J. (1978)
Comparison of chromatic-adaptation transforms.
Color Research and Application, 3 (3): 1

BARTLESON, C.J. (1979)
Predicting corresponding colors with changes in adaptation.
Color Research and Application, 4 (3):143-155.

BECKER, W. and JURGENS, R. (1979)
An analysis of the saccadic system by means of double step stimuli. Vision Res. 19: 967-983.

BERNOTAS, V. (1979)
Measurement and calculation of color contrasts.
Sov. J. Opt. Technol., 46 (9): 565-566.

BEVERLEY, K.I. and REGAN, D. (1973)
Evidence for the existence of neural mechanisms selectively sensitive to the direction of movement in space.
J. Physiol., 235: 17-29.

BLACKWELL, H.R. (1946)
Contrast Thresholds of the Human Eye. J. Opt. Soc. Am., 36 (11): 624-643.

BLACKWELL, H.R. (1963)
Neural Theories of Simple Visual Discrimination.
J. Opt. Soc. Am., 53 (1): 129-160.

BLYTHE, I.M., BROMLEY, J.M., KENNARD, C., and RUDDOCK, K.H. (1986).
Visual discrimination of target displacement remains after damage to the striate cortex in humans. Nature, 320: 619-621.

BOCH, R., FISCHER, B. and RAMSPERGER, E. (1984)
Express-saccades of the monkey: reaction-times versus intensity, size, duration and eccentricity of their targets. Exp. Brain Research, 55: 223-231.

BOULTON, J.C. (1986)
Two mechanisms for the detection of motion. Paper presented at the Ninth European Conference on Visual Perception.

BOYNTON, R.M. and CLARKE, F.J.J. (1964)
Sources of entopic scatter in the human eye.
J. Opt. Soc. Am., 54 (1): 110-119.

BOYNTON, R.M. (1983)
A system of photometry based on cone exitations.Presented at C.I.E., 20th Session, B1/1-B1/6.

BRADDICK,O. (1974)
A short-range process in apparent motion. Vision Res., 14: 519-527.

BRINDLEY, G.S., GAUTIER-SMITH, P.C. and LEWIN, W. (1969)
Cortical blindness and functions of non-geniculate fibres of optic tracts. Journal of Neurology, Neurosurgery and Psychiatry, 32: 259-264.

BROGAN, D. (1987)
Effect of noise and background structure on visual lobe and visual search. (submitted to: Ophthal. Physiol. Opt.).

BROWN, P.K. and WALD, G. (1963)
Visual pigments in Human and Monkey retinas. Nature, 200 (4901): 37-43.

BUCHSBAUM, G. (1981)
The retina as a two-dimensional array in the context of colour vision theories and signal detection theory. Proc. I.E.E.E., 69 (7):772-785.

BUCHSBAUM, G. and GOTTSCHALK, A. (1983)
Trichromacy, opponent colours coding and optimum colour information transmission in the retina. Proc. Roy. Soc. London B, 220:89-113.

BUCKINGHAM, T. and WHITAKER, D. (1985)
The influence of luminance on displacement thresholds for continuous oscillatory movement. Vision Res., 25 (11): 1675-1677.

BUCKINGHAM, T. and WHITAKER, D. (1986)
Movement displacement thresholds: a clinical use? Paper presented at the Ninth European Conference on Visual Perception.

BURR, D. (1980)
Motion smear. Nature, 284 (13): 164-165.

BURTON, G,J. (1981)
Contrast Discrimination by the Human Visual System. Biol. Cybern., 40: 27-38.

CAJAL, S.R. (1893)
The Vertebrate Retina. (Tr. Rodieck, R.W., in The Vertebrate Retina. (1973). (San Francisco: W.H.Freeman and Co.)

CAMPION, J., LATTO, R. and SMITH, Y.M. (1983)
Is blindsight an effect of scattered light, spared cortex, and near threshold vision?
Behavioural and Brain Sciences, 6 (3)

CAVANAGH, P., TYLER,C.W. and FAVREAU, O.E. (1984)
Perceived velocity of moving chromatic gratings.
J. Opt. Soc. Am. A, 1 (8): 893-899.

CAVANAGH, P., BOEGLIN, J. and FAVREAU, O.E. (1985)
Perception of motion in equiluminous kinetograms.
Perception, 14: 151-162.

CLARE, J.N. and SINCLAIR, M.A. (1979)
Search and the Human Observer. (London: Taylor & Francis Ltd).

CLARKE, F.J.J. (1960)
A study of Troxler's Effect. Optica Acta, 7:219-236.

COHN, T.E., THIBOS, L.N. and KLEINSTEIN, R.N. (1974)
Detectability of a luminance increment.
J. Opt. Soc. Am., 64 (10): 1321-1327.

COHN, T.E. and LASLEY, D.J. (1974)
Detectability of a luminance increment: Effect of uncertainty. J. Opt. Soc. Am., 64 (12): 1715-1719.

COHN, T.E. (1981)
Absolute threshold: analysis in terms of uncertainty.
J. Opt. Soc. Am., 71 (6):783-785.

COHN, T.E. and WARDLAW, J.C. (1984)
Effect of large spatial uncertainty on foveal luminance increment detectability. J. Opt. Soc. Am. A, 2: 6820

COOKE, K.J. and BELL, J.B. (1980)
Study of modelling and assessment techniques for ATGW.
Report no. BT 10420 of the British Aerospace Dynamics Group, April 1980.

CRAWFORD, B.H. (1936)
The dependence of pupil size upon external light stimulus under static and variable conditions.
Proc. R. Soc. Lond. B., 121: 376-395.

DAVIS, E.T., KRAMER, P. and GRAHAM, N. (1983)
Uncertainty about spatial frequency, spatial position or contrast of visual patterns.
Perception and Psychophysics 33 (1): 20-28.

DEMOTT, D.W. and BOYNTON, R.M. (1958)
Retinal distribution of entopic stray light.
J. Opt. Soc. Am., 48 (1): 13-22.

DENG, S.-Y., GOLDBERG, M.E., SEAGRAVES, M.A., UNGERLEIDER, L.G. and MISHKIN, M. (1985)
The effect of Unilateral Ablation of the Frontal Eye Fields on Saccadic Performance in the Monkey. In Adaptive Processes in Visual and Oculomotor Systems. (1986) Ed. KELLER, E.L. and ZEE, D.S. (Oxford: The Pergamon Press)

DEUBEL, H., WOLF, W. and HAUSKE, G. (1984)
The evaluation of the oculomotor error signal. In Theoretical and Applied Aspects of Eye Movement Research. (Amsterdam: North Holland, Ed. GALE, A.G. and JOHNSON, F.W.).

DE VALOIS, R., ABRAMOV, I. and JACOBS, G.H. (1966)
Analysis of Response Patterns of LGN cells.
J. Opt. Soc. Am., 56 (7): 966-977.

DITCHBURN, R.A. and FOLEY-FISHER, J.A. (1983)
Information concerning colour derived from a single boundary. Ophthal. Physiol. Opt., 3 (3): 233-238.

DIXON, W.J. and MOOD, A.M. (1948)
A method for obtaining and analysing Sensitivity Data.
J. Am. Statistical Assoc., 43: 109-126.

DRASDO, N. (1977)
The neural representation of visual space.
Nature, 266 (7):554-556.

DUBOIS, M.F.W. and COOEWIJN, H. (1979)
Optokinetic reactions in man elicited by localised retinal motion stimuli. Vision Res., 19 :1105 - 1115.

DUYSENS, J., ORBAN, G.A. and CREMIEUX, J. (1984)
Functional basis for the preference of slow movement in area 17 of the cat. Vision Res., 24 (1): 17-24.

ELLIS, C.J.K. (1981)
The pupillary light reflex in normal subjects.
B. J. Ophth. , 65: 754-759.

ESTEVEZ, O., SPEKREIJSE, H., VAN DEN BERG, T.J.T.P. and CAVONIUS, C.R. (1975)
The spectral sensitivities of isolated human colour mechanisms determined from contrast evoked potential measurements. Vision Res., 15: 1205 - 1212.

ESTEVEZ, O. and CAVONIUS, C.R. (1976)
Human colour perception and Stiles' < Mechanisms.
Vision Res., 17: 417 - 422.

ESTEVEZ, O. (1979)
On the fundamental data-base of normal and dichromatic color vision. Ph.D. Thesis, University of Amsterdam.

FARRELL, R.J. and BOOTH, J.M. (1984)
Design Handbook for Imagery Interpretation Equipment.
(Seattle: Boeing Aerospace Company).

FINDLAY, J.M. (1982)
Global visual processing for saccadic eye movements.
Vision Res., 22 ( ): 1033-1044.

FINDLAY, J.M. (1983)
Visual Information Processing for Saccadic Eye Movements.
In Spatially Oriented Observer. (Berlin: Springer-Verlag,
Ed. HEIN, A. and JEANNEROD, M.).

FINDLAY, J.M. (1985)
Saccadic eye movements and visual cognition.
L'Annee Psychologique, 85:101-136.

FINLAY,D. (1982)
Motion perception in the peripheral visual field.
Perception, 11: 457-462.

FINNEY, D.J. (1964)
Statistical method in biological assay. (London: Charles
Griffin and Company Ltd.)

FISCHER, B. and BOCH, R. (1983)
Saccadic eye movements after extremely short reaction times
in the monkey. Brain Research, 260: 21-26.

FISCHER, B. and RAMSPERGER, E. (1984)
Saccadic reaction times reflect different brain functions.
Exp. Brain Research, 57 (1): 191-195.

FROST, D. and POPPEL, E. (1976)
Different programming modes of human saccadic eye movements
as a function of stimulus eccentricity: indications of a
functional sub-division of the visual field.
Biological Cybernetics, 23: 39-48.

FUCHS, A.F. KANEKO, C.R.S. and SCUDDER, C.A. (1985)
Brainstem control of saccadic eye movements.
Ann. Rev. Neurosci., 8: 307-337.

GOILLAU, P. (1983)
Effect of display subtense on eye movement search.
2nd European Conference on eye movements Nottingham.

GOLDBERG, M.E. and WURTZ, R. (1972)
Activity of Superior Colliculus in Behaving Monkey. I.
Visual receptive fields of single neurons.
J. Neurophysiology, 35: 542-559.

GORDON, J. and ABRAMOV, I. (1977)
Color Vision in the peripheral retina. II. Hue and
saturation. J. Opt. Soc. Am., 67 (2): 202-207.

GOURAS, P. and ZRENNER, E. (1982)
The Neural Organisation of Primate Colour Vision.
Color Research and Application., 7 (2): 205-208.

GREEN, D.G. and MAASEIDVAAG, F. (1967)
Closed-Circuit Television Pupillometer.
J. Opt. Soc. Am., 57 (6): 830-833.

GREGORY, R.L. and HARRIS, J.P. (1984)
Real and apparent motion nulled. Nature, 307 (23):
729-730.

GUITTON, G., BUCHTEL, H.A. and DOUGLAS,R.M. (1985)
Frontal lobe lesions in man cause difficulties in
suppressing reflexive glances and in generating
goal-directed saccades. Exp. Brain Res., 58: 455-472.

HALLETT, P.E. (1969)
The variations in visual threshold measurement.
J. Physiol., 202: 403-419.

HALLETT, P.E. (1969)
Quantum efficiency and false positive rate.
J. Physiol., 202: 421-436.

HARMS, H. (1956)
Possibilities and Limitations of pupillomotor perimetry.
Klin. Mbl. Augenheilk., 129:518-534.

HARRIS, M.G. (1986)
The perception of moving stimuli: a model of spatiotemporal coding in human vision. Vision Res., 26 (8): 1281-1287.

HARTMANN, E., LACHENMAYR, B. and BRETTEL, H. (1979)
The peripheral critical flicker frequency.
Vision Res., 19: 1019-1023.

HARVEY, L.O. and POPPEL, E. (1972)
Contrast sensitivity of the human retina.
American Journal of Optometry and Archives of American Academy of Optometry, 49: 748-752.

HASTINGS, C. (1955)
Approximations for digital computers. (Princeton: Princeton University Press.)

HEGGELUND, P. (1984)
Direction asymmetry by moving stimuli and static receptive field plots for simple cells in cat striate cortex.
Vision Res., 24 (1):13-16.

HINTON, J.L. (1984)
The BAe D target acquisition model "oracle": An overview - 1984. Report no. JS 10009 of the British Aerospace Dynamics Group, February 1984.

HOLMES, D.L., COHEN, K.M. and HAITH, M.M. (1977)
Peripheral Visual Processing.
Perception and Psychophysics, 22 (6): 571-577.

HOME, R. (1978)
Binocular summation: A study of contrast sensitivity, visual acuity and recognition. Vision Res., 18: 579-585.

HUBEL, D.H., and WIESEL, T.N. (1965)
Receptive fields and functional architecture in two nonstriate visual areas (18 and 19) of the cat.
J. Neurophysiol., 28 : 229-289.

HUBEL, D.H. and WIESEL, T.N. (1979)
Brain Mechanisms of Vision.
Scientific American, 241: 130-145.

HUNT, R.W.G. (1977)
The Specification of Colour Appearance. II. Effects of Changes in Viewing Conditions.
Color, Research and application, 2 (3): 109- 119.

HUNT, R.W.G. (1978)
Colour Terminology. Color, Research and application, 3 (2): 79-87.

HUNT, R.W.G. (1982)
A model of colour vision for predicting colour appearance.
Color, Research and application, 7 (2): 95-112.

HUNT, R.W.G., and POINTER, M.R. (1985)
A Colour-Appearance Transform for the CIE 1931 Standard Colorimetric Observer.
Colour Research and Application, 10 (3): 165-179.

HUNT, R.W.G. (1986)
Colorimetry up to 1960. Paper presented at the Colour Group's W.D.Wright 80th Birthday Symposium, Imperial College, November 1986).

JOHNSTON, A. and WRIGHT, M.J. (1983)
Visual motion and cortical velocity.
Nature, 304 (5925): 436 - 438.

JOHNSTON, A. and WRIGHT, M.J. (1985)
Lower thresholds of motion for gratings as a function of eccentricity and contrast. Vision Res., 25 (2): 179-185.

KAHNEMAN, D. (1973)
Attention and Effort. (Englewood Cliffs: Prentice-Hall).

KAPOULA, Z. (1985)
Evidence of a range effect in the saccadic system. Vision Res., 25 (8): 1155-1157.

KELLER, E.L. (1980)
Oculomotor Neuron Behaviour. In Models of oculomotor behaviour and control. (Chicago: C.R.C. Press, Ed. ZUBER, B.L.) 21-41.

KOGA, K. and OSAKA, R. (1983)
A comparison of triple recording methods of eye movement. Japanese Psychological Research, 25 (4): 181-190.

KOENDERINK, J.J., BOUMAN, M.A., BUENO DE MESQUITA, A.E. and SLAPPENDEL,S. (1978)
Perimetry of contrast detection thresholds of moving sine wave patterns. II. The far peripheral visual field (eccentricity 0^{o}-50^{o}). J. Opt. Soc. Am., 68 (6): 850-854.

KOENDERINK, J.J., BOUMAN, M.A., BUENO DE MESQUITA, A.E. and SLAPPENDEL,S. (II) (1978)
Perimetry of contrast detection thresholds of moving sine wave patterns. III. The target extent as a sensitivity controlling parameter. J. Opt. Soc. Am., 68 (6): 850-854.

KOERNER, F. AND TEUBNER,H-L. (1973)
visual defects after missile injuries to the geniculostriate pathway in man. Exp. Brain Res., 18: 88-113.

KULIKOWSKI, J.J. and TOLHURST,D.J. (1973)
Psychophysical evidence for sustained and transient detectors in human vision. J. Physiol., 232: 149-162.

LAMAR,E.S., HECHT,S., SCHLAER, S. and HENDLEY, C.D. (1947)
Size, Shape, and Contrast in Detection of Targets by Daylight Vision. 1. Data and Analytical Description.
J. Opt. Soc. Am., 37 (7):531-545.

LAPPIN, J.L. and UTTAL, W.R. (1976)
Does prior knowledge facilitate the detection of visual targets in random noise? Perception and Psychophysics 20 (5): 367-374.

LASLEY, D.J. and COHN, T.E. (1976)
Further studies of the Effect of Stimulus Parameter Uncertainty upon Visual Detection Performance.
J. Opt. Soc. Am., 66: 1079

LASLEY, D.J. and COHN, T.E. (1981)
Detection of luminance increment: effect of temporal uncertainty. J. Opt. Soc. Am.,71 (7): 845-850.

LEE, D.N. (1980)
The optic flow field: the foundation of vision.
Phil. Trans. R. Soc. Lond. B, 290:169-179.

LEGGE, G.E. and CAMPBELL, F.W. (1981)
Displacement detection in human vision.
Vision Res., 21: 205-213.

LENNIE, P. (1980)
Parallel visual pathways: a review.
Vision Res., 20: 561-594.

LEVINSON, E. and SEKULER, R. (1980)
A two-dimensional analysis of direction-specific adaptation.
Vision Res., 20: 103-107.

LISHMAN, J.R. (1981)
Vision and the optic flow field.
Nature, 293 (24): 263-264.

LOWENSTEIN, O. and LOWENFELD, I.E. (1969)
The Pupil. In The Eye. Ed Davson, H. (New York: Academic Press)

LU, C. and FENDER, D.H. (1972)
The interaction of color and luminance in stereoscopic vision. Investigative Ophthalmology, 11 (6):482-490.

LUND, J.S., LUND, R.D., HENDRICKSON, A.B., BUNT, A.H. and FUCHS, A.F. (1975)
The origin of efferent pathways from the primary visual cortex, Area 17, of the Macaque monkey as shown by retrograde transport of horseradish peroxidase.
J. Comp. Neurol., 164:287-304.

LURIA, S.M. (1966)
Color Vision. Physics Today., 34(3): 34-41.

MACADAM, D.L. (1942)
Visual Sensitivities to Colour Differences in Daylight.
J. Opt. Soc. Am., 32 (32):247-274.

MARR, D. and ULLMAN, S. (1981)
Directional selectivity and its use in early visual processing. Proc. Roy. Soc. London., B., 211: 151-180.

MARRIAGE, A. (1955)
Science and Applications of photography. (London: The Royal Photographic Society).

MASLAND, R.H. (1986)
The Functional Architecture of the Retina.
Sc. Am., 12: 90-99.

MATEEF, S. and EHRENSTEIN, W.H. (1986)
Perceptual latencies are shorter for foveopetal motion. (Presented at Ninth European Conference on Visual Perception, Bad Nauheim).

MCKEE, S. and NAKAYAMA, K. (1984)
The detection of motion in the peripheral visual field.
Vision Res., 24 (1): 25-32.

MCKEE, S.P., SILVERMAN, G.H. and NAKAYAMA, K. (1986)
Precise velocity determination despite random variations in temporal frequency and contrast.
Vision Res., 26 (4): 609-619.

MEGAW, E.D. and BELLAMY, L. (1979)
Eye Movements and visual search. In Search and the human observer. Ed. Clare, J.N. and Sinclair, M.A. (London: Taylor and Francis Ltd.)

MEIENBERG, O., ZANGEMEISTER, W.H., ROSENBERG, M. and HOYT, W. F. (1981)
Saccadic Eye Movement Strategies in Patients with Homonymous Hemianopia. Ann. Neurol., 9: 537-544.

MERTENS, J.J. (1956)
Influence of knowledge of target location upon the probability of observation of peripherally observable test flashes. J. Opt. Soc. Am., 46 (12): 1069-1070.

MOHLER, C.W. and WURTZ, R.H. (1976)
Organisation of Monkey Superior Colliculus: Intermediate cells discharging before eye movements.
J. of Neurophysiology, 39 (4): 722-743.

MOHLER, C.W. and WURTZ, R.H. (1977)
Role of Striate Cortex and Superior Colliculus in visual guidance of saccadic eye movements in Monkey.
J. of Neurophysiology, 39 (4): 722-743.

MORGAN, M.J. (1980)
Analogue models of motion perception.
Phil. Trans. R. Soc. Lond. B, 290: 117-135.

MULLEN, K. and BAKER JR, C.L. (1985)
A motion aftereffect from an isoluminant stimulus.
Vision Res., 25 (5): 685-688.

NAKAYAMA, K. (1980)
Psychophysical isolation of movement sensitivity by removal of familiar position cues. Vision Res., 21: 427-433.

NAKAYAMA, K. (1985)
Biological image processing: A review.
Vision Res., 25 (5): 625-660.

NAYATANI, Y., TAKAHAMA, K. and SOBAGAKI, H. (1986)
Prediction of Color Appearance under Various Adapting Conditions. Color Research and application., 11 (1):62-71.

NOORLANDER, C., HEUTS, M.J.G. and KOENDERINK, J.J. (1981)
Sensitivity to spatiotemporal combined luminance and chromaticity contrast. J. Opt. Soc. Am., 71 (4): 453-459.

NOORLANDER, C., KOENDERINK, J.J., DEN OUDEN, R.J. and WIGBOLD EDENS, B. (1983)
Sensitivity to spatiotemporal colour contrast in the peripheral visual field. Vision Res., 23:1-11.

OESTERBERG, G. (1935)
Topography of the layer of rods and cones in the human retina. Acta Ophthal. Scand., Supplement.

OGDEN, T.E. and MILLER, R.F. (1966)
Studies of the optic nerve of the Rhesus monkey: nerve fibre spectrum and physiological properties.
Vision Res., 6:485-506.

ORBAN, G.A., DE WOLF, J. and MAES,H. (1984)
Factors influencing velocity coding in the human visual system. Vision Res., 24 (1): 33-39.

ORBAN, G.A., VAN CALENBERGH, F. DE BRUYN, B. and MAES, H. (1985)
Velocity discrimination in the central and peripheral visual field. J. Opt. Soc. Am., 2 (11): 1836-1847.

OTTES, F.P., VAN GISBERGEN, J.A.M. and EGGERMONT, J.J. (1984).
Metrics of saccade responses to visual double stimuli: two different modes. Vision Res., 24 (10): 1169-1179.

OTTES, F.P., VAN GISBERGEN, J.A.M. and EGGERMONT, J.J. (1985).
Latency dependence of colour-based target vs nontarget discrimination by the saccadic system.
Vision Res., 25: 849-862.

OTTES, F.P., VAN GISBERGEN, J.A.M. and EGGERMONT, J.J. (1986).
Visuomotor fields of the superior colliculus: a quantitative model. Vision Res., 26 (6): 857-873.

OTTOSON, D., and ZEKI, S.M., (1985)
Central and peripheral mechanisms of colour vision.
(Basingstoke: The Macmillan press Ltd)

OVERINGTON, I. (1976)
Vision and Acquisition. (London: Pentech Press)

OVERINGTON, I. (198?)
Extension of the ORACLE visual performance model to colour vision. Report no. BT13759 of the British Aerospace Dynamics Group.

OVERINGTON, I. (1982)
Towards a complete model of photopic visual threshold.
Optical Engineering, 21 (1): 2-13.

PASIK, T. and PASIK, P. (1973)
Extrageniculostriate vision in the monkey. IV. Critical structures for light vs. no-light discrimination.
Brain Research, 56: 165-182.

PERENIN, M.T. and JEANNEROD, M. (1978)
Visual function within the hemianopic field following early cerebral hemidecortication in man - 1. spatial localisation.
Neurophysiologica, 16: 1-16.

PIERSON, R.J. and CARPENTER, M.B. (1974)
Anatomical Analysis of Pupillary Reflex Pathways in the Rhesus Monkey. J. Comp. Neurol., 158 (2):121

POLYAK, S. (1957)
The Retina (Chicago: University of Chicago Press).

POPPEL, E., HELD, R. and FROST, D. (1973)
Residual visual function after brain wounds involving the central visual pathways in man. Nature, 243 (6): 295-296.

POSNER, M.I., SNYDER, C.R.R. and DAVIDSON, B.J. (1980)
Attention and the detection of signals.
J. Exp. Psychology 109 (2): 160-174.

POST, R.B. and LEIBOWITZ, H.W. (1985)
A revised analysis of the role of efference in motion perception. Perception, 14: 631-643.

PRABANC, C., MASSE, D. and ECHALLIER, J.F. (1978)
Error-correcting mechanisms in large saccades.
Vision Res, 18:557-560.

RAMACHANDRAN, V.S. and GREGORY, R.L. (1978)
Does colour provide an input to human motion perception?
Nature, 275:55-56.

REEVES, B. and ROSS, J.E. (1986)
Changes in contrast sensitivity performance with age: do young subjects really see worse than older ones? Paper presented at A.V.A. Annual meeting, Oxford, April, 1986.

REGAN, D. (1979)
Electrical Responses Evoked from the Human Brain. Scientific American, 241 (6):134-146.

REGAN, D. and BEVERLEY, K.I. (1978)
Looming detectors in the human visual pathway. Vision Res., 18: 415-421.

REGAN, D. and TYLER, C.W. (1971)
Some dynamic features of colour vision. Vision Res., 11: 1307-1324.

REICHARDT, W. (1961)
Autocorrelation, a Principle for the Evaluation of Sensory Information by the Central Nervous System. In Sensory Communication, ed Rosenblith. (Cambridge, Mass., M.I.T. press)

RIGGS, L.A. VOLKMANN, F.C. MOORE, R.K. and ELLICOTT, A.G. (1982)
Perception of suprathreshold stimuli during saccadic eye movement. Vision Res, 22: 423-428.

ROBERTSON, A.R. (1986)
Advances in Colour Science from 1960 to the present. Paper presented at the Colour Group's W.D.Wright 80th Birthday Symposium, Imperial College, November 1986).

ROBINSON, D.A. (1980)
Models of the mechanics of eye movements. In Models of oculomotor behaviour and control. (Chicago: C.R.C. Press, Ed. ZUBER, B.L.) 21-41.

RONCHI, L. and NOVAKOVA, O. (1971)
Luminance-Time Relation at Various Eccentricities: Individual Differences. J. Opt. Soc. Am., 61 (1): 115-118.

ROSS, L.E. and ROSS, S.M. (1980)
Saccade latency and warning signals: Stimulus onset, offset and change as warning events.
Perception and Psychophysics, 27 (3): 251-257.

ROVAMO, J., VIRSU, V. and NASANEN, R. (1978)
Cortical Magnification Factor predicts the photopic contrast sensitivity of peripheral vision.
Nature, 271 (1): 54-55.

ROVAMO, J. and VIRSU, V. (1979)
An estimation and application of the human cortical magnification factor. Exp. Brain Res., 37: 495-510.

ROVAMO, J. (1983)
Cortical magnification factor and contrast sensitivity to luminance-modulated chromatic gratings.
Acta Physiol. Scan., 119: 365-371.

ROVAMO, J. and VIRSU, V. (1984)
Isotropy of cortical magnification and topography of the striate cortex. Vision Res., 24 (3): 283-286.

ROVAMO, J. and RANINEN, A. (1984)
Critical flicker frequency and M-scaling of stimulus size and retinal illuminance. Vision Res., 24 (10):1127-1131.

RUDDOCK, K.H. (1975)
Visual Form Perception. Contemp. Phys., 16 (4): 317 - 348.

SAFRAN, A.B., WALSER, A., ROTH, A. and GAUTHIER, G. (1981)
Pupil cycle induction test, A way of evaluating the light reflex. Ophthalmologica Basel, 183:205-213.

SAGI, D. and JULESZ, B. (1985)
"Where" and "What" in vision. Science, 228: 1217-1219.

SCHANDA, J. (1981)
The effect of chromatic adaptation on colour rendering.
Color Research and Application, 6j (4): 221-227.

SCHILLER, P.H., TRUE, S.D. and CONWAY, J.L. (1980)
Deficits in Eye Movements Following Frontal Eye-Field and Superior Colliculus Ablations.
J. Neurophysiol., 44: 1175-1189.

SCHNEIDER, G.E. (1969)
Two visual systems. Science, 163: 895-902.

SEKULER, R. (1975)
Visual motion perception. In Handbook of perception, V (New York: Academic Press).

SEKULER, R. and BALL, K. (1977)
Mental set alters visibility of moving targets.
Science, 198: 60-72.

SLOOTER, J. and VAN NORREN, D. (1980)
Visual acuity measured with pupil responses to checkerboard stimuli. Invest. Ophthal. Visual Sci., 19 (1): 105-108.

SMITH, A.T. and HAMMOND, P. (1986)
Hemifield differences in perceived velocity.
Perception, 15: 111-117.

SPRAGUE, J.M. (1972)
The superior colliculus and pretectum in visual behaviour.
Investigative Ophthalmology. 11 (6): 473-482.

SRINIVASAN, M.V. (1983)
The impulse response of a movement- detecting neuron and its interpretation. Vision Res., 23 (6):659-663.

SRINIVASAN, M.V. (1985)
Shouldn't directional movement detection necessarily be "colour-blind"? Vision Res., 25 (7):997-1000.

STABELL, U. and STABELL, B. (1976)
Rod and cone contributions to peripheral colour vision. Vision Res, 16: 1099-1104.

STABELL, U. and STABELL, B. (1976)
Effects of rod activity on peripheral vision. Vision Res., 16: 1105-1110.

STILES, W.S. (1929)
The effect of glare on the brightness threshold. Proc. R. Soc. (London) Biol.

STONE, J. (1983)
Parallel Processing in the Visual System. (New York and London: Plenum Press.)

SUTHERLAND, N.S. (1961)
Figural aftereffects and apparent size. Q. Jl Exp. Psychol., 13:222-228.

SUZUKI, D.A. and KELLER, E.L. (1984)
Visual Signals in the Dorsolateral Pontine Nucleus of the Alert Monkey: Their Relationship to Smooth-Pursuit Eye Movements. Exp. Brain Res., 53: 473-478.

SWETS, J.A., TANNER, W.P. JNR. and BIRDSALL, T.G. (1961)
Decision processes in perception. psychol. Rev., 68: 301-340.

TEICH, M.C., PRUCNAL, P.R., VANNUCCI, G., BRETON, M.E. and MCGILL,W.J. (1982)
Multiplication noise in the human visual system at threshold: 1. Quantum fluctuations and minimum detectable energy. J. Opt. Soc. Am., 72 (4):419-431.

THOMPSON, P. (1984)
The coding of the velocity of movement in the human visual system. Vision Res., 24 (1): 41-45.

TROELSTRA, A. (1968)
Detection of time-varying light signals as measured by pupillary response. J. Opt. Soc. Am., 58 (5):685-690.

TROSCIANKO, T. and GREGORY, R.L. (1985)
How colour perception enables us to see the world. Paper given at the Colour Group meeting, London, 2nd October 1985

TUSA, R.J. ZEE, D.S. and HERDMAN, S.J. (1985)
Recovery of Oculomotor Function in Monkeys with Large Unilateral Cortical Lesions. In Adaptive Processes in Visual and Oculomotor Systems. (1986) Ed. KELLER, E.L. and ZEE, D.S. (Oxford: The Pergamon Press)

TYNAN, P.D. and SEKULER, R. (1982)
Motion processing in peripheral vision: reaction time and perceived velocity. Vision Res, 22: 61-68.

UKAI, K. (1985)
spatial pattern as a stimulus to the pupillary system.
J. Opt. Soc. Am. A, 2 (7):1094-1099.

VAN DE GRIND, W.A., VAN DOORN, A.J. and KOENDERINK, J.J. (1983)
Detection of coherent movement in peripherally viewed random-dot patterns. J. Opt. Soc. Am., 73 (12): 1674-1683.

VAN DE GRIND, W.A., KOENDERINK, J.J. and VAN DOORN, A.J. (1986)
The Distribution of human motion detector properties in the monocular visual field. Vision Res., 26 (5): 797-810.

VANDENBUSSCHE, E., ORBAN,G.A. and MAES, H. (1986)
Velocity discrimination in the cat.
Vision Res., 26 (11): 1835-1849.

VAN DOORN, A.J. and KOENDERINK, J.J. (1983)
Detectability of velocity gradients in moving random-dot patterns. Vision Res., 23 (8): 799-804.

VAN ESSEN, D.C., and ZEKI, S.M. (1978)
The topographic organisation of rhesus monkey prestriate cortex. J. Physiol., 277: 193-226.

VANEY, D.I. (1985)
Fireworks in the retina. Nature, 314 (6013): 672-673.

VAN SANTON, J.P.H. and SPERLING, G. (1984)
Temporal covariance model of human motion perception.
J. Opt. Soc. Am. A, 1 (5): 451-473.

VARJU, D. (1964)
The Influence of Sinusoidal Luminance Variations in the Mean Pupillary Diameter and on Subjective Brightness.
Kybernetik, 2: 33-43.

VARJU, D. (1967)
Reciprocal Nervous Effects in the Pupillomotor Pathway in Man. 1. Differences in the Pupil Reactions after Uniocular and Binocular Light Stimulation. Kybernetik, 3: 203-214.

VIRSU, V., ROVAMO, J., LAURINEN, P. and NASANEN, R. (1982)
Temporal contrast sensitivity and cortical magnification.
Vision Res., 22: 1211-1217.

WATSON, A.B., AHUMADA, Jr., A.J. and FARRELL, J.E. (1986)
Window of visibility: a psychophysical theory of fidelity in time sampled visual motion displays.
J. Opt. Soc. Am. A., 3 (3): 300-307

WATSON, A.B., BARLOW, H.B. and ROBSON, J.G. (1983)
What does the eye see best? Nature, 302 (5907): 419-422.

WATT, R.J. and ANDREWS,D.P. (1981)
APE: Adaptive Probit Estimation of psychometric functions.
Current Psychol. Rev., 1: 205-214.

WEISKRANTZ, L., WARRINGTON, E.K., SANDERS, M.D. and MARSHALL, J. (1974).
Visual capacity in the hemianopic field following a restricted occipital ablation. Brain, 97: 709-728.

WELLER, R.E., KAAS, J.H. and WETZEL, A.B. (1979)
Evidence for the loss of X-cells of the retina after long term ablation of visual cortex in monkeys.
Brain Research, 160: 134-138.

WESTHEIMER, G. (1966)
The Maxwellian view. Vision Res, 6: 669-682.

WILLIAMS, D., PHILLIPS, G. and SEKULER, R. (1986)
Hysteresis in the perception of motion direction as evidence for neural cooperativity. Nature, 324: 253-255.

WILLIAMS, E.D., and WARWICK, P.L. (1980)
Gray's Anatomy. (Edinburgh: Churchill Livingstone).

WOLF, E. and GARDINER, J.S. (1963)
Sensitivity of the retinal area of one eye corresponding to the blind spot in the other eye.
J. Opt. Soc. Am., 53 (12): 1437-1440.

WOODHOUSE (1975)
The effect of pupil size on grating detection at various contrast levels. Vision Res., 15: 645-648.

WOODHOUSE and CAMPBELL (1975)
The role of the pupil light reflex in aiding adaptation to the dark. Vision Res., 15: 649-653.

WRIGHT, W.D. (1986)
The origins of the 1931 C.I.E. system. Paper presented at the Colour Group's W.D.Wright 80th Birthday Symposium, Imperial College, November 1986).

WURTZ, R.H. and MOHLER, C.W. (1976)
Organisation of Monkey Superior Colliculus: enhanced visual response of superficial layer cells.
J. of Neurophysiology, 39 (4): 745-765

WYSZECKI, G. and STILES, W.S. (1967)
Color Science. (New York: John Wiley and sons Inc.)

YOUNG, R.S.L. and ALPERN, M.
Pupil responses to foveal exchange of coloured lights.
J. Opt. Soc. Am., 70: 697-706.

ZEKI, S.M. (1974)
Cells responding to changing image size and disparity in the cortex of the Rhesus monkey. J. Physiol., 242: 827-841.

ZEKI, S.M. (1974)
Functional organisation of a visual area in the posterior bank of the superior temporal sulcus
of the Rhesus monkey. J. Physiol., 236: 549-573.

ZEKI, S.M. (1978)
The third visual complex of the Rhesus monkey prestriate cortex. J. Physiol., 277: 245-272.

ZEKI, S.M. (1978)
The cortical projections of foveal striate cortex in the Rhesus monkey. J. Physiol., 277: 227-244.

ZEKI, S.M. (1978)
Functional specialisation in the visual cortex of the rhesus monkey. Nature, 274: 423-428.

ZEKI, S.M. (1985)
Colour Pathways and Hierarchies in the Cerebral Cortex. In: Central and Peripheral Mechanisms of Colour Vision. Ed. by Ottoson, D and Zeki, S.M. (Basingstoke: The Macmillan Press Ltd)

ZIHL, J. (1980)
"Blindsight": Improvement of visually guided eye movements by systematic practice in patients with cerebral blindness. Neurophysiologica, 18: 71-77.

ZINN, K.M. (1972)
The Pupil (Springfield, Illinois: Charles C. Thomas).

ZRENNER, E. (1983)
Neurophysiological Aspects of Color Vision in Primates. (Berlin Heidelberg New York: Springer-Verlag).

ZUIDEMA, P., BOUMAN, M.A. and KOENDERINK, J.J. (1985)
Detection of light and flicker at low luminance levels in the human peripheral visual system. II. A mechanistic model. J. Opt. Soc. Am. A, 2 (3): 408-415.